12-2013

Vascular Nanomedicine: Site specific delivery of elastin stabilizing therapeutics to damaged arteries

Aditi Sinha
Clemson University, aditis@clemson.edu

VASCULAR NANOMEDICINE: SITE SPECIFIC DELIVERY OF ELASTIN STABILIZING THERAPEUTICS TO DAMAGED ARTERIES

A Dissertation
Presented to
the Graduate School of
Clemson University

In Partial Fulfillment
of the Requirements for the Degree
Doctor of Philosophy
Bioengineering

---

by
Aditi Sinha
December 2013

Accepted by:
Dr. Narendra Vyavahare, Committee Chair
Dr. Ken Webb
Dr. Alexey Vertegel
Dr. Bruce Gray

ABSTRACT

Elastin, a structural protein in the extra-cellular matrix, plays a critical role in the normal functioning of blood vessels. Apart from performing its primary function of providing resilience to arteries, it also plays major role in regulating cell-cell and cell-matrix interactions, response to injury, and morphogenesis. Medial arterial calcification (MAC) and abdominal aortic aneurysm (AAA) are two diseases where the structural and functional integrity of elastin is severely compromised. Although the clinical presentation of MAC and AAA differ, they have one common underlying causative mechanism – pathological degradation of elastin. Hence prevention of elastin degradation in the early stages of MAC and AAA can mitigate, partially if not wholly, the fatal consequences of both the diseases.

The work presented here is motivated by the overwhelming statistics of people afflicted with elastin associated cardiovascular diseases and the unavailability of cure for the same. Overall goal of our research is to understand role of elastin degradation in cardiovascular diseases and to develop a targeted vascular drug delivery system that is minimally invasive, biodegradable, and non-toxic, that prevents elastin from degradation. Our hope is that such treatment will also help regenerate elastin, thereby providing a multi-fold treatment option for elasto-degenerative vascular diseases. For this purpose, we have first confirmed the combined role of degraded elastin and hyperglycemia in the pathogenesis of MAC. We have shown that in the absence of degraded elastin and TGF-β1 (abundantly present in diabetic arteries) vascular smooth muscle cells maintain their

homeostatic state, regardless of environmental glucose concentrations. However simultaneous exposure to glucose, elastin peptides and TGF-β1 causes the pathological transgenesis of vascular cells to osteoblast- like cells.

We show that plant derived polyphenols bind to vascular elastin with great affinity resulting in improved resistance to elastolytic digestion. We further show that the same polyphenols interact with monomeric tropoelastin released by the vascular cells and dramatically increase their self-assembly in-vitro. In addition, we demonstrate the elastogenic ability of these polyphenols in aiding the crosslinking of tropoelastin released by aneurysmal cells converting it into mature elastin.

Finally, we developed a nanoparticle system functionalized with elastin antibody on the surface that, upon systemic delivery, can recognize and bind to sites of damaged elastin in the aorta. We are able to show that this nanoparticle system works in representative animal models for MAC and AAA. These nanoparticles demonstrated spatial and functional specificity for degraded elastin.

In conclusion, our work is focused on understanding the role of elastin degradation in vascular calcification and aortic aneurysms. We tested approaches to halt elastin degradation and to regenerate elastin in arteries so that homeostasis can be achieved.

DEDICATION

गुरुर्ब्रह्म गुरुर्विष्णुः र्गुरुर्देवो महेश्वरः ।

गुरुःसाक्षात् परंब्रह्म तस्मै श्रीगुरवे नमः ॥

(Guru is the supreme of all)

I would like to dedicate this work to all my teachers, first of them being my parents. Baba, from you I imbibe courage, righteousness, and determination. Maa, your strength, compassion, and discernment I strive to match up to. Bhai, your jovial spirit carries me through the tougher days.

Thank you for your unending encouragement, love, and support.

ACKNOWLEDGEMENTS

I would like to express my sincere gratitude to my advisor Dr. Naren Vyavahare for giving me an opportunity to work with him on this project. I am thankful to him for showing extreme patience and belief in me and helping me complete my studies in a timely fashion. Most importantly, I am deeply indebted to him for being my teacher. His intellectual input, scientific acumen, and commitment to translational research inspire me to pursue my future undertakings with sincerity and integrity.

I am especially thankful to my PhD committee members Dr. Alexey Vertegel, Dr. Ken Webb, and Dr. Bruce Gray. Some of the work in this dissertation would not have been possible without the expertise and guidance from Dr. Vertegel. I would also like to thank Dr. Webb for being a wonderful teacher and introducing me to the world of molecular biology. Dr. Aleksey Shaporev and Dr. Vladimir Reukov offered me contributory advice and assistance with various aspects of nanoparticle formulation and characterization. I would next like to thank Dr. Guzeliya Korneva for her indispensable help with HPLC and invaluable friendship. Dr. Agneta Simionescu has shared her immense knowledge of biochemistry and molecular techniques through the first phase of my project. Linda Jenkins and Cassie Gregory have helped me over the years with histology and cell culture respectively.

This dissertation could not have been completed without the assistance of the entire staff at Godley Snell Research Centre, Electron microscope facility at Advanced Material Center, and Clemson Light Imaging Facility. I would also like to acknowledge

the administrative staff for being so friendly and cooperative at all times. Special thanks to Maria Torres for always being there! To all the past and present CIRL members – thank you for the incessant brainstorming, help and discussion – working in the lab wouldn't have been half as fun without all of you. To all my friends in Clemson, thank you for making the last five years so fun and productive! I would especially like to acknowledge Blessen Elias, Neha Shah, and Partha Deb; without their unconditional support and faith in me, completion of this dissertation would have been far from possible.

I am also grateful to the Department of Bioengineering and Clemson University for being my home for the last five years and instilling the "tiger spirit" in me. Finally, I would like to acknowledge the financial support provided by National Institute of Health: "GAGs: Function and fixation in bioprosthetic heart valves, R01HL070969", COBRE grant: P20RR021949, and the Hunter Endowment (All awarded to Dr. Naren Vyavahare).

TABLE OF CONTENTS

LIST OF TABLES

LIST OF FIGURES

CHAPTER 1

INTRODUCTION

Cardiovascular diseases (CVD) remain the leading cause of death in the United States. 2004 statistics indicate that 52% of CVD related deaths are due to coronary heart disease, 17% due to stroke, 4% due to diseases of the arteries and 6% due to high blood pressure. Congenital CVD and rheumatoid heart disease attribute to 0.5% and 0.4% respectively.[1] In addition, 8.3% of American population are suffering from diabetes, of which 68% die due to cardiovascular complications.[2] It has also been established that diabetic patients are at a 2-4 times greater risk of vascular disease than healthy people. These compelling statistics drive the need for research in the area of cardiovascular disease, both in the fundamental understanding of vascular pathology and in development of cost effective therapeutic options for vascular diseases.

Elastin is a structural protein present in the elastic fibers, which are of crucial importance in the well-being of blood vessels. Elastic fibers are organized as concentric layers in the medial portion of the artery. Its fundamental function is providing elasticity and resilience to arteries; expand during systole and recoil during diastole thereby enabling continuous blood flow through arteries. Needless to say, larger arteries are endowed with more elastin, the degeneration of which affects the physiology of larger arteries more severely than branching arterioles. Elastin is a highly cross-linked protein resistant to proteolytic degradation except by a special class of proteases called matrix metallo-proteinases (MMP), especially MMP2, 7, 9, and MMP12.[3] Two fatal arterial

diseases, namely medial arterial calcification (MAC) and abdominal aortic aneurysm (AAA), are primarily elastin degradation related diseases.

Elastin associated calcification observed in MAC is a common and central pathological trait of type II diabetes mellitus[4] and chronic kidney disease (CKD).[5] The hallmark characteristic of type II diabetes is high levels of circulating glucose and insulin. High glucose concentrations (hyperglycemia) by itself is not a disease, however, it is the single largest contributor of all the co-morbidities associated with diabetes including micro-vascular and macro-vascular diseases, retinopathy, nephropathy, neuropathy, cardiomyopathy, and infection. Amputation of lower extremities and death can occur due to all the above mentioned co-morbidities. MMP mediated elastin degradation is commonly observed in peripheral arteries of diabetic patients.[5,6] Degradation of elastin leads to the release of soluble elastin peptides in the blood stream, which further bind to elastin laminin receptors on fibroblasts and smooth muscle cells present in the artery, thus activating them and causing possibly unfavorable downstream activity such as transgenesis of smooth muscle cells to bone-like cells and increased production of elastin degradative enzymes like MMPs.[7,8] In fact, blood serum levels of circulating soluble elastin peptides are much greater in diabetic patients compared to healthy people.[9] Therefore, a useful structural protein, upon degradation can have potentially malevolent implications on overall vascular health. Additionally, high levels of circulating glucose undergo a series of oxidant-induced fragmentation leading to the formation of advanced glycation end products (AGEs) that generate irreversible crosslinks on structural proteins like collagen and elastin.[10,11] The exact pathological mechanisms involving glucose and

elastin peptides leading to elastin calcification in diabetic patients is not clearly understood and thus we investigated the mechanistic aspects of hyperglycemia and elastin peptides in the osteogenesis of vascular cells (pathological conversion of arterial cells to bone-like cells).

AAA is another arterial disease with potentially severe consequences, mainly due to its asymptomatic nature. AAA causes structural weakening of a local segment of the aorta primarily due to accelerated elastin degradation causing faulty load bearing and insufficient resilience of arteries leading to local ballooning and eventual rupture of the abdominal aorta. AAAs are characterized by degeneration of arterial ultra-structure, decrease in medial elastin content, fragmentation of elastic lamellae, infiltration of inflammatory cells, increased enzymatic activity (especially MMPs), atherosclerosis, intra-luminal thrombosis and calcification.[12] AAA is an idiopathic disease with an unknown etiology. Although atherosclerosis is a key feature of AAA, atherosclerosis in small arteries causes opposite remodeling of arteries (expansion in AAA vs. occlusion in small arteries). Regardless of its initiation mechanisms, AAA is a biomechanical problem, and rupture of aorta is essentially a mechanical failure of the structural proteins elastin and collagen. Current surgical methods for AAA treatment include 1) open aneurysm repair and 2) endovascular abdominal aneurysm repair (EVAR). Though these procedures have low mortality rates (<5%) and relatively short recuperation times, long term cardiac and pulmonary complications and other graft related complications can drop patient survival rates by ~ 50% at 10 years post-operation.[13] Currently there are no pharmacological options for treating AAA. The therapeutics options that have made it to

clinical trials include statins[14-16], β-blockers[17,18], ACE inhibitors[19], tetracyclines like doxycycline (mainly works as an MMP inhibitor),[20] and anti-inflammatory agents. However, systemic delivery of these drugs have undesirable side-effects and reduced effectiveness in treating aneurysms as we will discuss later. Since AAA has a complex pathology with multi-factorial causal factors, a multi-modal treatment option would serve as an ideal one. First, as the eventual rupture is due to poor biomechanics of the arterial tissue (which is because of progressive loss of elastin and collagen), biomechanical strengthening of the residual ECM and its protection against further proteolytic damage would lead to halting of further ballooning and rupture. Second, arterial elastin that is lost during disease development needs to be restored and regenerated to reverse the formed aneurysm. In this dissertation we explore the use of plant derived polyphenolic compounds in stabilizing elastin matrix from proteolytic damage and improving biomechanics of aneurysmal aorta. In addition, we also study whether the same treatment can aid in cellular deposition of newly formed cross-linked elastin and inhibition of MMPs. Thus we aim to provide a treatment using polyphenols that can solve multiple problems in AAA and can halt and reverse aneurysms.

As discussed earlier, diseases like MAC and AAA do not have any pharmacological treatment till date. The drugs that can be potentially used for vascular therapy have very low tolerance when delivered systemically. For instance the use to doxycycline for AAA repair has unpleasant side-effects like skin reactions, tooth discoloration, gastrointestinal symptoms and yeast infection.[21] Furthermore, due to first-pass effect, systemic delivery of drugs causes rapid loss and uneven distribution of drug

throughout the body and thus very little concentration is present in the diseased site. Especially in diseases like MAC and AAA, which are primarily matrix disorders, the drug-matrix interaction is of fundamental importance. Hence development of a drug delivery system that is capable of targeting the diseased site and delivering the well-defined therapeutic payload of drug to the site becomes an attractive option. The advent of nanotechnology offers a logical and clever solution making the aforementioned possible. Polymeric nanoparticles (NPs) can be loaded with drugs/proteins of choice. Additionally, surface functionalizing of these NPs with ligands capable of recognizing specific sites enables active targeting in the vasculature. Once these NPs reach the site, they can deliver drugs to the site in a controlled fashion. Such NPs have been successfully used for cancer therapy.[22] However, targeting therapeutics to diseased blood vessels still remains a challenge mainly due the heterogeneity of vascular diseases, tortuosity of arteries, hemodynamic environment within the vasculature with its high blood flow and limited and transient targets available in the blood vessels. Although several researchers have attempted targeting inflammation of blood vessels (very common feature in all vascular disease),[23-25] the unstable and relatively low antigen expression provides sub-optimal targeting efficiency. In the following chapters we will discuss the development of a novel technology that enhances targeting efficiency to the site of vascular damage thereby enabling the delivery of drugs to diseased site. As discussed earlier, elastin fragmentation and degradation is a common and prevalent feature in several diseases especially diabetic MAC and AAA. We turned this undesirable pathology to our advantage by using it as a potential target for sites of nanoparticle

attachment. We formulated polymeric nanoparticles decorated with elastin antibodies that can recognize and attach to damaged elastin of aorta. This technology can be extended for delivery of drugs, imaging agents and biomolecules to sites of elastic damage.

Organization of dissertation

1) In **chapter 2**, we present a comprehensive overview of:
    - ***Elastin:*** its structure, function, biomechanics, physiological relevance in blood vessels, ultrastructure, mechanisms of elastin synthesis and fiber assembly in-vivo and in-vitro.
    - ***Cardiovascular diseases:*** Pathological significance of elastin in MAC and AAA, underlying mechanisms causing MAC and AAA, current therapeutic options for MAC and AAA
    - ***Polyphenols:*** Their structure, properties and historical uses, interaction with extracellular matrices, cellular interactions, and role as therapeutics
    - ***Drug delivery:*** Local drug delivery options to the vasculature
2) **Chapter 3** describes the project goals, scope, and rationale
3) In **chapter 4**, we discuss the effect of high glucose, elastin derived peptides and transforming growth factor β-1 (TGFβ-1) on the pathogenic transformation of vascular cells to osteoblast-like cells. We investigate the receptors and molecular pathways responsible for osteogenesis of smooth muscle cells in hyperglycemic conditions.
4) **Chapter 5** details the utility of polyphenols for stabilizing elastin against proteolytic damage and potential use for AAA repair. We study the polyphenol

interactions with insoluble elastin and tropoelastin. We also compare the effect of polyphenols on healthy as well as aneurysmal cells in elastic matrix regeneration and its assembly.

5) **In chapter 6** we develop a novel technology which uses nanoparticles that can categorically target sites of damage in the aorta which can be used to deliver site-specific drugs for AAA and MAC repair. Herein, we use established animal models to test our technology and investigate the tolerance of these nanoparticles in-vitro and clearance rates in-vivo.

6) Finally **chapter 7** discusses preliminary trials of polyphenol loaded nanoparticles for in-vivo delivery; final conclusions derived from this multi-faceted project, recommendations and future directions of the current work.

CHAPTER 2

LITERATURE REVIEW

2.1 Vascular anatomy

The circulatory system of the body comprises of the heart, arteries, blood vessels and blood. The main function of the heart is to pump the primary circulatory fluid-blood through closed conduits called arteries. Arteries branch out into smaller blood vessels and capillaries that allow exchange of nutrients and waste metabolites from all body tissues. The metabolites are carried back to the heart via the venous system.

A healthy artery comprises of three fundamental layers (Figure 2.1) - (1) endothelium (tunica interna) comprising of a monolayer of endothelial cells (2) media (tunica media) composed of smooth muscle cells (SMC) (3) adventitia (tunica externa) containing mainly fibroblasts. The medial layer mainly comprising of insoluble mature elastin is responsible for maintaining structure of the artery during the contractile pulsations of smooth muscle cells. The elastic property of arteries is provided by elastin whereas the load bearing properties of the artery are mainly due to the collagen present in the adventitial layer. The intima is the innermost layer of the arteries which comprises of endothelial cells resting on a basement membrane made up of extracellular matrix (ECM) proteins like collagen type IV, laminin and heparin sulfate proteoglycans.[26] The internal elastic lamina (IEL) separates the intima from the media and the external elastic lamina (EEL) separates the media from the adventitia. The medial layer is usually the thickest layer in the artery consisting of concentric layers of circumferentially arranged smooth

muscle cells interspersed in alternating elastic lamellae. Vascular smooth muscle cells are responsible for the production of elastin, collagen and other ECM components.

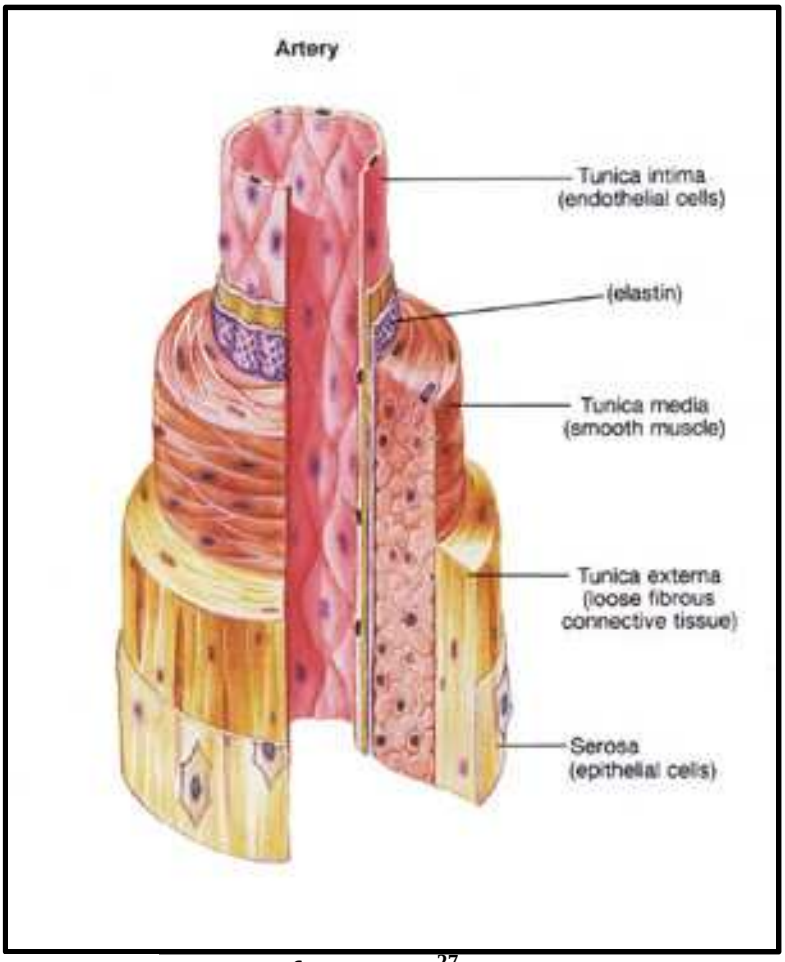

Figure 2.1: tructure of an artery[27]

2.1.1 Structure of aortic elastin

Elastin is the predominant structural protein of the arteries comprising of ~ 50% of the arterial ECM.[28] Elastin is primarily synthesized during embryogenesis, rarely undergoes remodeling and has a very low turn-over rate. It is a hydrophobic protein containing a highly conserved peptide sequence 'VGVAPG' (Table 2.1). Due to the

recurring hydrophobic amino acid residues (XPGX' where X and X' are hydrophobic residues), elastin is a highly hydrophobic and cross-linked protein and can undergo nearly 2 billion stretch-relaxation cycles in the aortic arch in a lifetime.[3]

Table 2.1: Amino acid composition of elastin derived from rat aorta. Values expressed as residues/1000 total amino acid residues[29]

Amino acid (AA)	**Residues per 1000 AAs**
Aspartic Acid(Asp)	3.6
Glutamic acid (Glu)	13.9
Serine (Ser)	15.9
Glycine (Gly)	382.1
Histidine (His)	0
Arginine (Arg)	6.6
Threonine (Thr)	10.3
Alanine (Ala)	214.6
Proline (Pro)	104.8
Tyrosine (Tyr)	35.9
Valine (Val)	81.4
Methionine (Met)	0
Cysteine (Cys)	0
Isoleucine (Ile)	24.1
Leucine (Leu)	64.8
Phenylalanine (Phe)	13.9
Lysine (Lys)	1.7
Iodesmosine (Ides)	2.2
Desmosine (Des)	3.4

Elastin is a biopolymer with tropoelastin as its single repeating monomeric unit. The typical amino acid composition consists of non-polar amino acids with few polar side chain residues. Elastin contains alternating hydrophobic segments and alanine and lysine rich segments (Figure 2.2).

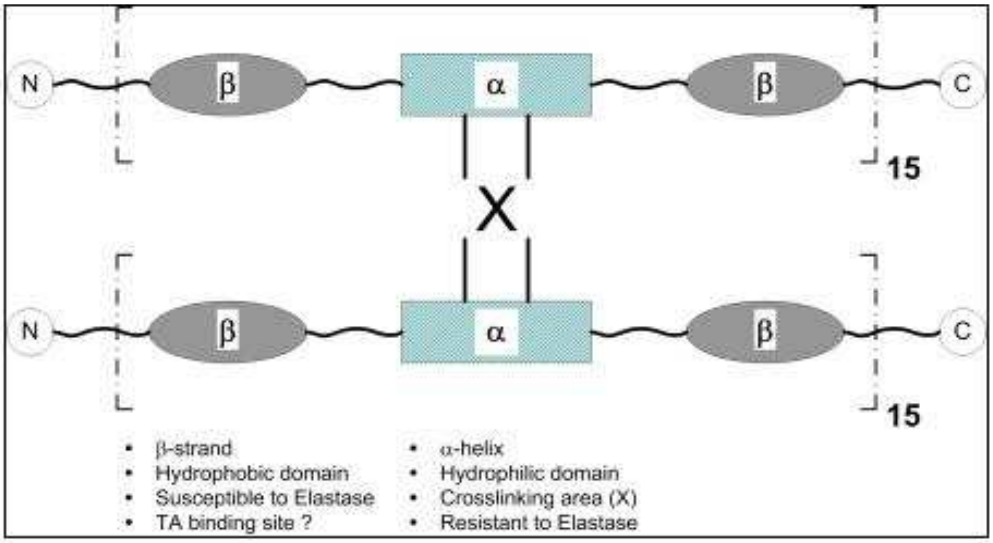

Figure 2.2: Structural features of elastin showing the repetitive alternating sequence (square brackets) of β-hydrophobic domains and α-crosslinking areas[30]

The hydrophobic short segment assumes β-sheet confirmation and is responsible for the elastic properties of elastin, whereas the α-helical segment of alanine and lysine rich residues mainly form crosslinks between adjacent molecules. In between these rigid cross-linking domains, the hydrophobic segments display motility and contribute greatly to the entropy of the system.[31] Despite being greatly hydrophobic, elastin is highly hydrated by water and swells in vivo.[31] The tropoelastin molecules are bound to each other with crosslinks that can either be bi- (lysinonorleucine) , tri- (merodesmosine) or tetra-functional (desmosine and iso-desmosine) in nature, and the increase in complexity

is thought to progress as the fiber matures and ages.[32] These internal links of desmosine and isodesmosine are extremely stable making elastin a very stable protein, resistant to conventional enzymatic or solvent based degradation. Extraction of elastin usually involves a stepwise procedure for the removal of tissue components under relatively mild conditions thereby preserving peptide bonds. Digestion of elastin using oxalic acid or boiling sodium hydroxide is commonly used to quantify insoluble mature elastin.[33] Being extremely stable and having a low turnover rate, it can be considered that elastin lasts the entire lifespan of the individual.

2.1.2 Mechanical properties of elastin

The two most prominent structural arterial proteins are collagen and elastin and these proteins primarily determine the mechanical properties of the aorta. Elastin plays rubber-like roles in physiological pressures leading to arterial expansion, whereas collagen bears high-pressure loads. The most important determinant of the arterial wall mechanics is the elastin to collagen ratio which varies significantly throughout the vasculature. Studies show that the uniaxial elastic modulus of collagen is between 0.3 to 2.5 X 10^{10} dynes/cm^2 which is at least a thousand times more than elastin.[34] The great mechanical stiffness of collagen is attributed to numerous inter-chain links that stabilize the helical structure of collagen. Elastin on the contrary is a stretchy protein that exhibits high degrees of reversible deformation with high resilience. The physiological properties of elastin include low stiffness, high extensibility and high resilience. It has been shown that at physiological pressures, arteries are mostly distensible, implicating the role of

elastin, whereas at higher pressures arteries tend to be much stiffer indicating the load-bearing tendencies of collagen.

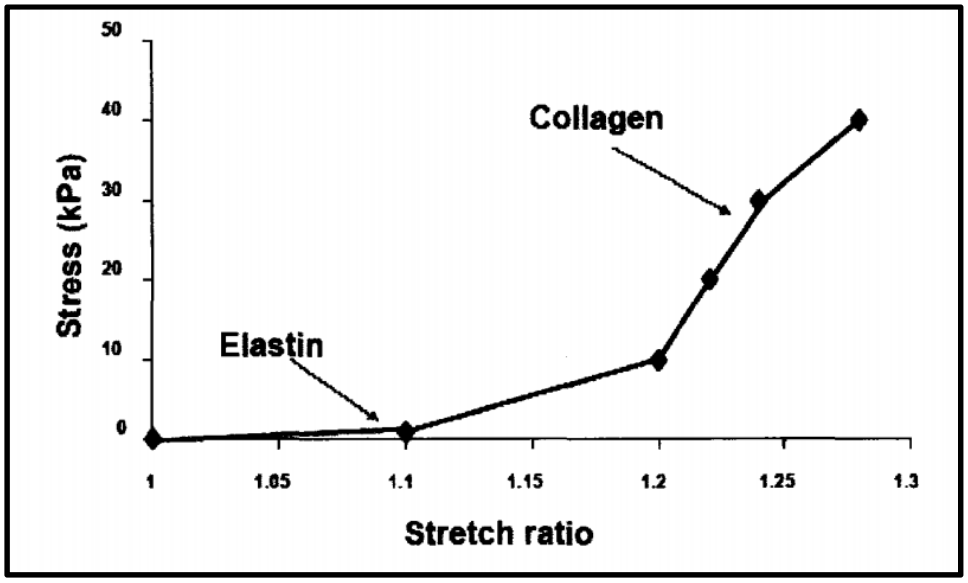

Figure 2.3: A typical stress-strain curve for a blood vessel. Shown are the respective regimes affected by physiologic state and organization of collagen and elastin.[35]

Roach and Burton have shown in their work that elastin mainly bears circumferential load, which explains their arrangement in the artery, whereas collagen mainly bears longitudinal loads at much higher pressure.[36] They separated the role of each protein by using trypsin to degrade elastin and formic acid to degrade collagen in human iliac arteries. Stromberg et al. in their experiments showed that pure collagen undergoes very small strain before they fracture, which is highly uncharacteristic of total arterial tissues. This indicates that collagen remains un-stretched in the arteries until the vessel is distended. They also showed the progressive alignment of collagen fibers in the

longitudinal direction with increasing stress.[37] Elastin is endowed with high resilience capable to undergoing cyclic stretching (Figure 2.4).

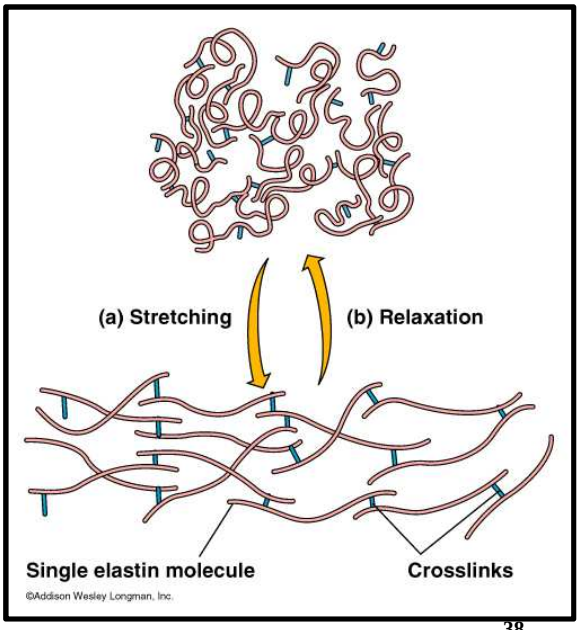

Figure 2.4:Depiction of elastin recoil[38]

2.1.3 Elastin ultrastructure

Insoluble elastin fibers are made up of 2 major structural components, a central core of amorphous elastin clumps which lacks a regular structure, and a periphery of microfibrils. The amorphous content consists about 90% of the mature elastin and is composed of exclusively elastin while the microfibrillar component consists 10-12 nm fibrils located around the periphery of the amorphous content with some interspersed within it.[39] Microfibrils contain a number of glycoproteins like microfibril-associated glycoproteins (MAGP-1,-2,-3,-4); however the majority of the protein is 350 kDa fibrillin playing an important role both in maintaining the elastic fibers and the matrix-cell interaction.[40] These microfibrillar components especially play an important role during

elastogenesis. The monomer tropoelastin interacts specifically with fibrillin and MAGP which is a vital step for the accurate crosslinking of elastin.

Under transmission electron microscope, elastin appears either in cross-section as amorphous clumps exhibiting low electron density measuring 100-800 nm at the core (Figure 2.5) or as longitudinally-aligned, laterally-associating bundles of elastin (Figure 2.6). TEM suggests that microfibrils are mainly tubular in nature appearing as a beaded chain. Multiple fibrillin molecules may align in a parallel head-to-tail fashion to form major microfibrils. The microfibrils are found in small bundles under the plasma membrane and with the development of fibers, elastin begins to appear as an amorphous bundle within each microfibrillar bundle. These amorphous areas gradually join together and generate the core of elastin with majority of the microfibrils orienting outwardly.[39]

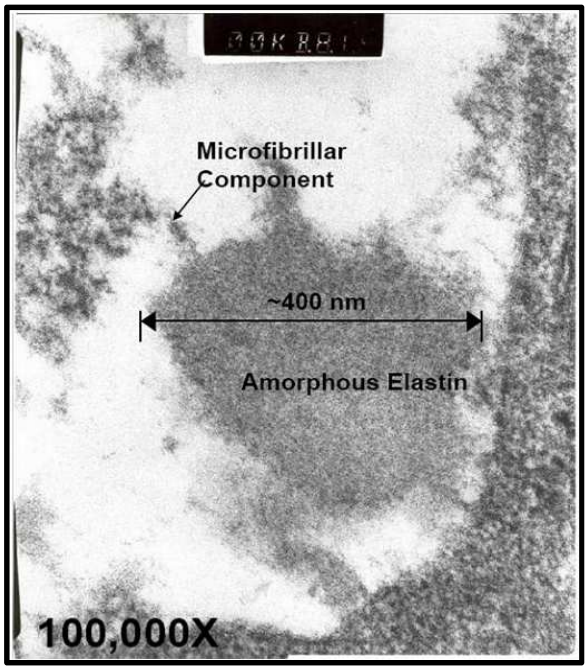

Figure 2.5: TEM of cross section of elastin and fibrillin fibers deposited by rat vascular cells in culture[41]

Besides directing the elastin growth, microfibrils have also shown to mediate cellular interaction with elastin fibers, regulating the cell phenotype and ensuring homeostasis.[42]

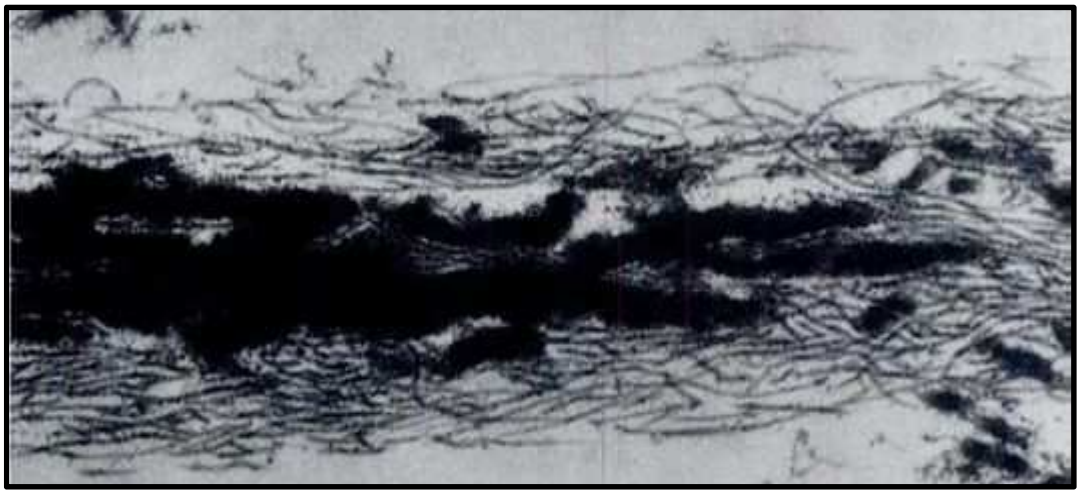

Figure 2.6: TEM of longitudinal section of elastin. Elastin is stained in black and is surrounded by microfibrils[39]

2.1.4 Mechanisms of elastin synthesis and fiber assembly

As mentioned earlier, elastin is a hydrophobic structural protein with an amorphous core and peripheral microfibrils. However, the cellular production, orientation, assembly, crosslinking and deposition of elastin is a tightly regulated hierarchical process which is poorly understood. The monomeric form of the bio-polymer elastin is a 72 kDa soluble tropoelastin which is released by cells. Human tropoelastin is encoded by a single gene with multiple isoforms. The elastin gene is present with a single copy on the chromosome-7.[43] The human tropoelastin mRNA encodes the 72 kDa soluble protein which on post translational modification, results in the mature 60 kDa protein. The tropoelastin protein is secreted by cells after being hydroxylated on a number of proline residues, mainly located on the protein segment corresponding to exon-18. The C-terminus is highly conserved regions in tropoelastin. It contains two cysteine residues which form disulfide bond. Human tropoelastin is unglycosylated[44] and is produced by smooth muscle cells, endothelial cells, and fibroblasts in response to mechanical stress.[32] The process of elastogenesis is broadly categorized into the following stages: (1) tropoelastin synthesis (2) coacervation (3) microfibrillar deposition (4) crosslinking (Figure 2.7).

Once the tropoelastin is released by cells, the process of self-aggregation (coacervation) begins wherein the ~ 15 nm monomers form larger spherical globules, primarily due to the inherent tendency of tropoelastin to coacervate due to its excessive hydrophobicity.[45] The tropoelastin coacervates remain attached to cell surface via glycosaminoglycans and integrins until deposition on microfibrils. Microfibrils play three

crucial roles, (1) provide a scaffold directing and propagating elastin growth[46] (2) further promoting coacervation[47] (3) recruit lysyl oxidase for the cross linking of elastin.[48]

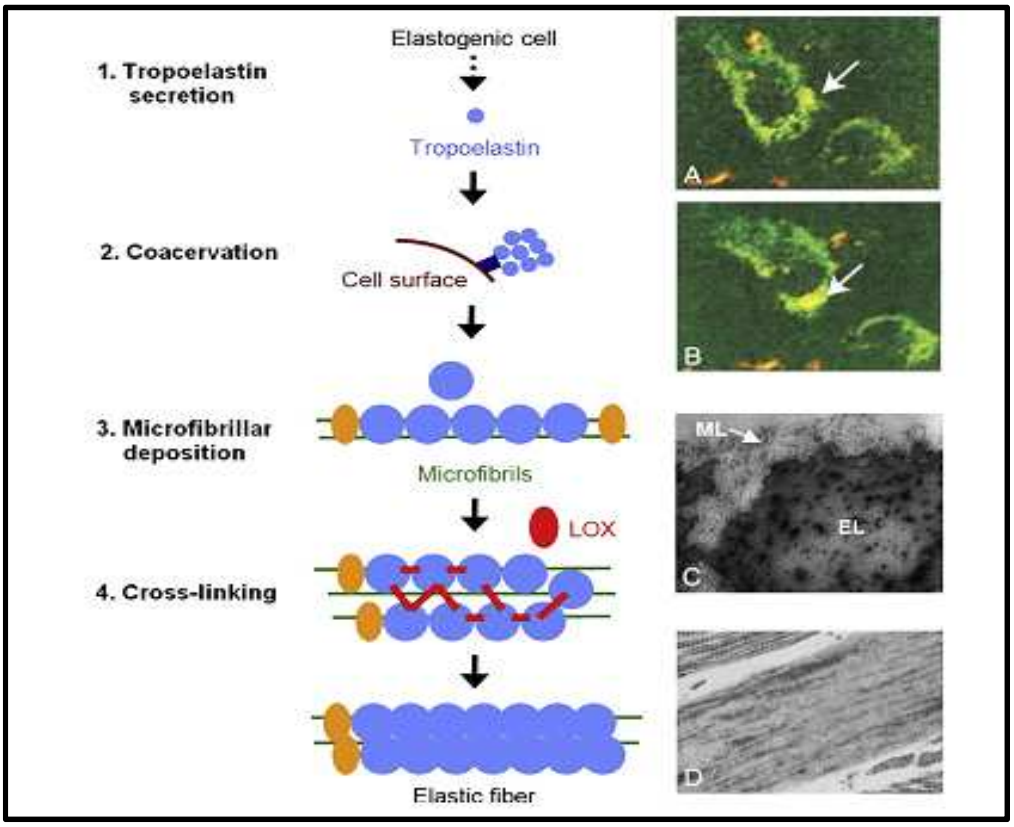

Figure 2.7: Elastogenesis schematic. Cells secrete tropoelastin coacervating on the surface. Coacervates remain attached to cells until deposition on microfibrils. Microfibrills recruit the crosslinking enzyme lysyl oxidase (LOX) which oxidizes the lysine residues, triggering the formation of intramolecular and intermolecular cross-links needed for formation of stable fibers.[49]

Once LOX is recruited to the site of tropoelastin-fibrillar complex, it deaminates specific lysine residues to form allysines[50] thereby initiating spontaneous formation of intra and intermolecular cross-links.[51] Once the intermolecular crosslinks are formed, elastin gets organized in the three dimensional network. Crosslinking inhibits mobility of elastin and makes elastin insoluble and a stable molecule.

2.1.5 Stages of in vitro tropoelastin self-assembly

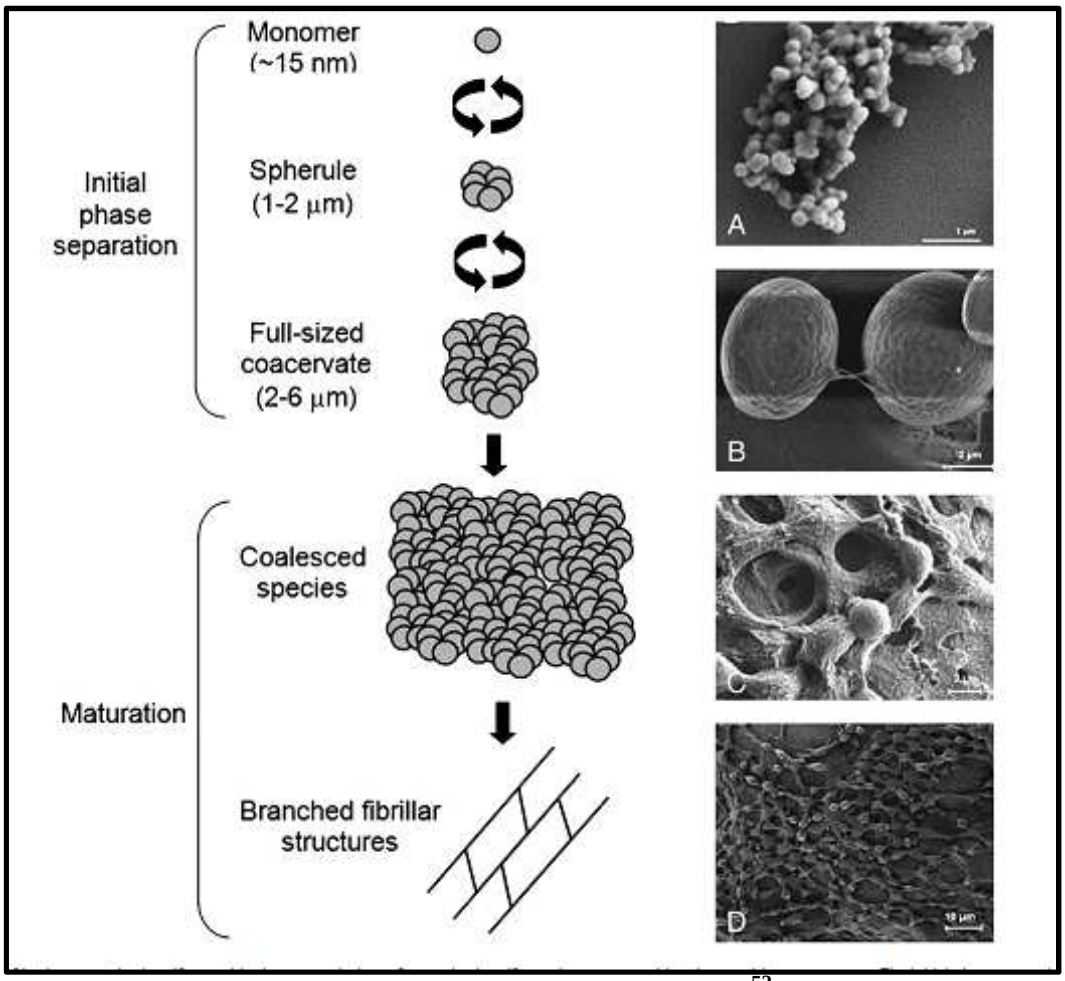

Figure 2.8:Stages of in vitro tropoelastin self-assembly.[52]

Tropoelastin displays a spontaneous self-aggregation in an acellular environment forming aggregates and fibers very similar to that in the presence of cells. This indicates the inherent ability of tropoelastin of assembly. This in-vitro coacervation can be divided into two main stages (1) initial phase separation (2) maturation phase (Figure 2.8).

Coacervation is an entropic process and over a very narrow range of temperature increase (<5°C) there is a rapid monomer-to-polymer assembly without any apparent intermediate stages.[53] Experimentally, this is observed as a sharp rise in turbidity in solution. With time, the droplets progressively grow until a stable size of 2-6 µm is reached. When allowed to settle, a liquid-liquid phase separation occurs. The bottom phase consists of a visco-elastic phase containing concentrated tropoelastin and the top phase consists of an aqueous solution of tropoelastin at its critical concentration.[54] The initial coacervation phase is a reversible process which dissipates back into solution upon cooling.[55] However, once polymerization is allowed for extended time period, the maturation stage occurs irreversibly and aggregates do not return back into solution upon cooling.[56] Maturation is observed as the formation of large globules which is experimentally detected as a decrease in turbidity/absorbance. During the coacervation phase, the increasing particulate matter scatter light increasing the absorbance. At the maturation phase, the light scattering ability of the spherules is reduced thereby decreasing turbidity.[57] Bressan et al. observed tropoelastin at 40°C for a few minutes isolated into filaments of 5 nm diameter and variable length. However, after 10 hours of incubation, formed a white precipitate consisting of 0.5-2 µm thick amorphous branching fibers, identical to those seen in normal tissues.[58]

As discussed earlier, cellular model of elastin assembly deploys microfibrillar proteins such as fibrillins, fibulins and MAGP promoting coacervation and intermolecular alignment. This phenomenon has also been observed in vitro using tropoelastin.[57] Interestingly, fibrillin shows an inhibition in tropoelastin coacervation in a dose-dependent manner (a property displayed by fibulin-4,-5 and MAGP-1). In the presence of these proteins, there is a significant delay in the time of maturation indicating the inhibitory effects of these species. Delaying the maturation enhances the clustering of tropoelastin into organized network. Also, fibulin-4,-5 deficiencies in humans are associated with the presence of large globules of tropoelastin in the extracellular space.[59] These findings indicate the importance of microfibrillar proteins in modulating the end size of tropoelastin prior to fiber assembly. Coacervation is a critical step to successful elastin crosslinking. Coacervation has shown to increase the intra-molecular structure of tropoelastin for downstream elastogenic events. Lysine oxidation of tropoelastin coacervates have shown to form spontaneous crosslinks.[60] This emphasizes the importance of coacervation in correct alignment of monomers and orienting lysine groups such that zero-length crosslinking can occur.[61]

2.2 Vascular diseases

Cardiovascular disease (CVD) has been the leading cause of death in the United States. The major risk factors include hypertension, high cholesterol levels, smoking, sedentary life style, poor eating habits and diabetes. CVD includes coronary arterial disease, heart valve disorders, high blood pressure, heart failure, aneurysms and stroke

(Figure 2.9). There is almost a 37% prevalence of CVD causing a mortality of around 830,000.[1]

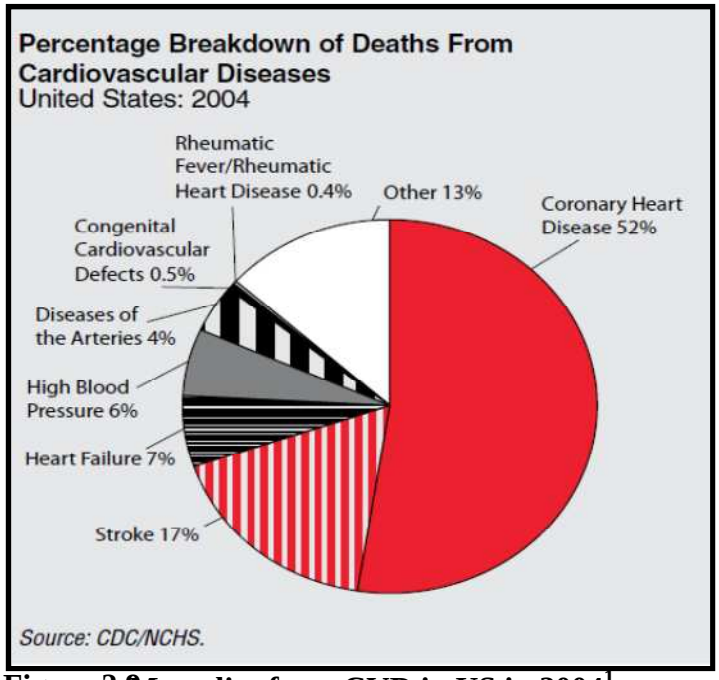

Figure 2.9 Mortality from CVD in US in 2004[1]

2.2.1. Atherosclerotic arterial disease

Atherosclerosis is an inflammatory disease characterized by luminal deposition of fatty plaque. Beginning with an initial endothelial injury, this disease progresses causing changes in endothelial cellular properties like permeability, response to stimulatory agents, and interaction with other cells types. Over time, the endothelium becomes increasing permeable to lipoproteins enhancing its uptake and retention in the sub-endothelial intima.[62] This gradual accumulation of low density lipoprotein (LDL) indirectly damages the arterial wall by inducing biochemical changes such as increasing the free radical content, initiating platelet adherence and activation, and secreting various

cytokines that cause proliferation of smooth muscle cells and recruitment of macrophages. Over a period of years, lipid-laden macrophages (called foam cells) accumulate in the intima attracting particles of lipid and calcium phosphate, eventually building upto a fibrous plaque narrowing the lumen and restricting blood flow[63] (Figure 2.10). Although atherosclerotic lesions may occur anywhere over the vascular tree, abdominal aorta, iliac, carotid and coronary arteries as well as vascular bifurcations are more prone to accumulation.[64] Lesions in small diameter arteries are especially fatal as they occlude the arteries obstructing blood flow possibly leading to myocardial infacrtion or stroke.

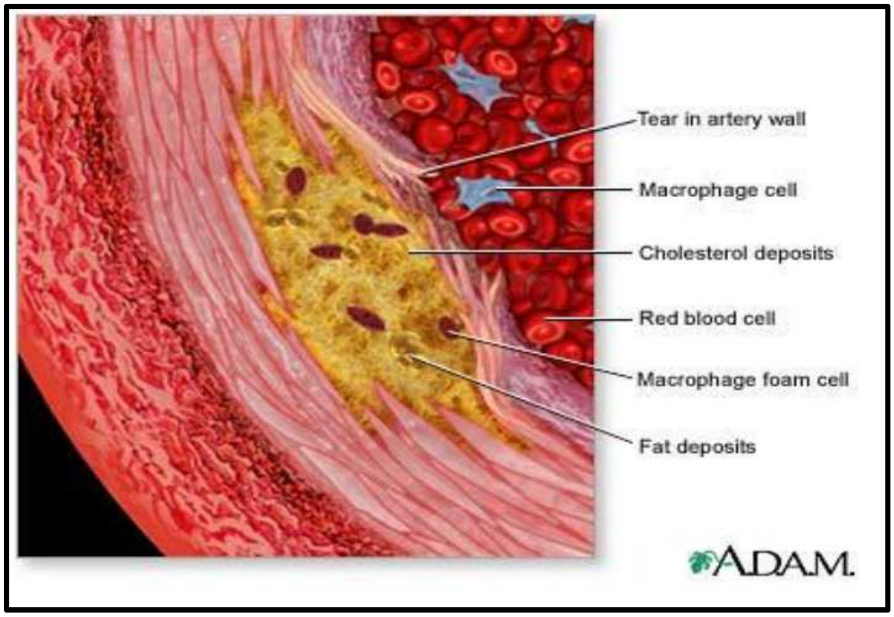

Figure 2.10 Cut section of an artery showing features of an atherosclerotic plaque[65]

2.2.2 Pulmonary arterial hypertension (PAH)

Pulmonary arterial hypertension (PAH) is a rare but fatal arterial disease causing an increased blood pressure in the pulmonary artery, pulmonary vein or capillaries causing a variety of symptoms such as shortness of breath, dizziness, fainting, and fatigue. The main manifestation of PAH is increased elevated mean pulmonary arterial pressure (MPAP). PAH is defined as an elevated MPAP of more than 25 mm Hg at rest, or 30 mm Hg after exercise.[66] Increase in MPAP can further correlate to other complications including increased pulmonary vascular resistance, intimal hyperplasia, smooth muscle hypertrophy, vascular matrix remodeling, thrombus formation, right ventricular hypertrophy, calcification, and all of them eventually leading to narrowing of arteries. PAH is an idiopathic disease with relatively slow progression, symptoms taking about 2-3 years to develop. Thus delay in diagnosis causes complications and high mortality of PAH patients mainly due to right ventricular failure. The exact etiology of PAH is unknown, however, the pathogenesis can be attributed to several pro-inflammatory conditions including exposure to toxins, proteolytic enzymes, imbalance between vasodilators and vasoconstrictors, elevated serotonin levels, and potassium ion channel dysfunction.[66] Arterial pericytes undergo differentiation into SMC causing abnormal proliferation and muscularization of distal alveolar ducts.[67] In addition, the reduction of nitric oxide[68] and thromboxane[69] (potent vasodilators) further causes narrowing of the arteries. Serine proteases that are potent elastases are also implicated in the pathogenesis of PAH. Further, up-regulation of elastases initiates a cyclic process of

increasing MMPs which further degrades the arterial matrix causing pathological matrix remodeling. Figure 2.11 gives a summary of the pathogenesis of PAH.

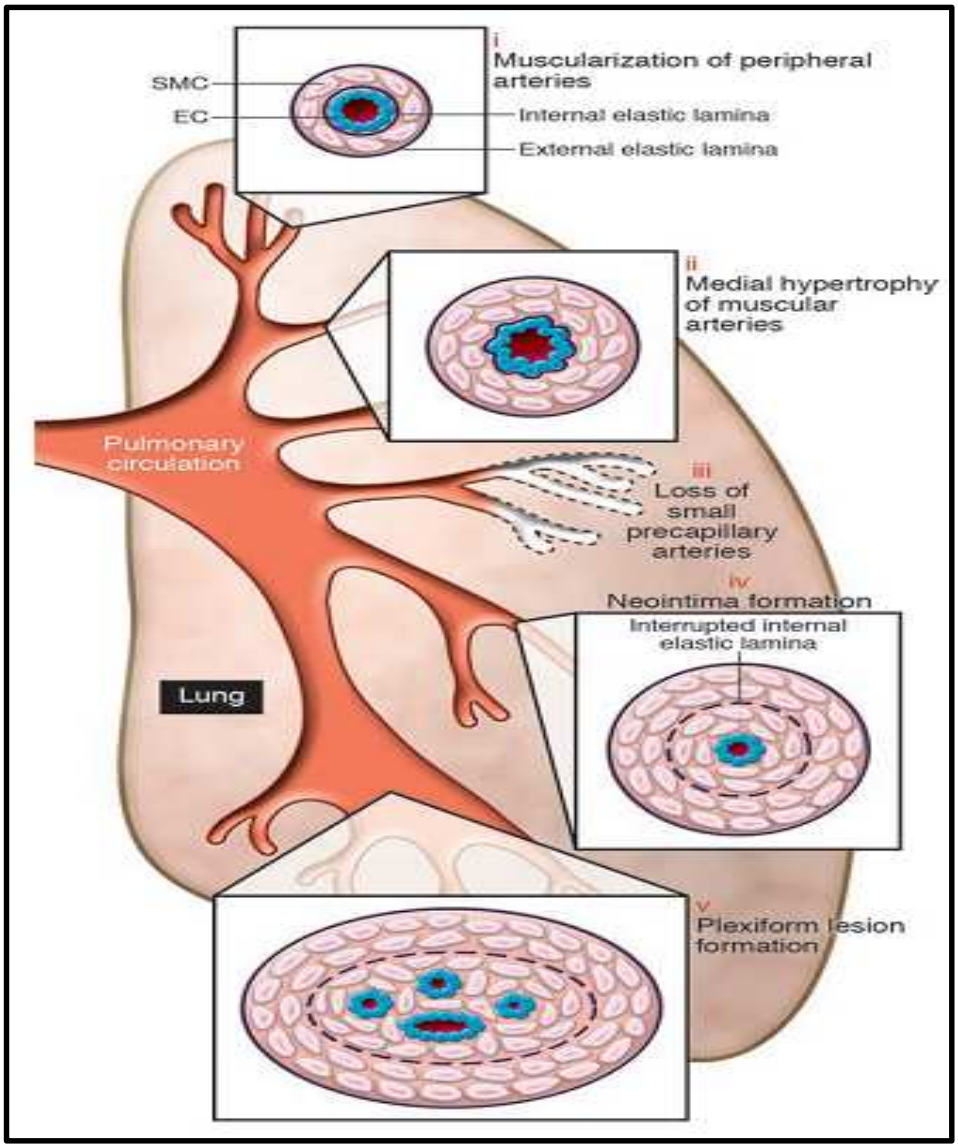

Figure 2.11: Pathogenesis of PAH. This schematic depicts the abnormalities throughout the pulmonary circulation, including (1) abnormal muscularization of distal precapillary arteries, (2) medial hypertrophy (thickening) of large pulmonary muscular arteries, (3) loss of precapillary arteries, (4) neointimal formation that is particularly occlusive in vessels 100–500 µM, and (5) formation of plexiform lesions in these vessels.[66]

2.2.3 Medial arterial calcification (MAC)

MAC is the mineral deposition in arteries which may exist with or without atherosclerosis and has different pathological initiation when compared to atherosclerotic arterial disease. Chronic deposition of bone-like hydroxyapatite into the elastic layers of arteries, alters the mechanical properties leading to higher blood pressure, poor circulation and eventual amputation.[70] The deposition of calcium in soft tissues can be four major variants: atherosclerotic calciphylaxis (discussed earlier), cardiac valve calcification, vascular calciphylaxis, and medial arterial calcification. This dissertation will deal majorly with medial arterial calcification (MAC).

MAC, also known as Monckeberg's sclerosis is a pathological ossification of the medial part of arteries (Figure 2.12).

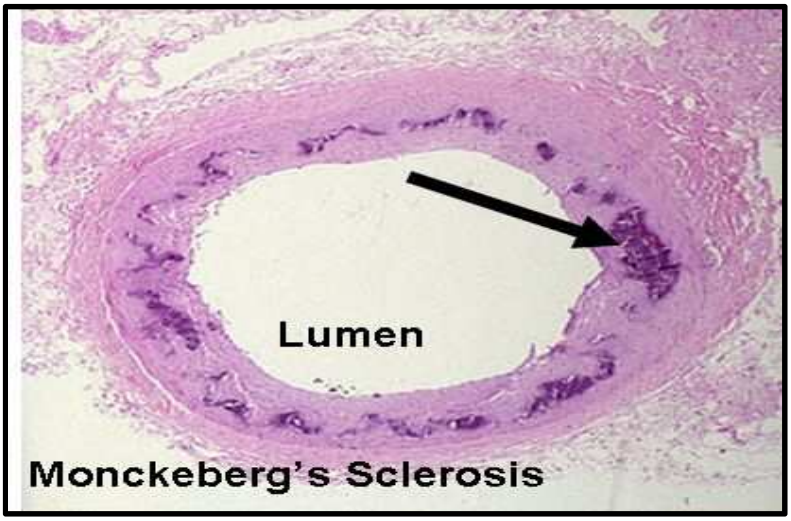

Figure 2.12:H&E of a patient with MAC. The arrow depicts calcium deposits within the media of a peripheral artery.[71]

MAC is highly characteristic of diabetes and chronic kidney disease (CKD) and is associated with significant morbidity and mortality.[72,73] The molecular finger printing and phenotypic traits of MAC in diabetic and CKD patients are strikingly similar.[70] Both CKD and diabetes have now been identified as pro-inflammatory conditions. Initially thought to be benign, MAC has now been recognized as a severe pathology causing morbidity and mortality in patients. Initially thought to be a passive deposition of calcium phosphate on the arteries, MAC has now shown to be active biological process. Calcification of arteries in diabetes and CKD is a series of well-orchestrated processes which are tightly regulated involving molecular reprogramming, structural and functional changes in arterial cells and matrix.[74,75] Additionally, the mineral deposition in arteries is not just amorphous calcium phosphate, but is complex hydroxyapatite. Although the exact pathological mechanistic links between diabetes and MAC are not clearly understood, the mineralization highly resembles calvarial (skull) bone formation and odontogenesis (teeth formation).[76] Both MAC and bone formation share similar features such as 1) no cartilaginous precursor required, 2) bone morphogenetic protein-2 – homeobox protein Msx-2 (BMP-2-Msx2) drives the process of osteogenesis and mineralization.[77] Up-regulation of Msx2 and Msx1 in diabetic aorta have been shown earlier.[74] Although diabetic patients are prone to both MAC and degenerative atherosclerotic calcification,[70] MAC is a significant predictor of lower limb amputation and cardiovascular mortality in patients with Type II diabetes[78] (Figure 2.13).

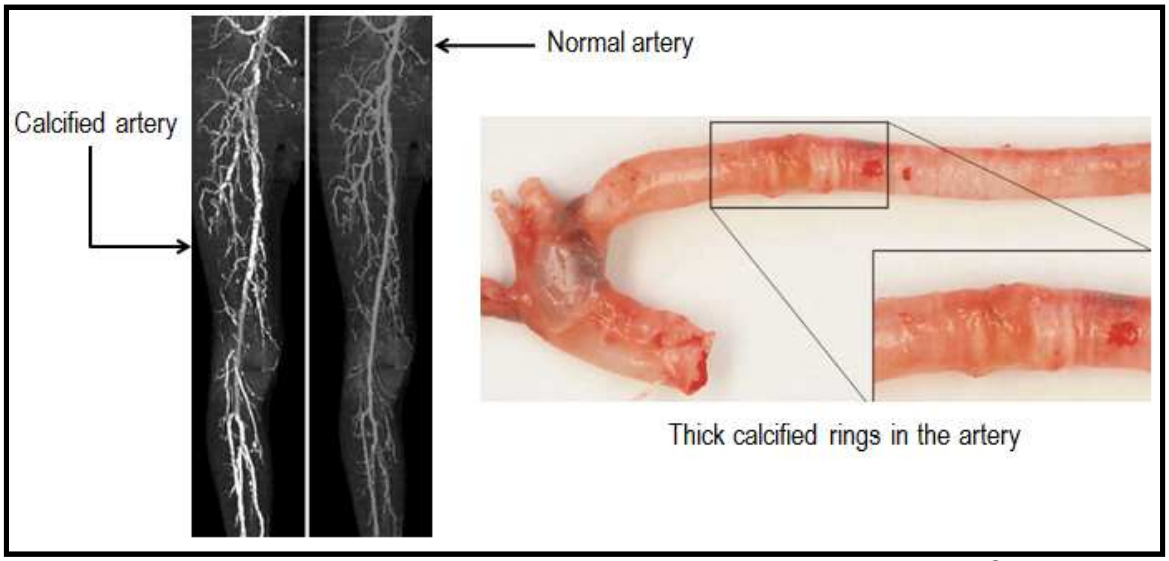

Figure 2.13: Normal arteries seen do not block x-rays whereas calcified arteries display the railroad pattern of calcific deposits, visualized as white thick calcified rings upon gross examination.[79,80]

2.2.3.1 Pathobiology of vascular calcification

Hydroxyapatite present in the vessels is very similar to that seen in bone, which instigated researchers to compare the molecular mechanisms leading to calcification in bone and arteries. There is now considerable evidence that arterial calcification is an active, cell controlled event wherein proteins control the initiation, progression and inhibition of calcification. Calcification in the arteries occurs mainly due to an inflammatory stimulus which is more pronounced in the presence of lipoproteins. However in diabetes and CKD, the native cells of the arteries like smooth muscle cells, and fibroblasts also participate in the process of calcification. Additionally tissue macrophages release a potent growth factor called tissue necrosis factor –α (TNF-α)[81] which turn smooth muscle cells into osteoblastic cells releasing the bone proteins like alkaline phosphatase (ALP), osteopontin (OPN), osteoprotegrin (OPG), and bone sialoprotein (BSP), very similar to what is seen in bone.[82] In medial calcification, the

cellular source of calcification is almost exclusively smooth muscle cells. In fact, the lesions of patients with MAC have stained positive for α-SMA and SM-22 (both of which are proteins expressed by smooth muscle cells).[83] In addition, these cells also express bone proteins like collagen type I, II, osteonectin, alkaline phosphatase, bone sialoprotein, bone morphogenetic protein (BMP)-2, indicating that SMC can also produce bone proteins.[83] In particular, a specific subpopulation of SMC responsible for exhibiting bone-cell-like characteristics in in-vitro cell culture studies have been nicknamed "calcifying vascular cells".[84] The most commonly identified proteins in the arteries of diabetic and CKD patients will be discussed below.

Bone morphogenetic protein-2 (BMP-2)/TGF-β

BMPs are a group of growth factors belonging to the same family sharing homology with transforming growth factor (TGF-β). All these proteins belong to the TGF-β super family of proteins.[85] There are seven different types of BMPs, however only BMP-2,-4 have shown to play an important role in osteogenesis and the downstream process for ossification. In fact recently, it has been suggested that only BMP-2 may be sufficient for the process of calcification. TGF-β also has shown to play an important role in calcification of smooth muscle cells. Watson et al. have shown that under the influence of TGF-β1 and 25-hydroxycholestserol, vascular smooth muscle cells turn into osteoblasts producing bone proteins and eventually depositing intense calcifying nodules in culture.[86] In particular, TGF-β1 has been observed in association with vascular calcification and smooth muscle cell trans-differentiation.[86,87] TGF-β1 is also up-regulated in elastin specific calcification.[88] It is known that TGF-β is sequestered by a

matrix-associated protein called Latent TGF-β Binding Protein (LTBP) on elastin fibers.[89] A pro-inflammatory environment, abundant with proteolytic enzymes, releases MMPs which cleave LTBPs thereby releasing active TGF-β1, which is not free to react with cells causing several downstream effects. Chapter 3 provides some experimental evidence of such downstream effects caused by TGF-β1 in vascular smooth muscle cells.

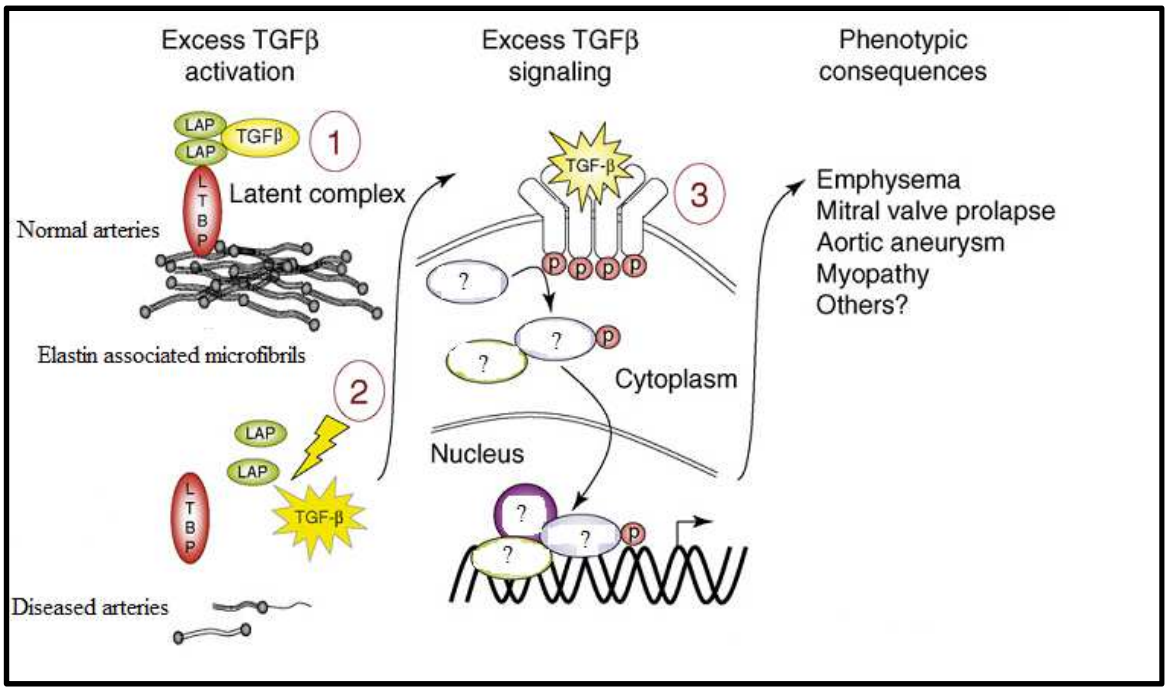

Figure 2.14: Schematic of regulation of TGF-β in normal and diseased arteries. (1)Extracellular matrix microfibrils bind latent TGF-β, latency associated peptide (LAP), LTBP. (2) MMP mediated degradation releases TGF-β in the environment thereby activating it. (3) Free TGF-β binds to its celluar receptor causing several downstream effects leading to phenotypic changes such as osteogenesis, aneurysm, and mitral valve prolapse. (adapted from Ramirez and Dietz[90])

Runt related transcription factor-2 (RUNX-2)

RUNX-2 also known as core binding factor alpha -1 (CBFA-1) is a key transcription factor associated with osteoblastic differentiation. RUNX-2 -/- mice exhibit complete lack of osteoblasts and die soon after birth.[91] RUNX-2 also plays an important

role in expression of different bone markers genes needed for terminal differentiation and maintenance of osteoblasts.[92] Jono et al. showed that human aortic smooth muscle cells respond to externally added phosphate concentrations in a dose dependent manner increasing RUNX-2 and mineral deposition.[93] We have previously shown in a series of cell culture and animal experiments that RUNX-2 is strongly up-regulated in the process of elastin calcification. When pure elastin is implanted sub-dermally in the back of rats, they undergo severe calcification and exhibit typical bone proteins including RUNX-2.[88]

Alkaline phosphatase (ALP)

ALP is an important component of matrix vesicles in increasing the orthophosphates required for the growth of the hydroxyapatite crystal. Hypophosphatasia is a disease characterized by the lack of ALP causes severe malformation in bone.[94] ALP has been implicated in the process of vascular mineralization. Lomashvili and group demonstrated that strips of normal aorta when cultured in vitro in the presence of ALP, calcified to form rings of hydroxyapatite similar to those seen in diabetic patients. In addition, they also showed that normal healthy aorta produced inhibitors of calcification which were destroyed by ALP.[95]

Osteocalcin (OCN)

OCN is also known as bone gla protein contains 3 gla residues and is the most commonly found non-collagenous bond extracellular matrix protein. OCN is almost exclusively produced by osteoblasts and thus may serve as a useful marker for identifying calcifying vascular cells. OCN-/- mice have increased bone density with normal

resorption in female mice. However, ovariectomized 6-month-old animals, the mineral content (mineral:matrix ratio) in the wild-type cortices increased from periosteum to endosteum, whereas, in the knockout animals' bones, the mineral:matrix ratio was constant. Ovariectomized knockout cortices had lower carbonate:phosphate ratios than wild-type, and crystallite size and perfection resembled that in wild-type trabeculae, and did not increase from periosteum to endosteum. These data provide evidence that osteocalcin is required to stimulate bone mineral maturation.[96]

Osteopontin (OPN)

As per Vattikuti and Towler, diabetic MAC is initiated by the migratory adventitial myofibroblasts population that respond to the osteopontin (OPN) production by smooth muscle cells in diabetic conditions (Figure 2.15). Increased OPN production in diabetic patients is a consistent observation[83,97,98] and surgical resection of adventitia has shown prevention of MAC in rat model.[99]

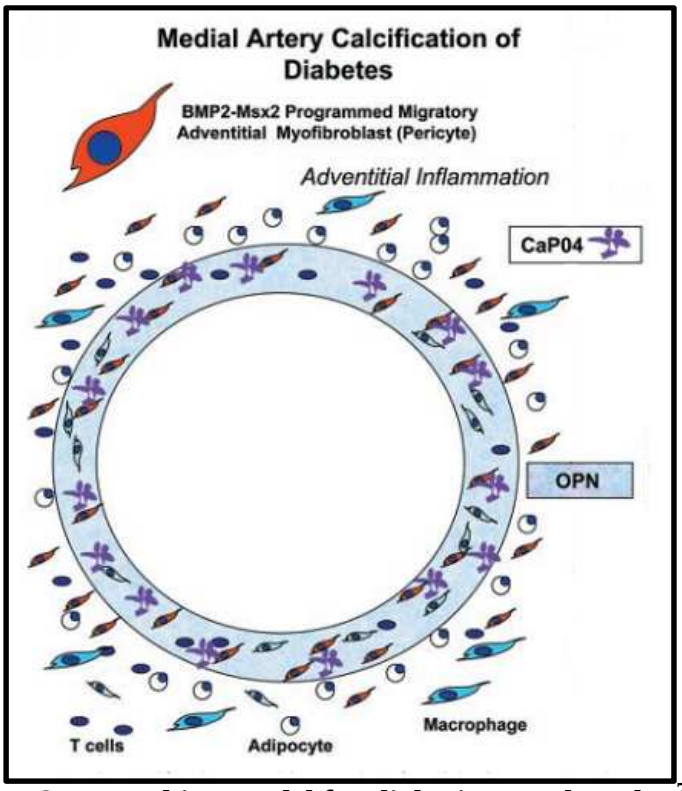

Figure 2.15:Working model for diabetic vasculopathy.[77]

2.2.3.2 Role of hyperglycemia in MAC

Hyperglycemia (high glucose concentrations) is the hallmark of diabetes, which in itself is benign, however, over long periods of circulation causes irreversible and devastating damage to almost every tissue in the body. There are four different mechanisms proposed to be working either independently or in tandem towards the pathology of diabetes: [100]

1) Increased flux through polyol pathway

2) Intracellular production of advanced glycation end products (AGE)

3) PKC activation

4) Increased hexosamine pathway activity

Although all the four pathways will be discussed, the main focus of this dissertation is the PKC activation and its implications in the pathobiology of diabetes.

Aldose reductase is an enzyme that normally reduces toxic aldehydes in the cells to inactive alcohols, however under hyperglycemic conditions, aldose reductase converts glucose to sorbitol, which later is oxidized to fructose. In the process, an essential cofactor NADPH is consumed, which is also critical for maintenance of intracellular oxidative stress. It has been shown that diabetic dogs treated with aldose reductase inhibitor for 5 years prevented diabetes-induced defect in nerve conduction[101] indicating the significance of aldose reductase and sorbitol in the complication of diabetes.

AGEs are proteins or lipids that get glycated after being exposed to sugars. Over time, as glucose circulates in the blood, it glycates the blood proteins (mainly albumin) causing the formation of AGEs. AGE interacts with its receptor (RAGE) causing a variety of microvascular complications. Generally, AGE crosslinks molecules in the vascular matrix permanently altering cellular structure, and interacting with RAGEs on cell surface altering the cellular functions.[102]

As glucose is metabolized by cells, diacyl glycerol (DAG) concentrations increase, which is an important cofactor for several protein kinases (PKC) like – β, δ and

α.[103,104] When intercellular hyperglycemia is increased, the cellular PKC concentrations increase which then activates several pathways leading to pathological consequences.

2.2.3.3 Treatment options

Currently there is ***no cure*** for MAC. However, treatment options for reversal of calcification are being extensively investigated by researchers. The mineral deposited in the arteries are crystals of hydroxyapatite which is a highly insoluble material.[105] Treatment for MAC entails removal of hydroxyapatite from arteries which is a great challenge. The first mode of action towards treatment is overall change in lifestyle like change in diet, elimination of smoking, exercise and such. Since reversal of calcification is faced with great challenges, most therapeutic options target prevention of progression of calcification instead. Discussed below are some strategies towards calcification therapy:

Chelation and demineralization therapy

Chelation therapy refers to the permanent removal of calcium phosphate crystals using chemicals with a very strong affinity for calcium. Most commonly, ethylenediamine tetraacetic acid (EDTA) combined with vitamins, trace elements and an iron supplement is injected intravenously repeatedly throughout the course of treatment.[106] Chelation therapy has shown to be effective in the reversal of atherosclerotic occlusive disease, and peripheral arterial disease (MAC).[107,108] It has been argued as a potentially valuable alternative in severe cases of MAC requiring amputation. Chelation therapy was initially used as a treatment for lead poisoning and a chance observation was

made where patients undergoing chelation therapy reported relief against angina pectoris.[109] Ever since its chance discovery, EDTA chelation therapy has been under scrutiny as a use for anti-calcification therapy for MAC. However, the debate remains if the benefits of chelation therapy outweigh its potentially severe side effects. A systematic review was conducted in 2000 that summarized all clinical evidence for or against the effectiveness of chelation therapy, which concluded that chelation therapy should be considered obsolete due to complete lack of evidence for efficacy and its adverse side effects.[110]

Vitamin K

Matrix gla protein (MGP) is a calcium binding protein that has glutamate residues which are carboxylated post translation. This process is vitamin K dependent process. Many of MGP's protective roles are unknown; however, it appears that many of its vital functions are dependent on the γ-carboxylation which is a vitamin K dependent process. Thus vitamin K, which can increase γ-carboxylation might be effective in preventing progression of calcification. Reversal of warfarin induced MAC has been observed when rats were fed Vitamin K making this an important therapeutic strategy.[111]

Statins

Statins (hydroxymethylglutaryl coenzyme A (HMG-CoA) reductase inhibitors) are a class of compounds, known to lower lipids by inhibiting the activity of HMG-CoA, which is a key enzyme in cholesterol anabolism in the liver.[112] Statins also exhibit pleiotropic effects on vascular vessel walls that increase release of protective factors like

eNOS and decrease pathological factors like MMP expression, interleukins production platelet activity and oxidative stresses.[112] Crisby et al. studied the effects of Pravastatin 24 patients with carotid artery stenosis. They found that Pravastatin significantly reduces lipid content in the plaque area (16% decrease), decreases oxidized LDL immunoreactivity (7% decrease), reduces MMP-2 and increases TIMP-1 immunoreactivity.[113] Thus, the benefits of statins on vascular health are established. Although the protective effects of statins on progressive coronary calcification in atherosclerosis has been demonstrated, statins have shown to be ineffective in diabetic and CKD patients with MAC.[114] Since statins are believed to lower inflammatory cytokines mediated by lipoprotein infiltration, it is possible that the pathology of medial calcification which is primarily due to infiltration of macrophages independent of lipid deposition is the reason for the ineffectiveness of statins in reducing calcification. Apparently, calcification progresses most rapidly when the volumetric calcification scores are low,[115] therefore the best option for calcification treatment in terms of regression or retarding progression with statins is during the early stages of the disease.

Estrogen

A strong association between gender and vascular calcification has been observed. Especially post-menopausal women exhibit greater tendencies for vascular calcification and osteoporotic disease. It has been shown that both men and women with post-menopausal arterial calcification have lower serum estradiol levels with gender controls.[116] Additionally, women on hormone replacement therapy have reported lower coronary artery calcium levels.[117] However, the cardio-protective effects of hormone

therapy is now under question. Participants in the HERS (heart and estrogen/progestin replacement study) who were post-menopausal with coronary artery disease were treated with estrogen and medroxyprogesterone. 4.1 years later, there was no difference in the cardiovascular outcomes of patients treated with our without estrogen.[118] On the contrary, estrogen treated groups had more events in the first year, but fewer in years 4 and 5.

Calcium channel blockers

Calcium channel antagonists can be proved effective in reducing arterial calcium deposition. Calcium channel blockers (CCB) have been studied extensively ever since the pioneering work of Fleckenstein in demonstrating its anti-atherosclerotic effects.[119] CCBs like Amlodipine, Aranidipine, Clevidipine, Felodipine, Nifedipine, etc, have been tested for the same. CCBs could prevent calcium overload in cells during atherogenesis in a rabbit experimental model.[120] However, the effect CCBs have on human arteries is unknown. One long term morbidity and mortality clinical trial done with amlodipine showed no benefit in the progression of arterial atherosclerotic lesions, however arterial calcification was not examined.[121]

2.2.3.4 Animal models

Animal models mimic human pathology and serve as a good platform to (1) study successive stages of the pathology providing insight about the mechanism and molecular pathways underlying the pathology (2) to test new therapeutics on target pathologies. Small animals like rodents serve as valid species for studying vascular diseases as they are easy to manipulate, relatively cost-effective, have a short lifespan of about 2 years,

resemble human physiology and metabolism, contain the same number of genes as the human genome which are also highly conserved throughout mammalian species.[122] There are several rodent models for vascular calcification that mimics calcification with or without the co-existence of atherosclerosis; however this literature review will deal only with non-atherosclerotic arterial calcification, a characteristic of medial arterial calcification.

A. Warfarin + vitamin D model

Administering warfarin to rats leads to increased levels of calcification throughout the vasculature.[123,124] Cerebral arteries, veins, and capillaries are not affected by this model.[123] It is believed that warfarin interferes with the γ-carboxylation of the matrix gla protein (MGP) causing the excessive calcification in major arteries. MGP has an important role in preventing arterial calcification. Because of the presence of gamma-carboxyglutamic acid (gla) residues, it is thought to bind to hydroxyapatite, creating a protein layer that inhibits further mineralization.[123] It has been shown that the N-terminus of MGP (with its 5 gla residues) is essential for MGP to bind to BMP-2.[125] Thus, MGP that is produced in the presence of warfarin is ineffective because of the lack of these vitamin K-dependent modifications. Recently it has also been shown in juvenile rats that vitamin D added to warfarin is highly synergistic to arterial calcification.[126]

B. Vitamin D3 and nicotine (VDN)

Upon delivering vitamin D3 and nicotine to young rats, a 20-35 –fold increase was recorded in the calcium content of the aorta. This increase in calcification was also

accompanied by subsequent stiffness in the aortic wall and systolic hypertension.[127] Vitamin D has shown to increase alkaline phosphatase production while suppressing expression of parathyroid hormone related peptide (PTHrp).[128,129] In cell culture studies, an inverse relationship between PTHrP and calcification has been demonstrated.[128] Calcium deposition by the VDN model occurs preferentially on the internal elastic lamina and other fibers leading destruction of elastin fibers of the artery. This clinical relevance of this model lies in that there is a decrease in elastin-specific amino acids desmosine and isodesmosine causing high concentration of these peptides in circulation.[130] There is also a strong negative correlation between the quantity of elastin-specific peptides and calcium content, clearly suggesting that VDN treatment cause calcification and loss of arterial compliance due to elastin degradation.

C. Genetically altered mice models

Several knock-out mice models of genes regulating bone formation have been used for understanding the pathogenesis of arterial calcification. MGP-/- mice have shown extensive calcification of the aorta, its branches, muscular arteries, elastic arteries, and coronary arteries.[131] MGP-/- mice do not survive past 2 months and die of vascular rupture essentially due to calcified and severely brittle aorta. There are several other genetic models for aortic calcification including osteoprotegrin-/-,[132] smad6-/-,[133] carbonic acid anhydrase isosyme-/-,[134] fibrillin-1-/-,[135] klotho-/-,[136] ApoE-/-,[137] and LDLr-/-,[138] the discussion of which is beyond the scope of this dissertation.

D. Animal models of local calcification

All the above models for calcification induce systemic calcification throughout the vascular tree. In addition, these models also cause calcification in the general organs. For studying effects of drugs locally, local and site specific models of calcification can be extremely valuable. To this end, there are two main models for studying calcification: (1) subdermal rat model (2) calcium chloride injury model. The subdermal model involves subdermal implantation of soft tissue (on which calcification needs to be evaluated) into the back of juvenile rats. The implanted elastin undergoes calcification without any other added factors. When pure elastin, for instance, is implanted sub-dermally, the calcification observed histologically is identical to that visualized in calcified arteries.[88] Similarly, Paule et al. have shown that when glutaraldehyde cross-linked prosthetic heart valves when implanted subdermally into juvenile rats develop severe calcification on both collagen and elastin fibers.[139] Calcium chloride injury model on the other hand is a circulatory model of vascular calcification. In this model, adult rat aorta is exposed and a localized portion of the aorta is perivascularly treated with calcium chloride. This acute insult to the artery induces an accelerated and extensive calcification accompanied by intense inflammation and severe elastin degradation.[140]

2.2.4 Abdominal aortic aneurysms

Abdominal aortic aneurysm (AAA) is a local dilatation of the aorta with respect to the original arterial size or the adjacent area of the artery (Figure 2.16). As a convention, arterial diameter greater than 1.5 times the normal size or greater than 3 cm in diameter, is considered aneurysmal, although the definition may vary somewhat by age

and body surface area.[1] AAA is a pathological condition characterized by structural weakening, wall thinning, arterial remodeling, luminal expansion, intra-luminal thrombus and trans-mural inflammation. Aneurysms can be classified based on the location they are found like cranial aneurysms, thoracic aortic aneurysms, thoraco-abdominal aneurysms, abdominal aortic aneurysms, peripheral artery aneurysms (popliteal artery aneurysm), visceral aneurysm (hepatic, spleen). Although they have different etiology, risk factors and clinical presentations, local dilatation in the vessel wall remains a common feature. Abdominal aortic aneurysm (AAA) will be the primary focus of this literature review.

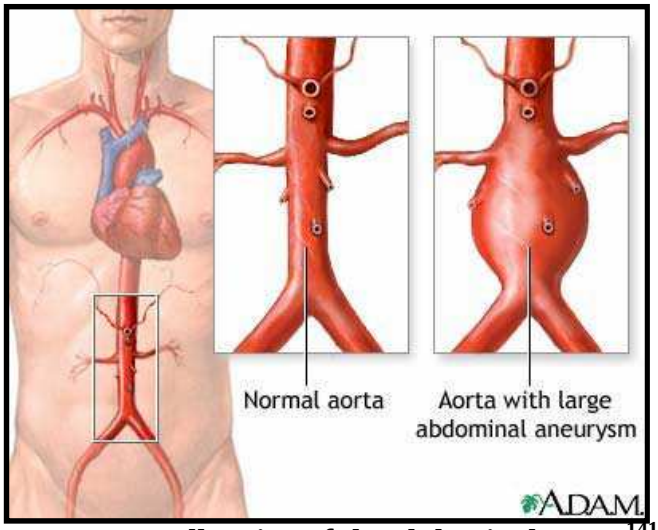

Figure 2.16:Ballooning of the abdominal aorta [141]

Based on the shape (Figure 2.17), AAA can be fusiform (the weakened portion is a near symmetric bulge), saccular (the weakened portion is an asymmetrical blister-like bulge) or pseudo-aneurysm (false aneurysm which develops only around the arterial wall).

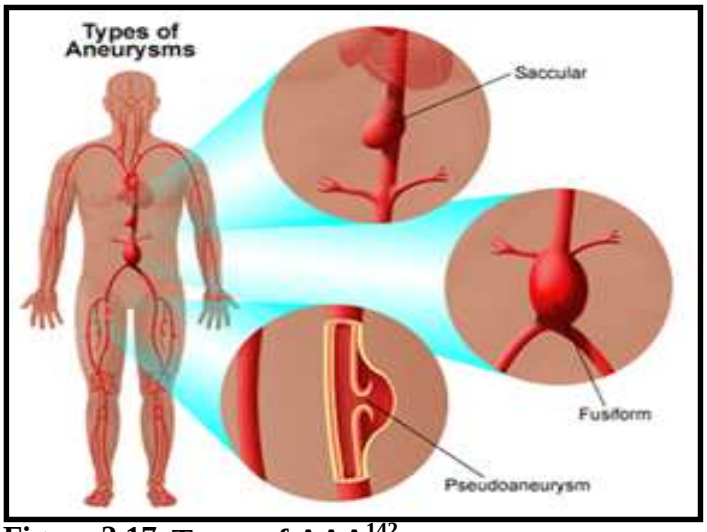

Figure 2.17: Types of AAA[142]

A. Epidemiology

AAA is 10 fold more commonly present in men than in women in an age range of 65-75 years.[143] Arterial occlusive diseases, however, almost has a similar male: female ratio. The incidence of AAA reported has increased in the last couple of decades due to increased smoking, poor life-style, ageing of population and improvements in diagnostic and screening techniques.

A. Risk factors

Age: the prevalence of acquired AAA under the age of 60 is almost insignificant. Screening studies by ultra-sonography have shown 8.8% prevalence of AAA in people over 60 years of age; 88% of these were 3.5 cm or less.[144]

Smoking: Cigarette smoking is shown to be the biggest environmental risk factor for AAA.[145] The smoking and AAA association is four times higher in smokers than in non-smokers. Also there is direct positive correlation between AAA development and the number of smoking years, which decreases significantly after quitting smoking.[146]

Race and gender: AAA development has an evident race and gender bias with Caucasian men having twice as much as propensity of developing AAA, although the trend is reversed in atherosclerosis.[147] Occurrence of AAA is four times greater in men than in women.[148]

Hypertension: According to the AHA, there is not significant relationship between hypertension and AAA prevalence[149], however, the prevalence of aneurysms were higher in patients treated for hypertension. The exact association between the two is yet to be determined. Most probable reason for increased aneurysms may be due to the increased stress on arteries in hypertension.

A. Clinical manifestations

Un-ruptured AAAs

AAAs are usually asymptomatic until rupture and early aneurysms are mostly detected accidently during an extensive vascular examination. AAAs develop at an exceedingly slow but steady rate of 1 cm/year, displaying very few symptoms, thereby making detection impossible.[150] Once detected, the patients are monitored once every six months for the increase in the arterial diameter. Medical intervention becomes necessary when the arterial diameter is more than 5.5 cm or if the rate of progression is more than 1 cm/year (Figure 2.18). Sometimes, AAAs are discovered in patients as a result of distal thrombotic/athero embolism. This is called disseminated intravascular coagulation (DIC), i.e., that is embolism due to dissociations of plaque or thrombus.

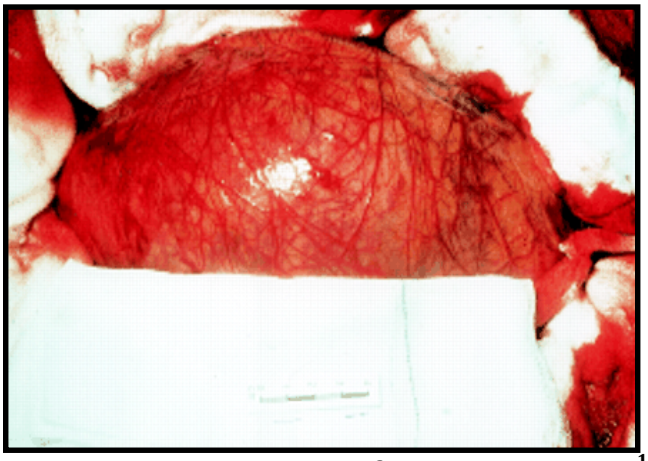

Figure 2.18:A large AAA before surgical repair[151]

Aboulafia and Aboulafia conducted a study of 67 patients of which only 2 patients had DIC.[152] In both instances, the coagulation was resolved post-surgery. The only symptom of an un-ruptured AAA is chronic lower back and abdomen pain, which can often be ignored by the patient. The pain occurs mainly due to direct pressure on adjacent tissues and its distention. Physical examination may also reveal a pulsatile and expansive mass right above the iliac bifurcation.

Ruptured AAAs

Figure 2.19:AAA rupture into the retro-peritonial space.[153]

When left undiagnosed, the rupture of an AAA is indicated by the onset of an excruciating pain in mid/lower abdomen and presence of palpation in abdominal mass. Rupture can be of 2 types: antero-lateral rupture, which almost always leads to exsanguinations and death, whereas, retroperitoneal rupture (Figure 2.19), which is more contained and the wall break is temporary sealed till surgical intervention.[154]

B. Classical features and pathobiology of AAA

The gross characterization of abdominal aortic aneurysms include locally dilated aorta, atheromatous plaque deposition and mural thrombosis, whereas typical histological characterization include trans-mural inflammation, increased pro-inflammatory and immune markers, extensive local proteolytic activity, apoptosis, local oxidative-stresses and neovascularization. In addition, genetic predisposition and certain infection can increase the propensity of AAA development and progression. Figure 2.20 gives a brief description of the events in AAA pathology. To date, the exact etiology of AAA is unknown and AAA has been established as a local disease with the interplay of multiple factors as discussed below.

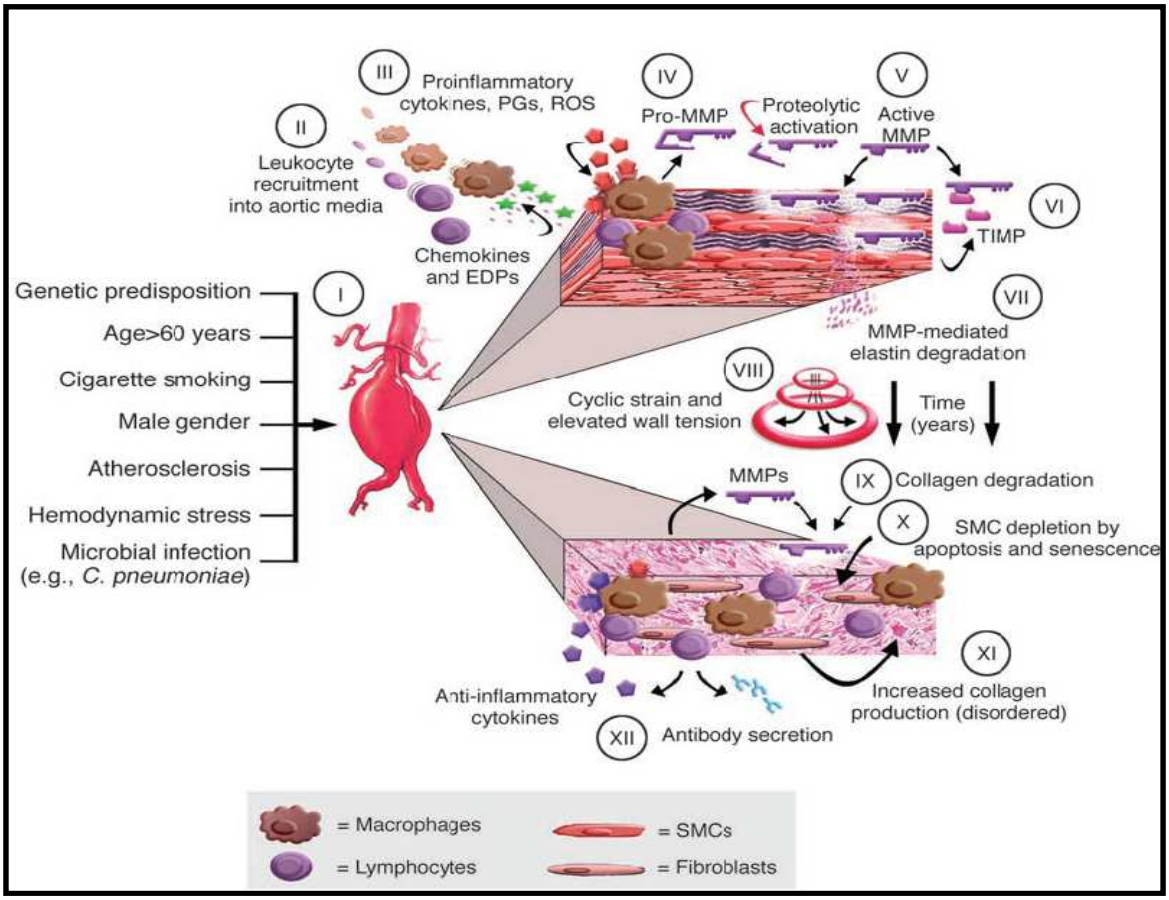

Figure 2.20: Schematic describing the events in AAA pathology. Known risk factors (I), leads to recruitment of leukocytes into the aortic media (II), macrophage activation, and production of proinflammatory molecules (III). Macrophages also produce proenzyme forms of MMPs (pro-MMPs) (IV), which are activated in the extracellular space (V). TIMPs may neutralize MMP activity (VI), but this appears insufficient to prevent degradation of structural matrix proteins(VII). Over a period of years, elastin degradation, cyclic strain, and elevated wall tension bring about progressive aortic dilatation (VIII). Collagen degradation further weakens the aortic wall (IX); apoptosis and cellular senescence cause SMC depletion (X), and interstitial collagen appears disorganized (XI). Aneurysm tissues exhibit infiltration by T cells, B lymphocytes, plasma cells and local deposition of immunoglobulins, reflecting a cellular and humoral immune response (XII).EDPs, elastin degradation peptides; MPh, macrophages; PGs, prostaglandins; ROS, reactive oxygen species.[155]

C. Matrix changes and luminal expansion: Role of matrix degrading proteinases

Proteinases or proteases, as the name suggests, are a class of enzymes that degrade a whole array of proteins. Proteases are classified into six major divisions based on the peptides they cleave. This includes serine proteases, cysteine proteases, aspartate proteases, threonine proteases, glutamic acid proteases and matrix metalloproteases. Abdominal aortic aneurysms are associated with a significant loss of matrix protein integrity (Figure 2.21) and tissue remodeling which alters the native mechanics of the artery, exposing it to increasing hemodynamic load and abnormal wall stresses.

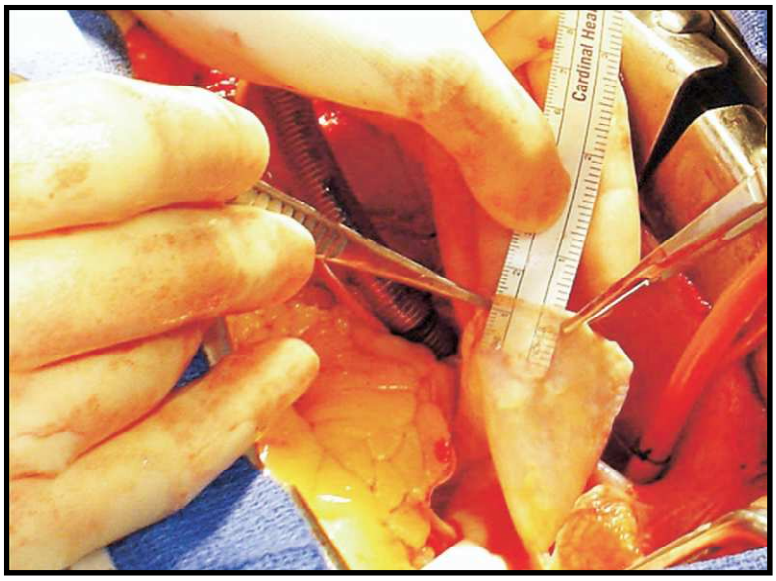

Figure 2.21: An aneurysmal wall so thin that a ruler can be read through the wall [156]

D. Matrix metalloproteinases (MMP)- MMP-1,2,9,12

Of particular interest are the class of Matrix Metalloproteases (MMPs) that are known to degrade insoluble matrix proteins like collagen and elastin. Although elastin is an insoluble protein resistant to most proteases, certain MMPs and elastases are potent in degrading elastin fibers. Until date about 20 different MMPs have been identified each one of them acting on one or more different types of matrix proteins. MMP-1 was the first identified MMPs isolated from fibroblasts. Welgus and colleagues were one of the first groups to identify the specificity of MMP-1 (collagenase) isolated from human skin fibroblasts on the degradation of collagen type1.[157] Their findings indicated that approximately 25 molecules of collagen are degraded per molecule of MMP-1. Only 10% of the collagen molecules are accessible for initial degradation, exclusively within their triple helix domains, the remainder 90% become prone to degradation only after the initial catalytic degradation. MMP-1 is physiologically found in fibroblasts, dermal cells, keratinocytes and inflammatory cells, which mark its involvement in cell proliferation, wound repair, and matrix remodeling. However, excessive localization of MMP-1 in the arterial tissues can prove damaging. Irazarry et al. demonstrated the localization of MMP-1 in the adventitia of eight AAA patients' aorta, which was almost undetectable in normal infra-renal aorta.[158]

MMP-2 (a 72-kDa protein) and MMP-9 (a 95-kDa protein), commonly known as gelatinases, exhibit specificity for collagen type IV. In the recent years both MMP-2 and MMP-9 have shown to be associated with the lysis of intact elastin fibers. Senior et al. showed that both MMP-2 and MMP-9 have a high ability to degrade Kappa-elastin in an

in-vitro system. MMP-9 especially has a 30% higher elastin degradation activity compared to human leukocyte elastase.[159] Both these gelatinases have been shown to degrade type IV collagen which is found in the basement membrane, in addition to elastin degradation. MMP-9 has been identified in abundance in human aneurysmal adventitia. Thompson et al. indicated almost eight-fold increase in the activity of MMP-9 in aneurysmal tissue compared to healthy tissues.[160] Furthermore, they indicated an eight-fold greater activity of the natural inhibitors of MMP-9, tissue inhibitors of matrix metalloproteinase-1 (TIMP-1), in the diseased tissue. This indicates the physiological homeostatic response to elevated MMP-9 levels; however, their successful interaction at the particular site is questionable. Pyo et al. used MMP-$9^{-/-}$ mice to investigate the role of MMP-9 in AAA formation.[161] They observed that MMP-9 gene knock out suppresses AAA formation despite the presence of macrophage infiltrate. This study led researchers to believe that a single MMP-9 gene is sufficient to cause the disease, at least in the mouse model. Longo et al. showed in their experiments that neither MMP-$9^{-/-}$ nor MMP-$2^{-/-}$ mice develop aneurysms, whereas wild type mice do.[162] This indicated to the fact that MMP-2 and MMP-9 work in concert and have complementary role in the pathogenesis of AAA. However, this understanding was recently challenged by Xiong et al.[163] They harvested macrophages from MMP-$9^{-/-}$ and MMP-$2_{-/-}$ mice and demonstrated that those macrophages degraded similar quantities of elastin in vitro as the wild-type macrophages. Thus, it appears from their studies that MMP-9 and MMP-2 may be indirectly influencing disease development. Some researchers believe that the frequency of rupture is directly related to proteolytic activity in the tissue. Freestone and colleagues indicated that small

aneurysms (4-5cm) had higher MMP-2 activity whereas larger aneurysms (>5cm) mainly consisted of MMP-9.[164] Although MMP activity is seen in aneurysms, which cells secrete these enzymes is still investigated. One of the sources may be polymorphonuclear leukocytes (PMNs). AAA is almost always associated with severe atherosclerosis and thrombosis in humans. The blood continues to flow through the mural thrombus. Fontaine et al showed the presence of PMNs at the luminal end of the thrombus along with a strong activity of MMP-9. This suggests that degranulation of these PMNs can potentially release MMP-9 around the thrombus.[165] MMP-2 activity is shown to be several fold higher in AAA tissues compared to normal or any other diseased tissue.[166] Smooth muscle cells constitutively produce MMP-2, however this production is elevated during pathological conditions.

Human macrophage elastase, also known as MMP-12, is a 22-kDa proteinase that was first identified in the peritoneal cavity of mice. This work also confirmed the ability of MMP-12 to efficiently degrade insoluble elastin.[167] MMP-12 is usually not evident in normal tissues, however, Curci et al. showed an eight time increased MMP-12 activity in aneurysmal aortas compared to normal arteries. They also showed macrophage co-localization with MMP-12.[168] Overall, MMPs are either secreted by inflammatory cells or native SMCs may take part in ECM degradation in aneurysms.

E. Diagnosis of AAA

Currently there are only a very few imaging techniques that are used to detect and monitor AAAs.

Ultra-sonography is currently the safest, easiest and most economic examination for the diagnosis of AAAs. It can be used as the initial assessment or as the follow-up surveillance. Ultrasound is reported to have a sensitivity of 99.99% for AAA detection with anterior-posterior diameter measurements more reproducible than the transverse diameter.[169] Ultrasound also gives a good definition of AAA associated abnormalities like intra-luminal thrombus, aortic dissections, extent of lesions, etc. Ultrasound definitely is the safest and easiest way of measuring luminal expansion, but this technique has certain limitations. Sonography can become difficult and imprecise with obese patients and with those with abundant bowel gas. It is the preferred mode of detection for initial assessment and monitoring, however once the diameter increases enough for medical intervention, a CT is performed to determine what kind of repair is preferable.

Computed tomography accurately demonstrates the size and extent of AAA and also detects thrombus (crescent sign) effectively. CT can also be used to visualize the retroperitoneum thus allowing the detection of abnormalities and complications like aneurysmal leaks, fibrosis and ureteral obstruction. Ct is the preferred detection method after surgical repair. One drawback of CT includes exposing the patients to ionizing radiation.

Magnetic resonance imaging (MRI) demonstrates features without the need for a contrasting agent. MRI is completely non-invasive.

Angiography is used to evaluate the state of the renal arteries and other smaller, but vital arteries in AAA patients. This method is especially important after an endovascular repair to ensure the optimal positioning of the graft.

2.2.4.1 Current treatment options

Once an aneurysm has been detected (>3 cm luminal diameter), it is monitored once every six months. Arterial diameter more than 5-5.5 cm or a rate of progression more than 1 cm/year often needs surgical intervention. Currently there are two different methods to manage AAAs in patients- an open repair or an endovascular approach.

A. Open repair

Aneurysmectomy is the most standard procedure for AAA treatment. This procedure involves a long midline incision or a wide transverse incision of the abdomen. Once the peritoneum is exposed, the neck of the aneurysm is identified and clamped using surgical hemostats. The weakened aorta is then excluded from circulation and a synthetic mesh is sutured to the normal portion of the aorta (Figure 2.22). The upper anastomosis is always end-to-end type and the distal anastomosis depends of the extent of AAA. The distal end of the graft can be sutured the aortic bifurcation, iliac bifurcations or the femoral arteries. The native diseased aortic wall is then sewn back. A retroperitoneal approach of repair is recommended for certain patients with pulmonary diseases. In this case, the patient is made to lie slightly tilted to the right side and the incision is made from right side of the belly to the supra-umbilicus region. Accessibility

of intraperitoneum and right iliac arteries can pose as a challenge to surgeons in this particular approach.[170]

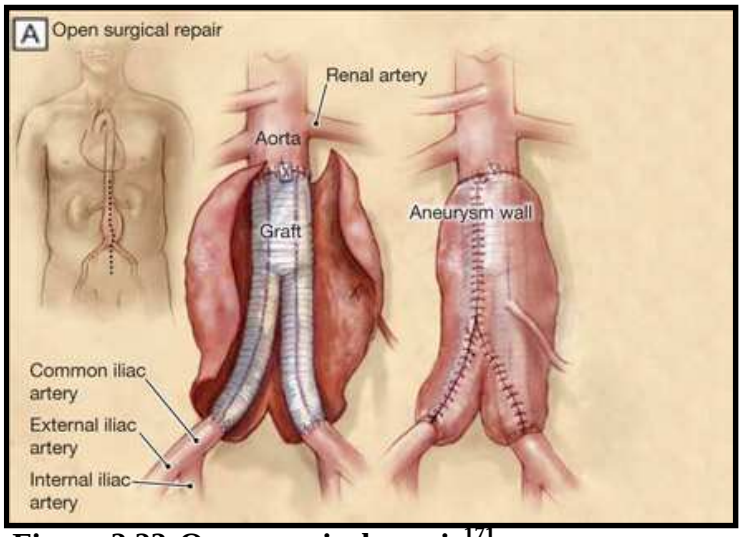

Figure 2.22:Open surgical repair[171]

Since the first open repair performed in 1952, significant advances have been made in pre-operative and post-operative care to reduce mortality rates. The mortality rates for elective open repair as low as 5%.[172] This procedure also has a long term durability and majority of the patients do not experience any noteworthy graft-related complications for the rest of their lives.[173] However, such an invasive procedure may be unfit for a substantial number of aged patients with co-morbidities. In addition, some patients who undergo distal anastomosis in the femoral arteries tend to develop infections. Open surgery may in some cases also cause myocardial infarction, renal failure or coronary artery disease.[174] This procedure also has post-operative recovery rates that take upto 3 months of more. In a very interesting and preliminary study, Coggia and group have described a total laparoscopic procedure for AAA tissue repair.

Laparoscopy evidently is a minimally invasive procedure with reduced pain and surgical trauma, however, a procedure as complex as described requires experience and further assessment.[175]

B. Endovascular repair

In 1991, Parodi et al introduced an endovascular technique for treating abdominal aortic aneurysm wherein a woven polyester or Dacron graft, mounted on a self-expanding stent is deployed within the vessel, at the site of aneurysm.[176] The basic design of a endoluminal stent-graft consist of a tubular synthetic graft that is supported by stents along the entire length. This technique is commonly referred to as endovascular aneurysm repair (EVAR). An interventional radiologist and a vascular surgeon perform the procedure. Two incisions are made in the groin region near both the femoral arteries to allow passage of the guide wire, sheath and crimped stent-graft. Using X-ray the catheter delivers the graft to the site of AAA. On identification of the proper position, the graft is deployed at the site (Figure 2.23). The tip of the catheter has a balloon which is inflated once the right position is located. This inflation, secures the proximal end of the graft to the healthy artery. The ends have anchors/hooks/barbs that facilitate the secure positioning of the stent-graft. Removal of the introducer system restores blood flow through the tubular stent-graft thereby relieving the wall stresses from the weakened aorta. Post-deployment, the aneurysmal sac wraps around the graft.

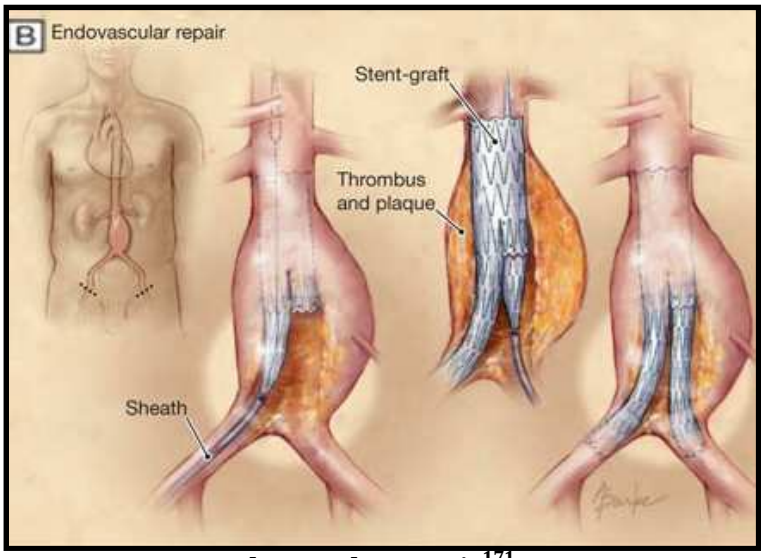

Figure 2.23:Endovascular repair[171]

EVAR may not be practical for all patients. The feasibility mainly depends on anatomical factors of the patient. A proximal neck shorter than 15 mm is widely accepted as a contraindication for EVAR. Diameter, length, angulations, tortuosity, calcification and thrombus in the neck region are the most frequent causes of exclusions from EVAR.[177]

Although EVAR is an attractive option for patients with significant co-morbidities and age, long-term cardiac, pulmonary and graft-related complications can occur in EVARs. Flow of blood into the diseased sac eliminated from circulation, referred to as 'endoleaks', is one of the most common complications of EVAR and occurs in 24% of the patients undergoing EVAR.[178] Post procedural leakage, if left un-attended, can cause fatal ruptures. Endoleaks are broadly categorized into four different types: [174]

Type I: inadequate seal at the proximal or distal ends of the grafts leading to leakage

Type II: blood flow from collateral arteries into the aneurysmal sac

Type III: Leakage from the graft modules due to compromised graft integrity

Type IV: porous graft material

Endotension refers to the progression of AAA and enlargement of arterial wall without any evident endoleaks into the sac.[179] It is a rare but a fatal complication seen in patients with EVAR. The exact reasons for the luminal expansion are unknown, however some evidence has been shown to believe the transmission of pressure into the sac through an attachment defect or through a thrombus, that seals an endoleak.[180]

Device migration is yet another EVAR associated issue that is reported in 4% of the patients.[181] Zarins et al. noted that patients whose length of neck covered by the stent was less than 10mm, had a greater chance of graft migration.[182] They pointed out that the fixation distance from the renal arteries was a predictor for migration. Thus, poor imaging at the time of graft deployment is one of the major causes for migration. Graft migration may be minimized by deployment of the graft right below the renal arteries.

In a study by Jacobs and group, 10% of all the grafts used had incidents of fracture within the first 4 years of implantation.[183] Fracture of stents may lead to type II endoleaks. In the first few years of EVAR, occlusions in the stent-graft limbs led to distal emboli formation. Infection, dissection and angulation are some other complications that may arise in endografts. Patients are generally kept under surveillance if any of these

complications are detected, which is usually followed by a re-intervention or an open surgical repair.

2.2.4.2 Pharmacological strategies for AAA repair

Currently there are no well-defined pharmacological therapies for the treatment of AAA. Once an aneurysm is detected, clinicians wait until surgical intervention is necessary. Therefore, early detection of small aneurysms followed by therapeutics that can inhibit further enlargement or regress already enlarged aneurysms will be a significant advancement in improving patients' lives. In this context three main approaches have been identified: (1) inhibition of further tissue damage and expansion (2) stabilization of the ECM and rendering it resistant to proteolytic damage (3) regression of aneurysmal tissue by regenerating the fundamental ECM proteins

Statins

Several animal as well as clinical studies have attempted to investigate the effect on statins on the progression of abdominal aortic aneurysms. Steinmetz et al. proved the suppression of development of AAA when treated with Simvastatin in wild type as well as $ApoE^{-/-}$ mice perfused with porcine elastase.[184] Subcutaneous delivery of Simvastatin reduced the incidence of AAA formation in wild type mice by 33% and in hyperlipidimic mice by 30%. 21% and 26% reduction in aortic diameter was noted in wild type and hyperlipidimic mice respectively. The statin treated mice also showed preservation of smooth muscle alpha actin in the medial layers. Relative MMP-9 gene expression went down 20 fold in the Simvastatin group compared to the vehicle treated controls, and

TIMP-1 mRNA expression was 9-fold higher in the drug treated group compared to vehicle control. In another study, Wistar rats perfused with porcine elastase, received Simvastatin daily in water and systemic effects of the drug was studied on the AAA development.[185] Arterial diameter was significantly less in Simvastatin group compared to control group (30% reduction) and statin groups reduced the MMP-9 expression by half. A complete gene microarray analysis indicated the down-regulation of genes responsible for inflammation, immune function and ECM remodeling. Organ culture of human infra-renal AAA has also shown around 50% reduction in total MMP-9 activity when treated with Cerivastatin for 48 hours.[186] In a clinical trial consisting of 108 men and 22 women diagnosed with AAA, only 5% of the patients treated with statins died, whereas 16% of the patients given placebo died due to rupture.[187] Evans et al. studied the effect of pre-operative administration of Simvastatin in 21 patients scheduled to undergo open surgical repair and showed a 40% reduction in MMP-9 activity in the excised tissue.[188] Schouten and colleagues also made similar findings where patients undergoing statin therapy had a 1.16 cm/year slower growth than patients without treatment.[189] Despite all these clinical results, in a systematic meta-analysis done by Twine and Williams, 12 human cohort studies with 11,933 patients did not show any significant reduction in 30-day post-treatment mortality rates. No significant difference was noted in the expansion of AAA either.[190] However, the 1, 2, 5 years post-operative survival rates were higher in statin treated patients. Thus, the ACC/AHA guidelines for AAA treatment do not recommend statin therapy in small AAA due to lack of substantial evidence in

randomized trials.[191] The reduction in mortality rates after statin therapy is probably attributed to the better vascular health due the lipid lowering ability of statins.

β-blockers

Beta androgenic blockers are a class of drugs that are known to benefit cardiac health by blocking the action of endogenous catecholamines like epinephrine and nor-epinephrine, which are stress hormones that mediate the 'flight or fight' response. One specific b-blocker, propranolol, has been extensively studied for AAA treatment. Studies show that propranolol when delivered to aneurysm prone turkeys/ blotchy mice, result in 150% increase in insoluble elastin and 54% increase in insoluble collagen, suggesting the direct effect of the drug on cross linking matrix proteins.[192,193] Slaiby et al. also demonstrated the AAA inhibitory effects of propranolol in a hypertensive rat model. They created AAA by perfusing elastase in genetically hypertensive wistar-kyoto rats and delivered propranolol subcutaneously for 14 days to find a 50% in arterial diameter in normotensive rats and a 25% in hypertensive rats.[18,194] Two retrospective cohort studies by Gadowski et al[195] and Leach et al[196] showed a 60% reduction in the aortic diameter expansion rates when treated with androgenic beta- blockers. These promising results led to the randomized trial for propranolol in 548 small aneurysm patients. This clinical trial indicated the complete failure of propranolol to prevent or inhibit AAA progression in patients.[197] There was no significant difference is rate of arterial expansion and mortality in the groups treated with and without propranolol. On the contrary, propranolol caused poor tolerance in patients leading to poor standards of life and subsequent discontinuation of medication. In another clinical study by Lindholt et al. 60% of AAA patients receiving

propranolol dropped out of the study because of dyspnea.[198] During follow-up, 16.7% patients in the beta-blocker group died compared to 4.2% in the placebo group. These findings led the investigators to terminate the study after 2 years. Thus current clinical status of the use of beta-blockers, at least propranolol, is of debatable efficacy based on the high rate of adverse effects.

ACE inhibitors and ATII receptor inhibitors (sartans)

Angiotensin II is one of the key hormones in the body that regulates blood pressure by vasoconstriction and release of aldosterone from the adrenal cortex. Angiotensin is implicated in several cardiovascular diseases including hypertension, atherosclerosis, and restenosis after angioplasty and heart failure. However, the mechanisms by which angiotensin functions to contribute to the pathology of the diseases are not well defined. Daugherty et al. described the probable role of angiotensin II in AAA development in a hyperlipidimic mouse model.[199,200] Angiotensin-I converting enzyme (ACE) plays a significant role in increasing blood pressure by two main mechanisms: catalyzing the conversion of angiotensin I to angiotensin II and by degrading bradykinin, a potent vasodilator. [201] Also Angiotensin II binds to two types of receptors, AT1 and AT2, both of which have equal affinity for angiotensin II. Therefore, inhibition of ACE and ATR (angiotensin receptor) are attractive pharmacological approaches to inhibit vascular diseases. In the Angiotensin II/ ApoE-/- AAA model, Inoue et al. subcutaneously delivered a ACE inhibitor (Lisinopril) and ATR inhibitor (Candesartan) and demonstrated a 18% and 23% reduction in the aortic diameter after 40 weeks.[202] Liao et al. confirmed similar results in a rat elastase model, with ACE inhibitor

Enalapril preventing increase in arterial diameter by 88%.[203] Without restraining inflammation, the inhibitors seemed to preserve the medial structure. Hackam and colleagues conducted a human cohort study to investigate the effects of ACE inhibitors on 3426 patients.[204] They showed that those patients who received the treatment for 1.25 years were more protected to rupture risk than patients not receiving ACE inhibitors. To corroborate this finding, they showed that patients who initially received ACE inhibitors for one year and discontinued its use for three months had increased rate of rupture. This study has certain shortcomings like a potential bias of healthier patients receiving ACE inhibitor treatment. Besides, Hackam did not address as to how discontinuation increased the propensity of rupture as compared to the patients not receiving the treatment. In a very recent retrospective cohort study, Sweeting et al. demonstrated a completely opposite finding.[205] In this study, 169 patients that were on ACE inhibitors had a significantly higher aneurysm progression rate compared to patients without treatment (0.33 cm/year Vs 0.27 cm/year). This necessitates an elaborate randomized trial to elucidate the efficacy of ACE on the AAA patients.

A lot of ongoing research strives to block ATR (receptors for angiotensin II) to prevent the progression of AAAs. Losartan is an AT I inhibitor which has shown promising results in animal models. Daugherty et al. indicated that subcutaneous delivery of Losartan completely inhibited the formation of AAA with 0% incidence, whereas delivery of a synthetic inhibitor for AT II receptor dramatically increased the blood pressure, incidence, complexity and atherosclerotic lesion in the AAA.[206] This study indicates the protective role of AT II receptor and the probably efficacy of Losartan as an

AAA drug. Fujiwara et al further exemplified the potential of Valsartan, another AT I inhibitor, as a therapeutic for AAA.[207] Valsartan inhibited macrophage infiltration followed by reduced MMP-2,3,9 and 12 expression and reduced elastin destruction. Further investigation is required to determine the efficacy of ATRs in AAAs in human populations.

Tetracyclines

Tetracyclines non-specifically inhibit MMP activity and inhibit neutrophil activation. The role of one particular tetracycline, Doxycycline, has been extensively studied in aneurysm tissue repair. Sho et al. showed that both systemic and local periaortic infusion of Doxycycline in rat-elastase model of AAA, significantly reduced AAA diameter, macrophage infiltration and SMC proliferation.[20] Local Doxycycline delivery and systemic subcutaneous delivery resulted in a 35.2% and 45.9% aortic diameter reduction respectively. However, elastic lamellae preservation was not apparent in this study. In the Angiotensin II model of AAA, Manning et al demonstrated a dramatic reduction in the incidence of AAA formation (35% in Dox group Vs 86% in control group) in the mice groups receiving oral Doxycycline.[208] A notable point is that the mice received Doxycycline a week before the infusion of Angiotensin II thereby implying a protective role of the drug. Curci et al. demonstrated a 2.5 fold reduction in MMP-9 activity and 5.5-fold reduction in mRNA compared to control group in eight patients treated with Doxycycline one week before elective repair.[209] Despite the promising results in animal studies, a population study by Baxter et al. did not show any significant contribution of Doxycycline in AAA repair. 36 AAA patients were monitored

for six months to evaluate the effect of Doxycycline. 92% of the patients completed the six-month program; however, the remainder patients discontinued the drug due to several side effects including cutaneous photosensitive reactions, tooth discoloration, gastro-intestinal symptoms and yeast infection.[210] Forty-seven percentages of the patients showed almost 50% reduction in plasma MMP-9 levels after 6 months, however no change in aortic diameter was recorded in the patients before and after the treatment. Due to the side effects of systemic Doxycycline delivery, Bartoli et al attempted to study the local effects of Doxycycline on AAA progression. They showed that local periadventitial delivery of Doxycycline was as effective as systemic delivery, even at doses 100-fold lower than that used in systemic delivery. Thus localized delivery of Doxycycline holds a promising future in AAA repair, perhaps as a pharmacological adjunct to EVAR.

Anti-platelet therapy

As discussed in section 2.3, the past few years have drawn the attention of researchers to investigate the role of ILT in AAA. Anti-platelet therapy can potentially mitigate the consequences of thrombosis in the development and progression of AAA. Dai et al. showed the effect of a synthetic inhibitor (AZD6140) of a platelet receptor (P2Y12), on inhibition of platelet activation and prevention of AAA progression in transplantation model in rats.[211] AZD6140 inhibited the aggregation and activation of platelets until 10 days, reduction in thrombus development and platelet CD41 expression. Subsequently, a 28% reduction in arterial diameter was observed at the end of 42 days. Karlsson and colleagues investigated the effect of an anti-platelet agent, acetylsalicylic acid (asprin), on 247 AAA patients.[212] Additionally patients were given statins as an anti-

inflammatory. The groups that received aspirin and statins had a significantly reduced expansion rate compared to the placebo group (0.14 cm/year Vs 0.27 cm/year). It is unclear if the observed results are due to the effects of statins or aspirin or the synergistic effect of both. Although anti- platelet therapy is not officially recommended by the AHA guidelines[191], these drugs can potentially improve life expectancy in AAA patients.

Anti-oxidant therapy- Vitamin E

Since local oxidative stress is high in aneurysmal tissue, reduction of oxidative stress can prove to be a potential therapy for AAA repair. Gavrila et al, showed for the first time, that dietary intake of Vitamin E, in the hyperlipidimic Angiotensin II mice model, decreases aortic diameter by 24%, reduces elastin fragmentation and fatal rupture by 44% and diminishes macrophage infiltration.[213] Vitamin E had no effect on blood pressure, MMP activity and serum lipid profile in the animals. As of date, the effect of Vitamin E has not been tested on patients with AAAs. However, a randomized trial conducted to see the effect of Vitamin E on lung cancer patients with a history of smoking, indicated no significant difference in AAA rupture and repair between the control and Vitamin E groups.[214] Since AAA repair was not the intention of this trial, there is no record of the true incidence and rate of development. Thus, the benefits from vitamin E in the context of AAA repair are yet to be determined. However, key points to be noted are, the dose of Vitamin E given to patients was a lot lesser than in rodent model (50IU/day in humans Vs 2IU/g of diet in mice). Additionally, the mice were fed Vitamin E a week before Angiotensin was delivered, suggesting the preventive role of Vitamin E. Most importantly, humans need supplementary Vitamin C to scavenge the pro-oxidant

tocopherols that Vitamin E yields (which was not provided in the human trials), whereas mice can synthesize Vitamin C de novo from L-gulono-□-lactone oxidase, an enzyme that humans lack.[215] Thus further trials are needed to elucidate the beneficial effect of tocopherols like Vitamin E in prevention/treatment of AAAs.

Anti-inflammatory agents

Since inflammation is a prominent feature of AAA, scientists have tried to dampen inflammation using anti-inflammatory agents to study its effect on AAA. As discussed earlier, cyclooxegenase (COX) converted to prostaglandin, mediates inflammation and MMP production. In a case control study, Walton et al. showed that 15 patients taking Non-steroidal anti-inflammatory drugs (NSAIDs), had a 50% retardation in AAA growth rate compared to 63 control patients that were not on NSAIDs.[216] Inhibition of COX-2 with Celecoxib decreased the incidence and severity of AAA formation in the Angiotensin-II mice model (drug delivered a week before Angiotensin infusion) but no difference was noted with inhibition of COX-1.[217] In addition, COX-2 knockout mice were completely resistant to Angiotensin induced AAA in mice.[218]

Using the elastase induced AAA in a rat model, Dobrin et al. demonstrated the inhibitory effects of prednisolone and cyclosporine in AAA progression. Nine days post perfusion, drug treated rats had a 33% reduced arterial diameter compared to the control groups. Cellular infiltration was dramatically reduced in the medial region of the drug treated rats compared to the control group by day 14.[219]

Blocking of pro-inflammatory cytokine TNF-α[220] and MCP-1 inhibits the progression of AAA in rat elastase model, however blocking receptors for IL-1 shows no change in post-perfusion arterial diameter.[220]

2.2.4.3 Animal models for AAA

Over the years researchers have developed several animal models that somewhat simulate the human AAA pathology in terms of matrix degradation, inflammatory infiltration, atherosclerosis and mural thrombus formation. These animal models are discussed below. Every model has distinct advantages as well as disadvantages over others and none of the models completely mimic the true human aneurysms formation.

A. Elastase perfusion model

AAA induction in the rat model by perfusion of porcine elastase was first described by Anidjar et al. in 1990.[221] A midline incision was made on anesthetized rats and the abdominal aorta was exposed. After clamping the infra-renal and supra-iliac regions of the aorta, the artery was catheterized and perfused with porcine elastase for 2 hours. This intra-luminal perfusion leads to an aortic dilation of 100-120% in a period of 2-4 weeks. This is one of the most frequently used animal models to investigate the mechanisms of AAA pathology and to deliver therapeutics. The elastase model is characterized by chronic infiltration of mononuclear leukocytes leading to extensive elastin fragmentation and luminal expansion, all of which are key features of human AAA. Although elastase is delivered exogenously, after a week several endogenous proteases like MMPs have been detected in this model.[222] The major drawbacks of this

model include the lack of atheromatous plaque and mural thrombus formation. Besides, this procedure involves a very challenging micro-surgery, lacks calcification of arteries and causes significant necrosis due to prolonged exposure to aesthesia. Nackman et al. also showed that this model induces adventitial angiogenesis, as observed in human AAA.[223] To elucidate the involvement of specific factors responsible for AAA formation, the elastase model was adopted in genetically deficient mice. For instance, Pyo et al. showed that MMP-9 knock-out mice do not develop AAA in the elastase model illustrating the role of MMP-9 in AAA formation.[161] Additionally, MMP-12 knock-out mice do not contribute in any protective role against AAA development, at least in the elastase perfusion model. MMP-9 and MMP-12 double knock-out mice however, enjoy greater preservation of aorta compared to other groups.

B. Calcium chloride model

The calcium chloride injury model was first established in a rabbit carotid aneurysm model by Gertz et al.[140] By then, the presence of calcific deposits in atherosclerotic plaque was well established. Gertz and group showed the link between calcification and aneurysm formation by peri-adventitially applying calcium chloride to carotid arteries. Later Chiou et al. adopted the same method of peri-adventitial calcium chloride application to develop AAAs in a mouse model. They described the presence of inflammatory infiltrates and elastin fragmentation which contributed to the AAA formation.[224] Similarly Isenburg et al. described the increase in MMP-2 and MMP-9 activity in the aortas exposed to calcium chloride in a rat model.[225] They also detected calcific deposits in the aneurysmal arteries, which is a common feature in human AAA.

C. Genetically altered mice models

One of the latest models of AAA have been developed by Daugherty et al.[199] They discovered this model based on the role of Angiotensin II in promoting atherogenesis and vessel wall inflammation. They showed that subcutaneous delivery of Angiotensin II via osmotic mini-pumps into ApolipoproteinE (ApoE) knock-out mice for upto one month led to the development severe atherosclerotic lesions as well as massive aneurysms throughout the vasculature. The atherosclerotic lesions had abundant macrophages and lymphocytes. Although Angiotensin is a potent hypertensive agent, no significant change in blood pressure was detected in their studies. The most interesting result of this study was that the aneurysmal tissue had all the characteristics of human AAA tissues, which no other animal model currently has to offer. The site of aneurysm was characterized by medial fragmentation, luminal expansion, thrombus formation, neovascularization and extensive inflammation. Very similar observations were also made by subcutaneously delivering Angiotensin II to Low density lipo-protein receptor (LDLR) knock-out mice.[226] According to Daugherty et al, the earliest (within 48 hours) event occurring in this model, is the infiltration of macrophages into the media leading to elastin fragmentation and dissection.[227] Between 4 and 10 days a vascular hematoma was also observed in the animals which was histologically characterized by abundant macrophages at the edge of the thrombus. After 14 days, aneurysmal tissue matured with increased matrix deposition in the regions which was previously filled with thrombus. Elastin fragmentation continued until 28 days. Atherosclerotic lesions were detected only beyond 28 days, at least in the ApoE-/- mice. One drawback of this model is that the

aneurysms develop in the aortic arch, thoracic aorta and supra-renal abdominal aorta, whereas in human, infra-renal abdominal aortic aneurysms are the most common. However, this particular model has provided significant insight on the pathogenesis and factors involved in the progression of aneurysms.

2.3 Plant derived polyphenols

Based on the literature reviewed so far, it is clear that MAC and AAA are fatal diseases of the arteries. Although there are limited clinical management strategies, there is still no cure for either of the diseases. It has been shown in literature and also by several animal and cell-culture models in our lab that elastin degradation is a key characteristic of both MAC and AAA. Degradation of elastin accelerates calcification and also causes aneurysm formation. Depending on several other factors such as inflammation, hyperglycemia, hyperuremia, duration of disease, nature of vascular insult, presence/absence of atherosclerosis, life style choices of individuals, the fate of aorta might lead to arterial calcification or aneurysm or both. Regardless, the common feature to both diseases is elastin degradation. This research explores the use of plant derived polyphenols for stabilizing elastin and therefore preventing elastin degradation mediated MAC and AAA. Polyphenols are reviewed in the following section.

Polyphenols are chemicals derived from plants that have a hydrophobic core and multiple external phenolic (-OH) groups. They can be typically divided into condensed, complex or hydrolysable varieties. They are micronutrients found in plant sources such as green tea leaves and have been under the scrutiny of research for the past decade for its

multiple valuable properties. Depending on the number of phenol rings and structural elements between phenolic rings, polyphenols can be divided as: phenolic acids, flavonoids, stilbenes, and ligans.[228]

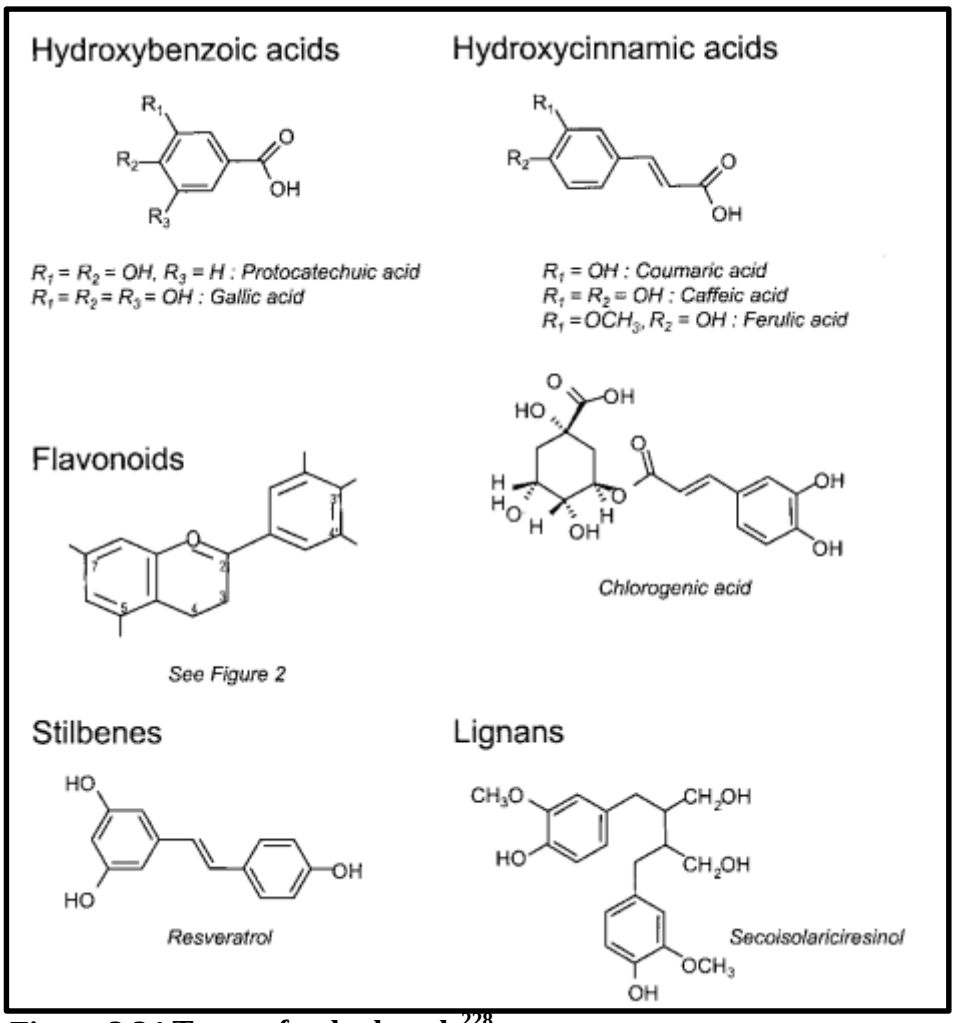

Figure 2.24:Types of polyphenols[228]

Phenolic acids are further classified as derivatives of benzoic acids or derivatives of cinnamic acids. Structure of flavonoids consists of two aromatic rings (A and B) bound together by three carbon atoms that comprise an oxygenated heterocycle (ring C).

Flavonoids are categorized into 6 subclasses based on type of heterocycle involved: flavones, isoflavones, flavanones, anthocyanidins, and flavanols (catechins and proanthocyanidins).[228] For our studies we have chosen three different polyphenols for comparing and investigating their interactions with elastin. We used pentagalloyl glucose (PGG), (-)-Epigallocatechin-3-O-gallate (EGCG) and (+)-Catechin, the structures for which are shown in Figure 2.25.

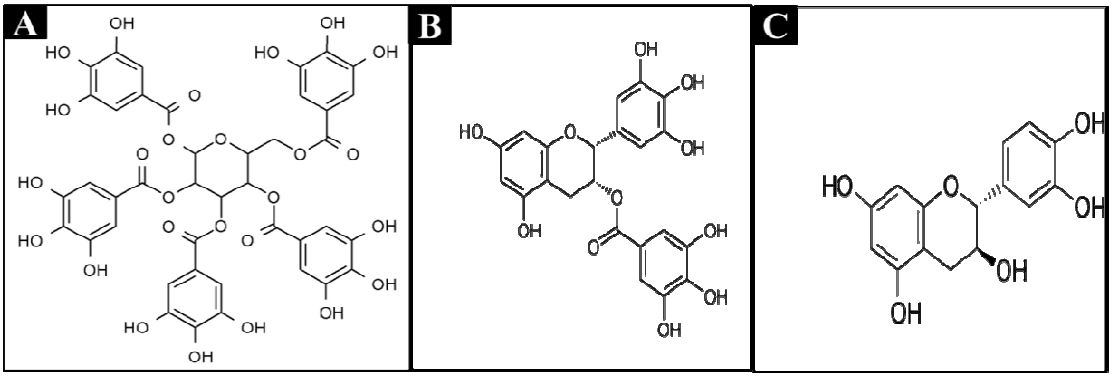

Figure 2.25: Structure of (A) PGG, (B) EGCG, (C) Catechin

2.3.1 Polyphenols interaction with matrices

Phenolic gallotannins have been shown to bind to hydrophobic regions of elastin and collagen specifically to the proline-rich regions.[229,230] Tannic acid (another polyphenol) has been used commonly in electron microscopy, sometimes in combination with glutaraldehyde for visualizing the ultra-structure of elastin.[231] This observation suggested that tannic acid like polyphenols bind to elastin with great affinity. Polyphenols are also effective antibacterial agents and reduce inflammation and antigenicity.[232] Tannic acid and PGG has also shown to bind strongly to vascular elastin

preventing it from proteolytic degradation.[30,233] Previously, we have also shown that a single time peri-adventitial application of PGG to abdominal aorta of rats prevents formation and progression of AAA without any detectable changes in serum or toxic effects in liver.[225] This suggests the biological safety and efficacy of PGG as an AAA treatment when applied as a single dose. Recently PGG has been used for tissue engineering and regeneration applications as a matrix stabilizer. Moderately crosslinking collagen scaffolds from porcine pericardium with PGG exhibited excellent mechanical properties, inhibited in-vivo calcification, prevented enzymatic degradation and supported cellular infiltration, thereby making a suitable scaffold for tissue engineered heart valve.[234] Similarly, elastin scaffolds treated with PGG served as excellent arterial scaffolds conducive to cellular infiltration and neo-matrix deposition.[235] Finally, PGG-treated scaffolds resisted diabetes-induced crosslinking and stiffening, were protected from calcification, and exhibited controlled remodeling in vivo, supporting future use of diabetes-resistant scaffolds for cardiovascular tissue engineering in patients with diabetes.[236]

2.3.2 Polyphenols interaction with cells

Pharmacological properties have been investigated for many years mainly for their anticarcinogenic, antimutagenic, antiviral, and antimicrobial capabilities.[237] Observations such as inverse correlation between green tea consumption and frequency of gastric cancer led to deeper investigation between the molecular interaction of polyphenols and cells.[238] Animal research produced evidence in that the use of tea polyphenols inhibited skin cancer in mice,[239] and colon tumors in rats.[240] Polyphenols

also act as scavengers for free radicals thereby proving very effective anti-oxidants. Anti-oxidant properties of polyphenols have been demonstrated both in-vitro and in-vivo. Polyphenols are shown to reduce oxidative stress by inhibiting activation of nuclear factor κB (NF-κB) and activator protein-1 (AP-1) in culture cells.[241] EGCG is particular has shown several anti-inflammatory properties. Human umbilical vein endothelial cells (HUVECs) when treated with EGCG, exhibited lower monocyte adhesion due to TNF-α.[242] EGCG also has protective effects against ultraviolet B induced AP-1 and NF-κB dependent transcriptional activation.[243] PGG has shown to inhibit cellular proliferation by arresting cell cycle at G1 phase through the down-regulation of cyclin dependent kinases 2 and 4 and cyclin dependent kinase inhibitors p27 and p21 in human breast cells.[244,245] More recently polyphenols like tannic acid and ellagic acid have demonstrated the ability to help in regeneration of elastin in cell culture models. Skin fibroblasts when treated with polyphenols showed greater and well oriented elastin fiber orientation compared to untreated controls. Additionally, once the polyphenols were removed from culture and reverted back to normal growth medium, the groups previously treated with polyphenols showed resistance to enzymatic attack.[246]

2.4 Local drug delivery options in the vasculature

AAA is a focal condition and MAC occurs heterogeneously along the vascular tree, concentrating on some areas. Thus local therapy directed to the diseased site will be an attractive option for the treatment of MAC and AAA. This is advantageous for two reasons: (1) For treatment of matrix disorders such as that in MAC and AAA, greater efficacy of treatment is expected with direct drug-target interaction, (2) systemic delivery

of drugs may have adverse effects on other organs (as mentioned in the human trials of Doxycycline).

Although regression of the aneurysmal/calcified tissue appears to the ideal treatment, early detection and inhibition of progression is a more realistic approach to clinically deal with AAA/MAC. Historically, small aneurysms have different rates of growth, both within and between patients. Current diagnostic techniques are not very precise in predicting growth rate and rupture risk of AAAs. This emphasizes the need to develop sensitive and accurate methods for detecting biomarkers of AAAs in circulation or other easily accessible body fluid. Also, MAC is almost inevitable in patients with diabetes and CKD, hence early detection and prevention of elastin degradation and calcification is required.

The next section will discuss the local delivery options for AAA/MAC repair. The two main aims of local delivery are: (1) maximize drug effects in the tissue and (2) minimize undesired systemic effects. The ideal delivery device would deliver and maintain required amounts of drug in the vessel wall for a period adequate to ensure therapeutic effect, without causing local damage and hindrance to blood flow. In theory, two possible approaches to deliver drugs to the vasculature include: (1) intra-luminal delivery or inside-out delivery and (2) peri-adventitial delivery or outside-in delivery

Currently there are no FDA approved drugs for the systemic/local treatment of AAA/MAC, thus there is a dearth of literature pertinent to devices for local delivery of therapeutics in vasculature. However, in the past decade, researchers have made great

efforts to develop local vascular drug eluting devices to inhibit restenosis after successful percutaneous transluminal angioplasty (PTA). To the best of my knowledge, all the clinically approved devices employ percutaneous intraluminal route instead of peri-adventitial routes. However, varieties of peri-adventitial delivery devices have exhibited their efficacy and potential in animal studies. The following section discusses the list of intra-luminal devices approved for clinical use and the peri-adventitial devices used in animal studies. Knowledge of drug delivery devices of small arteries like coronary arteries is beneficial for development of devices for large arteries like abdominal aorta.

2.4.1 Intra-luminal delivery devices – FDA approved product designs

1) Balloon catheter systems

The three basic mechanisms used to design catheter systems are passive diffusion, pressurized infusion and electrical and mechanical infusion.

Passive diffusion

The first balloon catheter used to deliver drugs was the double balloon catheter. This device comprises of two inflatable balloons at the distal and proximal end with perforations in the catheter between the balloons for delivery of drug solution (Figure 2.26). Deployment of the balloons creates a closed circuit for delivery of drugs, allowing passive drug diffusivity through the lumen. Adequate drug delivery requires 15-30 minutes perfusion leading to the risk of local ischemia. Besides, this method leads to drug loss into collateral or bifurcating vessels. Jorgensen et al. used double balloon catheter in 6 patients undergoing PTA to deliver tissue-type plasminogen activator and heparin for

30 minutes and observed recanalization and remission of symptoms at the end of 30 days.[247]

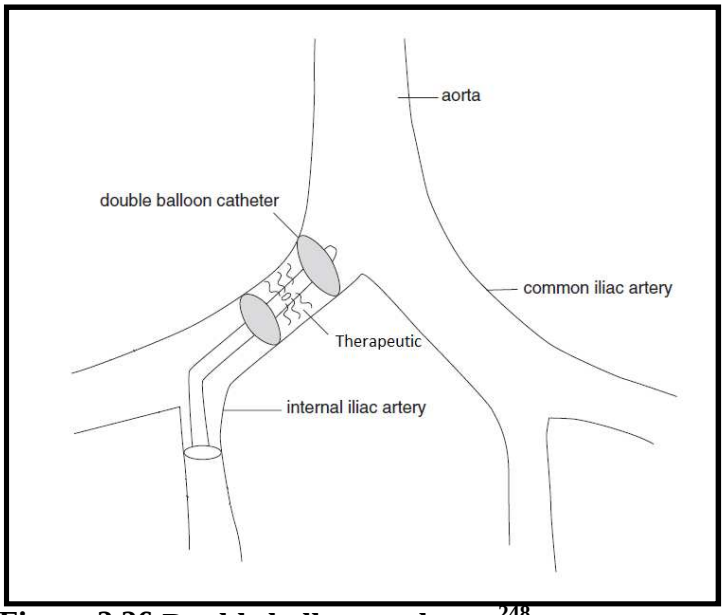

Figure 2.26:Double balloon catheter [248]

The coil balloon catheter is another modification of the basic balloon catheter. The Dispatch™ (Boston Scientific Scimed) consists of a perforated helical infusion balloon wrapped around a non-porous sheath (Figure 2.27). The sheath allows antegrade blood flow and the helical inflation coil diffuses drugs to the vessel lumen on deployment. This device has shown some clinical success, however homogenous drug delivery remains an issue. Intracoronary infusion of heparin using Dispatch™ after balloon angioplasty has shown improved patency and reduced thrombosis in 22 patients compared to patients depending solely on systemic anti-thrombotic agents. [249]

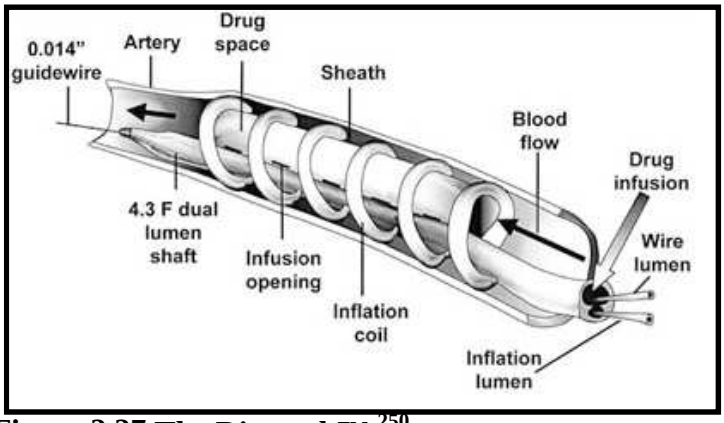

Figure 2.27:The Dispatch™ [250]

The hydrogel coated balloon catheter swells like a sponge on perfusion of the drug solution and allows passive diffusion of drugs once the balloon is inflated. A clinical study suggested that hydrogel coated balloons can be safely used to locally deliver urokinase to attain coronary thrombolysis.[251] Ninety-five patients receiving urokinase displayed reduced thrombus after angioplasty. However, around 10% of the patients suffered from other complications like distal emboli, abrupt closure, no reflow and late closure. Since these devices are designed to diffuse drugs rapidly, speedy release of the drugs immediately after entry into the blood stream may prove problematic. Therefore incorporation of a protective sheath over the balloon helped overcome this concern.

Pressure delivery

The porous balloon catheter is one of the best examples for a pressure driven device. The balloon itself has pores/micropores that directly deliver drugs to the wall after deployment. The depth of penetration is proportional to the perfusion pressure. The Vascular ClearWay™ is a micro-porous balloon catheter designed especially for the removal of soft, fresh emboli and thrombi before angioplasty. Traditional pressure

devices are known to cause damage to the intima at the time of delivery, but the ClearWay™'s soft and tough material exerts similar pressure as conventional porous balloon, but does not cause as much tissue damage (Figure 2.28). It consists of an inner balloon with an array of pores and an outer membrane with thousands of micropores.

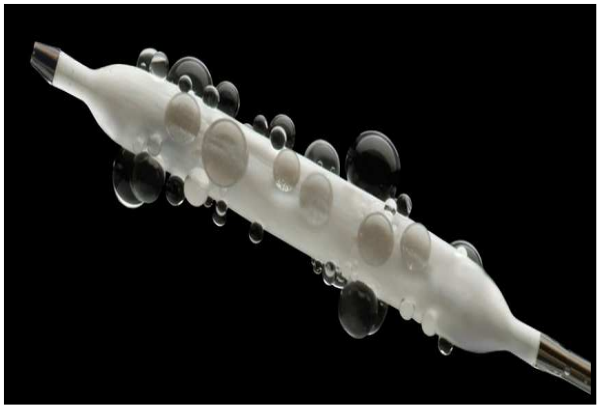

Figure 2.28:The ClearWay™ micro-porous catheter [252]

Mechanical or electrical devices

The needle injection catheter has fine needles that penetrate the media to deliver therapeutics to the perivascular tissue including the adventitia. Despite its invasive nature, this device is shown to cause limited injury and trauma. Ikeno's group successfully delivered Tacrolimus into the adventitia of swine coronary arteries using this system (Figure 2.29).[253]

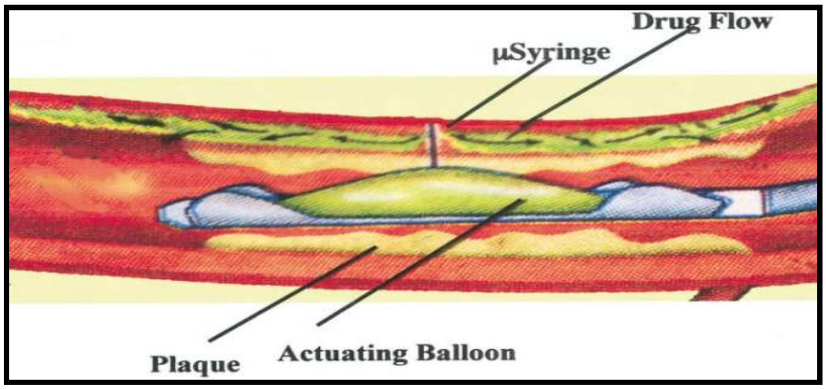

Figure 2.29: Periadventitial delivery using needle injection catheter [253]

The Trellis infusion catheter is a novel percutaneous device that is employed for embolic protection in peripheral vessels especially in Deep vein thrombosis (DVT). This system has two balloons (distal and proximal end) with infusion holes located between the balloons. The catheter has a central lumen which facilitates the movement of the guide wire and a dispersion wire. The dispersion wire is oscillated after the perfusion of the lysis agent. Once the thrombus has been lysed, the contents are aspirated through the pores in the catheter. The balloons that had isolated the vessel is deflated to allow restoration of circulation (Figure 2.30).

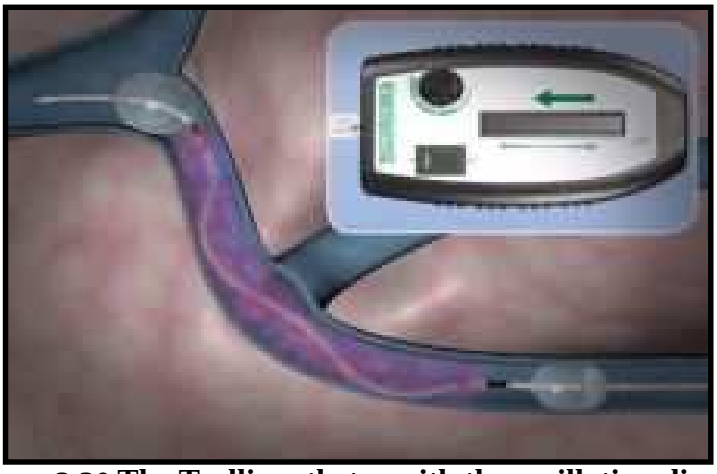

Figure 2.30: The Trellis catheter with the oscillating dispension wire [254]

Drug eluting stents

Bare metal stents are the clinical standard therapy for arterial occlusive diseases. Stents coated with biodegradable polymer containing drugs like Paclitaxel are deployed to the site of occlusion. While most of these drug eluting stents reduce the incidence of restenosis, they are shown to cause greater incidence of late stage thrombosis.[255] Although these drug eluting stents are being questioned about their efficiency in terms of vascular healing, they still exhibit an efficient way to delivery drug locally.

2.4.2 Peri-adventitial delivery methods- research in animals

Several studies conducted in animals demonstrate the successful peri-adventitial delivery of therapeutics/growth factors in local AAA tissue. In a canine vein-patch aneurysm model, Kajimoto et al. implanted basic fibroblast growth factor (bFGF) coated stent-graft to study the reduction of endoleaks. The stent graft was impregnated with 10% soluble elastin and 0.5% heparin salt to bind the materials. Later, these grafts were soaked in a solution containing bFGF, dried and implanted. At the end of four weeks,

there was a six-time greater intimal proliferation in the groups treated with bFGF than the ones without growth factors.[256]

Villa et al used a silicone polymer matrix loaded with dexamethasone to study neointimal proliferation after balloon angioplasty in a rat–carotid model.[257] The drug-loaded matrix wrapped around the carotid artery, was harvested three weeks later (Figure 2.31). From their observation, local dexamethasone delivery at two different concentrations markedly inhibited neo-intimal proliferation after three weeks. The use of silicone rubbers enclosing hydrophobic drugs has distinct advantages as an arterial implant because it does not exhibit swelling effects as any water-soluble drugs in synthetic polymer does. Hydrophobic drugs like dexamethasone come to equilibrium with the extracellular fluid or plasma and form a solid phase solution when implanted.

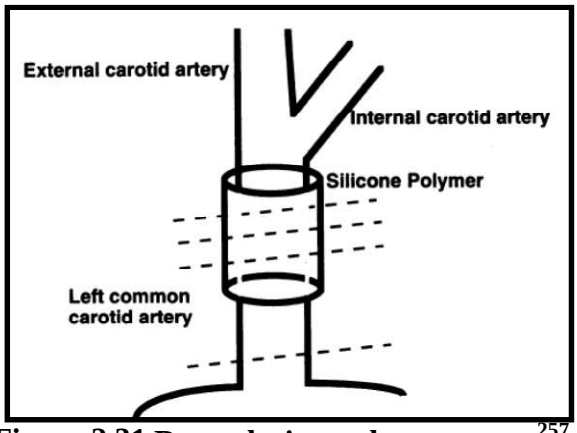

Figure 2.31: Drug eluting polymer wrap [257]

Research groups have also used polyvinyl alcohol (PVA) foams loaded with drugs for peri-adventitial delivery.[20,258] Sho et al. used a mini-osmotic pump loaded with Doxycycline guided by a catheter into a PVA foam (Figure 2.32). Controlled and site-specific delivery of Doxycycline was achieved by placing the PVA foam on the abdominal aorta of the rat. Although they did not display the local release profile of Doxycycline, Doxycycline in the blood did not vary at the end of 14 days, indicating the local drug metabolism in the tissue. Besides, the inhibition of disease progression was comparable in both local as well as systemic delivery. Thus, peri-aortic treatment might improve clinical outcome of AAA treatments.

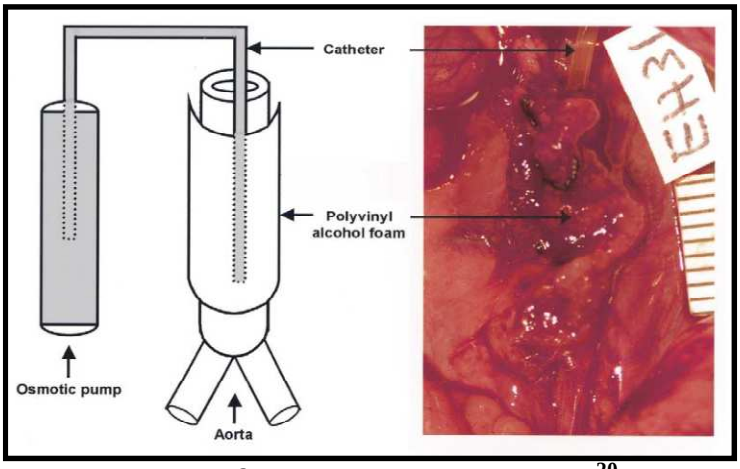

Figure 2.32: PVA foam sutured to the artery[20]

Simons et al used a novel in-situ polymerization technique for delivering drugs peri-adventitially for upto two weeks. They used Pluronic® F-127 gel, which facilitates solubilization of water-insoluble compounds. This gel has a unique property of being soluble at 4°C and solidifying on contact with tissues at 37°C. Their intent was to study the effect of peri-adventitial delivery of anti-sense phosphorothioate in neo-intimal accumulation of cells after balloon angioplasty.[259]

In another experiment, Brauner et al. developed one sided Ehtylene Vinyl-Acetate (EVA) based peri-adventitial matrices for Verapamil to inhibit experimental neointimal cell proliferation. The EVA copolymer and Verapamil hydrochloride was dissolved in methylene chloride and molded into rectangular pieces for peri-adventitial delivery. To facilitate uni-directional drug release, one side of the matrix was sealed with blank EVA using methylene chloride as glue. These polymer patches were then sutured to rabbit vein grafts.[260]

Pires and colleagues developed perivascular cuffs made out of poly-caprolactone (PCL) to reduce restenosis. The cuffs (cylinder with 0.5mm and 1mm internal and external diameter respectively) were loaded with drugs like Paclitaxel and Rapamycin and secured around the femoral arteries of mice. Sustained release of Paclitaxel and Rampamycin caused a 76% and 75% reduction in intimal thickening respectively.[261]

2.4.3 Novel vehicles for drug delivery

Endovascular delivery methods discussed above, focus on the direct delivery of drugs to the site of pathology. However, sustained release of drug to the particular site may be an attractive option to minimize side effects and optimize drug-effects. Some examples of novel drug-delivery vehicles for the vasculature are discussed below.

Very recently, Ogata et al. developed a Doxycycline loaded controlled release biodegradable fiber (DCRBF) for local administration in AAA tissue (Figure 2.33).[262] These Doxycycline incorporated poly-lactic acid fibers showed a controlled in-vitro drug release of 28 days and in-vivo release of upto 84 days. The research group further tested

the efficacy in an ex-vivo mouse model and in-vivo Angiotensin-II model. 14 days co-culture of DCRBF and arteries showed 33% greater quantity of elastin. DCBRF reduced protein expression of MMP-2,9, IL-6 and TNF-α and increase in the TIMP-1 activity in the Angiotensin-II model.

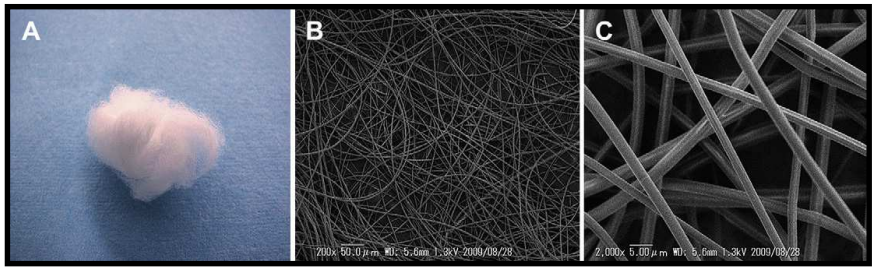

Figure 2.33:(A) gross appearance of DCBRF (B),(C) TEM images of DCBRF [262]

Frank et al. successfully created Hydrocortisone loaded microspheres and delivered them via perforated balloon catheters into rabbit arteries after balloon angioplasty.[263] Westedt et al. also formulated nanoparticles that were infused coupled with porous balloon catheter (Figure 2.34).[264] This prevented the second deployment as in the case of Frank's study. Both these studies showed the successful delivery of particles to the site of disease.

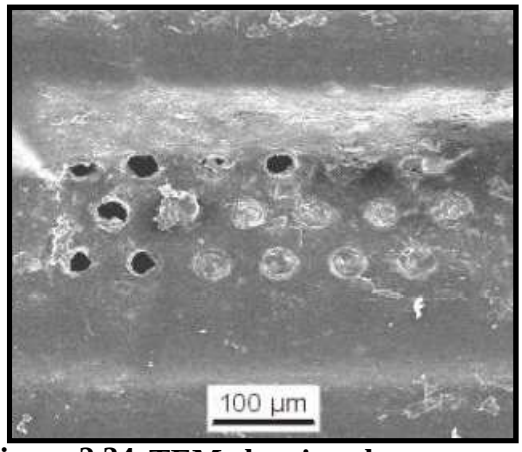

Figure 2.34: TEM showing the nanoparticles eluting out of the porous balloon [264]

The literature reviewed above discusses the different methods of delivering drugs to the vasculature. However, all these methods require surgical manipulation which makes these techniques less than desirable in certain cases. Also, in several vascular pathologies like that of MAC, the diseased area is spread heterogeneously along the vascular tree. Thus, an ideal delivery method should be able to recognize the precise site of calcification/damage and deliver drugs at the precise site. This dissertation talks about one such approach in Chapter 6.

CHAPTER 3

PROJECT RATIONALE

3.1 Project objective and aims

Based on the literature reviewed earlier, the main objectives of this project are:

a) Investigate the potential combined action of glucose and elastin peptides in the presence of transforming growth factor beta-1 (TGF-β1) in the osteogenesis of vascular smooth muscle cells
b) Evaluate the impact of polyphenols like PGG, EGCG and catechin on the quality and quantity of elastin matrix synthesis and stabilization of mature elastin preventing it from elastolytic degradation
c) Develop a minimally invasive nanoparticle mediated drug delivery system that can target damaged elastin, attach and degrade to deliver drugs to diseased vessel

3.2 Specific aims and rationale

Specific Aim 1:

Determine the combined effect of soluble elastin peptides (a result of degradation of insoluble mature elastin) along with TGF-β1 and high levels of glucose in the osteogenesis of vascular smooth muscle cells.

Rationale: From the literature reviewed in Chapter 2, it is clear that diabetes mellitus causes severe calcification of elastin in the artery causing hardening of arteries which affects the mechanical properties of the arteries, leads to poor circulation, infection, and eventual amputation of lower extremities in affected individuals. From research that has been done in MAC observed in CKD or diabetic patients, it is understood that calcification of arteries is a multi-factorial process and works in two fundamental pathways: (1) A passive deposition of hydroxyapatite on the arterial matrix and (2) a tightly regulated and active cell mediated deposition of hydroxyapatite by native cells of the artery. Whether these two processes have a chronological occurrence, work independently or work together has been an unclear debate for decades. MMP mediated elastin degradation is accelerated in diabetic patients which is observed as soluble elastin peptides in circulation. Also, diabetic tissues have abundant TGF-β1 which is released due to MMP mediated conversion of its inactive to active. Chapter 2 discusses the sequestration of latent TGF-β1 by matrix associated glycoproteins like LTBP. With increasing inflammation and MMP activity, there is a progressive degradation of elastin and LTBP. This cleavage activates latent TGF-β1 into active forms available for cellular interaction. It is unclear whether elastin peptides and TGF-β1 interact with glucose contributing to the overall process of vascular calcification. Thus, the first aim of this project is to isolate these factors and test their pathological effect in a cell culture experimental set up.

Specific Aim 2:

- Evaluate the efficacy of plant derived polyphenols like PGG, EGCG and catechin in binding to vascular elastin and protecting against proteolytic degradation**.**
- Determine the benefits of delivering exogenous polyphenols towards elastin synthesis and matrix deposition in a cell culture model. Study the difference between elastin fiber deposition between healthy and aneurysmal cells.

Rationale: From Chapter 2, we know that elastin degradation is a primary cause of MAC and AAA. Currently there is no FDA approved clinical therapy for reversal of arterial calcification or for aneurysm repair. Patients with diabetes and CKD almost inevitably develop vascular calcification, and AAA shows elastin degradation. Since elastin degeneration is a common causal factor for both MAC and AAA, there is a pressing need to develop a therapeutic that can prevent elastin degradation in the early stages of AAA, diabetes and CKD. With the prevention of elastin degradation, we can protect the progression of vascular calcification and aneurysm. Based on earlier work, we tested if polyphenols that are known to have strong affinity to elastin can prevent elastin degradation and at the same time allow deposition of new elastic fibers.

Specific Aim 3:

Develop elastin-antibody coated PLA nanoparticles (ENPs) for luminal targeting in elasto-degenerative diseases for drug delivery and imaging.

Rationale: Delivering drugs specifically to the arteries is a considerable challenge for several reasons: (1) Vascular diseases in large arteries like MAC and AAA, are heterogeneous and the precise spatial identification remains a challenge (2) Because of their anatomy and general inaccessibility, drugs can be delivered to arteries either via laparoscopic route (peri-adventitial) or through endovascular route (intra-luminal), both of which require surgical intervention. We have seen in chapter 2 that current attempts of delivering drugs to the blood vessels are relatively invasive causing probable damage to the luminal side of the artery. It is not sufficient to discover novel drugs for vascular therapy. In the case of pre-emptive drugs (as we suggested in aim 2), surgical drug delivery options are undesirable and will have minimal patient compliance. This necessitates the invention of a drug delivery technique that does not mandate surgery, is cost-effective and provides desired therapeutic effect without causing systemic side effects. The third aim of this project is to use nanotechnology to formulate polymeric nanoparticles that can recognize sites of vascular damage and home themselves to the site and deliver drugs in time dependent fashion.

3.3 Clinical significance

Cardiovascular diseases are the leading cause of death worldwide. The global diabetic epidemic further accentuates the statistics of cardiovascular events. Blood vessel

replacement is a common treatment option for diseases such as atherosclerosis, restenosis and abdominal aortic aneurysms. Although synthetic vascular replacements have a high success rate, they still warrant surgical intervention, increase overall cost of treatment and lead to complications requiring revision surgeries. Currently there are no FDA approved drugs for MAC and AAA treatment and the very few that have reached clinical trials have failed either due to lack of therapeutic value or extreme side effects. By understanding the fundamental mechanisms that cause vascular calcification, exploring novel chemicals with therapeutic potential and exploiting current advances in nanotechnology, we can develop minimally invasive treatment options for MAC and AAA.

It has been shown that PGG and polyphenols as such bind to elastin with strong affinity and protect it from degradation in an elastolytic environment.[265] In small animal models PGG has shown to prevent AAA progression[225] and also dramatic protection against MAC in diabetic rat models.[236] It has been shown earlier that MMP mediated elastin degradation is a precursor to elastin calcification.[88] Additionally, these degraded elastin products provoke osteogenesis in smooth muscle cells turning them into osteoblast like cells.[7] Taken together, polyphenols can bind to elastin in the arteries and (1) prevent AAA progression by directly binding to elastin and preventing inflammatory degradation (2) prevent diabetic MAC by directly binding to elastin, preventing its degradation and indirectly maintaining vascular homeostasis.

The long term goal of this research is to bring about a new site-specific delivery of agents for more effective treatment in patients suffering from elastin related disorders such as MAC and AAA.

CHAPTER 4

ROLE OF ELASTIN PEPTIDES AND GLUCOSE IN OSTEOGENESIS OF SMOOTH MUSCLE CELLS

4.1 Introduction

Cardiovascular calcification has been shown to be an independent marker for mortality in patients with advanced cardiovascular diseases.[26,266] Two pathological patterns of vascular calcification include: intimal calcification and medial calcification. Intimal calcification occurs mostly in association with atherosclerosis subsequent to lipid deposition, macrophage infiltration, and smooth muscle cell proliferation.[267] Medial arterial calcification (MAC) on the other hand may exist with or without atherosclerosis and is characterized by the presence of calcific deposits on the elastic lamellae.[268] As MAC progresses, it forms dense circumferential sheets in the medial layer of the artery which depicts features very similar to that of physiological calcification in bone. MAC is most commonly observed in the distal arteries of patients with diabetes and end-stage renal failure, or with advanced age. It can lead to stroke and lower limb amputations.

In recent years it has been established that vascular calcification is an active and tightly regulated biological process that involves cross-talk between cells and extra-cellular matrix of the arteries and resembles physiological bone formation.[269] In vitro cell culture studies with high concentration of glucose exposure has been shown to accelerate vascular smooth muscle cell (VSMC) calcification. For example, Chen et al showed that bovine VSMCs when incubated with high concentrations of glucose (25 mM), coupled

with inorganic calcifying agents like β-glycerophosphate and ascorbic acid, underwent a more pronounced osteogenic differentiation compared to cells with normal glucose (5 mM) concentrations, indicating the role of hyperglycemia in the increased vascular calcification.[270]

The role of elastin degradation on medial calcification as observed in MAC is not understood well, specifically in diabetic high glucose conditions. Matrix metalloproteinases (MMPs) are known to degrade elastic fiber and it has been shown that MMP activity is increased in diabetic arteries.[5,6] This may lead to an accelerated degradation of elastic fibers. Elastin derived peptides (EDPs), a product of elastin degradation, can be detected in the serum of diabetic patients.[9,271] In fact, a direct positive correlation has been established between the concentrations of serum elastin-derived peptides (EDPs) and the development of micro-vascular complications in diabetic patients.[9,271] Elastic fiber degradation in arteries, along with degradation of TGF-β binding protein associated with elastic fibers, releases sequestered TGF-β.[89,272] Thus elastic fiber degradation can increase concentration of free TGF-β. In our previous study, to test the effect of EDPs and TGF-β1 on VSMCs, we incubated rat VSMCs in vitro with increased concentrations of TGF-β1 and EDPs. We showed that EDP and TGF-β1 have a synergistic effect in the process of osteogenesis of vascular smooth muscle cells, which was characterized by the over-expression of runt-related transcription factor 2 (RUNX2), alkaline phosphatase (ALP) and osteocalcin (OCN).[7] We found increased osteogenesis in absence of any external calcifying agents added to the cell culture such as β-glycerophoshate. However, previous studies were performed in high glucose culture

medium and the effects of normal glucose levels were not clearly examined. To elucidate the effects of glucose concentrations, we compared the degree of osteogenenis of VSMCs in the presence of EDPs and TGF-β1 in high and low concentrations of glucose.

4.2 Materials and methods

Cell isolation and cell culture

Primary rat aortic smooth muscle cells (VSMC) were purchased from Cell Applications, Inc. Passage number 4-8 were used for all the experiments. Cells were cultured in 6 well plates ($1.5x10^5$ /well) in either Dulbecco's modified Eagle's Medium with Low glucose (HyClone Laboratories, Inc., Novato, CA) or Dulbecco's modified Eagle's Medium with High glucose (Cellgro-Mediatech, Herndon, VA), containing 10% fetal bovine serum (HyClone Laboratories, Inc., Novato, CA), 100 units/ml penicillin and 100 units/ml streptomycin (Cellgro-Mediatech, Herndon,VA) in a humidifier incubator at 37°C, with 5% CO_2. Media was replenished every 3 days.

Elastin peptides were purchased from Elastin Products Company (Owensville, Missouri, USA) which were a mixture of elastin fragments, purified from bovine neck ligament, ranging between a molecular weight 1000 to 60,000 kDa, and were highly soluble in water. Recombinant TGF-β1 was purchased from Peprotech (Rocky Hill, NJ). Cells were also treated with SB-431542 and lactose (Sigma, St. Louis, MO) to block the activin receptor-like kinase (ALK-5) and Elastin laminin receptor (ELR-1) respectively. In addition, cells were treated with GF109203X (Enzo Life Sciences, Farmingdale, NY) to block intracellular protein kinase C βII (PKCβII).

Experimental design and time points

VSMCs were grown in low glucose DMEM (LGC), low glucose DMEM with elastin peptides and TGF-β1 (LGET), high glucose DMEM (HGC), high glucose DMEM with elastin peptides and TGF-β1 (HGET). Test additives were administered to sub confluent cells (n=6 per group) as follows: 100 µg/ml elastin peptides and 10 ng/ml TGF-β1.

Additionally, to study the response of inhibition of the respective receptors of elastin peptides (ELR-1) and TGF-β1 (ALK-5), 5 mM lactose or 10 ng/ml SB-431542 was added along with elastin peptides and TGF-β1. For PKCβII inhibition studies, 10µM GF109203X was added to cell cultures and relative gene expression of representative osteogenic genes were investigated.

Cells were grown for 1, 3, and 7 days at the end of which total cellular protein and total cellular RNA were isolated. The spent media was collected for protein analyses at the end of each time point.

Gene expression

At each time point, cell monolayers were scraped and homogenized using a PowerGen 125 homogenizer (Fisher Scientific, MA). The total RNA from the cells was isolated using the RNeasy mini kit (Qiagen, Valencia, CA). The quality and quantity of the RNA was analyzed by Agilent 2100 Bioanalyzer using 6000 Nano lab-on-a chip kit (Agilent Technologies, Foster City, CA). 1µg of RNA was reverse transcribed using Qiagen RT kit. The cDNA samples were then amplified using Qiagen SYBR green kit in

Rotorgene RT-PCR machine (Corbett Research, Mortlake, NSW, Australia). The primer sets used (forward and reverse primers) are tabulated in Table 4.1 along with their accession numbers and PCR product sizes. All primers were procured from Integrated DNA Technologies (IDT, Coralville, IA). Each sample was normalized to the expression of β-2 microglobulin (β2-MG) as a housekeeping gene and compared to LGC group cells (cells cultured in low glucose DMEM alone), using the $2^{-\Delta\Delta CT}$ method.[273]

Table 4.1: PCR primers used in the study

Gene	Name	Primer (forward)	Primer (reverse)	Product size (bp)	Accesion number
ß2-MG	Beta 2-microglobulin	CGTGATCTTTCTGGTGCTTGTC	ACGTAGCAGTTGAGGAAGTTGG	123	NM_012512
CBFA 1	Core binding factor alpha-1	CAACCACAGAACCACAAGTGC	CACTGACTCGGTTGGTCTCG	120	AF053950
ALP	Alkaline phosphatase	TCCCAAAGGCTTCTTCTTGC	ATGGCCTCATCCATCTCCAC	108	J03572
OCN	Osteocalcin	TATGGCACCACCGTTTAGGG	CTGTGCCGTCCATACTTTCG	123	NM_013414
ELR1	Elastin-laminin receptor	GTCAGCGTCATCTCCTCCAG	GAAGGTCCCAGGTGTGAAGC	105	NM_017138

Protein isolation

Cell monolayers were washed twice in PBS and cells were isolated in a mammalian extraction buffer. To prepare the buffer, 1 tablet of protease inhibitor cocktail (Sigma, St.Louis, MO) was added to 10 ml of Solulyze-M mammalian extraction buffer (Genlantis, San Diego, CA). Cell layers were homogenized using PowerGen 125 homogenizer and centrifuged at 10,000 g for 15 minutes. The supernatant was collected and assayed for different proteins of interest.

Immunofluorescence for ELR-1 and ALK-5

VSMCs were grown on glass chamber slides (Lab-Tek II Chamber Slide system, nunc, Thermo Fisher Scientific, Rochester, NY) and then incubated with elastin peptides and TGF-β1 for 3 days. The cells were then washed twice with PBS and fixed in 4% formaldehyde for 10 minutes in room temperature followed by incubation with a 5% bovine serum albumin blocking serum. The primary antibody, a rabbit polyclonal anti-67kDa laminin receptor (Abcam, Cambridge, MA) or a rabbit polyclonal anti-TGF beta receptor I antibody (Abcam, Cambridge, MA) at 1:100 dilution was applied overnight at 4°C. Alexafluor 488 chicken anti-rabbit IgG secondary antibody (Molecular Probes, Eugene, OR) was applied at a dilution of 8µg/ml for 2 hours at room temperature. Coverslips were mounted in glass slides using aqueous mounting medium with anti-fading agents (Biomedia corp., Foster city, CA). The slides were examined by fluorescent microscopy.

ALP assay

After quantifying the total cellular protein, cell lysates were analyzed for alkaline phosphatase using p-nitrophenol phosphate (pNPP) (Thermo Fisher Scientific, Rochester, NY) as a substrate in diethanolamine buffer (Pierce, Rockford, IL). Alkaline phosphatase level was calculated using a p-nitrophenol standard curve and was normalized to the total protein content. Additionally, cells in culture were stained with 0.2 mg/ml 5-bromo-4-chloro-3-indoyl-phosphate, 0.4 mg/ml 4-nitroblue tetrazolium, and 5 mM MgCl2 in 50 mM Tris buffer, pH 9.5 (Sigma,St. Louis, MO) to localize the activity of ALP in cell cultures.

Osteocalcin assay

Culture medium samples from each group were analyzed in triplicates for secreted soluble osteocalcin, using a rat osteocalcin enzyme-linked immunoassay kit (Biomedical Technologies, Stoughton, MA) and values were normalized to the total protein.

Inhibition of ELR-1 and ALK-5 receptors

Lactose (5 mM) was used to block the ELR-1 receptor, the concentrations of which were optimized in previous studies.[7] SB-431542 (10µM) was used to block ALK-5 receptor.[274]

Live dead assay

A live-dead assay (Molecular Probes) was performed as per the manufacturer's protocol. Cells were observed under a fluorescent microscope. Red fluorescence indicated dead cells while green fluorescence indicated live cells.

Statistical data analysis

Results are expressed as means ± standard error of the mean (SEM). Statistical analyses of the data were performed using single-factor analysis of variance (ANOVA). Subsequently, differences between means were determined using the least significant difference (LSD) with an alpha value of 0.05.

4.3 Results

To examine the cytotoxicity of the concentrations of elastin peptides and TGF-β1 used in this study, we performed a live-dead assay. None of the groups were significantly more cytotoxic compared to the low glucose control group at the end of 3 days (Figure 4.1). However, there was a distinct morphological change in the VSMCs from a typical spindle shaped one to that of an atypical rounded morphology (Figure 4.1). This effect was evident only in the groups treated with EDP and TGF-β1 and high concentrations of glucose did not seem to contribute to the effect.

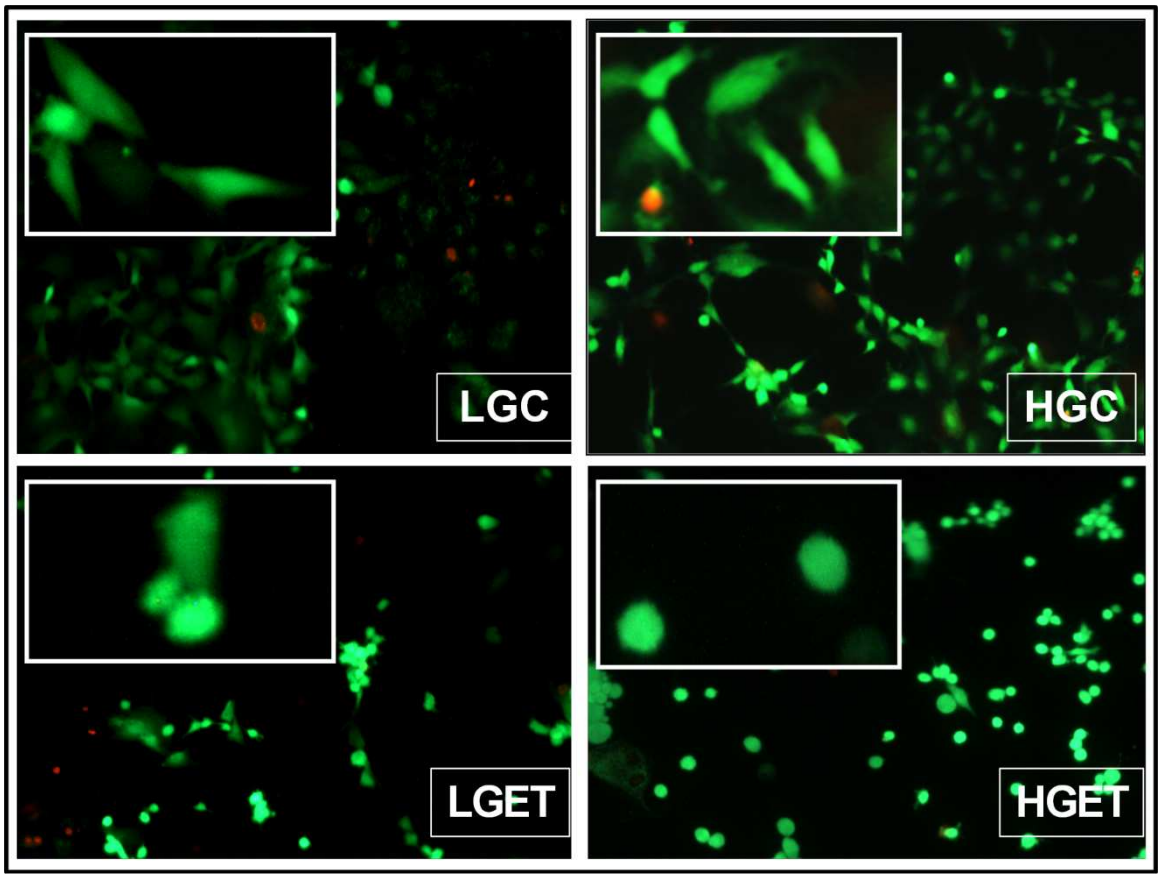

Figure 4.1:Live-Dead assay of VSMCs cultured in the presence of low glucose baseline control (LGC), high glucose (HGC), low glucose + elastin peptides + TGF-β1 (LGET) and high glucose + elastin peptides + TGF-β1 (HGET). Live and dead cells are indicated by green and red fluorescence respectively. Original magnification, 100X. Inset demonstrates cellular morphological differences among the groups.

High glucose is required for expression of osteogenic markers in VSMCs

To investigate the effect of high glucose concentration coupled with growth factor TGF-β1 (10 ng/ml) and elastin peptides (EDP) (100 µg/ml), VSMCs were incubated with both these additives either under the presence of high concentrations of glucose (4.5 g/L) or normal concentrations (1.1g/L) of glucose. Cells were cultured for 1d, 3d, and 7d to study the relative gene expression of RUNX2, OCN and ALP, all three of which are

known to be commonly associated with osteogenesis.[275,276] At the end of 1d, there was ~1.5 times ($p < 0.05$) over-expression of the RUNX2 relative gene expression in high glucose control (HGC), low glucose (LGET) and high glucose (HGET) groups with additives as compared to cells grown in low glucose control DMEM alone (Figure 4.2).

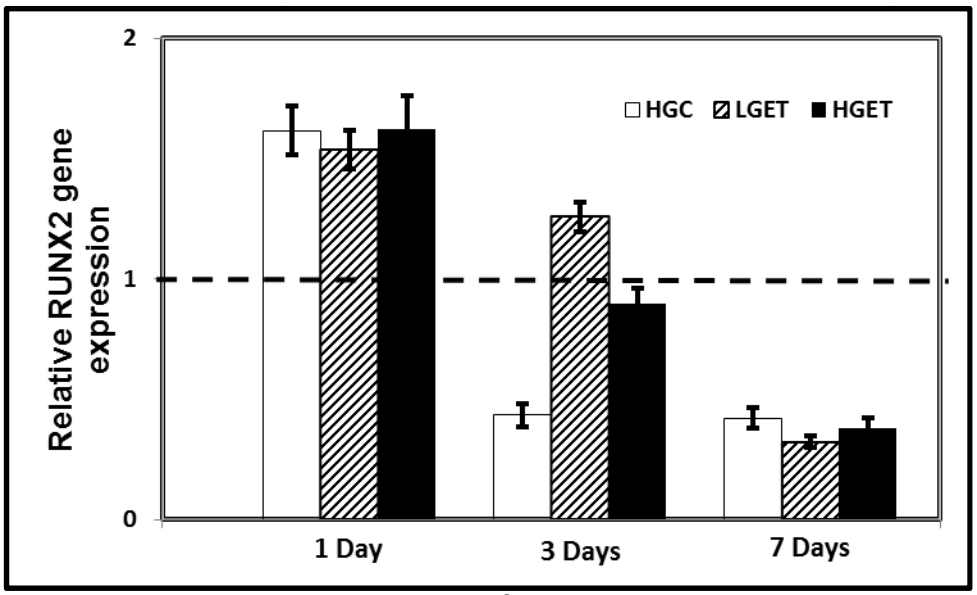

Figure 4.2:Relative gene expression of VSMCs cultured in the presence of low glucose baseline control (LGC), high glucose (HGC), low glucose + elastin peptides + TGF-β1 (LGET) and high glucose + elastin peptides + TGF-β1 (HGET). Bars represent gene expression relative to cells exposed to low glucose baseline control. Relative RUNX2 gene expression after 1, 3 and 7 days of exposure to glucose, elastin peptides and TGF-β1.

This early over-expression was independent of glucose concentration and by the end of 3d; its expression was significantly suppressed. RUNX2 is a transcription factor and it is the earliest marker for osteogenesis; so its over-expression at 1d was expected. In contrast to RUNX2, the relative gene expression for ALP, a key enzyme in the

physiological and pathological calcification, and OCN, bone specific marker, were significantly greater in the presence of high glucose (HGET) groups compared to the low glucose (LGET) groups at 3d and 7d, clearly showing that high glucose levels are essential for the overexpression of these important bone markers (Figure 4.3a and 4.3b).

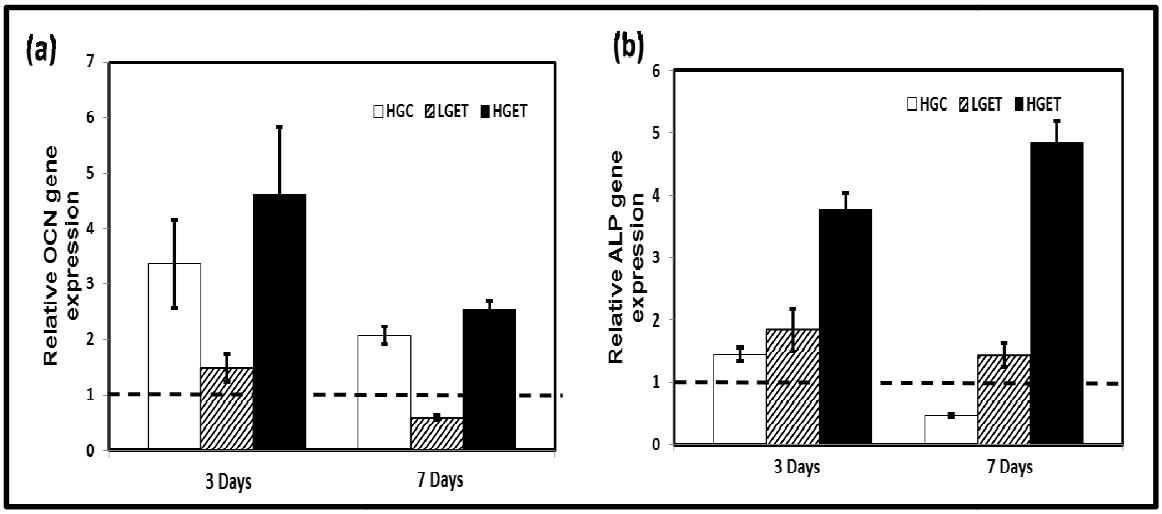

Figure 4.3: Relative gene expression of VSMCs cultured in the presence of low glucose baseline control (LGC), high glucose (HGC), low glucose + elastin peptides + TGF-β1 (LGET) and high glucose + elastin peptides + TGF-β1 (HGET). Bars represent gene expression relative to cells exposed to low glucose baseline control. (a) Relative ALP gene expression after 3 and 7 days of exposure to glucose, elastin peptides and TGF-β1. (b) Relative OCN gene expression after 3 and 7 days of exposure to glucose, elastin peptides and TGF-β1.

We also measured the protein activity of ALP by a colorimetric quantitative method using a BCIP/NBT that is a specific for ALP.[7] At 7d, there was almost a 4-fold ($p < 0.05$) increase in the activity of ALP enzyme seen in the HGET groups, (Figure 4.4a). Staining for ALP in cell cultures showed notably higher purple coloration in the HGET samples around the cells indicating a higher activity of ALP (Figure 4.4b). In addition,

we observed a clustering of VSMCs under the influence of EDP and TGF-β1 which indicates the probable initiation of calcification nodules (Figure 4.4b).

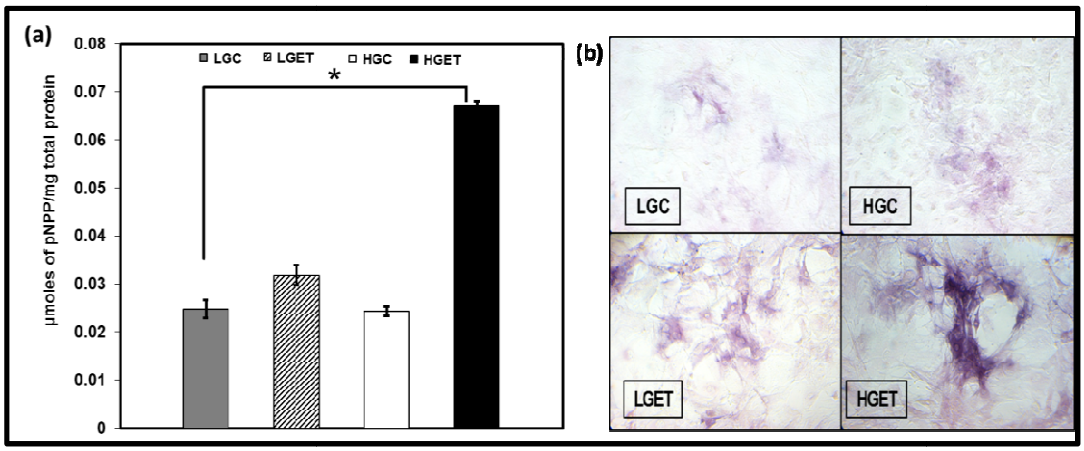

Figure 4.4: Regulation of osteogenic protein activity by VSMCs cultured in the presence of low glucose baseline control (LGC), high glucose (HGC), low glucose + elastin peptides + TGF-β1 (LGET) and high glucose + elastin peptides + TGF-β1 (HGET). (a) Alkaline phosphatase activity in cell lysates. (b) Histochemical staining of enzyme activity in VSMCs.

Osteocalcin protein activity was also found to be 2-fold ($p < 0.05$) higher in the cell culture media of HGET group as compared to any other group at 7 days (Figure 4.5). The protein expression was higher in HGET group as compared to high glucose control (HGC) clearly showing that high glucose levels were not sufficient to increase the osteogenic protein activity in SMCs and exposure to high glucose in combination with high EDP and TGF-β1 was necessary.

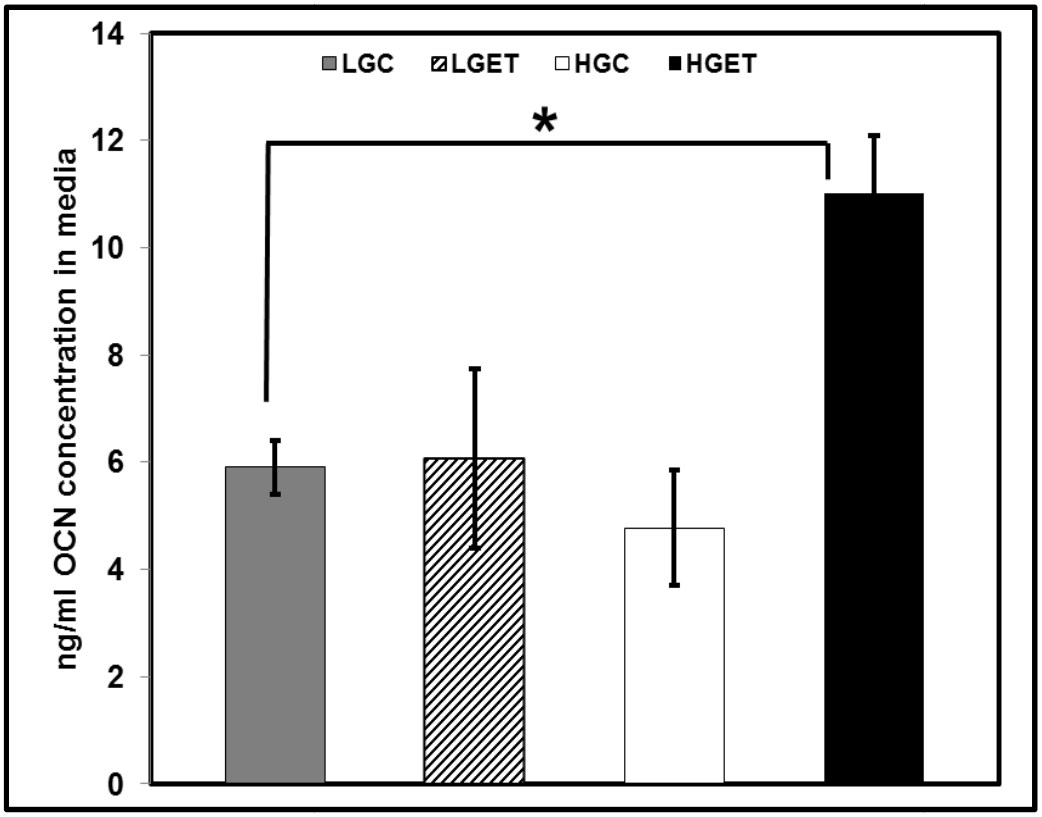

Figure 4.5:Regulation of osteogenic protein activity by VSMCs cultured in the presence of low glucose baseline control (LGC), high glucose (HGC), low glucose + elastin peptides + TGF-β1 (LGET) and high glucose + elastin peptides + TGF-β1 (HGET). Levels of OCN protein secreted by VSMCs in the culture media.

Role of ELR-1and ALK-5 in osteogenesis

It is been shown that TGF-β1 binds to the ALK-5 receptor on cells to cause a series of cellular cascade that are responsible for a variety of cellular phenomenon.[277] Similarly EDPs bind to elastin-laminin receptor on VSMCs. Activation of ELR-1 has been shown to regulate a variety of biological and pathological phenomena including cell proliferation[278] and chemotaxis.[279] Thus we wanted to test if these receptors are involved in rendering osteogenic response in VSMCs. When cells were exposed to high

concentration of glucose, along with EDP and TGF-β1, both ELR-1 (Figure 4.6a) and ALK-5 (Figure 4.6b) receptors on VSMCs were overexpressed showing that these receptors may be involved in signaling towards osteogenic pathway. Glucose concentration in the culture medium did not affect the expression of ELR-1 and ALK-5 as negligible signal was detected in the LGC and HGC groups and no detectable difference was observed between the LGET and HGET treatments.

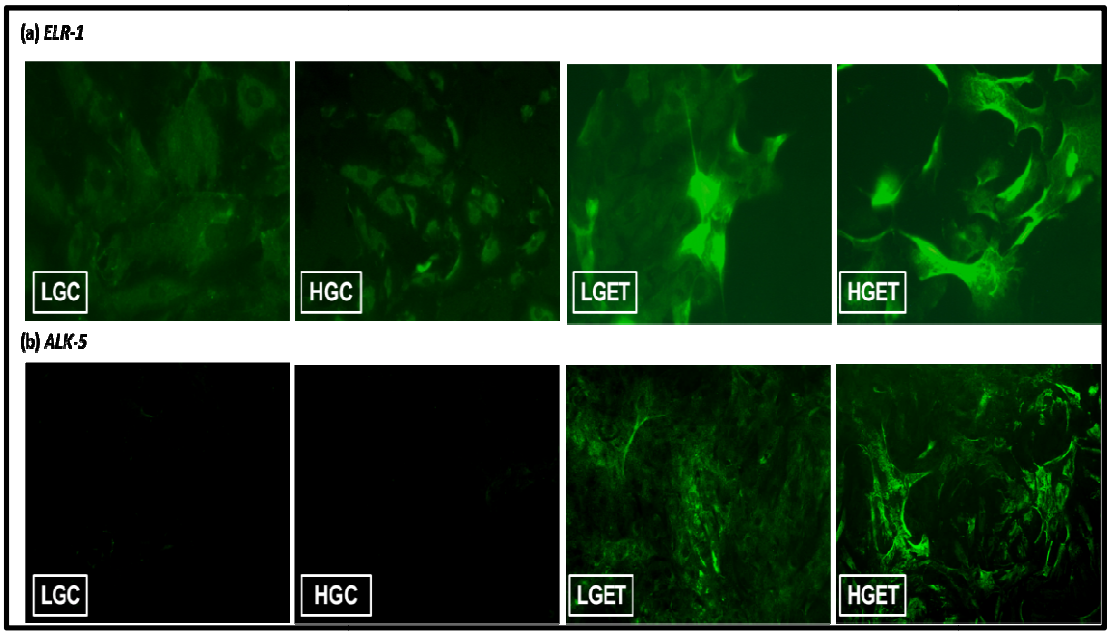

Figure 4.6:**Immunocytochemical detection of (a) ELR-1 and (b) ALK-5 on VSMCs when exposed low glucose baseline control (LGC), high glucose (HGC), low glucose + elastin peptides + TGF-β1 (LGET) and high glucose + elastin peptides + TGF-β1 (HGET). Original magnification, 200X.**

We further blocked the respective receptors by incubating cells with agents known to block their activities: ELR-1 with 5mM lactose and TGF-β1 receptor ALK-5 by 10μM SB-431542. Relative gene expression was studied at the end of 1d and 3d. Figure

4.7 shows inhibition of ELR-1 and ALK-5 caused significant down-regulation in the RUNX2, ALP and OCN relative gene expression in these cells even though they were exposed to high concentration of glucose, EDPs and TGF-β1. These data clearly suggest that ELR-1 and ALK-5 mediated signaling is required for osteogenesis of VSMCs. Interestingly blocking only one of the two receptors had similar effect in inhibition of osteogenic markers (Figure 4.7). This data is suggestive of cross-talk between the two receptors; suppression of one leading to the down-regulation of the other.

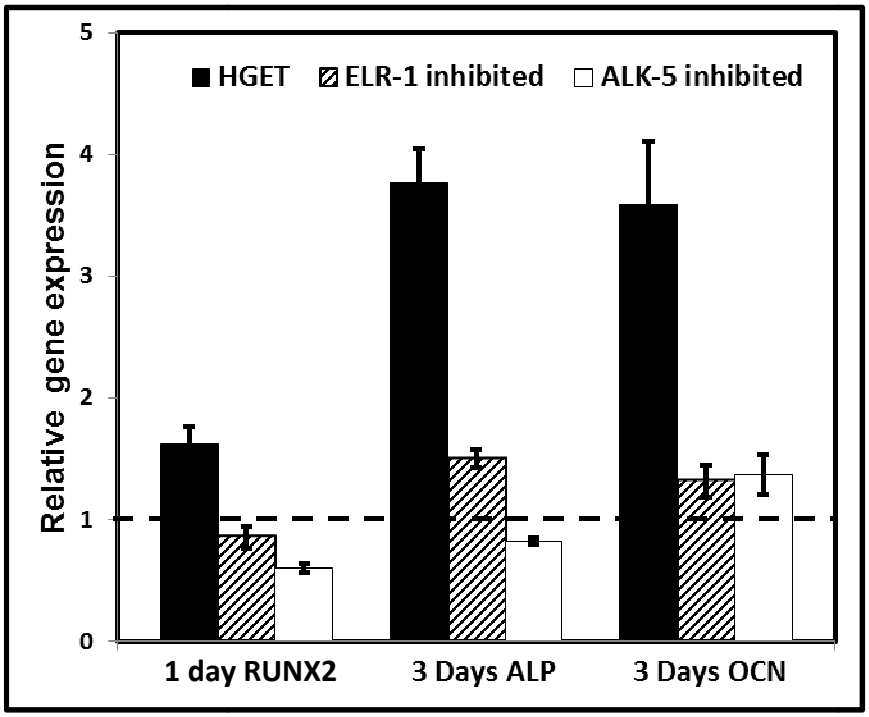

Figure 4.7:Relative gene expression of RUNX2, ALP and OCN by VSMCs when exposed to high glucose + elastin peptides + TGF-β1 (HGET), 5 mM lactose (ELR-1 inhibited), 10μM SB-431542 (ALK-5 inhibited). Bars represent gene expression relative to cells exposed to HGET positive control

Involvement of PKCβII in osteogenesis

Involvement of the PKC signaling pathway in the up-regulation of RUNX2, OCN and ALP has also been studied in literature.[270] We wanted to investigate the involvement of PKCβII in our cell culture model of osteogenesis. At the end of 7 days, cells exposed to high glucose, elastin peptides and TGF-β1, showed a five times greater PKCβII relative gene expression (Figure 4.8a), which was confirmed by higher immunofluorescence staining for PKCβII in HGET (data not shown). Furthermore, exposing cells to GF109203X (a potent inhibitor of PKCβ) in the presence of high glucose, elastin peptides and TGF-β1, a strong down-regulation of 2 representative osteogenic markers (RUNX2 and ALP) were noticed (Figure 4.8b).

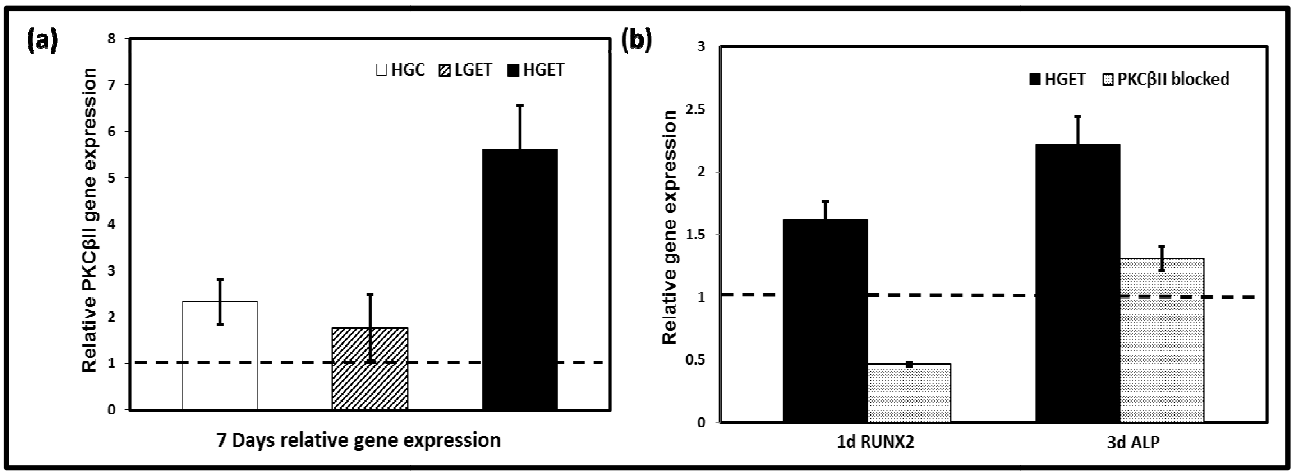

Figure 4.8:(a) PKCβII expression showing highest levels in HGET group as compared to others relative to LGC. (b) Blocking of PKCβII reduces gene expression of RUNX2 and ALP.

4.4 Discussion

Our results indicate that the presence of high concentration of glucose amplifies the osteogenesis of vascular smooth muscle cells in the presence of elastin peptides and TGF-β1. Our data also indicates that a cross-talk in the ELR-1 and ALK-5 receptor mediated transduction pathways is involved in osteogenic response.

Medial arterial calcification (MAC) is a commonly observed pathology in diabetes, end stage renal disease (ESRD) and ageing. MMP mediated elastin degradation releases soluble elastin peptides, which have been shown to induce a wide range of chemotactic effects, angiogenesis,[280] cell proliferation,[281] and proteolytic activity.[282] In previous publications, we have demonstrated that TGF-β1 when coupled with elastin peptides in a dose-dependent manner, induce osteogenesis in vascular smooth muscle cells[7] and skin fibroblasts[8] by activating the elastin laminin receptor-1 and over-expressing three representative osteogenic markers namely, RUNX2, ALP, and OCN. In addition, these additives also increase the cellular production of MMP-2, which can further exacerbate elastin degradation and release of soluble elastin peptides. However, in that study normal DMEM medium was used that contains a very high level of glucose. It was unclear if the osteogenic transformation effects were due to exposure of cells to high glucose.

Our results here indicate that under high glucose conditions, relative gene expression of RUNX2 is up-regulated by 1.5 ($p < 0.05$) times compared to baseline low glucose control group at 1d. RUNX2 expression decreases at 3d onwards, however, two

other osteogenic genes namely ALP and OCN show a 4.7 and 2.5 fold ($p < 0.05$) over-expression respectively, at 3d and continually overexpressed at 7d. Interestingly, although RUNX2 is equally up-regulated in both LGET and HGET groups after 24 hours, the sustenance of ALP and OCN relative gene expression is visible only in the presence of high glucose. In addition, the ALP enzymatic activity is significantly greater in the HGET groups at the end of 7 days. Our data suggests that exposure to elastin peptides and TGF-β1 alone may initiate the process of osteogenic transformation by overexpression of RUNX2, earliest transcription factor marker for osteogenesis, however; progression of osteogenic pathway needs high glucose conditions. ALP and OCN genes and proteins were only overexpressed when cells were exposed to EDPs, TGF-β1 in presence of high glucose.

It should be noted that high glucose alone did not affect osteogenic gene expression. Hyperglycemia has been implicated in vascular calcification in several in-vitro studies. Chen et al. have shown the increase in the relative gene expression of ALP and OCN and formation of calcifying nodules by vascular smooth muscle cells in a hyperglycemic culture medium.[270] Liu et al. have also corroborated the importance of RUNX2 in diabetic vascular calcification. They have shown an increase in intracellular calcium content, greater relative expression of RUNX2, ALP and BMP2 in vascular smooth muscle cells in the presence of high glucose concentrations.[283] Subsequent BMP2 inhibition via noggin partially blocked RUNX2 expression and osteoblastic differentiation of smooth muscle cells. BMPs, which belong to the TGFβ superfamily, have also shown to strongly mediate arterial calcification in diabetic rats as well as in a

cell culture model of hyperglycemia.[284] Our results are in agreement with current understanding of hyperglycemic induction of calcification of smooth muscle cells; however, it is of notable importance that our experimental setup is devoid of any external calcifying/phosphate elevating agents such as β-glycerophosphate that are used in aforementioned in vitro cell culture studies. Addition of these agents itself can cause cells to show osteogenic activity.[93,285] We show that exposure of elastin peptides (due to degradation of elastic fibers[9]) and TGF-β1 (due to its release from TGF-β1 binding protein associated with elastic fiber[89]), and high local concentration of glucose (diabetic), conditions known to occur in in diabetic vascular pathology, can cause smooth muscle cellular transformation to osteoblast-like cellular behavior.

Transforming growth factor-β1 (TGF-β1) is a cytokine with a wide-range of biological functions regulating cell-matrix interactions, cellular proliferation and inflammation. In particular, TGF-β1 has been observed in association with vascular calcification and smooth muscle cell trans-differentiation.[86,87] TGF-β1 has also been shown to mediate apoptosis induced calcification of sheep aortic valve interstitial cells.[286] These cells develop characteristic calcifying nodules under the effect of TGF-β1 and express ALP and apoptosis markers. Our results indicate that TGF-β1 and elastin peptides cause a visible morphological shift in the vascular smooth muscle cells, which is independent of glucose levels in the culture medium. This is in agreement with previous publications where vascular smooth muscle cells have undergone a spindle to cuboidal morphological shift under the effect of the cytokine tumor necrosis factor-α (TNFa).[287] It is unknown how high glucose levels alter cellular interactions of growth factors and

EDPs. Some previous studies shed light on these events. For example, TGF-β1 has been shown to increase the cellular uptake of glucose by activating the GLUT1 receptors in mesangial cells.[288] This TGF-β1-GLUT1 axis can influence the cellular glucose metabolism resulting in vascular pathology. Induction of protein kinase C (PKC) pathway in diabetic tissues has been co-related with several vascular complications. Up-regulated activation of the diacylglycerol (DAG) – PKC pathway in the aorta and heart has been demonstrated in diabetic animal models[289,290] and subsequent blocking of PKC has shown mitigation of vascular[291] and glomerular dysfunction.[292] In-vitro cellular PKC activation by vascular endothelial and smooth muscle cells under hyperglycemic conditions has also been established.[293-295] Blocking of PKCβ has also shown a significant down-regulation in the TGF-β1 activity in diabetic rat models suggesting positive correlation between them.[292,296]

Elastin-laminin receptor (ELR-1) is also suspected to increase cellular DAG concentrations thereby facilitating PKC translocation in the cells.[297] Thus, EDPs in presence of high glucose may enhance ELR-1 activity and PKC translocation and thus increase ALK-5 activity. Consistent with current understanding, our data indicates an increased PKCβII expression by vascular smooth muscle cells under the influence of high glucose, EDP and TGF-β1. Finally, involvement of the PKC signaling pathway in the up-regulation of RUNX2, OCN and ALP has also been identified.[270] We show that blocking PKCβII does decrease osteogenic gene expression in SMCs. Taken together; these findings suggest the possible role of PKCβII in the osteogenic responses of vascular smooth muscle cells. Based on current research, (shown in the schematic in Figure 4.9)

we hypothesize that EDPs and TGF-β1 released by elastic fiber degradation under high glycemic condition in vessels can lead to increased ELR-1, ALK-5, and PKCβII expression in SMCs and lead to osteogenic transformation of SMCs. Overexpression of bone proteins can lead to mineral deposition on degraded elastin. Elastin is known to have calcium binding sites.[298] This in turn can lead to elastin specific medial calcification as seen in diabetic patients. Further in vivo research with diabetic animal models is needed to confirm the findings of this in vitro cell culture results.

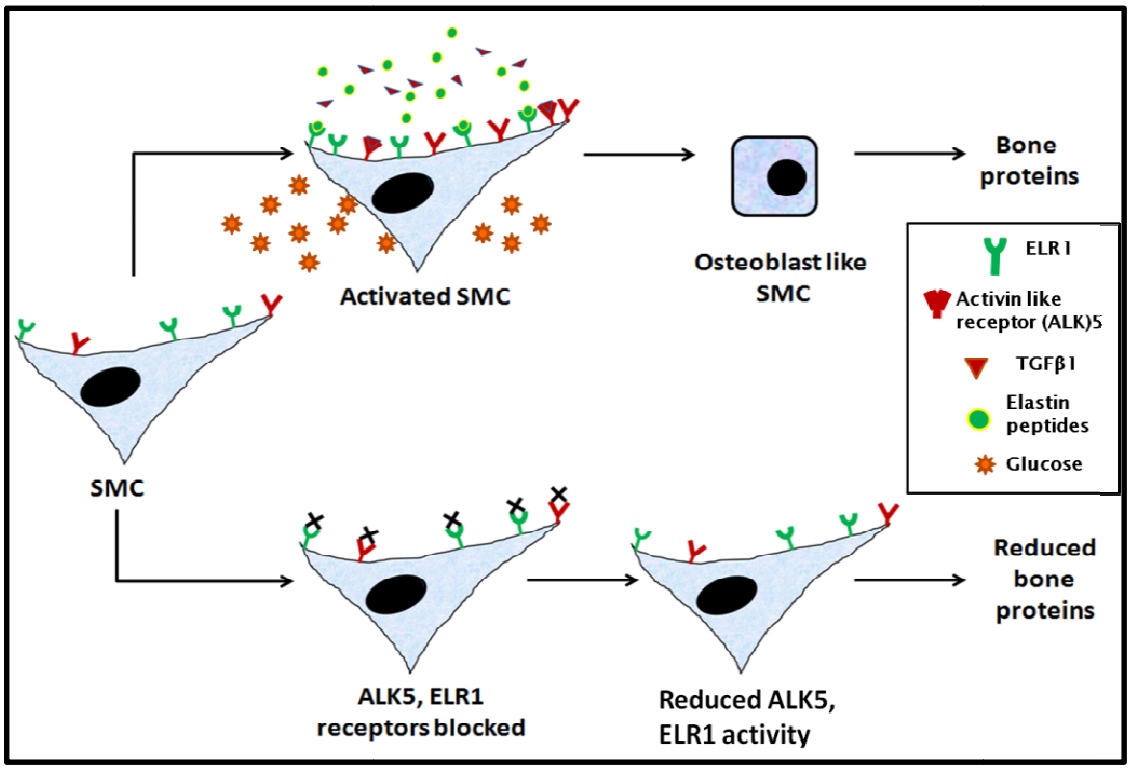

Figure 4.9:Schematic illustrating the osteogenesis of SMC and the responsible receptors

4.5 Conclusion

In conclusion, we have demonstrated that glucose plays a fundamental role in the osteogenesis of smooth muscle cells when coupled with EDP and TGF-β1. Blocking of ELR-1, ALK-5, or PKCβII suppresses the osteogenic response in the cells thereby suggesting a possible cross talk among various pathways. This glucose mediated accelerated osteogenesis of vascular smooth muscle cells can broaden our understanding of medial arterial calcification in diabetic patients.

CHAPTER 5

ELASTO-PROTECTIVE AND ELASTO-REGENERATIVE PROPERTIES OF POLYPHENOLS

5.1 Introduction

As discussed in detail in Chapter 2, abdominal aortic aneurysms (AAA) is a fatal disease of the artery characterized by accelerated inflammation mediated loss of matrix proteins such as elastin and collagen leading to structural weakening and eventual rupture of the artery.[299] There are approximately 18,000 deaths each year due to aneurysms in the United States making it the 15th largest cause of death.[300] Currently, there are no pharmacological repair options for AAA. Aneurysmectomy is the most standard procedure for AAA treatment, wherein the weakened aorta is excluded and replaced with synthetic graft.[301] A lesser invasive option includes the endovascular deployment of stented vascular grafts.[176] Surgical intervention may not be a suitable option for elderly patients, especially since AAA is a disease of the elderly.[144] Endovascular surgical repair, although minimally invasive, has undesirable complications like endotension,[179] graft migration[181] and endoleaks.[178] Additionally, the heterogeneity of AAA, tortuosity of artery, presence of thrombus and calcific deposits may deem EVAR unfit for many patients.[177] Most importantly, none of these clinical interventions provide therapeutic relief in preventing or reversing the pathology.

Since AAA is primarily an inflammatory disease, non-surgical treatment options mainly include inhibitors of matrix metalloproteinases (MMPs) like doxycycline,[302,303]

proteinase inhibitors such as tissue inhibitors of MMPs[304] and chemical crosslinking of artery.[305] However these options provide a one handed approach in stabilizing the damaged artery and prevention from further damage. Although of great importance, the ideal treatment option should work dually in preserving elastin, protecting from further damage and regenerate new elastin leading to disease reversal and cure.

In prior studies, we have demonstrated the ability of plant derived polyphenols to bind to elastin and prevent it from elastolytic degradation.[306] We have also shown, in a rat model, that a single time application of pentagalloyl glucose (PGG) can bind to aortic elastin with minimal toxicity and stabilize AAA.[305] An added impetus in terms of elastogenic factors can enhance the formation and accumulation of net elastin thereby regressing AAA. This work explores the potential of polyphenols as a multi-folded treatment option in AAA by stabilizing elastin, preventing enzymatic degradation, renewing cross-linked mature elastin and inhibiting MMPs.

5.2 Materials and methods

Pure elastin preparation

Pure porcine elastin was prepared and characterized as described earlier.[88,306] Briefly, ascending porcine aorta were procured from local slaughterhouse, cleaned to remove fat and adherent tissues and finely shredded in a food processor. Aortic elastin shreds (~2 mm) were subjected to 4-5 washes in 2 L of 0.9% NaCl to remove cloudy waste, following which they were washed with 1 L cold saline every hour for 3 hours (4°C) and left in shaking overnight in saline at 4°C. After washing, 1ml of the wash

solution is removed, centrifuged at 12,000 × g for 15 mins and evaluated for soluble protein using Peirce BCA protein assay (Thermo Scientific, Rockford, IL). The washing steps were repeated until no protein was detected in the supernatant. The tissue shreds were then autoclaved, 2-3 times in water, and were replaced with fresh warm water after each autoclave cycle. Finally, the aorta were defatted and dehydrated with ethanol and diethyl-ether and lyophilized. This procedure eliminates cellular, collagenous and non-collagenous material including elastin-associated glycoproteins and leaves elastin intact.[307]

Polyphenol binding kinetics

Pure aortic elastin (10 mg, as described above) was suspended in 1 ml of 10, 25, 50, 100 µg/ml concentrations of Pentagalloyl glucose (PGG), Epigallocatechin gallate (EGCG) and catechin. Pentagalloyl glucose (PGG) was a gift from Ajinomoto, Epigallocatechin gallate (EGCG) and Catechin were purchased from TCI America (Portland, OR). The polyphenols were dissolved in 10% ethanol in Phosphate buffered saline (PBS). 100 µl of the sample buffer was drawn at various times and absorbance was measured at 280 nm.

Methanol extraction of polyphenols

~10 mg elastin was treated with 10, 100, 1000, 10000µg/ml of PGG, EGCG, Catechin for 48 hours in 37°C. Unbound polyphenols were washed in de-ionized water and elastin samples were dialyzed against water overnight, lyophilized, and weighed. Samples were homogenized and polyphenols were extracted in methanol and were

quantified using a standard curve for polyphenols. The amount of polyphenols bound to pure elastin was expressed as micrograms of polyphenols bound per mg dry elastin. All experiments were conducted in triplicates.

Resistance to enzymatic degradation

Lyophilized elastin (~5 mg) was treated with 10, 100, 1000, 10000µg/ml of PGG, EGCG, Catechin for 48 hours in 37°C. Unbound polyphenols were washed in de-ionized water and elastin samples were dialyzed against water overnight, lyophilized and weighed. Elastin samples were treated with high purity porcine elastase (10U/ml, 24hrs) (Elastin products company, Owensville, MO). Elastase was dissolved in 10 mM Tris buffer, 1 mM $CaCl_2$, 0.02% NaN_3, (pH 7.8). Dry weights before and after enzyme digestion were used to calculate percent digestion (n=3). The supernatant from elastase digestion experiment was collected and assayed for fragmented elastin using poly-acrylamide gel electrophoresis (PAGE) followed by Coomasie blue staining.

Histology and polyphenol stain

Elastin samples were incubated with polyphenols for 48 hours, and washed to remove free unbound polyphenols. Elastin samples were embedded in Tissue Tek OCT compound (Sakura Finetek, U.S.A. Inc., Torrance, CA), and frozen at -80°C. Sections (6 µm) were cut using a cryostat (Microm HM 505 N, Mikron Instruments, Inc.) and collected on glass slides. Sections were acclimated at room temperature for 5 minutes, fixed in cold acetone for 5 minutes and stained with 10% ferric chloride ($FeCl_3$) in methanol and counterstained with 1% light green. Ferric chloride stains polyphenols

deep-purple to black. In addition, elastin samples were stained with Verhoeff's Van Gieson (VVG) (Poly Scientific, Bay Shore, NY) to study structural integrity of elastin.

Cell culture

Primary rat aortic smooth muscle cells (RASMC) were freshly isolated. Briefly, freshly harvested abdominal aorta from healthy adult male Sprague Dawley rats were isolated and cleaned. Endothelium was scraped off and the adventitia was removed with scalpel blade. The medial layer was minced and digested in 125U/ml Collagenase (Worthington, Biochemicals Lake-wood, NJ) and 3U/mg elastase (Elastin products company, Owensville, MO) in Dulbecco's modified Eagle's Medium-F12 (Hyclone, Thermo Scientific, Rockford, IL) with 10% fetal bovine serum. The SMCs leave aorta and attach and grow in petri dishes.

RASMCs isolated from rat aorta with advanced abdominal aortic aneurysm were received from Dr. Ramamurthi at Cleveland Clinic, the experimental procedure for which has been described in detail earlier.[308] Briefly, the posterior lumbar aortic branches were ligated; infra-renal aorta was surgically exposed and injured via catheter mediated intra-luminal elastase perfusion. The aortic diameter was measured before aortotomy, after aortotomy and after harvest. The aneurysms were allowed to develop for 14 days before they were harvested and cells were isolated with the same procedure as described above for normal aorta.

Passage numbers 4-8 were used for all the experiments. Cells were cultured in 12 well plates (200,000/well) in Dulbecco's modified Eagle's-F12 medium containing 10% fetal bovine serum (HyClone Laboratories, Inc., Novato, CA), 100 units/ml penicillin and

100 units/ml streptomycin (Cellgro-Mediatech, Herndon,VA) in a humidifier incubator at 37°C, with 5% CO_2. Media was replenished every 3 days.

Experimental design

Healthy RASMCs / aneurysmal RASMCs (EaRASMC) were cultured in medium containing polyphenolic additives (1 µg/ml, 10 µg/ml; n=3/condition) for 14 days. Polyphenols were dissolved in Dimethyl sulfoxide (DMSO) (Sigma Aldrich, St. Louis, MO) to prepare stock concentration of 10 mg/ml and filter sterilized using 0.2 µm membrane filters (Corning Incorporated, Corning, NY) prior to addition. Control groups received only vehicle (DMSO) and no polyphenols. Cell culture media was changed every 3 days and spent medium was collected at each media change, frozen at -20°C and biochemically assayed for tropoelastin and lysyl oxidase. After 14 days, the cell layers and soluble proteins were collected and analyzed.

Protein isolation

Cell monolayers were washed twice in PBS and cells were isolated in a mammalian extraction buffer. To prepare the buffer, 1 tablet of protease inhibitor cocktail (Sigma, St.Louis, MO) was added to 10 ml of Solulyze-M mammalian extraction buffer (Genlantis, San Diego, CA). Cell layers were homogenized using PowerGen 125 homogenizer and centrifuged at 10,000 ×g for 15 minutes. The supernatant was collected and assayed for different proteins of interest. Total soluble protein was quantified using Peirce BCA protein assay.

Fastin assay for elastin

Total insoluble elastin deposited in the cell layers and soluble monomeric tropoelastin released in the media were quantified using Fastin assay (Accurate Scientific and Chemical Corporation, Westbury, NY). For each treatment group, tropoelastin was assayed individually after each media change to generate a trend curve, and also evaluated as cumulative tropoelastin released over 14 days. To quantify the mature elastin deposited within the cell layers, the cell pellet generated after the protein isolation procedure mentioned above, was lyophilized and digested in oxalic acid as per manufacturer instruction manual. Since fastin assay quantifies only soluble α-elastin, the dried insoluble pellet was subjected to 3 digestion cycles with 0.25 M oxalic acid (100 °C, 1 h in water bath) and the pooled digests were assayed in the exact same procedure as tropoelastin in media. The total α-elastin was normalized to the total soluble protein released by the cells which is assumed to be directly proportional to the total cell count.

Cell viability studies

EaRASMCs were treated with 1, 10 µg/ml polyphenols for 48 hours and proliferation of cells was estimated using the MTT (3-(4, 5-Dimethyl-2-thiazolyl)-2,5-diphenyl-2H-tetrazolium bromide) assay. Briefly, 5 mg of MTT (Sigma Aldrich, St.Louis, MO) was dissolved in 10 ml of serum-free media and added to cells. After 4 hours, media was carefully aspirated and the insoluble formazan dye was collected with dimethyl sulfoxide (DMSO) (Sigma Aldrich, St. Louis, MO). Absorbance was read at 560 nm and normalized to control (no treatment) readings.

Gene expression

RASMCs and EaRASMCs were plated as mentioned earlier. At 70% confluency, cells were switched to serum-free media for 24 hours and treated with polyphenols in serum-free conditions. Only gene expression studies were conducted in serum free conditions, to evaluate solely the effect of polyphenols and negate the effects of serum and growth phase of cells. After 24 hours of treatment, cell monolayers were scraped and homogenized using a PowerGen 125 homogenizer (Fisher Scientific, MA). The total RNA from the cells was isolated using the RNeasy mini kit (Qiagen, Valencia, CA). The quality and quantities of the RNA were analyzed by Take3 micro-volume plate (BioTek, Winooski, VT). One µg of RNA was reverse transcribed using Qiagen RT kit. The cDNA samples were then amplified using Qiagen SYBR green kit in Rotorgene RT-PCR machine (Corbett Research, Mortlake, NSW, Australia). All primers were procured from Integrated DNA Technologies (IDT, Coralville, IA). Each sample was normalized to the expression of β-2 microglobulin (β2-MG) as a housekeeping gene and compared to their respective untreated control groups (cells cultured in DMEM-F12 alone), using the $2^{-\Delta\Delta CT}$ method.[273]

Gelatin zymography

Active MMP-2 was analyzed in the cell lysates (intracellular soluble proteins) by gelatin zymography.[309] The total protein was quantified using BCA kit and 12 µg total protein was loaded per well alongside with pre-stained molecular weight standards (Precision Plus Protein Standard, Bio-Rad, Hercules, CA). All lanes were loaded in duplicates with equal amounts of protein in each well. After development, coommasie

staining and de-staining, the gels were photographed and density of clear bands (MMP-2 at 68kDa) was analyzed using ImageJ software and reported as relative density units.

Immunofluorescence for elastin, fibrillin-1

RASMCs/ EaRASMCs were treated in similar conditions as mentioned earlier. After 14 days, the cell layers were washed twice with PBS and fixed in 4% formaldehyde for 15 minutes in room temperature followed by incubation with a 5% bovine serum albumin blocking serum. The primary antibody, rabbit anti-rat elastin antibody (United States Biological, Swampscott, MA) or a rabbit polyclonal anti-fibrillin I antibody (Abcam, Cambridge, MA) at 1:100 dilution was applied overnight at 4°C. Alexafluor 488 chicken anti-rabbit IgG secondary antibody (Molecular Probes, Eugene, OR) was applied at a dilution of 8µg/ml for 2 hours at room temperature. Cell layers were mounted using aqueous mounting medium with anti-fading agents (Biomedia corp., Foster city, CA). The samples were examined by fluorescent microscopy. Importantly, all samples were imaged under exactly similar conditions for impartial analyses.

In-vitro coacervation and maturation of tropoelastin

The kinetics of tropoelastin coacervation and maturation were performed using UV-Vis plate reader (BioTek, Winooski, VT) equipped with temperature, stir controllers and kinetic measurement features. 1 mg of human recombinant tropoelastin (Advanced BioMatrix, Poway, CA) was dissolved in 100% glacial acetic acid (Fisher Scientific, MA). Polypeptides were diluted in coacervation buffer (50 mM Tris, pH 7.5) to either 25 µM for one set of experiments and 10 µM for another set of experiments. The

temperature of coacervation was 37°C. Samples were stirred at the rate of 1000 rpm and absorbance was measured at 440 nm every minute throughout the reaction time. Polyphenols at 10 µg/ml were added to the polypeptides (in ice) immediately before the absorbance measurement.

Statistical data analysis

Results are expressed as means ± standard error of the mean (SEM). Statistical analyses of the data were performed using single-factor analysis of variance (ANOVA). Subsequently, differences between means were determined using the least significant difference (LSD) with an alpha value of 0.05.

5.3 Results

Polyphenols bind to mature elastin

In order to determine the binding kinetics of polyphenols to elastin, pure porcine elastin (the method described earlier) was incubated in 1.5 ml polyphenols of different concentrations (10, 25, 50, 100 µg/ml) and the solutions were assayed for 48 hours. Respective control polyphenol solutions without elastin were also maintained to evaluate the stability of polyphenols in solution over time. Within 1 hour of incubation, at 100 µg/ml PGG, there was a reduction of 68.67% ± 6.89% of initial PGG quantity which further reduced to ~42.09% ± 5.4% after 6 hours and less than 5% ± 0.63% of initial PGG after 24 hours, clearly indicating the binding of PGG to elastin (Figure 5.1). Furthermore, the control groups without elastin showed no absorbance variability over time (data not shown) indicating the stability of PGG in solution and confirming the

binding of PGG to elastin. The Langmuir rate of adsorption of PGG after 60 minutes was calculated to be 0.052 µg PGG/mg dry elastin/min. Likewise, EGCG quantities in the solution reduced by ~72% ± 3.8% after 60 mins, ~45% ± 7.63% after 6 hours and less than 25% ± 5.35% after 24 hours. The Langmuir rate of adsorption of EGCG after 60 minutes was calculated to be 0.044 µg EGCG/mg dry elastin/min (Figure 5.2). Catechin quantities in the solution reduced by ~77% ± 1.8% after 60 mins, ~65% ± 0.1% after 6 hours and less than 60% ± 1.25% after 24 hours. The Langmuir rate of adsorption of EGCG after 60 minutes was calculated to be 0.045 µg catechin/mg dry elastin/min (Figure 5.3). It is interesting to note that although catechin shows greater and faster adsorption compared to PGG in the first 6 hours, the total reduction after 24 hours is greater in PGG compared to EGCG and Catechin groups. This may be attributed to the smaller molecular weight of catechin and fewer phenolic groups, therefore displaying higher initial binding but low overall binding. Figure 5.1, 5.2, 5.3 depicts the binding kinetics of polyphenols to elastin over time. It also indicates the direct positive correlation of polyphenol concentration to rate of binding.

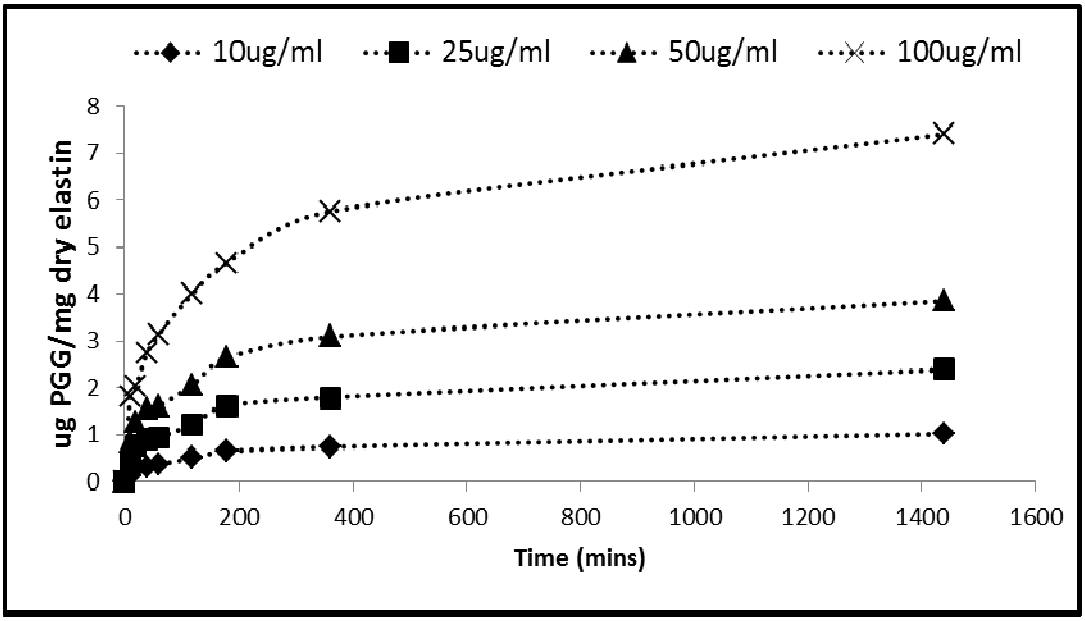

Figure 5.1: Binding kinetics of PGG to insoluble elastin. Quantity of PGG bound to elastin increases with time which was measured indirectly as the decrease in absorbance of PGG over time.

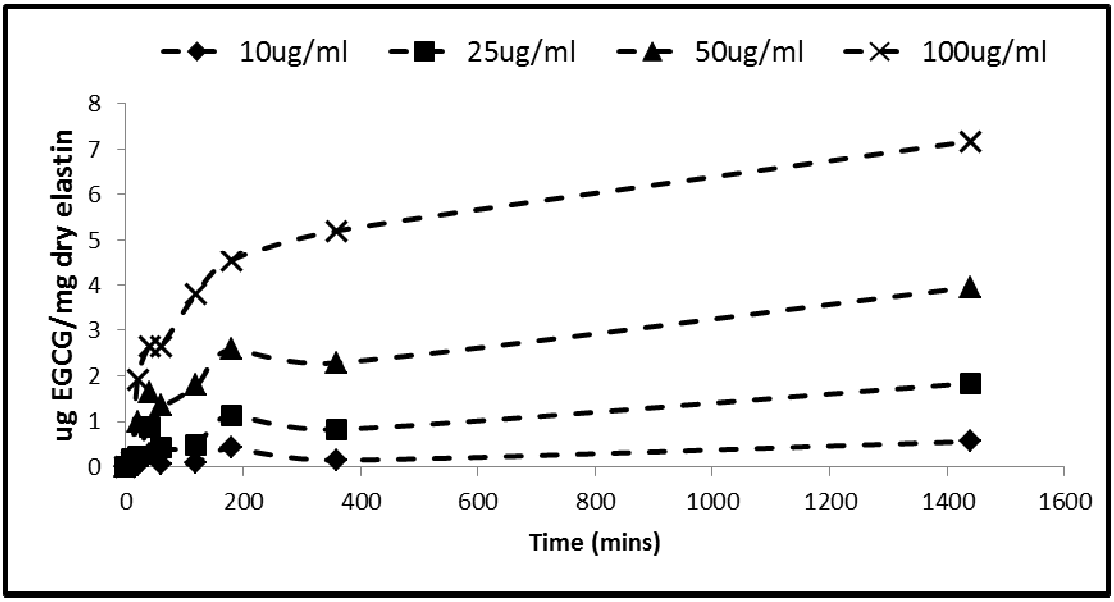

Figure 5.2: Binding kinetics of EGCG to insoluble elastin. Quantity of EGCG bound to elastin increases with time which was measured indirectly as the decrease in absorbance of EGCG over time.

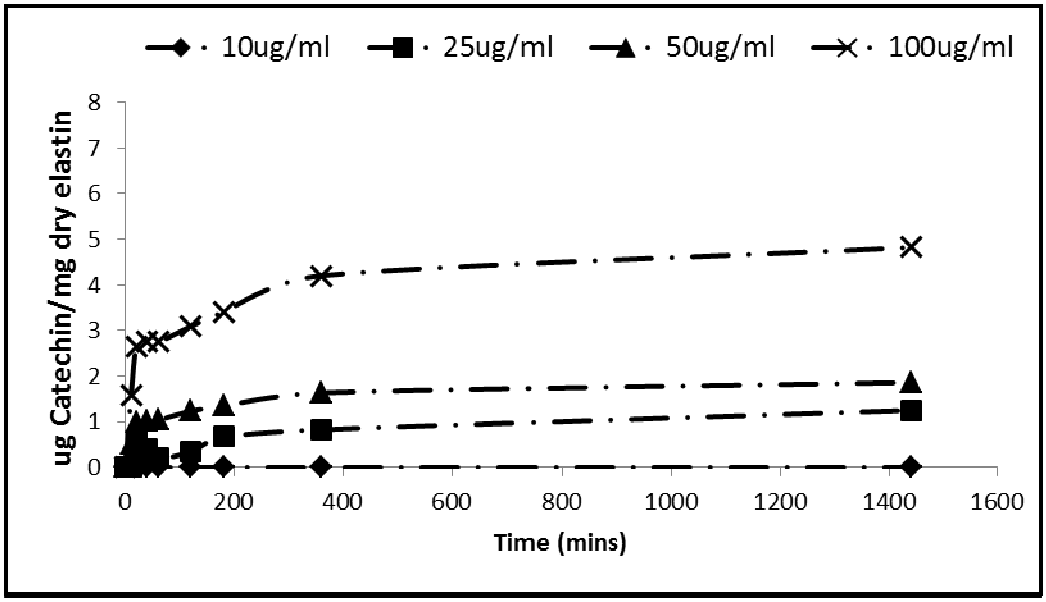

Figure 5.3: Binding kinetics of EGCG to insoluble elastin. Quantity of EGCG bound to elastin increases with time which was measured indirectly as the decrease in absorbance of EGCG over time.

In a separate set of experiments, much higher concentration of polyphenol solution (10, 100, 1000, 10000µg/ml) was used to validate the binding of polyphenols to elastin. Figure 5.4 shows the amount of polyphenols bound to elastin after 48 hours of incubation. At 1:1 polyphenols to elastin w/w ratio (10000 µg/ml polyphenols), ~ 140 µg PGG, 183 µg EGCG and 105 µg catechin / mg dry elastin was bound to elastin. Corresponding control groups (without polyphenols) showed no absorbance indicating the absence of polyphenols.

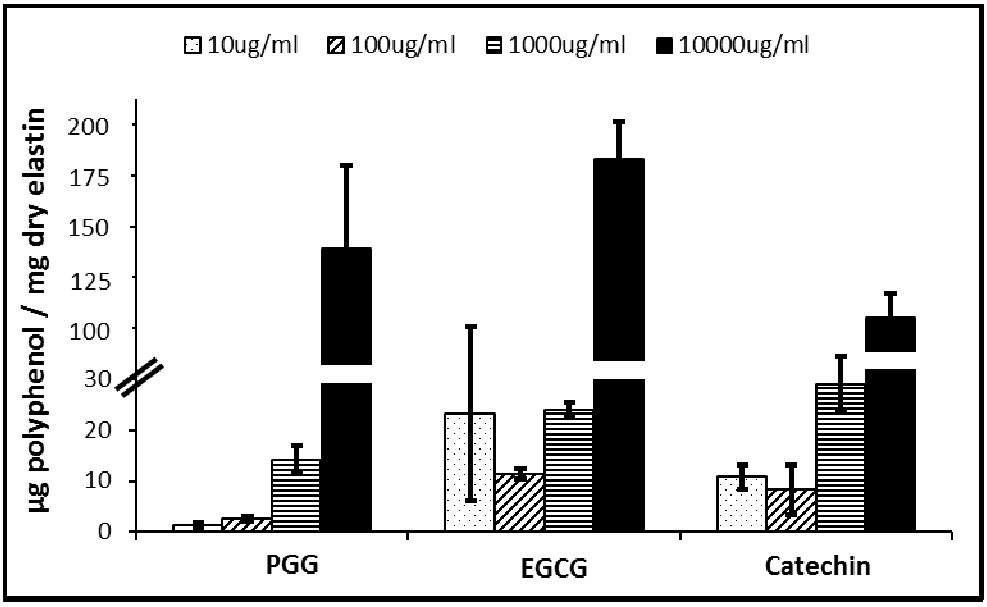

Figure 5.4:Quantity of polyphenols bound to elastin after 48 h of incubation

Further, the binding of polyphenols was histologically verified using a ferric chloride stain that binds to phenolic compounds imparting a deep purple to black color. Untreated control groups (Figure 5.5 A) showed no visible stain for phenolic groups when compared to PGG (Figure 5.5 B), EGCG (Figure 5.5 C) and catechin (Figure 5.5 D) treated groups. All the histological images were representative pictures taken for elastin samples treated with 10000 µg/ml polyphenol solutions.

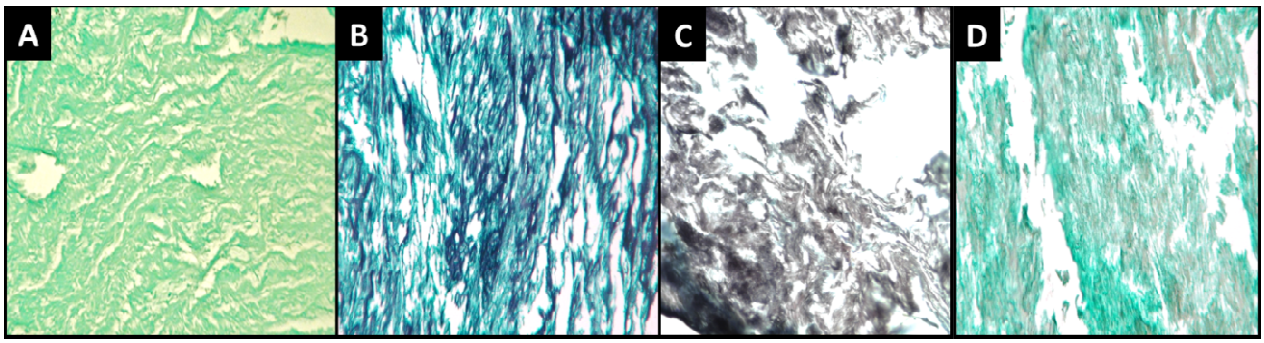

Figure 5.5:Phenol specific stain shows incorporation of polyphenols into pure aortic elastin

Polyphenols provide vascular elastin with elastolytic resistance

Resistance against elastase degradation was tested using aortic samples treated with polyphenols followed by porcine elastase degradation. The difference in the dry weights before and after elastase treatments indicated the elasto-protective effects of polyphenols. Control elastin preparations (without polyphenol treatment) lost ~80% total mass (Figure 5.6). Treatment with 10, 100 µg/ml polyphenol solutions did not apparently prevent from elastolytic degradation ($p>0.05$) whereas 1000 and 10000 µg/ml reduced the susceptibility of elastin degradation by ~25% and 88% in PGG, 17% and 88% in EGCG, 15% and 33% in catechin groups respectively.

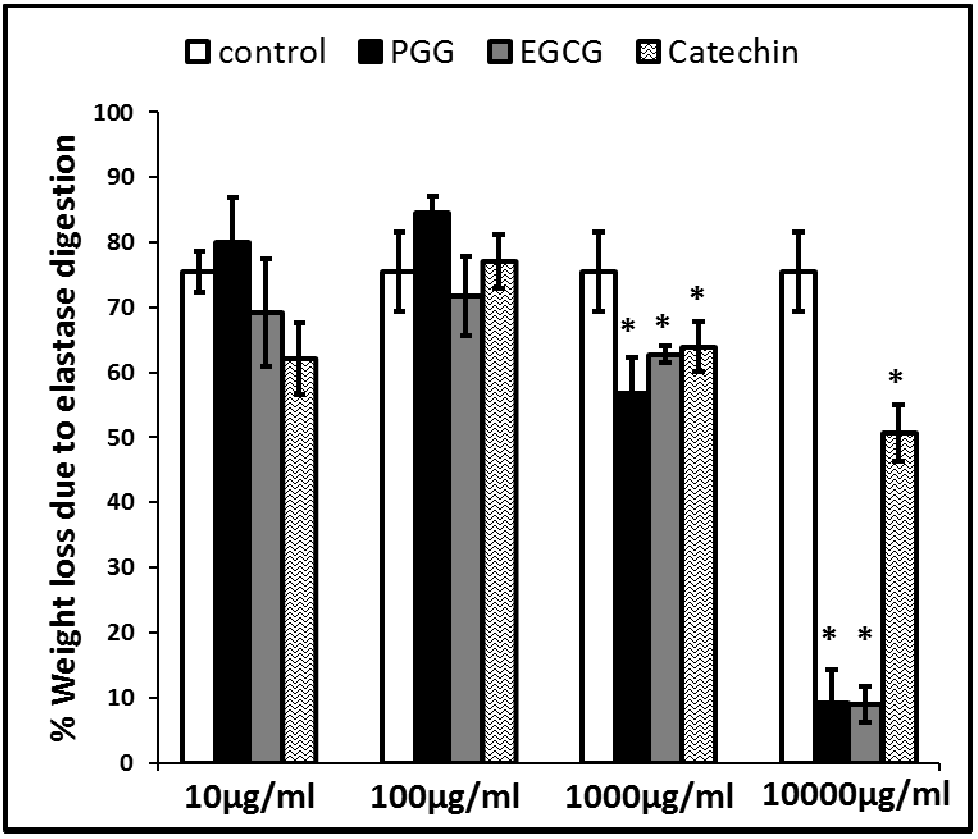

Figure 5.6:Efficacy of polyphenols as elastin-stabilizing agent.

The elasto-protective feature of polyphenols was further confirmed histologically with VVG staining. Untreated control elastin groups display clear signs of fiber degradation and matrix degeneration (Figure 5.7 A) while elastin stabilized with 10000 µg/ml polyphenols exhibit little to none fiber degradation (Figure 5.7 B, C, D).

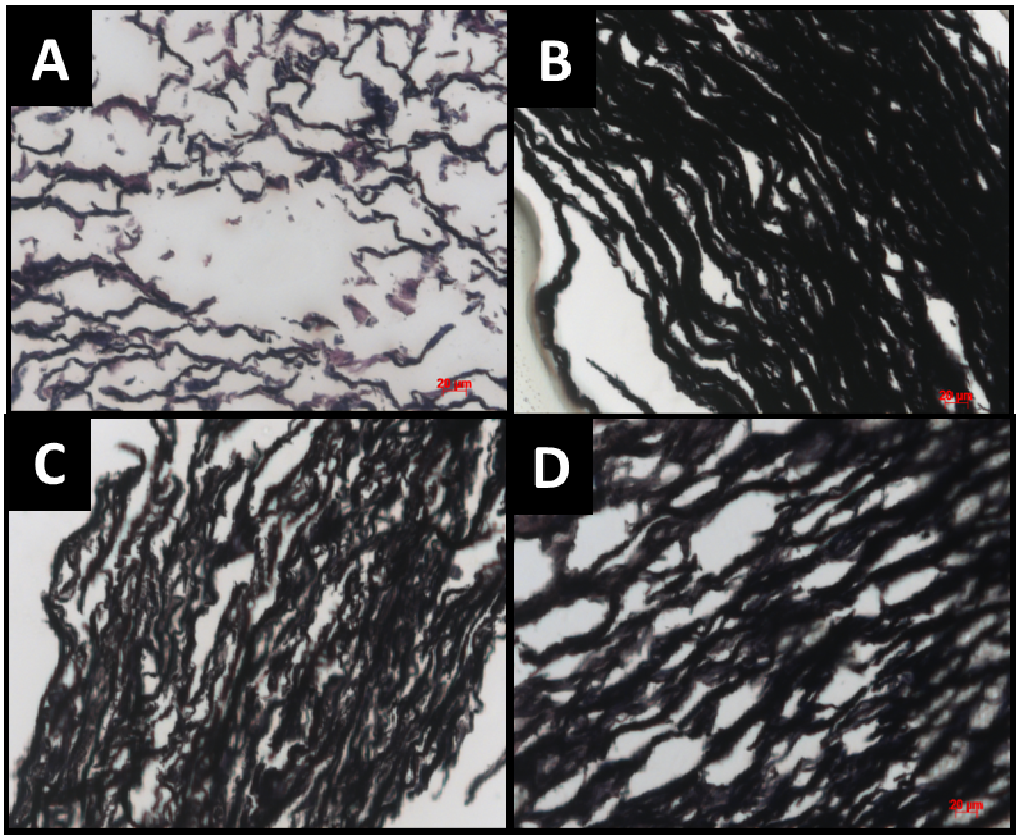

Figure 5.7:Histology of pure elastin after digestion with elastase. PGG (B), EGCG (C), catechin (D) show intact elastin fibers compared to untreated control (A).

Additionally, the digestate after elastase digestion was run through SDS- PAGE to evaluate the elastin fragments in solution. The untreated control groups showed a dark smear of elastin fragments at different molecular weights indicating severe elastic damage which was evidently inhibited by 1000 and 10000 µg/ml polyphenol treatments, especially in the PGG and EGCG groups (Figure 5.8). It must be noted that the solution assayed had elastase which might be contributing to the band density.

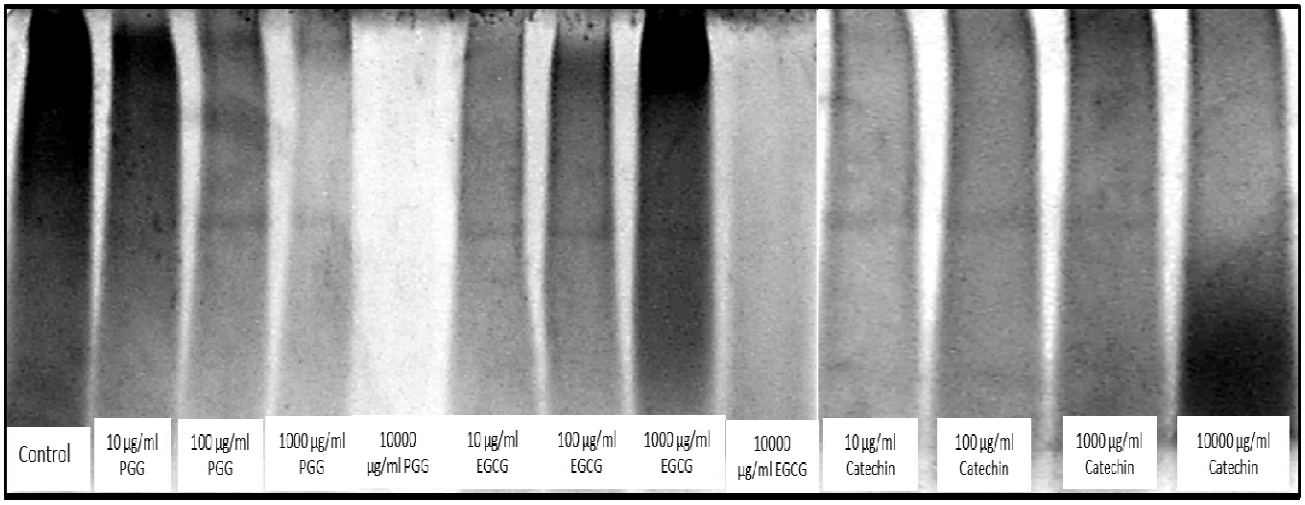

Figure 5.8:Degradation products after elastase digestion. Polyphenol treated group show less band density indicating greater protection against elastase digestion

Polyphenols bind to tropoelastin and accelerate rate of self-assembly in-vitro

Kinetics of tropoelastin coacervation was examined in-vitro using a UV-Vis spectrophotometer enabled with stir rate controllers and temperature monitoring device. In initial experiment (Figure 5.9), tropoelastin "coacervation phase" was marked by a rapid increase in absorption at 440 nm. This initial rise in absorbance is thereafter followed a steady decrease in absorbance; a stage termed as "maturation phase".

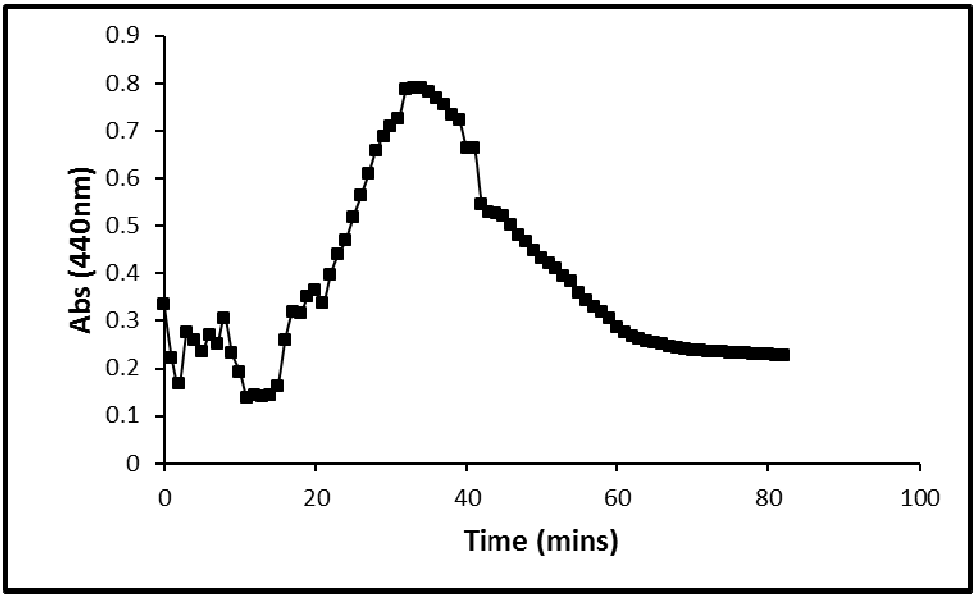

Figure 5.9:In-vitro elastin self-assembly kinetics

Addition of polyphenols dramatically increased the rate of coacervation (Figure 5.10 A) (PGG by 1.6-fold, EGCG and catechin by 7.5-fold) and delayed the onset of maturation (20 mins for pure polypeptides Vs. ~200 mins for polypeptides + polyphenols).

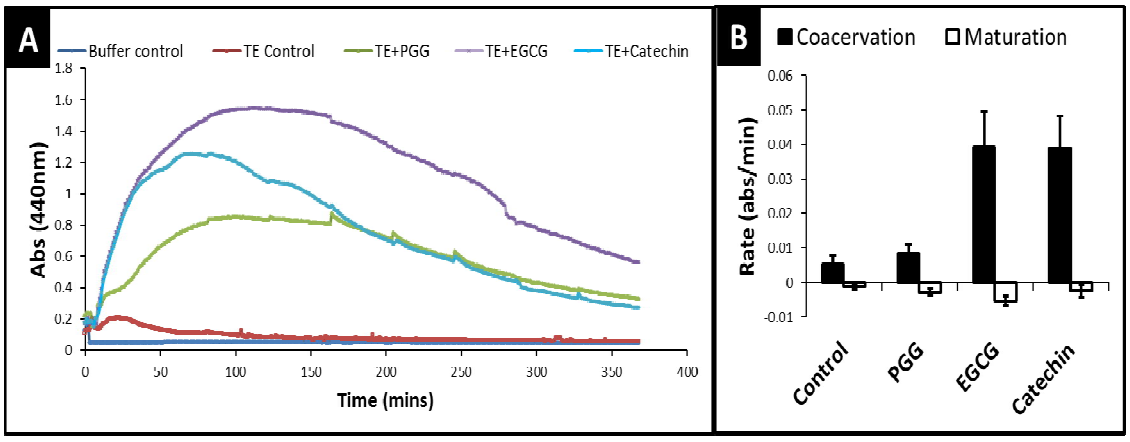

Figure 5.10:(A) Shows the self-assembly kinetics of tropoelastin after polyphenol addition. (B) The rate of coacervation and maturation of tropoelastin after addition of polyphenols

MTT assay for cellular proliferation

A colorimetric cell proliferation assay was used to evaluate the viability of aneurysmal smooth muscle cells in vitro. MTT showed a significant retardation in cell proliferation when cells were exposed to 10 µg/ml PGG and catechin, whereas 1 µg/ml polyphenols showed minimal difference in cellular proliferation. EGCG appeared indifferent compared to control groups at both 1, 10 µg/ml concentrations (Figure 5.11).

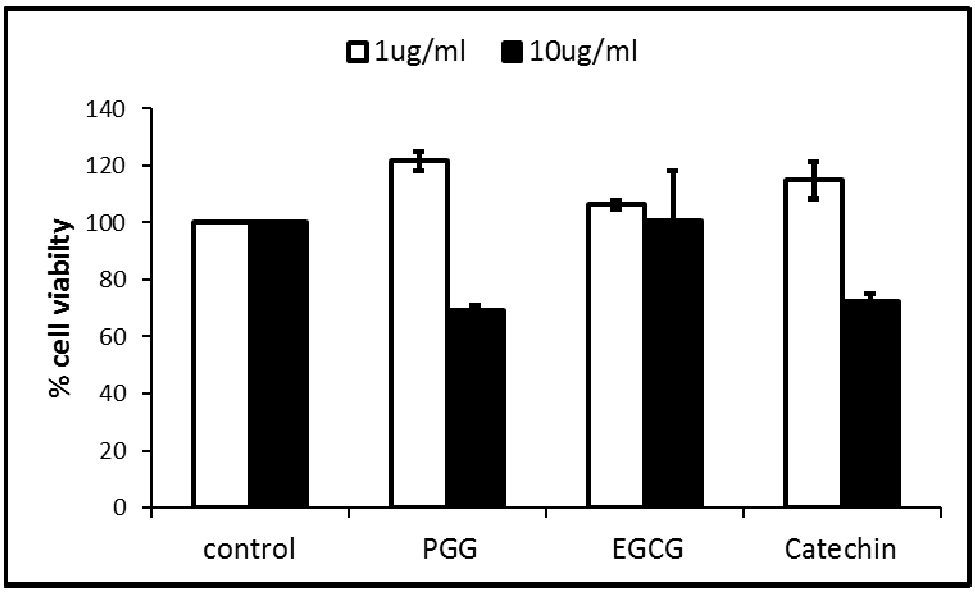

Figure 5.11:MTT cell proliferation assay after polyphenol treatment

Tropoelastin and cross-linked elastin production

Figure 5.12 A depicts the cross-linked insoluble elastin deposited by healthy vascular cells after 14 days. Evidently, all the polyphenols significantly enhanced the deposition of insoluble elastin. Interestingly, the quantity, kinetics and dynamics of

tropoelastin released in the media were not changed by the addition of polyphenols (Figure 5.12 B).

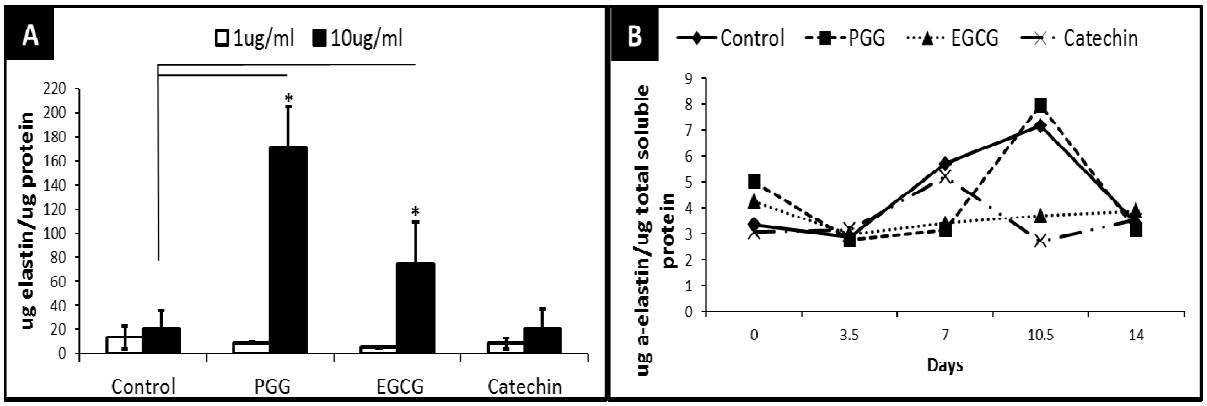

Figure 5.12:(A) Shows the deposition of insoluble elastin by healthy RASMCs in response to polyphenols (B) shows the tropoelastin produced in the media in response to polyphenols

The exact same trends were also observed in passage matched aneurysmal cells (Figure 5.13 A, B). Polyphenols added at 1 µg/ml did not exert any elastogenic effects, at least after 14 days in culture. At 10 µg/ml, PGG induced ~8-fold greater mature elastin in healthy RASMCs and 6-fold more elastin in aneurysmal EaRASMCs. EGCG at the same concentration, increased elastin fiber deposition by ~ 4 times in RASMCs and 2 times in EaRASMCs. Catechins showed ~ 1.7 fold greater insoluble elastin deposition in EaRASMCs. Due to the infectivity of polyphenols at 1 µg/ml in elastic matrix enhancement, all further studies were carried out using polyphenols at 10 µg/ml concentrations.

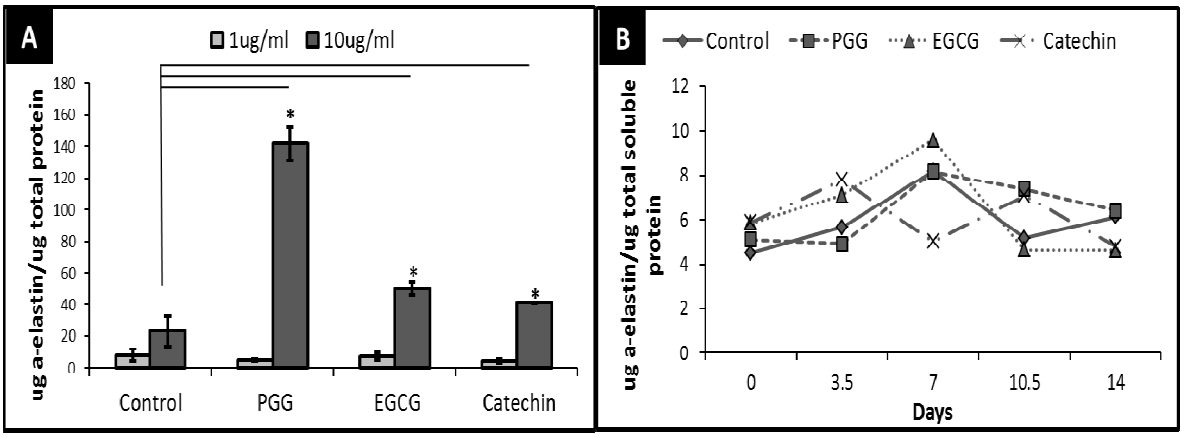

Figure 5.13: (A) Shows the deposition of insoluble elastin by aneurysmal EaRASMCs in response to polyphenols (B) shows the tropoelastin produced in the media in response to polyphenols

Figure 5.14 A is a comparative graph displaying the total tropoelastin elastin production by RASMCs and EaRASMCs. None of the polyphenols influenced the cellular tropoelastin production after 14 days by both healthy and aneurysmal cells. Counter-intuitively, aneurysmal cells released ~ 1.6 times greater soluble tropoelastin compared to healthy cells, however, failed to translate into increased matrix production in a comparable time period of 14 days (Figure 5.14 B). In addition, even with unchanged levels of tropoelastin, healthy RASMCs deposited nearly double the elastin quantity in the presence of polyphenols when compared to aneurysmal EaRASMCs.

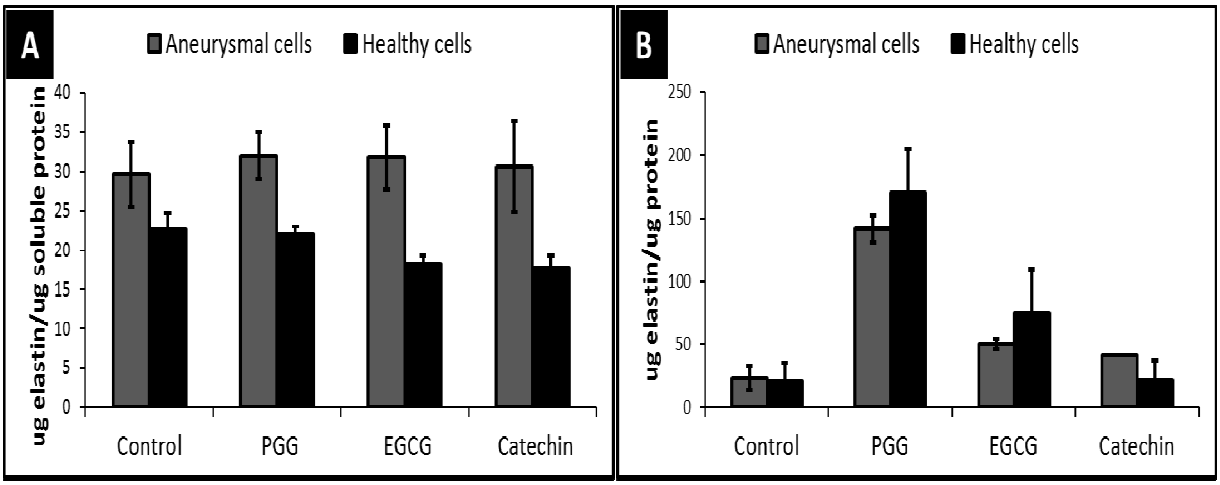

Figure 5.14: A) Total tropoelastin released by RASMCs and EaRASMCs after 14 days (B) total insoluble elastin deposited by RASMCs and EaRASMCs after 14 days of treatment with 10 µg/ml polyphenols

LOX functional activity

The trend curves of LOX activity revealed that healthy RASMCs maintain relatively stable expression and activity of LOX throughout the culture period (Figure 5.15 A); however, there is a progressive increase in the LOX activity in the presence of polyphenols in aneurysmal EaRASMCs (Figure 5.5 B), which is not as pronounced in untreated control groups.

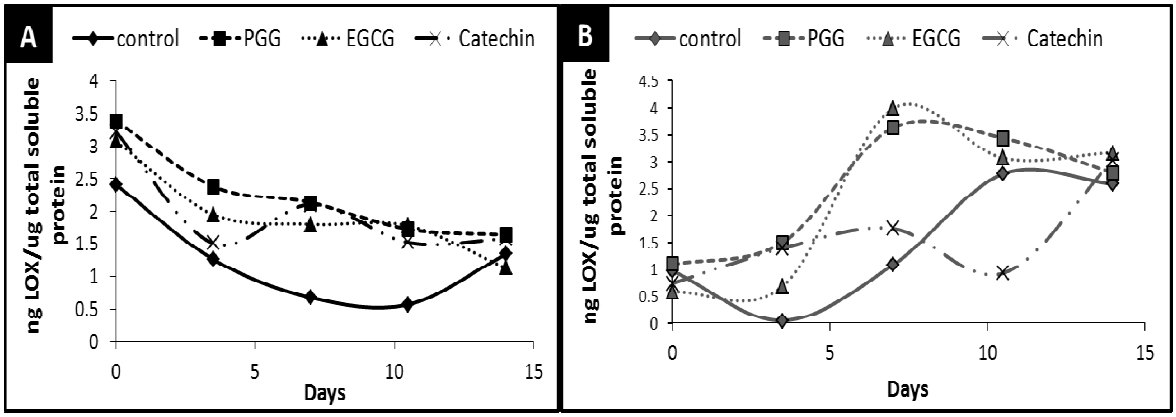

Figure 5.15: LOX released by (A) RASMCs and (B) EaRASMCs with 10 µg/ml polyphenols treatment over 14 days

Furthermore, the overall activity of LOX over 14 days was significantly greater in untreated healthy RASMCs compared to EaRASMC (~ 2 times). PGG addition enhanced LOX activity by ~ 4 times in healthy and 5 times in aneurysmal cells. Following similar trends, EGCG up-regulated LOX activity ~ 3-fold and catechin by 1.5 times in RASMCs and EaRASMCs. (Figure 5.16)

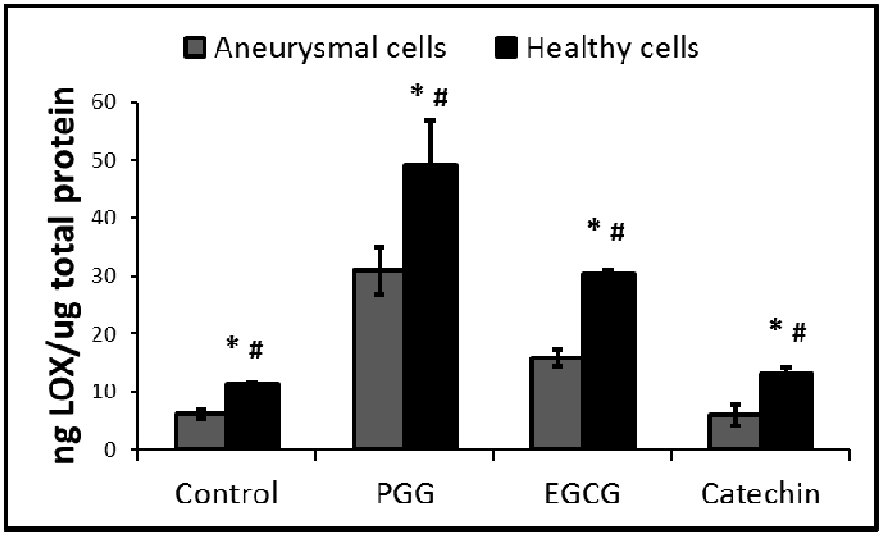

Figure 5.16: Total LOX produced by RASMCs and EaRASMCs after 14 days.
*** - significant difference compared to healthy control cells**
 # - significant difference compared to aneurysmal cells

ELN, Fib-1 immunofluorescence

All cell cultures attained confluency and deposited sufficient extracellular matrix (confirmed by routine phase contrast microscopy) by the end of 14 days. The cells were fixed and immunolabeled for elastin and fibrillin-1. It was noted that cell density was visibly lower in the treatment groups as expected from the MTT results. Immunofluorescence micrographs of 14 day cultures of EaRASMCs showed higher amounts and well-oriented elastin fibers (green fluorescence) in the polyphenol groups (Figure 5.17 B, C, D) as opposed to the control groups (Figure 5.17 A). Nuclear DAPI stain reveals relatively uniform cell layers in all the groups, however, the groups treated with PGG and EGCG showed granular localization of elastin fibers indicating greater deposition of elastic matrix.

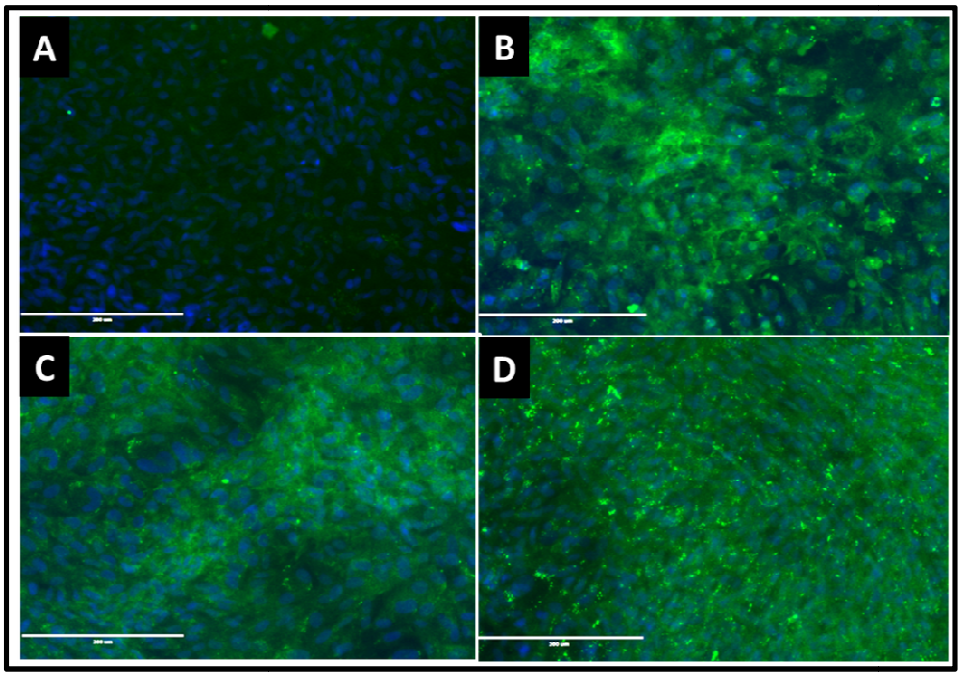

Figure 5.17:Immunofluorescence for elastin by EaRASMC in (A) control, (B) PGG, (C) EGCG, (D) catechin groups

Fibrillin-1 immunofluorescence also showed slightly greater staining in the PGG treated groups (Figure 5.18 B) compared to control cell layers (Figure 5.18 A).

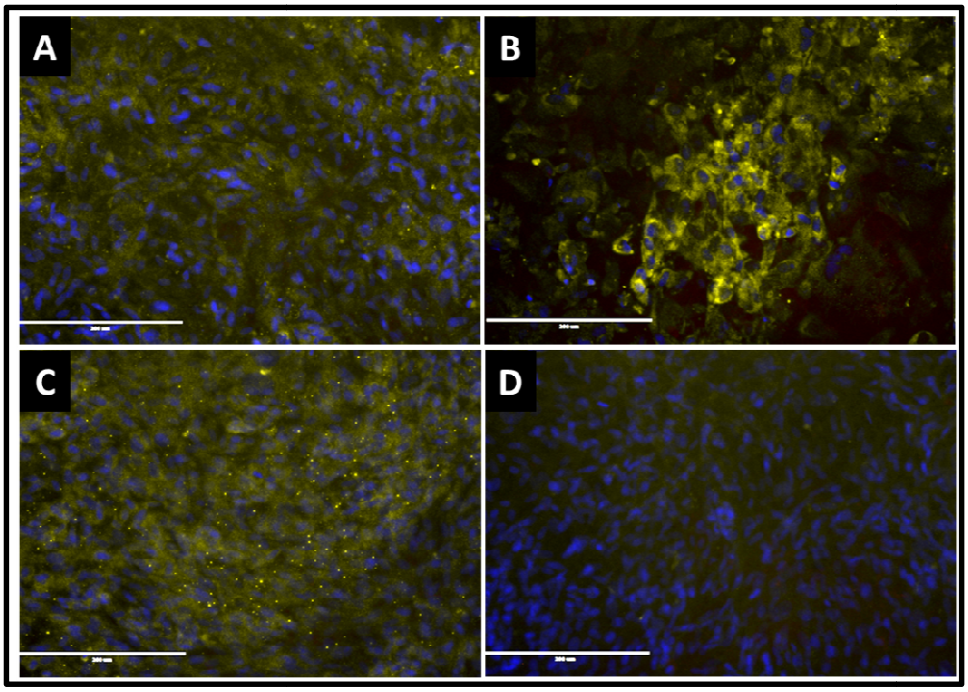

Figure 5.18:Immunofluorescence for Fibrillin-1 by EaRASMC in (A) control, (B) PGG, (C) EGCG, (D) catechin groups

Elastin and LOX relative gene expression

RT-PCR studies revealed that compared to healthy RASMCs, EaRASMCs have ~ 2-fold elastin gene expression. PGG groups were used as a representative polyphenol for mRNA expression studies. Addition of PGG did not significantly alter the relative gene expression of elastin gene, implying the extracellular involvement of PGG in the process of elastic matrix deposition (Figure 5.19).

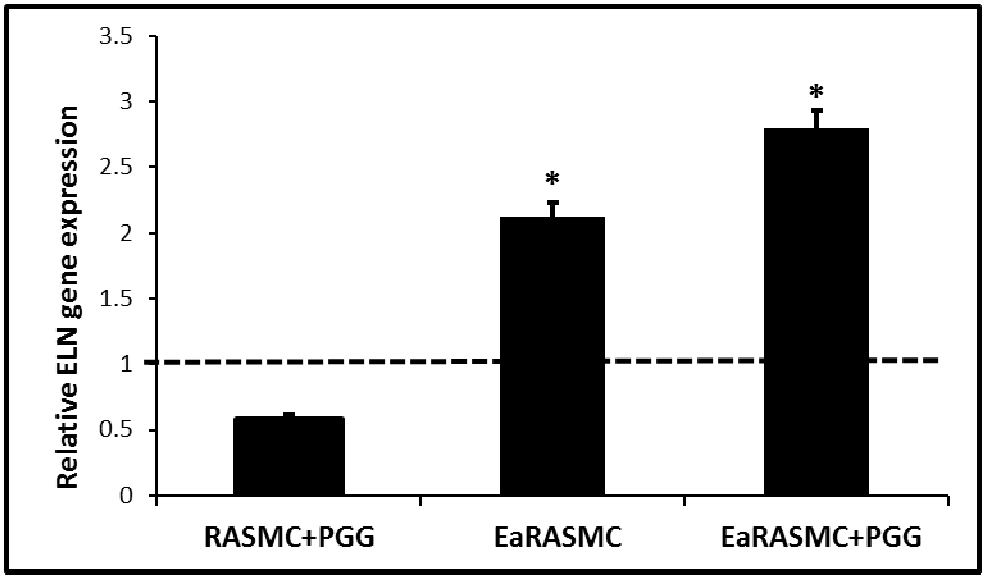

Figure 5.19:Relative gene expression of elastin gene by RASMC and EaRASMC. All groups normalized to β-2mg expression and healthy RASMC was used as baseline control.

Unexpectedly, there was a dramatic increase (~9 fold greater) in the relative gene expression of LOX in the EaRASMCs groups compared to the healthy RASMCs (Figure 5.20), which seemed down-regulated by the addition of PGG. The gene expression of LOX did not translate into co-relatable enzymatic activity. Speculatively, defunct translation of the LOX gene in aneurysmal cells may be the causal factor for impaired elastin deposition.

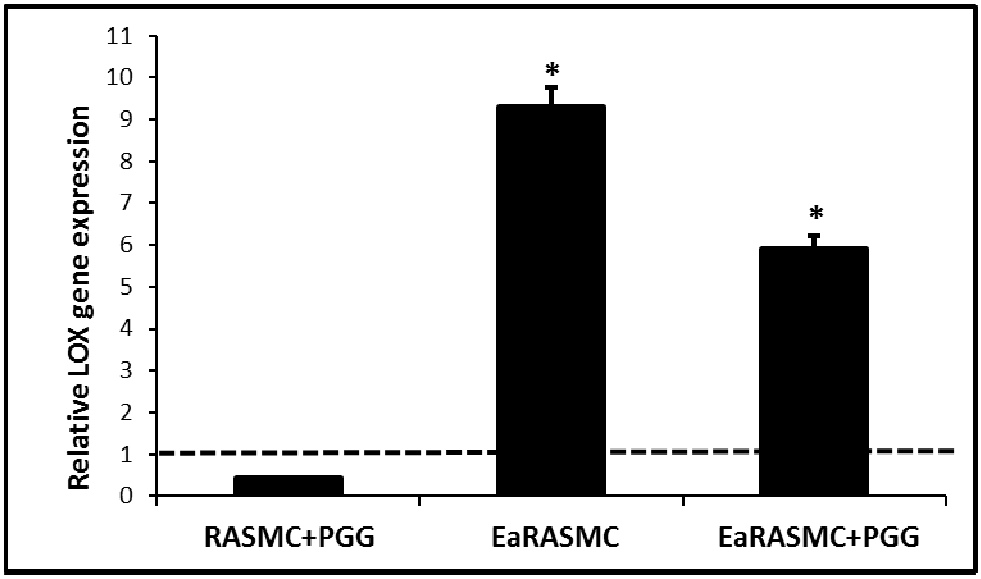

Figure 5.20:Relative gene expression of LOX gene by RASMC and EaRASMC. All groups normalized to β-2mg expression and healthy RASMC was used as baseline control

MMP-2 enzymatic activity

Gelatin zymography revealed that the total MMP-2 (66 kDa) activity was ~ 2-fold greater in the EaRASMCs when compared to healthy RASMCs, which was reduced by ~ 62% ± 12.9% by PGG, 58% ± 2.3% by EGCG and 67% ± 4.4% by catechin. Healthy cells did not display any difference in their MMP-2 activity under the influence of polyphenols. (Figure 5.21)

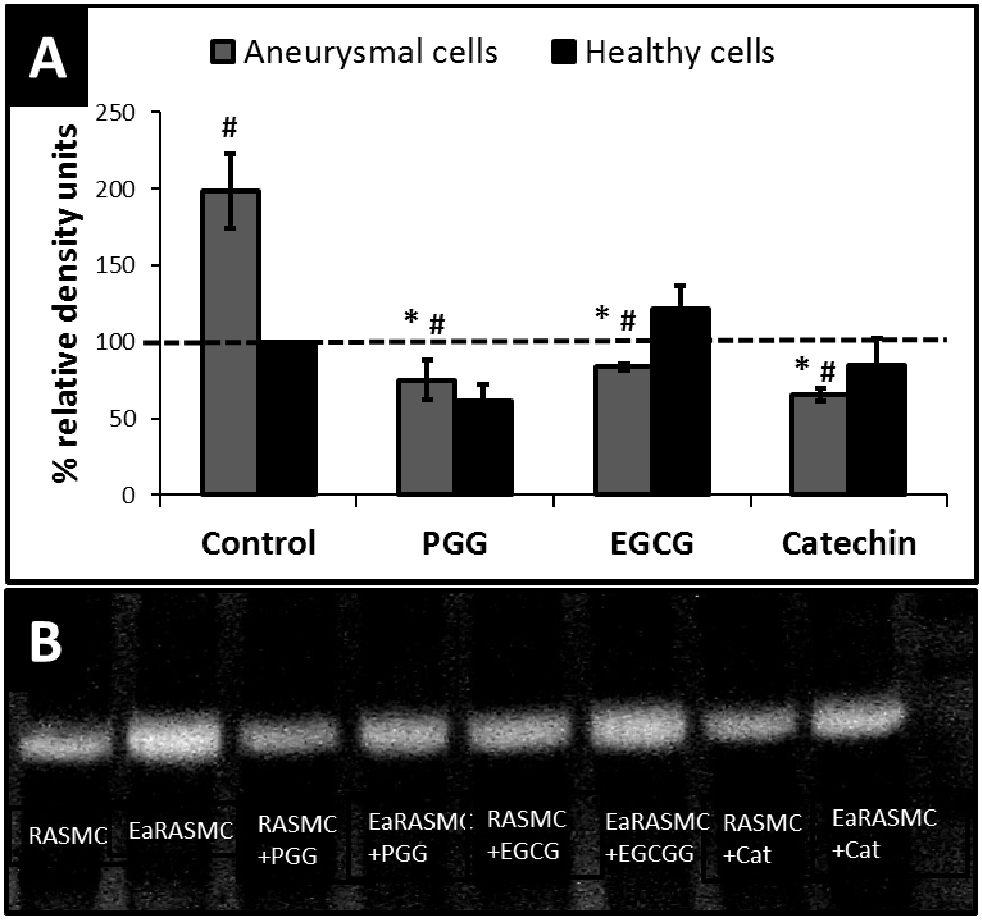

Figure 5.21:(A) Relative density units of MMP-2 cellular activity (B) clear bands indicating MMP-2 activity by cells

5.4 Discussion

Abdominal aortic aneurysm (AAA) is a life threatening vascular disease with no available pharmacological therapy. AAA is a multi-factorial pathology involving several biological, physical, bio-mechanical and hemodynamic factors that eventually lead to the pathological thinning of the artery, ballooning and rupture. Current clinical repair options include surgical repair and deployment of endovascular stent grafts. Both these options are surgically invasive, have their own demerits and do not provide a permanently viable

cure to the damaged artery. Given the nature of the disease, poor turnover of elastin fibers, and eventual failure being a result of acute mechanical loss of elastin, the ideal treatment option would be a combination of strategies working synergistically towards preventing elastolytic degradation, halting proteolytic activity, stabilizing matrix and regenerating arterial proteins and matrix. In a series of prior publications we have investigated the interactions of polyphenolic compounds with elastin and its ability to stabilize elastin as a potential AAA treatment.[30,233,305,310] It has been previously demonstrated that tannic acid and PGG bind to elastin and render it resistant to elastolytic damage, which makes it an attractive elastin-stabilizing agent for cardiovascular prosthesis.[310] In a relevant rodent model, a single time peri-adventitial application of PGG has also prevented the formation and progression of AAA.[305] Although the polyphenols under investigation proved valuable in stabilizing healthy aortic elastin, the interaction between polyphenolic compounds and tropoelastin in the process of elastogenesis was never studied. The aim of this work was to investigate the biological aspect of polyphenols like PGG, EGCG and catechin in aiding in the process of elastogenic matrix formation in a cell-culture model.

The first finding of our studies was that polyphenols rapidly bind to insoluble mature elastin and the interaction is dose dependent. These trends are in agreement with previous studies.[30] The binding kinetics is a time and concentration dependent process. At concentrations of 1000 µg/ml polyphenol solution, 14 µg PGG/mg elastin, 23 µg EGCG/mg elastin, 29 µg catechin/mg elastin were bound to elastin after 48 hours. At these treatment concentrations, pure elastin preparations showed significant protection

against elastase degradation (Figure 5.4). MMP mediated elastin degradation is a characteristic feature of AAA leading to progressive degeneration of elastin and expansion of aorta.[311,312] Elastases from various sources such as, macrophage elastase and neutrophil elastase attack the hydrophobic domains of elastin resulting in enzymatic cleavage.[313] Plant derived polyphenols like tannins and flavanols have demonstrated their potential in inhibiting human leukocyte elastase activity [314] and preventing MMP-2/-9 activity in cancer cells.[315] Catechin derivatives have also displayed MMP inhibition therefore preventing elastin degradation.[316] Use of polyphenols such as PGG, EGCG, and Catechin can therefore provide a novel strategy for stabilization and prevention of AAA progression.

Stabilizing aneurysmal elastin and protection against proteolytic damage resolves only one half of the pathological complication of AAA. A larger challenge in treating AAA is the inherently poor elastin turn-over by adult cells[317,318] that prohibits the repair and regeneration of degraded elastin. Knowing polyphenols bind to hydrophobic amino acid residues with strong affinity,[229] we hypothesized that cellular tropoelastin will interact rapidly with polyphenols helping the process of coacervation and self-assembly accelerating the process elastin crosslinking, thereby enhancing elastic fiber deposition. In this current in vitro cell culture study, we demonstrated that addition of polyphenols to healthy vascular cells enhances the mature cross-linked elastin fiber deposition at 10 µg/ml concentration. Anti-proliferative effects of polyphenols have been established in literature before[319], however only PGG at 10 µg/ml displayed anti-proliferative tendencies in our cell culture set-up (Figure 5.11). Although encouraging, we wanted to

verify if similar trends are evident in a diseased model as well. For this purpose, we used late-stage aneurysmal cells and treated them with polyphenols. The motive behind using cell culture models was for better monitoring of intra-cellular and extracellular dynamics. The aneurysmal cells were procured from rats with advanced abdominal aortic aneurysm induced by luminal elastase perfusion, the description and characterization for which has been described elsewhere.[308] Under the influence of polyphenols, aneurysmal cells deposited significant higher quantities of matured elastin compared to untreated control groups. Interestingly, the trend curve of tropoelastin did not very with or without the addition of polyphenols (Figure 5.12 B, 5.13 B). Furthermore, the total tropoelastin released by cells remained constant in all the groups; in both healthy and aneurysmal cells (Figure 4.14 A). This suggests that polyphenols exert their elastogenic effect extra-cellularly and do not directly enhance the cellular tropoelastin production. Surprisingly, the total tropoelastin production was higher in diseased cells compared to healthy cells. This observation is similar to the past studies showing that AAA tissues produce greater tropoelastin compared to healthy tissues.[320 321] However, failure of desmosine crosslinks cause ineffective elastin maturation. As per our findings, the mRNA expression of elastin by aneurysmal cells is also greater compared to healthy cells (Figure 5.19). This may be compensatory feedback mechanism to replenish degraded elastin in AAA. However, elastic fiber assembly may be the limited by factors acting at the post-transcription level. It should be noted here that the addition of PGG (representative polyphenol) did not alter the tropoelastin mRNA expression, therefore substantiating the external role of PGG in elastic matrix formation.

To further understand the mechanisms involved in the process of elastic fiber deposition, we evaluated the LOX mRNA expression and enzymatic activity. LOX is a vital enzyme required in the process of elastin crosslinking[42] and is strongly suppressed in aneurysmal tissues.[321] Our results indicate that aneurysmal cells have significantly lower LOX activity when compared to healthy cells (Figure 5.16), which is, however, increased in the presence of polyphenols. Although the mRNA expression does not correlate with the post-translation enzymatic activity of LOX, it appears that LOX is regulating the crosslinking of elastin in the cell layers.

To further elucidate the sole interactions between tropoelastin and polyphenols, we incubated recombinant tropoelastin with polyphenols to study the self-assembly kinetics of elastin in-vitro. Due to the presence of excess hydrophobic domains in tropoelastin, coacervation is an endothermic and entropically-driven process. Self-assembly can be broadly divided into reversible "coacervation phase" leading to increasing turbidity in solution and irreversible "maturation phase" causing the growth of the coacervates.[57] Microfibrillar scaffolding proteins such as MAGP-1, fibulin-5 are known to interact with tropoelastin coacervates and also recruit LOX for the oxidation of lysine residues leading to formation of intermolecular crosslinks.[322,323] The presence of microfibrillar proteins have also shown to increase tropoelastin coacervation and retard maturation in-vitro that aids in better alignment of coacervates and systematic oxidation of lysine residues.[48,57,322] The importance of increased coacervation lies in greater and more specific increase in the intermolecular structure of individual tropoelastin molecules facilitating downstream elastogenic events. Our results suggest that the addition of

polyphenols dramatically alter the self-assembly kinetics of tropoelastin. The interaction of polyphenols with tropoelastin is evident in the coacervation phase which is significantly accelerated compared to pure tropoelastin in solution (Figure 5.10). While control tropoelastin molecules enter maturation by ~ 20 minutes, PGG takes ~ 180 minutes, EGCG and catechin takes ~200 mins to start maturing. In addition, the polyphenols also increase the rate of coacervation as evident from the sharp increase initial turbidity. It is thus a safe conclusion that polyphenols dramatically aid in the process of tropoelastin self-assembly; partly by increasing the rate of coacervation and partly by inhibiting maturation, thereby providing greater inter-molecular interaction for lysine oxidation.

5.5 Limitations of the studies

There are certain limitations to this study. Firstly, the ranges of polyphenol concentrations used were different in the elasto-protective studies and elasto-regenerative studies (10-1000 times more in the elasto-protective studies). The intent of this experiment was to determine the ability of polyphenols to provide elastolytic protection. High concentration of polyphenol (1000 µg/ml) is extremely toxic in cell culture system, whereas low concentrations of polyphenol (10 µg/ml) fail to show elasto-protective effects. Previously, a single time application of PGG on rat aorta at ~ 3000 µg/ml did not show any hepatotoxic effects.[225] Therefore, it can be assumed that in-vivo applications of polyphenols will have higher tolerance compared to cell culture studies. Secondly, the polyphenols were dissolved in DMSO, the combined effect of polyphenols and DMSO could have potentially toxic effects on the cells. From the studies done, all the

experiments were normalized to total soluble protein for fair comparison; however there was a significantly lower protein concentration in the groups treated with PGG (data not shown). This might have caused an over-estimation of the quantities of insoluble elastin reported. Regardless, the absolute quantities of cross-linked elastin in the PGG groups were still higher compared to control groups. Thirdly, our results show that polyphenols bind to insoluble elastin and protect from degradation. It is a strong possibility that polyphenols are merely binding to cross-linked elastin in cell culture system and preventing it from MMP mediated degradation. It is also unclear if polyphenols are exerting their effects indirectly by reducing MMP concentrations (as seen in the Figure 5.21). Finally, elastin synthesis and fiber assembly is a well-orchestrated, complex and relatively poorly understood process (as discussed in Chapter 2). We have not studied the effect of polyphenols on critical assembly proteins like fibulin-4, 5, latent TGF-β binding protein, fibrillin-2, and matrix associated gla protein-1. It is clear that polyphenols accelerate coacervation; however maturation phase is a complex interplay of all the above mentioned proteins. Further experiments need to be done to understand clearly the exact stage of elastogenesis at which polyphenols are exerting their effect.

5.6 Conclusion

We show that use of polyphenols works dually, firstly by binding to cross-linked insoluble elastin and rendering it resistant to elastolytic degradation; secondly by interacting with monomeric tropoelastin and accelerating the elastic matrix deposition by vascular cells. Thus such treatments could be locally applied to treat and repair elastic fiber degradative diseases such as aortic aneurysms. Such treatments would halt the

progression of elastic fiber degradation and at the same time allow cell secreted tropoelastin molecules to assemble to create new elastic fiber assembly so that degradative damaged could be repaired and the disease can be reversed.

CHAPTER 6

NANOPARTICLE TARGETING TO INJURED VASCULATURE FOR IMAGING AND THERAPY

6.1 Introduction

Targeting drugs to diseased vessel walls is difficult. Due to high shear flow conditions in arteries, oral, parenteral, or intra-arterial administrations of therapeutics have shown limited success and unwanted systemic side effects in treating vascular diseases.[324] For instance, anti-coagulants administered for coronary thrombotic occlusions present with severe unwanted side-effects of hemorrhage[325] and systemic doxycycline delivery for treatment of abdominal aortic aneurysm (AAA) have negligible therapeutic benefit due to side-effects such as cutaneous photosensitive reactions, tooth discoloration, gastro-intestinal symptoms and yeast infection.[21] In order to maximize therapeutic benefit and minimize off-target effects, a considerable effort has been spent in developing local vascular drug delivery. Various approaches to target vasculature are mostly focused on cell markers on activated endothelium, vascular smooth muscle cells, or inflammatory cells such as macrophages. Although abundantly over-expressed in inflammatory conditions, these markers provide limited targeting as they are heterogeneous, transiently expressed in the vasculature and also undergo physiological receptor recycling. As an alternative approach, we developed a novel biodegradable nanoparticle system that can be targeted to the site of vascular degraded elastic fibers which is a hallmark of many vascular diseases. For example, elastin degradation is

observed in vascular calcification in age-related elastocalcinosis (Monckenberg's sclerosis),[326] diabetes[327] and end-stage renal disease.[328,329] Another very different yet serious disease of vascular matrix is aneurysm. In particular, abdominal aortic aneurysm (AAA) is a degenerative disease of the artery characterized by severe protease-mediated degradation of extracellular matrix, especially elastin, causing dilatation of the aortic wall leading to rupture and in certain cases death.[330] In addition, vascular proliferative diseases of smaller arteries including coronary arterial occlusion and atherosclerotic mediated stenosis share common pathological features such as elastin degradation[331,332] and accumulation of vascular smooth muscle cells in the intima.[333] Thus, successful targeting of only degraded elastin provides the advantage of particle retention in the extracellular matrix as opposed to rapid cellular uptake thereby enabling delivery of several agents to the extracellular space.

In this chapter, we show that elastin specific targeting of nanoparticles is possible by the delivery of Polylactic acid (PLA) nanoparticles decorated with elastin-specific antibodies on to the surface of the particles. This minimally invasive technique can augment drug concentrations at the site of vascular damage, mitigate the undesirable effects of drugs and increase drug efficiency.

6.2 Methods

Fabrication of nanoparticles

Poly(D,L-lactide) (PLA) nanoparticles were prepared using a nanoprecipitation method based on solvent diffusion. Briefly, 10 mg PLA (Average M_W 75,000-120,000) (Sigma Aldrich, St.Louis, MO) was dissolved in 1ml acetone (VWR International, Radnor, PA). ~2.5 mg of 1, 2-distearoyl-*sn*-glycero-3-phosphoethanolamine-N-[maleimide (polyethyleneglycol)-2000] (PEG maleimide) (Avanti Polar Lipids, Inc., Alabaster, AL) and 250 µg of 1, 1-dioctadecyl-3, 3, 3, 3-tetramethylindotricarbocyanine iodide (DIR) (Biotium, Inc., Hayward, CA) were added to the PLA solution in acetone. ~300 µl of polymer solution was added drop-wise at a uniform rate to 8 ml of water kept under sonication in a water bath sonicator and solutions were sonicated for 1 hour. The resulting suspension contained nanoparticle with encapsulated DIR dye. The particles were purified 3 times by centrifugation at 3000×g for 15 minutes followed by re-dispersion in water.

Characterization of particle size and surface charge measurement

Particle size in suspension was determined using 90Plus Particle Size Analyzer (Brookhaven Instruments Co, Holtsville, NY). 10 µl of nanoparticle suspension was diluted in 3 ml of HPLC-grade water in a disposable plastic cuvette. Particle size and degree of aggregation were visualized using an Asylum Bio-MFP3D atomic force microscope (Asylum Research, Santa Barbara, CA).

Surface charge measurements (zeta potential) were made by dissolving stock solutions as 1:100 in water in a disposable cuvette and the zeta potential was measured using the 90Plus Particle Size Analyzer (Brookhaven Instruments Co, Holtsville, NY). The zeta potential was expressed in millivolts (mV) as a combined mean (±SD).

Nanoparticles were characterized using an atomic force microscope (Asylum Bio-MFP3D, Asylum Research, Santa Barbara, CA). AFM experiments were conducted in tapping mode in ambient conditions using Olympus AC240TS cantilevers backside-coated with aluminum with a spring constant of ~2 N/m. Nanoparticle samples were diluted 50 times, and then a 100 µl drop was placed onto freshly peeled Muscovite mica surface, incubated for 15 minutes, then dried under air flow.

Nanoparticle conjugation with antibodies

10 µg of rabbit anti-rat elastin antibody (United States Biological, Swampscott, MA) or rabbit anti-rat IgG antibody (Thermo Scientific, Rockford, IL) were thiolated using 34 µg of freshly prepared Traut's reagent (G-Biosciences, Saint Louis, MO) in HEPES buffer for 1 hour. Thiolated antibodies were washed thrice with HEPES buffer (20 mM, pH=9.0) and dialyzed through 10 kDa MWCO filters to remove Traut's reagent. Purified and thiolated antibodies were then added to particles (4µg antibody / mg polymer) and incubated overnight at room temperature for conjugation. After conjugation antibody coated particles were purified twice (3000×g for 15 minutes) and suspended in PBS at 4°C until further use. For optimization experiments, 0.1-25µg antibody/mg polymer was used.

Antibody concentration and correlation

An independent set of experiments was performed to establish the effect of antibody concentration on the binding yield of antibody to the particles. The PLA nanoparticles were prepared as described earlier, known amounts (0.1-25µg) of Alexa fluor 594 conjugated IgG solution in HEPES was added to 1 ml of 1 mg/mL PLA nanoparticles (final volume was 1.025 ml in all cases) and incubated overnight. Samples were centrifuged, and supernatant was analyzed using fluorescent spectrometry. Three replicates were used for each concentration. A calibration curve was plotted from standard solutions (0.1-25µg of antibody in 1.025 ml of HEPES) fluorescence data obtained under similar conditions. Calibration curve was fitted using 2^{nd} order polynomial equation, and a reverse equation for accurate calculation of antibody content from fluorescence data was derived. The differences in the fluorescence of bound and unbound dyes were used to calculate the binding yield percentage. Concomitantly, the number of antibody molecules per nanoparticle was calculated by dividing the number of antibody molecules by the average number of nanoparticle (n) using the following equation:

$$n = 6m/(\pi \times D^3 \times \rho)$$

where m is the nanoparticle weight, D is the mean diameter determined by DLS, ρ is the density (assuming PLA density of 1.25 g/cm^3).

Transmission electron microscopy of immunogold-stained nanoparticles

The nanoparticles were prepared as described earlier. The IgG antibody coated nanoparticles (INPs) (30µg) were incubated with 10 nm gold stained goat-anti-rabbit IgG ($5X10^{11}$ gold particles) (Sigma Aldrich, St.Louis, MO) overnight in 0.018M tris buffered saline (TBS), pH=8, with 0.9% bovine serum albumin and 17% glycerol. Following incubation, the particles were washed twice with TBS to remove unbound antibodies at 14,000×g for 15 minutes, deposited in a formvar-coated copper grid followed by negative staining with 2% phosphotungstic acid and examined directly with transmission electron microscopy.

Cytotoxicity and cellular uptake of ENPs

Rat aortic vascular smooth muscle cells (passage 6) were treated with 2.5, 10 and 25 µg elastin antibody concentration and 100, 500 µg/ml PLA concentrations to evaluate cytotoxicity and cellular uptake of ENPs. Cells were seeded at 10,000 cells/cm^2. At 70% confluency, cells were incubated with nanoparticles for 4 hours following which cell viability was determined using a LIVE/DEAD Cell Viability assay (Molecular Probes, Grand Island, NY). Cells fluorescing green are considered alive while cells fluorescing red are considered dead. Additionally, proliferation of cells was estimated using the MTT (3-(4,5-Dimethyl-2-thiazolyl)-2,5-diphenyl-2H-tetrazolium bromide) assay. Briefly, 5 mg of MTT (Sigma Aldrich, St.Louis, MO) was dissolved in 10 ml of serum-free media and added to cells. After 4 hours, media was carefully aspirated and the insoluble formazan dye was collected with dimethyl sulfoxide (DMSO) (Sigma Aldrich, St. Louis, MO). Absorbance was read at 560 nm and normalized to control (no treatment) readings.

To visualize the internalization of nanoparticles, nanoparticles of different sizes and surface charge were tested. Low molecular weight PLA (Average M_W 9,000) were used to prepare nanoparticles by the exact same procedure as mentioned earlier. To modulate the surface charge density, purified ENPs were incubated with 0.2 mg poly-L-lysine / mg of polymer (Sigma Aldrich, St. Louis, MO, Average M_W 150,000-300,000) for 2 hours at room temperature. Following incubation, the nanoparticles were thoroughly purified 2 times (centrifuged at 7000×g for 2 hours) to eliminate excess poly-L-lysine and re-suspended in water. 24 hours after nanoparticle incubation, the cells were thoroughly washed with Phosphate buffered saline (PBS) to eliminate unbound nanoparticles, fixed with 4 vol.% formaldehyde, labeled with the lipophilic membrane stain DiI (Invitrogen, Carlsbad, CA), and then mounted with Vectashield containing the nuclear dye 40 ,6-diamidino-2-phenyindole (DAPI; Vector Laboratories, Burlingame, CA). Imaging of cells was performed using fluorescent microscopy (EVOS fl. Microscope, Advanced Microscopy Group, Bothell, WA).

Ex-vivo nanoparticle binding studies for elastase treated aorta

High purity porcine pancreatic elastase (Elastin products company, Owensville, Missouri) was prepared (5U/ml) in 100mM Tris Buffer, 1mM calcium chloride, 0.02% sodium azide, pH 7.8. Aortas from Sprague-Dawley rats were explanted, rinsed and treated with elastase for 10, 20, 30, 60 mins. The aortas were clamped on either ends, and ENPs/INPs (prepared following the same method as described earlier) were injected intra-luminally for 1 hour at room temperature. Following injection, the aortas were thoroughly washed (3 times) with PBS to minimize non-specific adherence of

nanoparticles. Simultaneously, ENPs/INPs were also injected in control aorta (without elastase treatment). Following nanoparticle infusion and washing, the aortas were lyophilized. The dry weights of the aorta were recorded. A small portion was embedded in Tissue Tek OCT compound for histological analysis. The lyophilized aorta were homogenized using a PowerGen 125 homogenizer (Fisher Scientific, MA) in Dimethyl sulfoxide (DMSO), placed in an orbital shaker for 1 hour, 37°C, 200 rpm. Tissues were centrifuged for 15 minutes at 4000×g. The supernatant was purified by filtering through 0.2 µm nylon membranes were loaded into the HPLC for DIR quantification.

A separate set of experiments was conducted to evaluate the effect of antibody concentration on nanoparticle surface and binding efficiency to elastase treated aorta. ENPs were fabricated with 0.1-25µg antibody/mg polymer. Rat aortas were treated with porcine pancreatic elastase for 60 minutes and washed 3 times with PBS. 1 mg ENP suspension (0.1-25µg antibody/mg polymer) was injected intraluminally to each rat aorta. Aortae were washed, lyophilized, weighed, digested and DIR was quantified, as described previously.

In vivo nanoparticle targeting – calcium chloride injury model

Adult male Sprague-Dawley rats weighing approximately 250-300 g (Harlan Laboratories, Indianapolis, IN) on a normal diet were used for creating local elastic fiber damage. All animal procedures were in accordance with the local, state and federal regulations and approved by the Institutional Animal Care and Use Committee.

Vascular injury was created in rats (n=6) by peri-adventitial application of 0.5M $CaCl_2$ for 15 minutes to the infra-renal abdominal aorta using a strip of pre-soaked sterile cotton gauze. The area was briefly rinsed with warm saline and the abdominal cavity was closed with subcutaneous suture, followed by surgical staples. The elastin degradation was allowed to develop for 10 days.[334] After 10 days, the rats were anesthetized, PLA anti-elastin nanoparticles (ENPs) or PLA IgG control nanoparticles (INPs) were injected in 0.3% rat serum albumin (Sigma Aldrich, St.Louis, MO) through the tail vein of the rats (10 mg of polymer/kg body weight). The rats were euthanized 24 hours post injection. The harvested aortae were imaged using Caliper IVIS Lumina XR (Hopkinton, MA) with Ex/Em of 745/795.

Brain, heart, blood, muscle skin, liver, kidneys, spleen, and lungs, were examined for fluorescence for determining bio-distribution. Only the organs that presented with fluorescence were lyophilized and the total fluorescence was normalized to the total dry weight of each organ. Targeting was calculated as follows:

$$\%\text{targeting} = \left(\left(\frac{fluorescence\ in\ aorta}{total\ fluorescence\ in\ all\ organs}\right) * 100\right) / (\textit{dry weight of organ})$$

The aortic injury was a non-spontaneous locally induced damage. Hence, only the damaged portion of the aorta was considered “diseased (potential target)” and the dry weight of the local diseased portion was assumed to be ~10 mg (from separate experiment).

In vivo nanoparticle targeting – Warfarin + Vitamin K model

6 week old male Sprague Dawley rats (n=6) were given subcutaneous injections Vitamin K1 (10 mg/ml, 15 mg.kg-1.day-1 subcutaneous injection, every other day) and Warfarin (20 mg.kg-1.day-1) in drinking water. Small needles (25 G or smaller) were used and the subcutaneous injection sites were rotated between the 4 quadrants of the back to reduce stress. This routine was maintained for 3 weeks. The control group rats were age-matched and maintained normally with no treatment. At the end of 3 weeks, elastin antibody coated nanoparticles (ENPs) were injected through the tail vein of the rats. Following 24 hours of circulation, whole animals were euthanized and imaged using Calliper IVIS imaging system. The individual organs were also imaged to calculate the biodistribution and targeting of the nanoparticles. Explanted aorta were rinsed with phosphate buffered saline (PBS), embedded in Tissue CT compound, and frozen at -80°C.

Local delivery of nanoparticles to damaged abdominal aorta

For local NP delivery, injury to the abdominal aorta was created as mentioned earlier. After 10 days, the abdominal cavity of the anesthetized rat was exposed, the injured infra-renal aorta was clamped on either ends, catheterized, and particles (10 mg polymer/kg body weight) were locally perfused intra-luminally for 5 minutes (100 µl/min). Following local perfusion, blood flow in the aorta was established and animals were allowed to recover. After 24 hours, animals (n=4) were sacrificed and aortic sections were imaged using Caliper IVIS Lumina XR (Hopkinton, MA) with Ex/Em of 745/795.

Nanoparticle clearance study

To assess the clearance time of nanoparticles in the body, adult male Sprague Dawley rats were injected with INP (same concentration and preparation as mentioned earlier). The rats were imaged every other day for 8 days to observe the rate of clearance of nanoparticles. Live imaging was performed using Caliper IVIS Lumina XR with Ex.EM of 745/785. The fluorescent signal was normalized to the total body weight of the rats.

Histological assessment

Explanted aorta were rinsed with phosphate buffered saline (PBS), embedded in Tissue Tek OCT compound (Sakura Finetek, U.S.A. Inc., Torrance, CA), and frozen at -80°C. 6 μm thick sections were cut using a cryostat (Microm HM 505 N, Mikron Instruments, Inc.) and collected on glass slides. Sections were acclimated at room temperature for 5 minutes, fixed in cold acetone for 5 minutes and stained with Verhoeff's Van Gieson (VVG) (Poly Scientific, Bay Shore, NY) to study structural integrity of elastin. Sections were also stained routinely with H&E and Alizarin red stain to observe calcium deposits.

Quantitative assessment

DIR was quantified in all ex-vivo experiments using multi lambda fluorescent detector Waters 2475 utilizing Waters HPLC system with binary pump 1525 and autosampler 2707. Since we were interested in analysis of already purified samples, chromatography column was not used. Samples were injected automatically by the

autosampler, injection volume was 50 µl. 100% acetonitrile (Sigma Aldrich, St.Louis, MO) was used as a mobile phase at flow rate of 0.5 ml/min. Spectra were collected with excitation/emission wavelength of 745/795 nm, using Breeze operating software (Waters). Samples were prepared in DMSO, and the system was flushed three times after each injection with DMSO followed by acetonitrile. To eliminate residual signal from previous injection, blank DMSO was injected prior to sample injection. Preceding the analysis of the samples the series of standard dilutions of the dye in DMSO was run at the same conditions, and calibration curve was constructed (R^2 = 0.97). In addition, DIR encapsulation efficiency was calculated as per:

$$= \frac{quantity\ of\ DIR\ in\ digested\ nanoparticles}{(quantity\ of\ DIR\ in\ nanoparticles + DIR\ in\ supernatant)}$$

All measurements were performed at room temperature. Data was collected in emission units full scale (EUFS) from peak area.

Statistical data analysis

Results are expressed as means ± standard error of the mean (SEM). Statistical analyses of the data were performed using single-factor analysis of variance (ANOVA). Subsequently, differences between means were determined using the least significant difference (LSD) with an alpha value of 0.05.

6.3 Results

Characterization of antibody-nanoparticle conjugates

Particle size was determined using dynamic light scattering (DLS) for bare, elastin and IgG antibody coated nanoparticles. Over multiple experiments, all groups consistently sized approximately 200 ± 16 nm (Table 6.1).

Table 6.1: Characterization of nanoparticles

Type of nanoparticle	Size (nm)	Poly dispersity index	ζ- potential (mV)
Blank PLA	222	.136	-27.91
PLA+PEGmaleimide+DIR	226	.152	-66
NP+0.1µg elastin antibody	238	.30	-50.69
NP+0.25µg elastin antibody	208	.326	-45.89
NP+1µg elastin antibody	255	.209	-45.91
NP+2.5µg elastin antibody	242	.277	-41.74
NP+10µg elastin antibody	238	.26	-41.93
NP+25µg elastin antibody	100	.203	-39.57

It was observed that increasing surface density of antibodies decreased the ζ-potential of the nanoparticles, however; all NPs had negatively charged surfaces (Table 6.1). For all further experiments, 4 µg elastin antibody/mg total polymer was used for surface conjugation to nanoparticles. The antibody conjugated nanoparticles were generally spherical with uniform size when examined under AFM (Figure 6.1A).

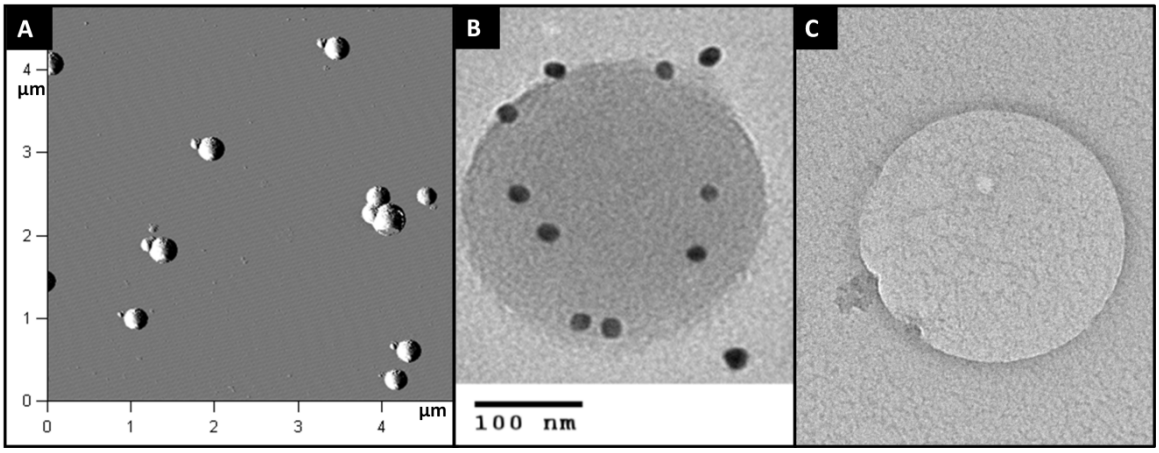

Figure 6.1:Nanoparticle morphology and size characterization. (A) Atomic force microscopy (AFM) of ENP indicating a general spherical morphology and ~ 200nm size, (B) TEM fpr immunogold labeling of antibody coated nanoparticles. Gold-stained IgG (seen as small dark spots) indicate the presence of antibody on the particle surface. (C) Negative control without antibody on surface.

PLA-antibody conjugation was studied under TEM. As seen in Figure 6.1B, the dark 10 nm gold particles are a direct indication of the presence of conjugated antibody on the nanoparticle surface. Control particles without antibody on the surface showed no gold staining (Figure 6.1C).

Antibody binding yield depends on initial antibody concentration

The binding yield of antibody increased with increase in the concentration of antibody used in the experiment (Figure 6.2). The increase in antibody binding leads to decrease in free PEG hydroxyl groups on the surface. Thus, to balance the amount of antibody and PEG groups so that optimum circulation time (provided by PEG) and site specific binding (provided by antibody) could be achieved, we picked the 4 µg/mg concentration for further studies which demonstrated ~30% binding yield.

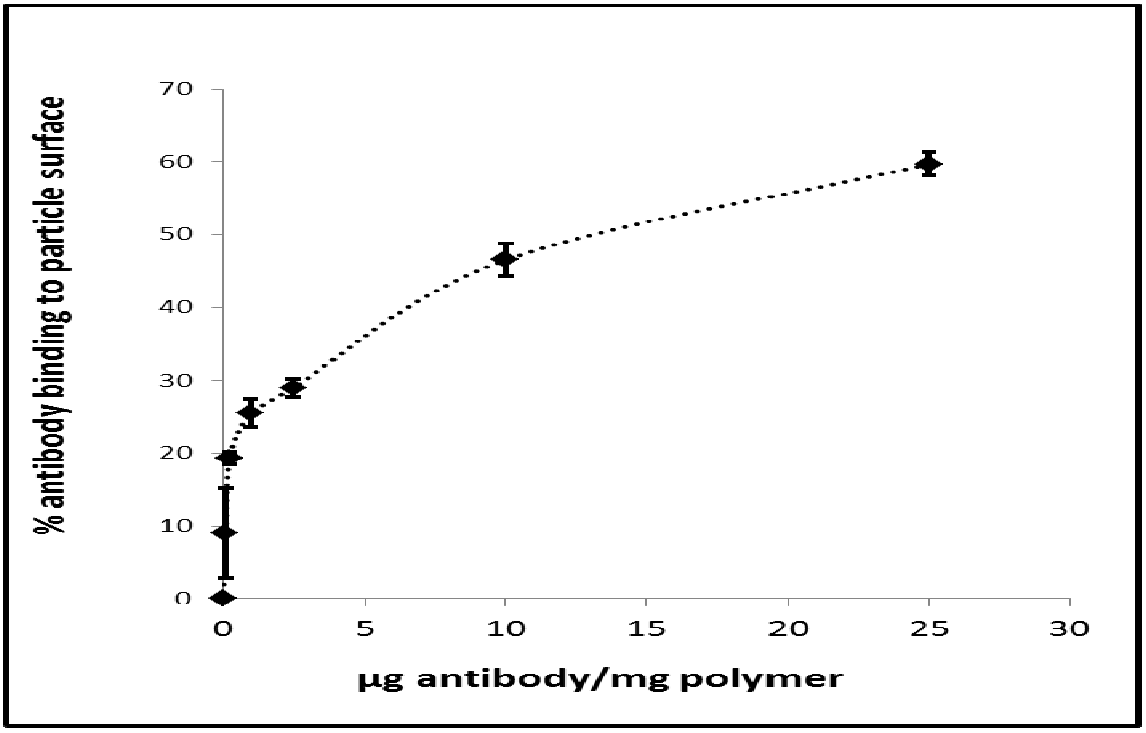

Figure 6.2:Antibody binding yield increases with increasing starting antibody concentration.

Ex-vivo determination of ENP binding specificity to degraded elastic matrix

To test NPs targeting to degraded elastin in vitro, isolated rat aortae were treated with elastase and NPs were delivered intraluminally. Whole rat aortas were exposed to 10, 20, 30, 60 minutes of elastase treatment in vitro to create increasing degrees of elastic damage. The elastic fiber damage was confirmed by VVG stain (Figure 6.3A, 6.3B).

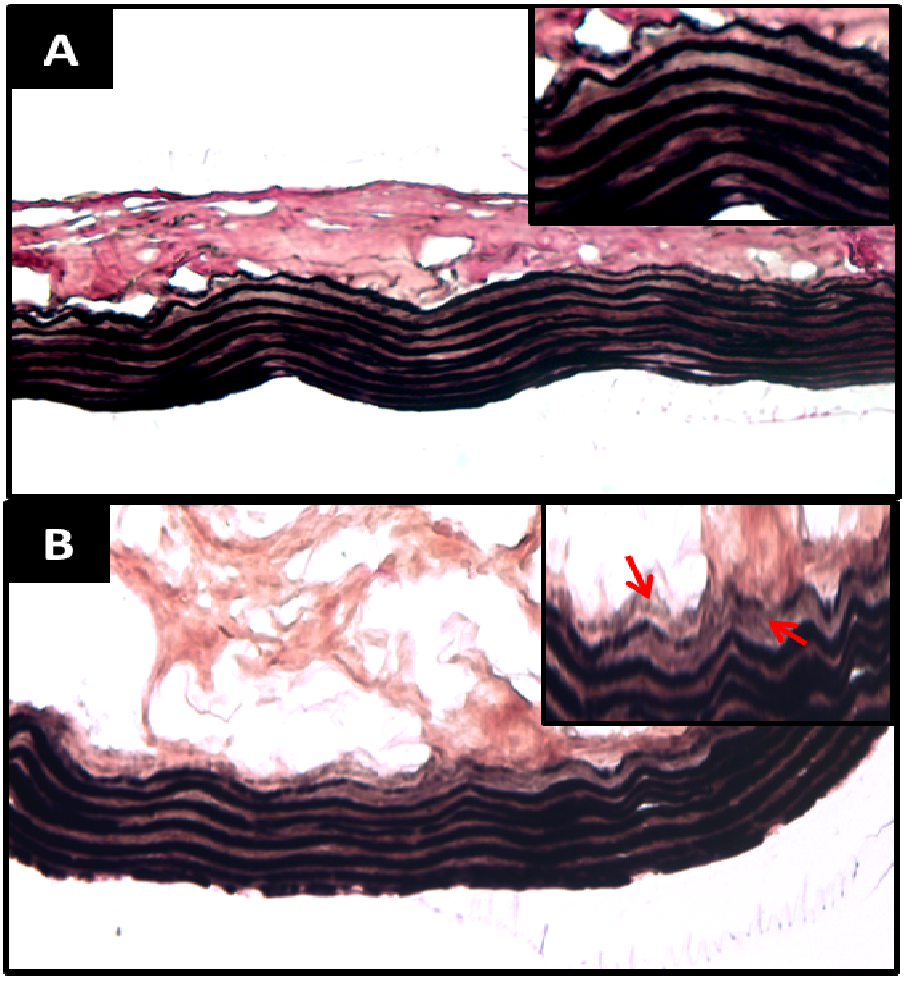

Figure 6.3:(A) VVG stain on untreated aorta depicting native wavy elastin fibers. (B) VVG stain for elastase treated (60 min) aorta showing disrupted elastic fibers. Insets show damaged fibers (marked by red arrows).

On intraluminal injection of INPs and ENPs, an increasing adherence of ENPs with greater elastic damage was observed (Figure 6.4) as assessed by quantitative fluorescence in the tissue. After 60 minutes of elastase mediated elastic lamina degradation, there was ~2 fold greater ENP attachment in comparison with INP groups.

The aortas that were not treated with elastase (control groups) showed negligible adherence of NPs suggesting that elastic fiber degradation is essential for NP targeting.

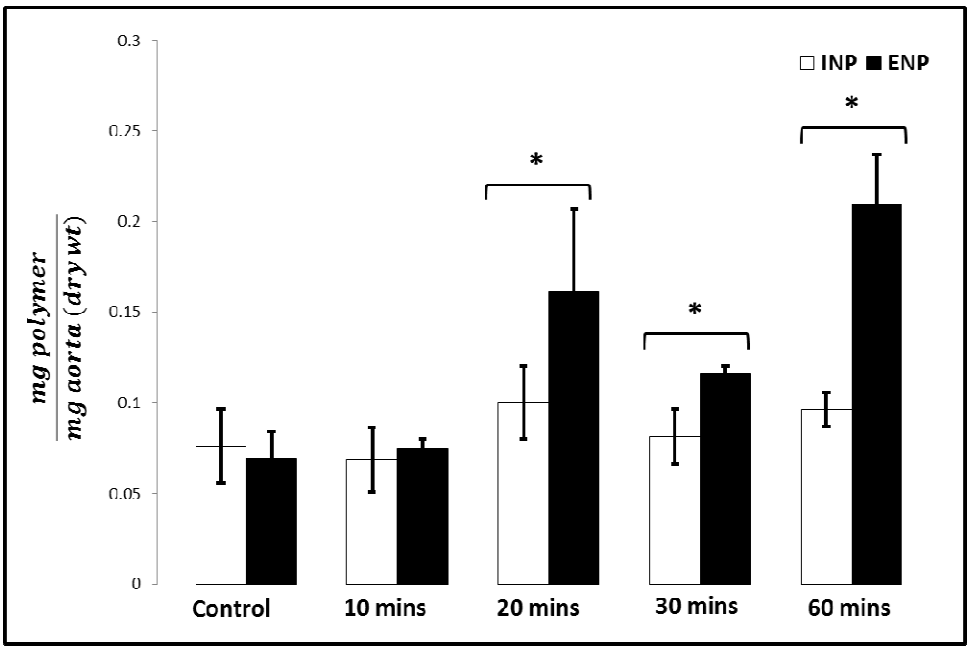

Figure 6.4:Rat aorta treated with elastase for various times showing NP attachment. INPs/ENPs were administered intraluminally and incubated for 60 minutes.

An increase in ENPs attachment efficiency was found with increase in surface antibody concentration (Figure 6.5). At 2.5 µg/ mg polymer ~2.8 fold increase in attachment was recorded when compared to INP control group. Further increase in surface antibody concentration did not increase attachment efficiency. ENP uptake by aorta was reconfirmed with histological assessment, where NPs were visualized as purple dots along the fragmented media (Figure 6.6A) which were evidently absent in the control INP groups (Figure 6.6B).

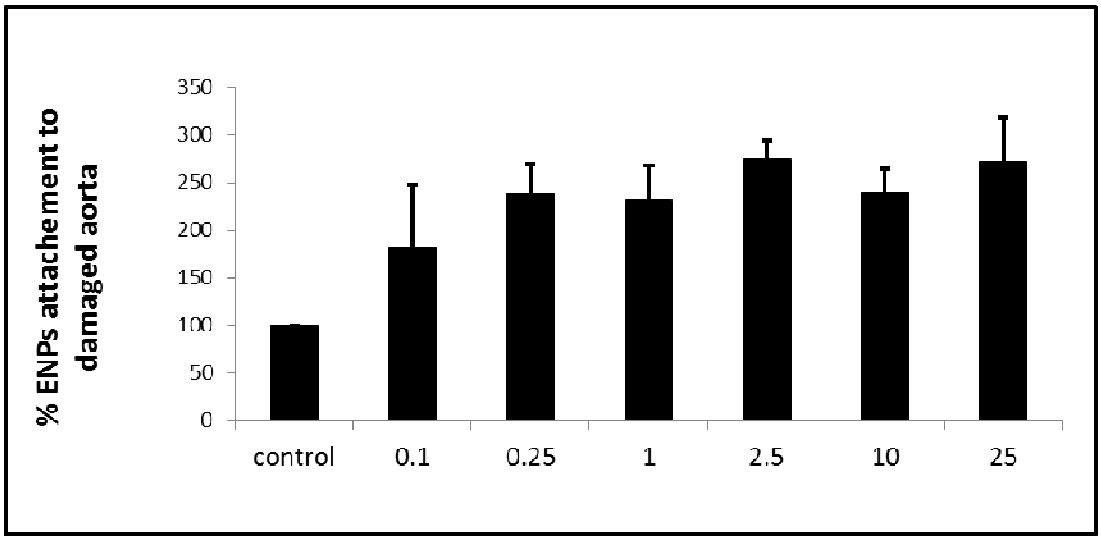

Figure 6.5:Increasing antibody surface density enhances target attachment efficiency up to 0.25 µg /mg polymer and stabilizes with further increase in surface antibody density.

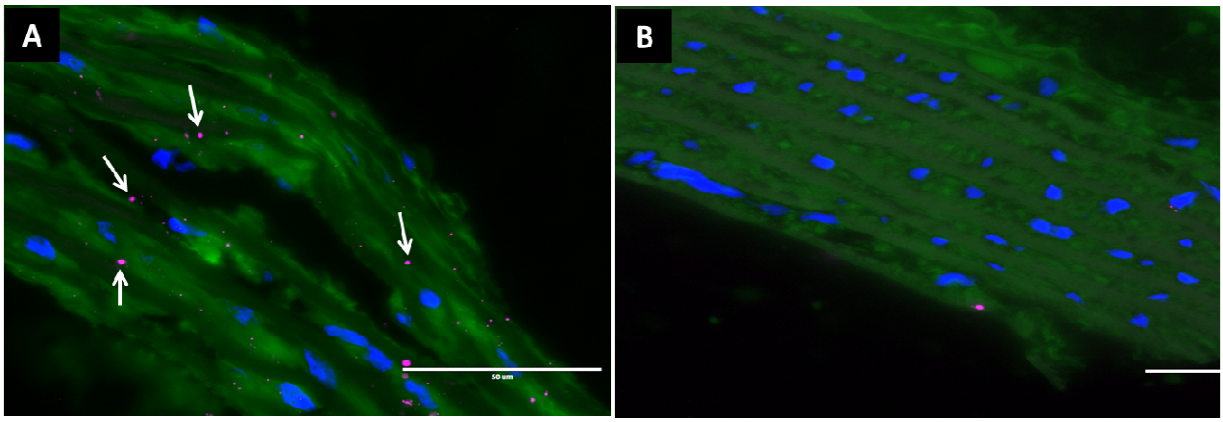

Figure 6.6:ENPs attach to elastase treated aorta (A) compared to lack of INPs adherence in elastase treated aorta, (B). Original magnification=200X

In-vitro cell culture studies

Determination of concentration specific toxicity of ENPs

The effect of elastin antibody coated NPs on the viability of rat aortic smooth muscle cells in vitro was assessed using quantitative (MTT) and qualitative (LIVE-DEAD) assays. MTT assay showed a significant retardation in cell proliferation when 500 µg/ml NP were placed in the cell culture media with more than 10 µg/mg levels of surface antibody concentration. Reducing NP concentration to 100 µg/ml still led to retardation of cellular proliferation. Positive control (70% ethanol) showed more than ~95% cell death (Figure 6.7A). As gauged by the absence of any dead (red) cells in the Live/Dead assay (Figure 6.7B), none of the groups appeared cytotoxic at any of the tested concentrations.

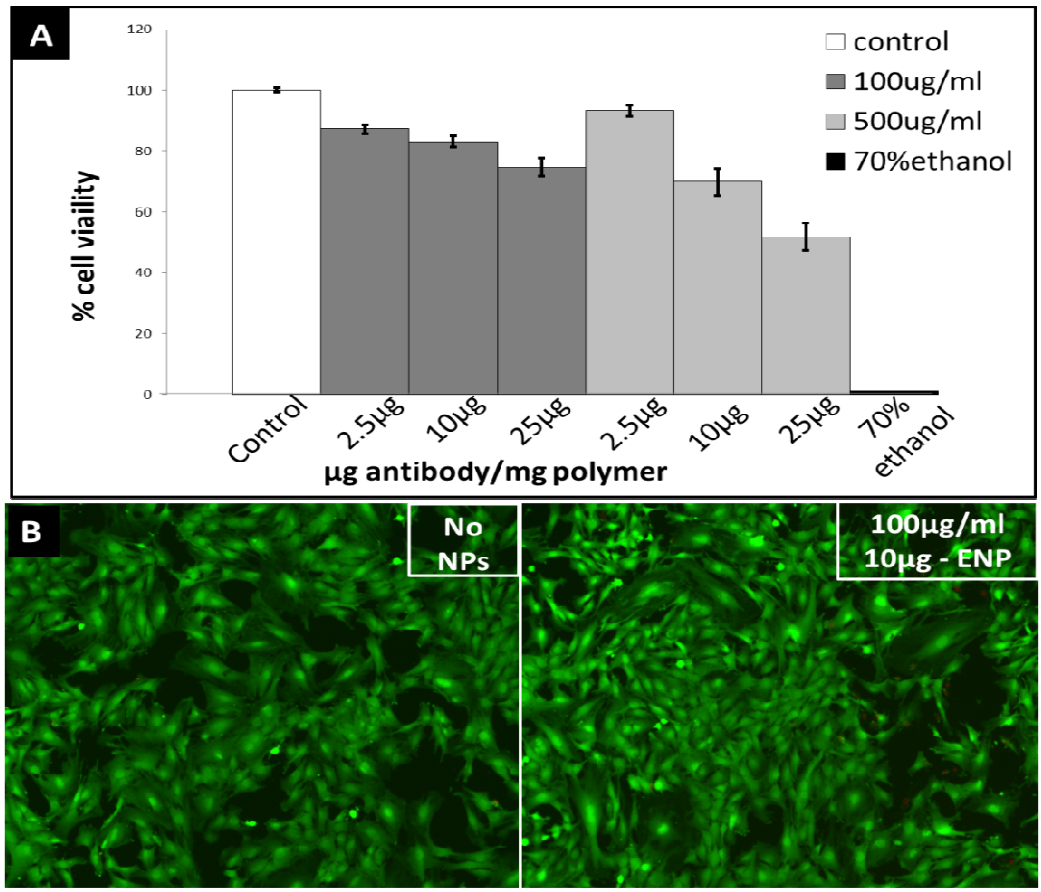

Figure 6.7:Cell viability and evaluation of cellular uptake of ENPs. (A) MTT assay quantifying the viability of cells when treated with 100 µg/ml and 500 µg/ml of 2.5,10,25 µg/mg polymer ENPs. (B) Live-dead assay on cells treated with and without ENPs; green = viable cells, red = dead cells). At 100 µg/ml, 10 µg/mg polymer does not show significant morphological changes or cytotoxicity compared to untreated controls.

ENP internalization by vascular smooth muscle cells

We examined the effect of particle size and charge on the intracellular uptake of DIR loaded-ENPs. Majority of the particles (>200nm) were excluded in the extracellular space at the end of 24 hours (Figure 6.8A) while particles below 100 nm were taken up

by cells (Figure 6.8B). To determine the effect of surface charge on cellular uptake of NPs, ENPs were incubated with poly-L-lysine to create positively charged particle surface (ζ-potential ~28.76 mV). When cells were presented with these positively charged particles, an enhanced cellular uptake was found; more so in smaller positively charged ENPs (Figure 6.8C) when compared to larger positively charged ENPs (Figure 6.8D). Overall, both size (>200 nm) and negative charge of the ENPs was essential to target them to the extracellular matrix with minimal cellular uptake.

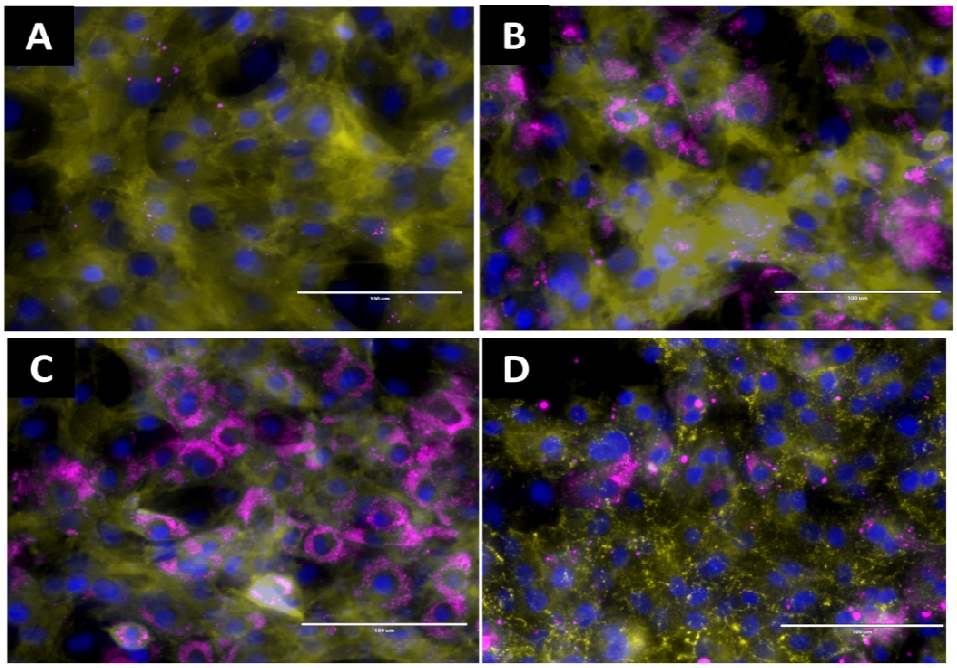

Figure 6.8: Cellular exclusion of ENP of large (>200nm) nanoparticles (A) and uptake of small (<100nm) nanoparticles (B), small particles treated with poly-L-lysine (C) and large particles treated with poly-L-lysine (D). Negatively charged ENPs are excluded by cells when size >200nm compared to <100nm particles. Increasing positive surface charge enhances cellular uptake even of larger particles.

In vivo model for targeting NPs to diseased vasculature

We created calcium chloride mediated injury in the abdominal aorta of rats that has been shown earlier to create elastic lamina degradation[305,334] to assess in vivo targeting of NPs. We confirmed elastic lamina fragmentation and degradation in this model by histological assessment. Perivascular application of 0.5 mol/L $CaCl_2$ to the infra-renal abdominal aorta induced elastic fiber degradation (Figure 6.9A) showing a distinct discontinuity/ thinning of elastic fibers in the medial layer of the artery while uninjured control aorta showed undisturbed wavy elastin fibers (Figure 6.9B).

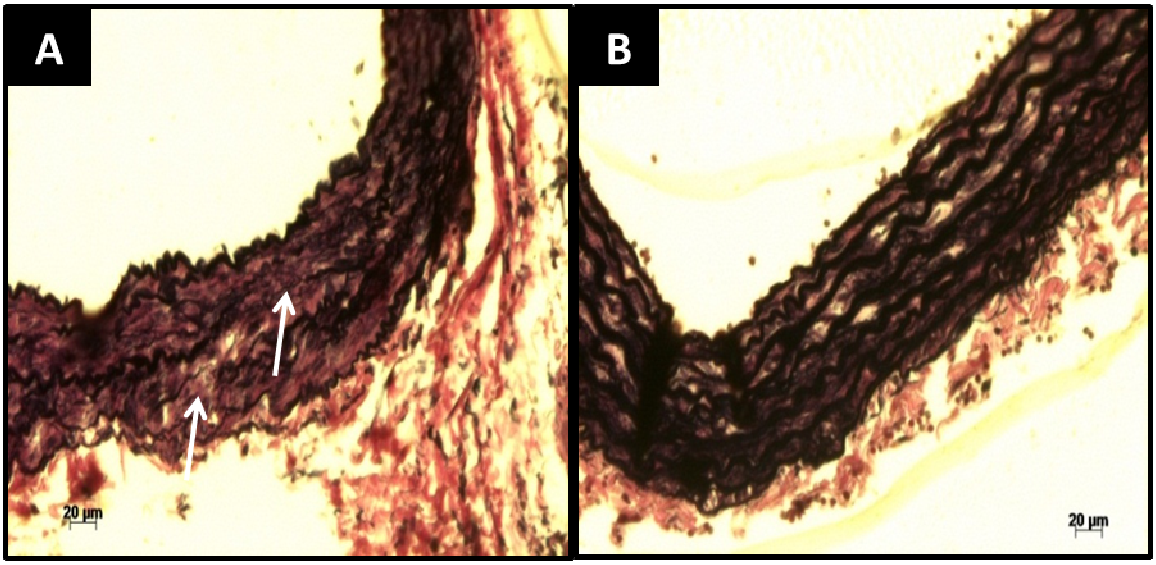

Figure 6.9:(A) VVG of rat aorta after 10 days of calcium chloride treatment, (arrow marks indicate fragmented elastin fibers) (B) healthy rat aorta.

We then evaluated the targeting efficacy of the ENPs/INPs to the vasculature with degraded elastic lamina after intravenous delivery. Based on our in-vitro cytotoxicity experiments, we determined ~100 µg/ml nanoparticle concentration is well within

tolerable range. Assuming 20 ml total blood volume in rats, we administered 10 mg of polymer/kg body weight NPs suspended in PBS as one time bolus intravenous injection. We allowed NPs to circulate and target for 24 hours. Nanoparticles with surface elastin antibody showed ~3.5 times greater targeting to the injured abdominal aorta as compared to nanoparticles with surface IgG antibody as measured by % total fluorescence/g tissue weight (Figure 6.10).

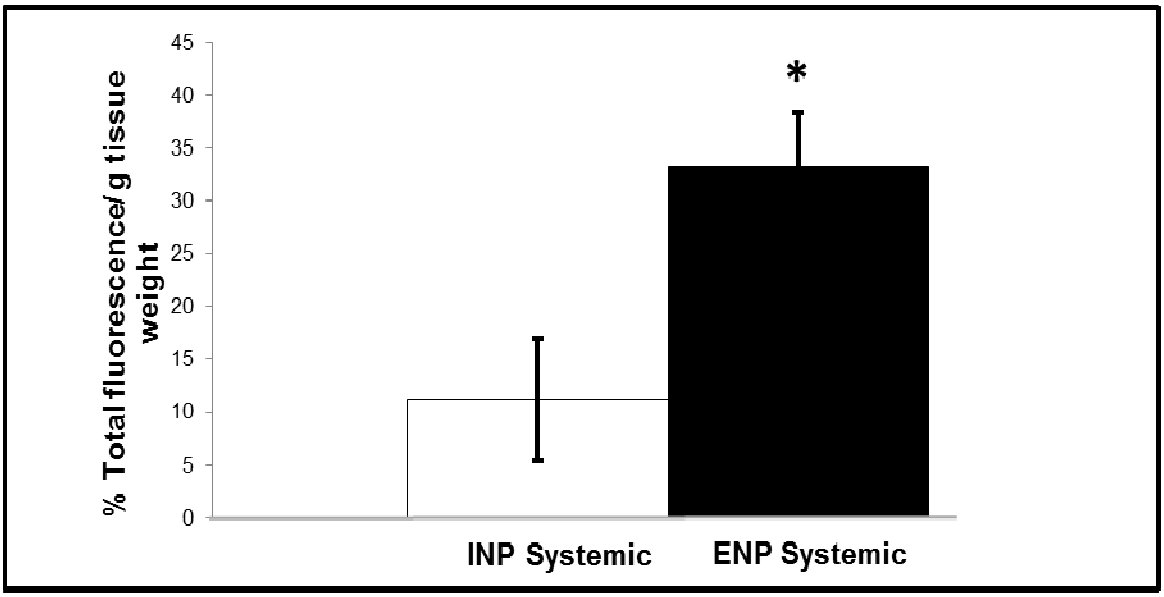

Figure 6.10:Targeting of ENPs to degraded elastic lamina in rat abdominal aorta. % targeting of INPs vs ENPs at 24 hours after intravenous injection

When the whole aortae were imaged with IVIS instrument, we observed strong fluorescence in the area of elastin degradation site in ENP group (Figure 6.11A, boxed area). In comparison, control nanoparticles with surface IgG antibody showed no fluorescence in the damaged aorta (Figure 6.11A). Histological assessment showed nanoparticles with surface elastin antibody were located deeply within medial layers of

aorta, clearly showing that they penetrate the aorta even under high shear flow conditions while no detectable fluorescence was observed in INP control group (Figure 6.11B). This data clearly suggests the targeting of elastin antibody coated NPs to sites of elastic damage.

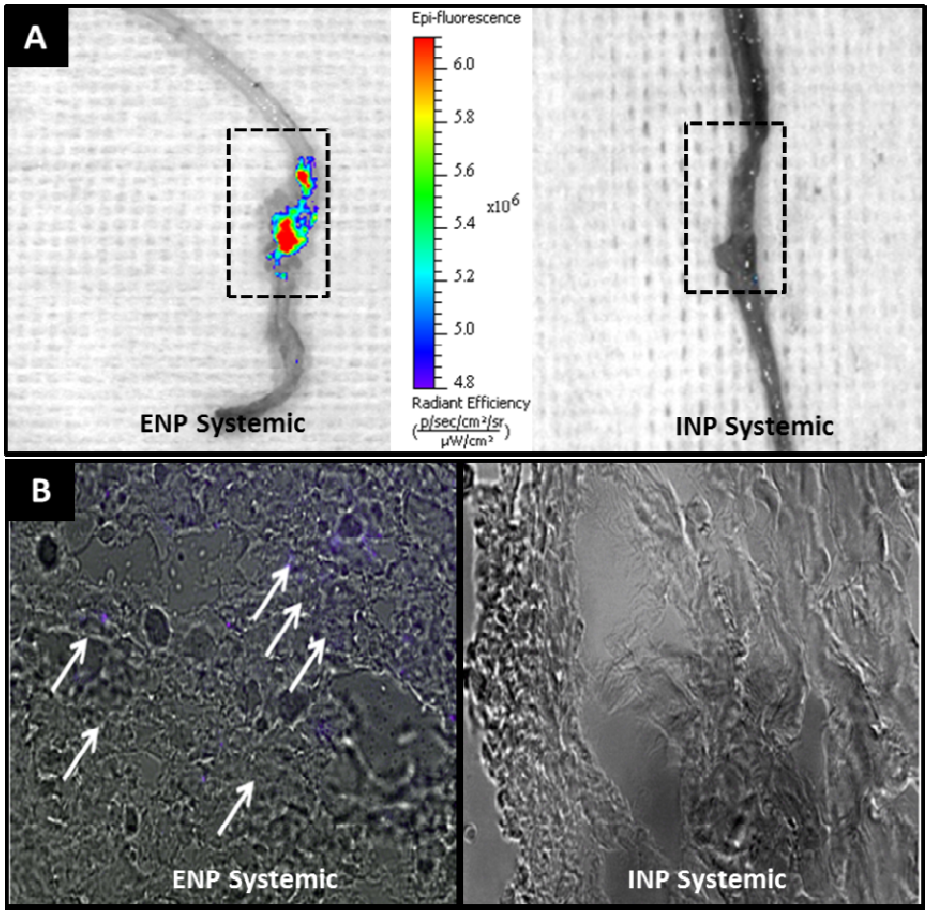

Figure 6.11:Targeting of ENPs to degraded elastic lamina in rat abdominal aorta. (A) IVIS imaging of whole aorta at 24 hours after intravenous injection of INPs/ENPs. Boxed area indicates the site of elastic damage. (B) Fluorescent microscopy of damaged abdominal aortic with INPs/ENPs. Purple coloration indicates the presence of nanoparticles in ENP group while no staining in INP group.

We also assessed organ distribution of NPs by measuring fluorescence. At the end of 24 hours, no residual fluorescence was found in the blood, heart, brain, muscle and skin. A biodistribution plot of the organs that exhibited fluorescence, revealed that high amount of signal was detected in the organs of mononuclear phagocytic system (MPS), namely the liver and spleen (Table 6.2). Splenic uptake was ~ 2.7 times lower in the ENP group than INP groups, possibly because of the higher accumulation in the damaged aorta. It must be noted that rabbit-anti-rat antibodies were utilized for this experiment which might be a major contributing factor to the splenic activation. Also, a small amount of fluorescent signal was observed in the kidneys probably because of the partial metabolism of low molecular weight un-encapsulated DIR molecules.

Table 6.2: Biodistribution of nanoparticles at 24 hours after intravenous delivery

Organ	**% total fluorescence/ g dry weight (INP)**	**% total fluorescence/ g dry weight (ENP)**
liver	16.97 ± 1.24	19.09 ± 1.00
aorta	11.19 ± 5.74	33.19 ± 5.19
lungs	14.304 ± 2.96	13.37 ± 7.62
kidneys	3.58 ± 1.95	1.05 ± .32
spleen	175.61 ± 35.12	63.79 ± 13.97

We tested these ENP in another clinically relevant animal model (discussed in Chapter 2) for medial arterial calcification (MAC). 24 hours after delivery of ENPs via tail veins of diseased rats, we harvested the aorta and imaged under IVIS and observed a strong florescence in the aortic arch and iliac bifurcation which was not seen in healthy animals treated with ENPs (Figure 6.12). VVG also confirmed elastin damage in warfarin+vit K treated rats (Figure 6.13).

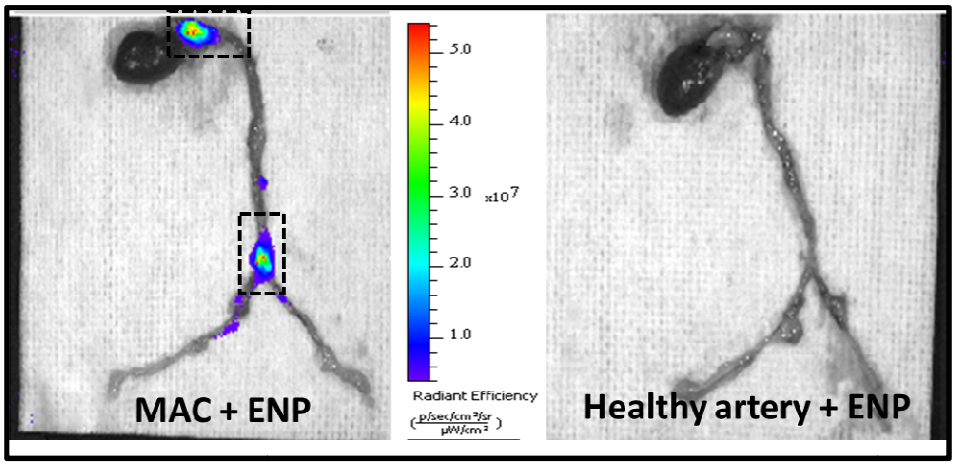

Figure 6.12:Targeting of ENPs to sites of damaged artery in MAC. Boxed area indicates elastin damage.

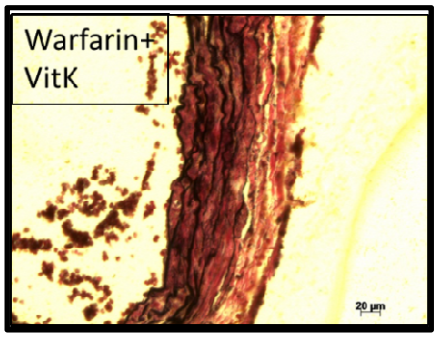

Figure 6.13:Elastin damage confirmed with VVG stain in MAC artery

Next, we tested if local perfusion of NPs at the site of elastic damage would increase accumulation of NPs. Thus, nanoparticles were endoluminally perfused into the damaged artery via a catheter mediated micro-vascular surgical procedure. 24 hours after injection, direct local perfusion of ENPs into site of matrix damage showed ~10 fold higher adherence and retention when compared to INPs control groups (Figure 6.14) (ENPs groups were assumed to display 100% attachment).

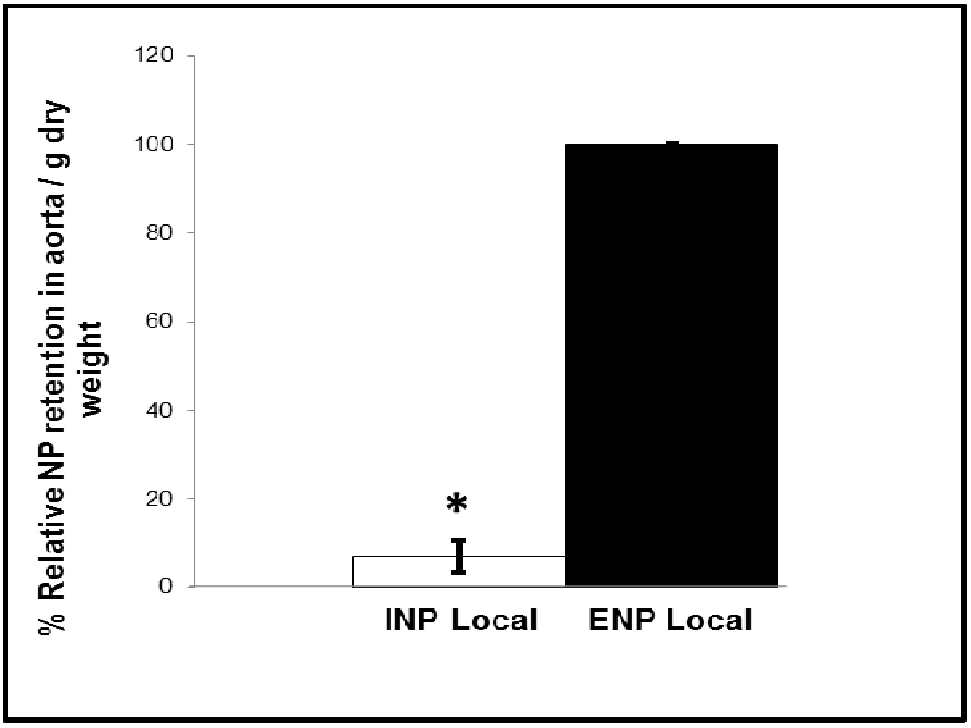

Figure 6.14:Local administration of INPs/ENPs to degraded elastic lamina in rat abdominal aorta. Relative adherence of INPs/ENPs at 24 hours after local delivery of nanoparticles to injured abdominal aorta.

The imaging of the whole aorta and histological assessment further confirmed that targeting of nanoparticles with surface elastin antibody was significantly higher than control INPs (Figure 6.15A, 6.15B) and the nanoparticles penetrated deep in the medial layers. The relative amount of ENPs attached to the injured area was ~43 times higher when delivered locally as compared to systemic delivery.

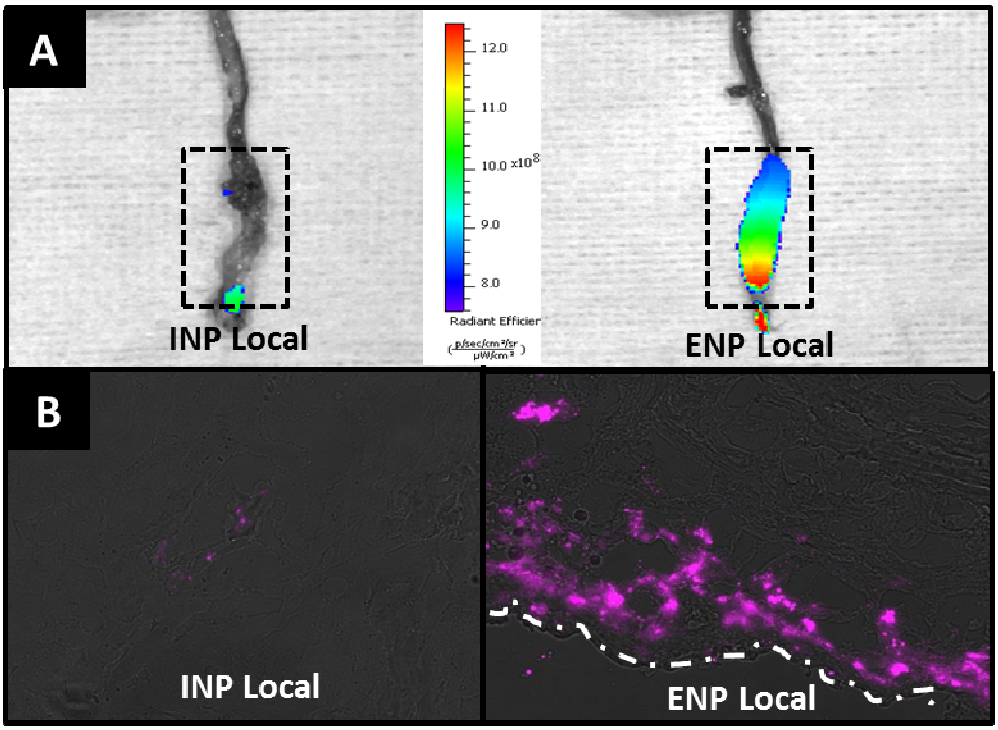

Figure 6.15:Local administration of INPs/ENPs to degraded elastic lamina in rat abdominal aorta. (A) IVIS imaging of whole aorta at 24 hours after local perfusion of INPs/ENPs. (B) Fluorescent microscopy of damaged abdominal aortic with INPs/ENPs. Purple coloration indicates the presence of nanoparticles. Dashed lines indicates the intima of the aorta.

NP clearance study

Whole body animal imaging revealed minimal to no fluorescent signal after 8 days of INP injection (Figure 6.16). However, upon imaging the organs individually, there was distinct signal observed largely from the liver and spleen even after 8 days of injection. The signal observed in the liver was ~ 40 times lesser after 8 days compared to day 1 , whereas spleen showed almost 50% reduction in signal after day 8. These results are encouraging as it shows the ability of the nanoparticles to clear out RES therefore making multiple dosages a possible option.

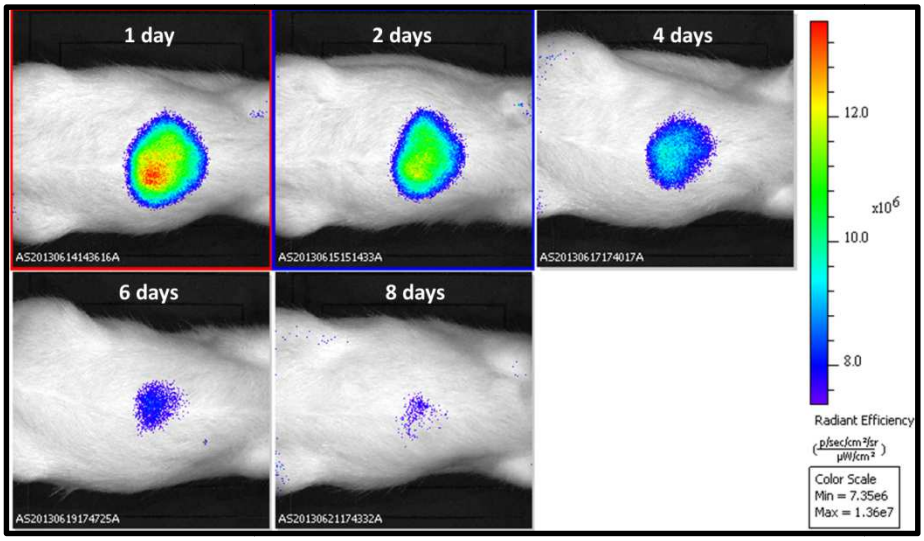

Figure 6.16:NP clearance study. Undetectable fluorescence after 8 days of INP injection

6.4 Discussion

There are a number of challenges associated with developing nanoparticles that specifically target the site of diseased artery for drug/gene therapy applications. First, the heterogeneous nature of vascular diseases poses a significant challenge for spatial and temporal delivery of drugs or imaging agents to the diseased site. Secondly, the hemodynamic environment in major arteries exposes the delivery vehicle to both convective and diffusive forces which retards target-specific binding and local retention. Thirdly, cellular and molecular targets of the vasculature that are intermittently expressed during different stages of the pathology, although useful for molecular imaging, may prove sub-optimal for site-specific delivery of therapeutic payload. Our overall goal was to develop a minimally invasive nanoparticle system that can achieve matrix targeting of a compromised vasculature. We have achieved this goal by employing elastin antibody coated PLA nanoparticles that recognize specific sites of matrix damage and adhere to the damaged vessel. This delivery technology can potentially be used for medical diagnostic as well therapeutic applications.

Most of the previous research has been primarily focused on delivering drug/genes to arteries by targeting vascular cells. For example, several researchers have used molecular markers which are transiently over-expressed in sites of vascular inflammation. In particular, endothelial cell adhesion molecules (CAMs) have been extensively studied as potential targets for homing drug delivery vehicles.[23,24] Anti-vascular cell adhesion molecule-1 (VCAM-1) liposome targeting has shown some promising results in an ldlr-/- mice model in mitigating atherosclerosis.[25] Although, these

constitutively expressed endothelial markers show several fold increase in its surface density in local sites of inflammation, they pose a major obstacle in serving as consistent and heterogeneous molecular target due to their shedding from the plasma membrane as a negative feedback mechanism to prevent leukocyte adhesion.[335] Besides, cellular targeting leads to uptake and intracellular delivery of drugs. We wanted to develop a delivery system for drugs intended to function in extracellular environment. For example, MMP inhibitors known to prevent degradation of matrix in diseases such as aortic aneurysm need to be present in the ECM for effective function.[336] Similarly compounds that specifically bind to elastic fibers such as polyphenols and prevent elastic fiber degradation [305] need to be delivered to the ECM with minimal to no cellular uptake. Deliveries of fibrinolytic agents in the case of coronary thrombosis also need an extra-cellular drug release for rapid clot dissolution. In such cases, negligible cellular uptake of drug-loaded nanoparticles maximizes the therapeutic benefit. Previous research has utilized exposed collagen type IV of basement membrane as a viable vascular target.[337] However, insufficient quantity of the fibrous protein may provide sub-optimal matrix targeting.

We wanted to develop NPs that specifically target degraded elastin and prevent non-specific attachment to native elastic fibers hence localizing NPs only to diseased site and not throughout the vasculature. Elastic fiber degradation which is a characteristic feature of several vascular pathologies including aortic aneurysms and arteriosclerosis can be used as a stable and abundant extracellular matrix target for nanoparticle adherence and delivery. Elastic fiber consists of two main components- 90% of the

mature elastic fiber is a core of amorphous cross-linked elastin protein while the remaining 10% consists of 10-12 nm fibrils that are located around the periphery of the amorphous elastin that include fibrillins, fibulins, and some other glycoproteins like microfibril-associated glycoproteins (MAGPs).[39,338] It has been shown earlier that MMPs in vascular disease pathologies specifically degrade peripheral glycoprotein cover on elastic fibers prior to elastin degradation.[339,340] This proteolytic degradation exposes the hydrophobic core of elastin allowing us to target only elastic fiber degradation site and not healthy aorta.

We first tested NP targeting in ex-vivo conditions using whole rat aortas. Inducing elastase mediated matrix damage exhibited a nanoparticle adherence that was elastin-specific (high in ENP group and minimal in INP groups) and damage-dependent (minimal ENP attachment in healthy undamaged aorta) (Figure 6.4). This data clearly suggested that ENPs were specifically attaching to degraded elastic lamina and not to the healthy aorta. The data also confirmed that intraluminal delivery was possible as NPs could pass through intact endothelium.

Next we decided to test if such NPs with surface elastin antibody could be targeted to diseased aorta in vivo. One of the biggest barriers faced by nanoparticle mediated targeted therapy *in vivo* is the rapid clearance of particles by the mononuclear phagocytic system (MPS), especially by the liver and spleen.[341,342] It has been established that PEGylation of carrier surface significantly increases circulation time, minimizes immune responses and increases flexibility and hydrophilicity.[342,343] In our preliminary

studies, we used un-PEGylated PLA nanoparticles and confirmed a rapid hepatic clearance (<1 hour) as opposed to PEGylated ENPs (>24 hours) (data not shown). We specifically chose ~200 nm particle size and negatively charged surfaces to avoid cellular uptake. Nanoparticle size is an important determinant in its cellular uptake and tissue accumulation. Studies have shown that 100 nm sized nanoparticles show greater uptake compared to 500 nm nanoparticles in vascular smooth muscle cells.[344] Similarly, particle size plays an important role in penetrating the endothelium when delivered endoluminally. It has been shown that smaller size nanoparticles (~ 100 nm) achieve 3-fold greater arterial uptake compared to larger (~ 275 nm) in an ex-vivo canine carotid artery model.[264,345] Our result indicated that nanoparticles with ~200 nm size were able to penetrate endothelium and basement membrane. Another vital parameter that determines the endocytosis or the lack thereof is the surface charge of nanoparticles. Due to the inherent negative charge on mammalian cell membrane, positively charged nanoparticles show superior cellular uptake when compared to negatively charged particles.[346-348] We also confirmed in our studies that positively charged surfaces increased cellular uptake. Overall, keeping size to ~ 200 nm and sufficient surface negative charge, we were able to keep nanoparticles in the extracellular matrix with minimum cellular uptake by SMCs. Although our results suggest that size and charge are important parameters in deciding the cellular uptake of nanoparticles, other critical factors like surface protein density, nanoparticle concentration, antibody affinity and shear rate may all contribute to the phagocytic effect of nanoparticles.

Overall, our results indicate that specifically designed NPs with elastin targeting antibody on the surface can be used to deliver agents to the site of elastic lamina damage while avoiding uptake by healthy vasculature (Schematic in Figure 6.17). One of the most exciting observations was that NPs only accumulated where elastic lamina injury was induced and remaining healthy vasculature was spared. In addition, ENPs delivered in healthy rats failed to display targeting (Figure 6.12) proving the specificity of ENPs and the need for elastic tissue degradation as seen in various vascular disease pathologies such as aortic aneurysms. However, there are several unanswered questions that need to be addressed with further research. The possible assimilation of NPs by inflammatory cells like macrophages present locally at the site of vascular disease is unclear. The maximum duration of NP retention at the damaged site is also unknown, however, such systems can be used to deliver imaging agents[349] or drugs that act quickly such as elastin stabilizing compounds.[265] Also this study was performed with single dose; one can envision using multiple doses to achieve constant supply. We used antibody mediated elastin targeting. However, presence of antibodies on the surface makes nanoparticles highly prone to Fc-receptor-mediated phagocytosis which causes rapid clearance by liver and spleen.[341,350] Antibodies have been investigated extensively in the last couple decades and antibody-mediated tissue targeting for clinical practice has been approved by the FDA.[351-353] Besides, with advancements in hybridoma technology, antibodies can be engineering and chimeric, humanized and fully human antibodies with minimal immunogenicity can be exploited for active site targeting.[354] This study was performed with encapsulated fluorescent labeled dye for tracking particle trajectory. Further studies

with drug or imaging agents loaded particles are underway to see effectiveness of the targeting in vivo.

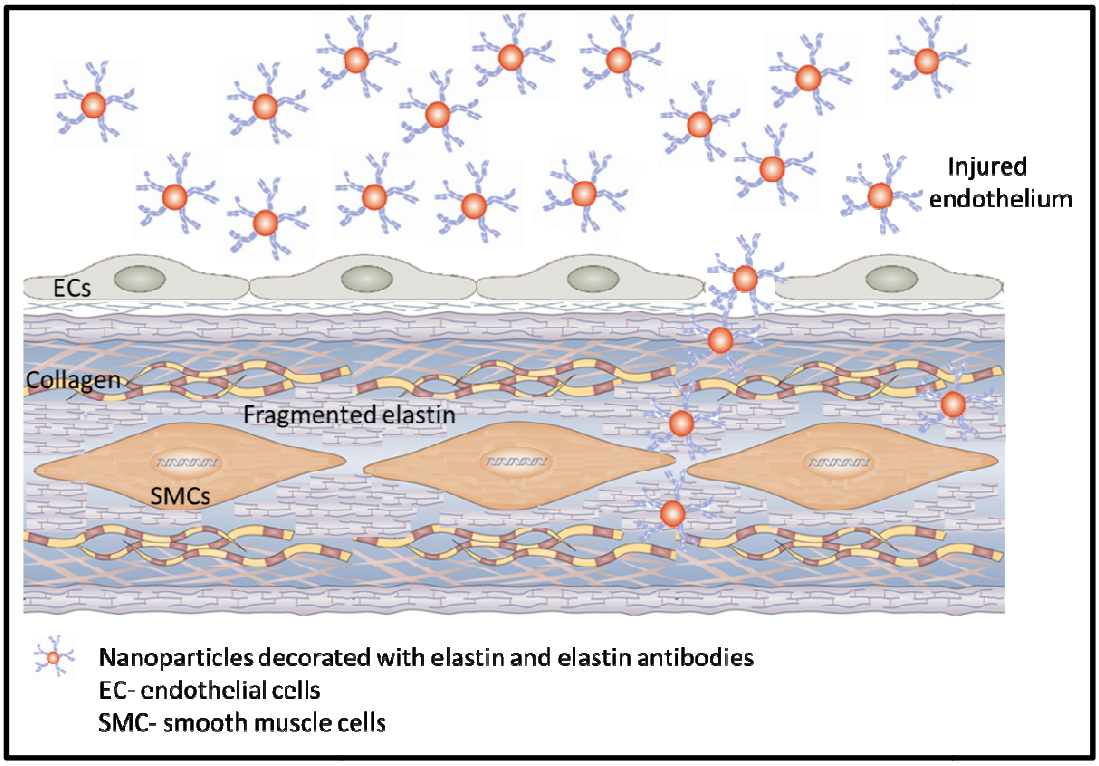

Figure 6.17:Schematic showing elastin antibody coated nanoparticle attaching to fragmented elastin of aorta

6.5 Conclusion

We show that nanoparticles can be designed to specifically target degraded elastic lamina, which is a key feature of a variety of vascular diseases, for site specific delivery of therapeutics and imaging. After several optimization experiments, we developed a nanoparticle system which was minimally cytotoxic, displayed ex-vivo and in vivo specificity, and hydrodynamic stability. Our results indicate that elastin antibody coated PLA nanoparticles are excluded by cells, display high affinity to degraded elastin when

delivered ex-vivo in rat aorta, injected intravenously and perfused locally into damaged arteries in rats. Nanoparticles with irrelevant control antibody (INPs) did not show such specificity. The ENP attachment was specific to injury site and healthy elastic lamina was spared. Thus such systems can be used to target vascular pathologies such as aortic aneurysms or arteriosclerosis.

CHAPTER 7

PENTAGALLOYL GLUCOSE (PGG) ENCAPSULATED NANOPARTICLES AS POTENTIAL THERAPY FOR MEDIAL ARTEIRAL CALCIFICATION AND ABDOMINAL AORTIC ANEURYSM

7.1 Introduction

From the previous chapters, we identified the elastogenic and elastoprotective properties of polyphenols making it a desirable candidate for AAA and MAC repair. In addition, we also developed a minimally invasive nanoparticle technology that can target sites of damaged elastin in the artery. The next goal was to load these polymeric nanoparticles with polyphenols for delivery to sites of diseased vessel for therapeutic benefit. We chose PGG as a model polyphenol for the same.

7.2 Materials and methods

Preparation of PGG loaded nanoparticles

Poly(D,L-lactide) (PLA) nanoparticles were prepared using a nanoprecipitation method based on solvent diffusion. Briefly, 10 mg PLA (Average M_W 75,000-120,000) (Sigma Aldrich, St.Louis, MO) was dissolved in 1ml acetone (VWR International, Radnor, PA). ~2.5 mg of 1, 2-distearoyl-*sn*-glycero-3-phosphoethanolamine-N-[maleimide (polyethyleneglycol)-2000] (PEG maleimide) (Avanti Polar Lipids, Inc., Alabaster, AL) and 500 µg/ 1 mg PGG were added to the PLA solution in acetone. ~300 µl of polymer solution was added drop-wise at a uniform rate to 8 ml of water kept under sonication in a water bath sonicator and solutions were sonicated for 1 hour. The

resulting suspension was expected to contain nanoparticle with encapsulated PGG. The particles were purified 3 times by centrifugation at 3000×g for 15 minutes followed by re-dispersion in water. Three different groups were tried: (a) blank (without PGG) (b) 500 µg PGG in 3 mg polymer (c) 1000 µg PGG in 3 mg polymer.

Percentage loading calculation

After purification of the nanoparticles, the samples were lyophilized, weighed and digested in DMSO and quantified against a standard curve of PGG in DMSO. The % loading was calculated as follows:

$$\%\ loading = \frac{mg\ of\ PGG}{mg\ of\ total\ polymer + mg\ of\ PGG}$$

Release profile of PGG in PLA nanoparticles

Known amounts of nanoparticles were taken and added to dialysis units (Slide-A-Lyzer® MINI Dialysis Units, Thermo Scientific, Rockford, IL) and incubated at 37°C in infinite dilution conditions in phosphate buffered saline (PBS). After each time interval, PGG loaded nanoparticles were removed, lyophilized and digested to evaluate the amount of PGG remaining in particles.

7.3 Results

Using high molecular weights of PLA yielded very poor % loading in the PGG groups. We obtained 1% PGG loading (2% encapsulation efficiency) and 3% PGG loading (5% encapsulation efficiency) with initial 500 µg and 1000 µg of loading PGG.

Such low encapsulation efficiency indicates that majority of the PGG was eliminated in the bulk aqueous phase instead of staying in the organic phase.

We tried another approach of using low molecular weight PLA (Average M_W 9,000) for the nanoparticle preparation using the same nanoprecipitation method. We noted a 25% encapsulation of PGG in ENPs using 50mg/ml PGG solution (Figure 7.1).

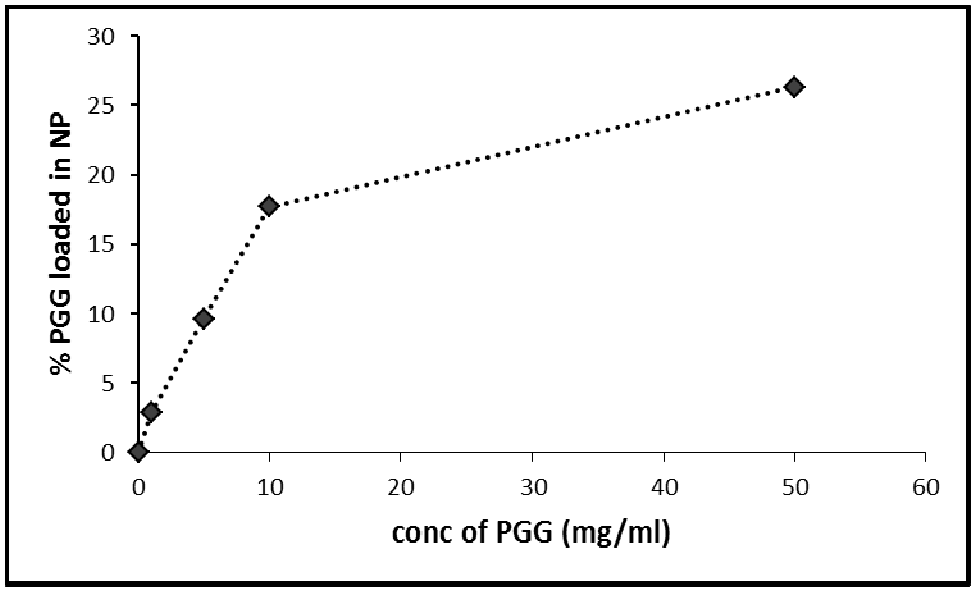

Figure 7.1:Increasing concentration of PGG starting solution shows greater PGG loading percentage

Further, we selected the highest loading percentage to quantify the release profiles, however ~ 90% of PGG was released 46 hours (Figure 7.2).

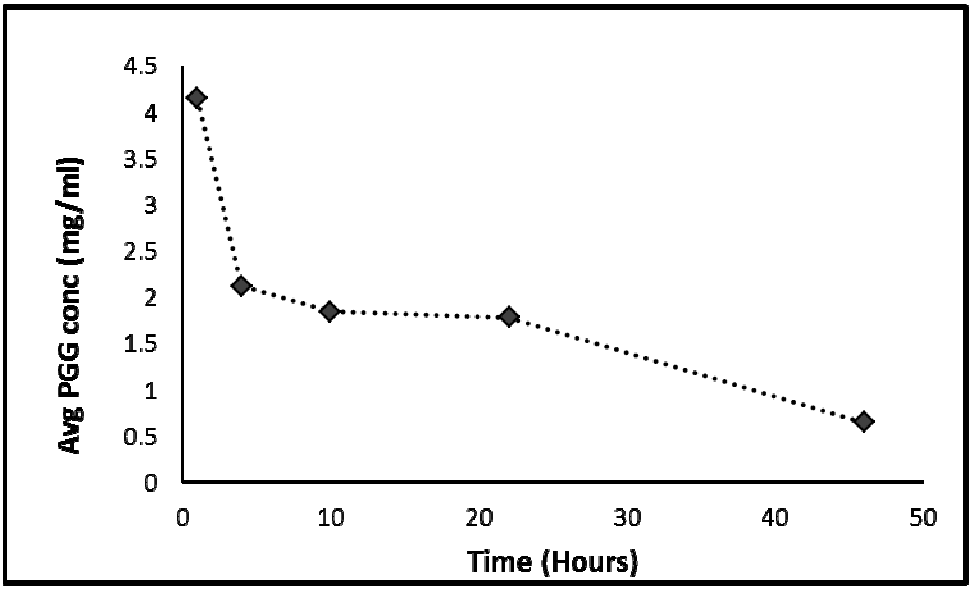

Figure 7.2:Release profile of PGG up to 46 hours

7.4 Conclusion

We tried loading PGG into PLA nanoparticles but achieved very poor drug loading efficiency. Although varying the molecular weight of PLA increased the loading efficiency by ~ 8 times (3% with high MW PLA vs. 25% with low MW PLA) almost 90% of PGG was released by 46 hours. Since PLA displays relatively show rate of hydrolytic degradation, the initial release of PGG appears to be a diffusive loss and not due to degradative properties of PLA.

CHAPTER 8

CONCLUSIONS AND RECOMMENDATIONS

8.1 Conclusions

Elastin is an extracellular matrix protein found in abundance in vascular tissue. Elastin degradation is a natural part of ageing; however pathological elastin degradation can lead to severe vascular diseases including abdominal aortic aneurysms (AAA) and medial arterial calcification (MAC). Unfortunately, innate ability of cells to repair degraded elastin is highly diminished in adults and cells cannot recapitulate elastic fiber assembly that happens during development. The broad goal of this project was to understand the role of elastin degradation in diabetic vascular calcification and to develop minimally invasive drug therapy that can target degraded elastin and deliver polyphenolic compounds to prevent disease progression. We show the following:

1) In the first part of the project, we set out to determine the pathological relevance of elastin degradation products and TGF-β1 in a hyperglycemic milieu. Hyperglycemia is a hallmark feature of diabetes mellitus. There is an overwhelming amount of evidence linking diabetes with medial arterial calcification (MAC). In fact, calcified arteries are the unfortunate fate of diabetic patients' arteries eventually requiring amputation of lower extremities. Of the several factors causing calcification of diabetic arteries, our experiments isolated three clinically relevant parameters - elastin peptides, TGF-β1, and glucose – and tested their effects on vascular smooth muscle

cells. Our results indicate that in the presence of elastin peptides and TGF-β1, smooth muscle cells turn into osteoblast like cells, an effect which is dramatically aggravated in the presence of high glucose concentrations. Conversely, without the elastin peptides and TGF-β1, high glucose concentrations alone did not cause this osteogenic shift, indicating the importance of elastin peptides in the process of calcification. Our results therefore validate the importance of intact elastin, the degradation of which plays an acute role in diabetic vascular calcification.

2) The second stage of this project was examine the elasto-protective and elasto-regenerative effects of polyphenols like PGG, EGCG and catechin. All the three polyphenols bound to elastin in a concentration and time dependent manner, providing resistance against elastolytic damage. Furthermore, these polyphenols exhibited a strong affinity for binding to soluble tropoelastin, thereby aiding in the coacervation and maturation of tropoelastin to cross-linked elastin. Aneurysmal smooth muscle cells generated greater tropoelastin compared to healthy vascular cells; however they did not produce commensurate amounts of lysyl oxidase, a key enzyme needed for cross-linking elastin. Polyphenols helped aneurysmal cells to deposit greater quantities of mature elastin without altering the quantity of tropoelastin in the media. These features of polyphenols make them a desirable candidate for treating elasto-degradative diseases like AAA and MAC.

3) In anticipation of using these polyphenols as elastin protective agents, we invented a novel minimally invasive method that can recognize degraded elastin. We fabricated PLA nanoparticles loaded with a tracer dye and elastin antibodies attached on the surface. One time intravenous injection of these nanoparticles showed ~ 33% attachment of nanoparticles which was ~ 3.5 times greater than non-specific control. Furthermore, these nanoparticles were relatively cyto-compatible and bio-compatible. After 8 days of nanoparticles injection, ~ 55% of the particles were removed by the reticulo-endothelial system. Therefore, this technology can be used to load therapeutics, imaging agents, drugs, and molecules for site specific delivery to damaged vascular matrix.

8.2 Limitations of this project and recommendation for future work

1) Scope for improvisation in the physical aspect of nanoparticle system (synthesis and characterization)

In this project we have chosen PLA nanoparticles to test our hypothesis that degraded elastin is a stable and viable target for therapeutic delivery. Spherical nanoparticles have been traditionally used both clinically and in research laboratories. The importance of size has been discussed in Chapter 6. However, the importance of geometry has been neglected in this project. Nanovector geometry has shown to play an important role in defining its transport in vasculature and its adhesion to target receptors as well as mode of nanovector-

cell interactions such as endocytosis, vesiculation, and phagocytosis. Geng et al. have shown that long cylindrical micelles display longer and higher tumor targeting compared to spherical counter parts.[355] Muro et al. have also shown that large elliptical discs exhibited higher targeting efficiency compared to spheres.[356] Champion and group also show that "worm-shaped" particles exhibit negligible phagocytosis compared to spherical particles of equal volume.[357] With current advancements in "shape engineering", it is possible to formulate nanosized particles of different shapes that are capable of achieving greater molecular targeting with minimal off-target accumulation.[358]

The PEG used in our studies has a molecular weight of ~ 3000. We have tested nanoparticles made of only one molecular weight of PEG and a single PLA:PEG ratio (4:1). It has been shown often times in literature that surface PEG groups are easily tunable and provide a "hairy" outer surface to nanoparticles.[359,360] The greater and longer the PEG chains on the surface, the longer the circulation time, thereby greater targeting efficiency. However, higher circulation time also makes the particles prone to untimely degradation, thereby reducing its effectiveness. On the other hand, lesser PEG groups on the surface, makes the particles more prone to protein adsorption (opsonization), thereby activating the RES system and leading to an accelerated undesirable clearance of the nanoparticles. Further studies need to be done to investigate the effect of varying PEG molecular weight and ratio on the targeting efficiency. However, in doing so, the available maleimide groups available for antibody conjugation must

not be compromised; as such groups decide the eventual functional capacity of the nanoparticles. An elaborate experimental analysis must be performed such as employment of surface plasmon resonance (SPR) to investigate the interaction of elastin antibody coated nanoparticles with elastin. Further, the in-vivo response to varying PEG groups must be studied for creating a more effective delivery system.

It must be noted that the nanoparticles tested for our use were fabricated in pure deionized water as the bulk aqueous phase. Since the intent of nanoparticle formulation was in-vivo testing, this system helped with the preparation of nanoparticles free from toxic surfactants. However, this compromised the stability of the particles. Since we used freshly prepared particles for each experiment, the stability was not a critical component of our system. However, as we envision a clinical scalability of this project, sterile formulation and stable storage becomes a crucial parameter that needs much research. In addition, as we are dealing with biodegradable systems, it is imperative that the nanoparticles must be stored in a dry environment. Nanoparticles are commonly isolated by freeze-drying. This process should have certain desirable characteristics such as (a) preservation of physical and chemical characteristics of polymeric system (b) an acceptable relative humidity (c) long term stability (d) functional retention of antibodies. Freeze drying is a stressful process that can de-stabilize colloidal suspension of nanoparticles especially during dehydration. This process may cause unwarranted and sometimes permanent fusion of nanoparticles dramatically changing its

physical properties. To avoid this, either cryoprotectants (prevents freeze stress) or lyoprotectants (prevents drying stress) are used for long term storage. Some commonly used stabilizers are sucrose, lactose, glucose, mannitol, treahlose, glycerol, hydroxymethyl starch, etc.[361] It has been shown that PLGA nanoparticles could be freeze-dried successfully without changing structural conditions after freezing, (no macroscopic aggregation) when sucrose and glucose were added.[362] Thus experiments must be performed on the PLA nanoparticle system proposed in Chapter 6 to confirm its storage, shelf-life, and stability.

2) ***Scope for improvisation in the biological aspect of nanoparticle system (biological response to nanoparticles)***

The nanoparticles have been tested in two different animal models as described in Chapter 6. Although these models simulate the pathological presentation of MAC and AAA, the induction of the pathology is very acute and clinically dissimilar. Especially, the calcium chloride injury model causes an acute caustic injury to the aorta leading to elastin fragmentation. In addition, the model is devoid of atherosclerosis and fatty deposition (a common clinical presentation). As evidenced, there is a direct positive correlation between the quantity of nanoparticle attachment and degree of elastin damage. An important question, and possibly a limiting parameter of this project, is if the amount of elastin damage in the calcium chloride model is comparable to that in diseased patients. Therefore, it becomes necessary to test the functionality of these

particles in a clinically relevant animal model such as Angiotensin II in ApoE-/- mice (discussed in detail in Chapter 2).

Due to the size of nanoparticles tested (~ 200 nm) it is clear that a vast majority of the particles are cleared by the Kupffer cells of the liver and spleen. This is due to a rapid opsonization of nanoparticles which causes instant (minutes to hours) trafficking of nanoparticles to liver and spleen (non-targets). The clearance study indicates that ~ 50% of the particles are cleared from the liver and spleen by 8 days. Thus this technology can be used to safely deliver multiple doses of nanoparticles to attain required therapeutic effect. However, clearance follows a first order exponential decay rate, thus it becomes important to identify the time that particles take for complete clearance, as multiple dosing should not cause toxic accumulation of nanoparticles in off-target organs.

3) Loading of polyphenols for drug delivery

The greatest shortcoming, thereby the largest future scope, of this project is the un-successful loading and release of drugs in the nanoparticle system. We attempted PGG loading two times using two different molecular weights of PLA and obtained sub-optimal encapsulation efficiency. It has been documented in literature several times about the challenges of loading water-soluble drugs in PLA/PLGA nanoparticle systems. Consequently, the advent of liposomes provided a novel solution to loading water soluble drugs. Liposomes are bilipid micelles that mimic cell membranes but lack membranous proteins. Liposomes

can be single membrane layer or multiple membrane layers.[363] Just like polymeric nanoparticles, liposomes can be manipulated to add surface PEG groups, conjugate proteins on surface and engineered for controlled release of drugs. Thus, liposomes can be used for encapsulating water soluble drugs such as PGG, EGCG and catechin to achieve desirable loading efficiency and release profiles, which can then be administered for elastin stabilization.

CHAPTER 9

REFERENCES

1. Writing Group M, Lloyd-Jones D, Adams RJ, et al. Heart Disease and Stroke Statistics--2010 Update: A Report From the American Heart Association. *Circulation.* February 23, 2010;121(7):e46-215.

2. http://www.cdc.gov/diabetes/pubs/pdf/ndfs_2011.pdf.

3. Urry DW, Luan C-H, Peng SQ. Molecular Biophysics of Elastin Structure, Function and Pathology. *Ciba Foundation Symposium 192 - The Molecular Biology and Pathology of Elastic Tissues*: John Wiley & Sons, Ltd.; 2007:4-30.

4. Moon J CVMBJWSRGDP. A controlled study of medial arterial calcification of legs: Implications for diabetic polyneuropathy. *Archives of Neurology.* 2011;68(10):1290-1294.

5. Chung AWY, Yang HHC, Sigrist MK, et al. Matrix metalloproteinase-2 and -9 exacerbate arterial stiffening and angiogenesis in diabetes and chronic kidney disease. *Cardiovascular Research.* December 1, 2009 2009;84(3):494-504.

6. Signorelli SS, Malaponte G, Libra M, et al. Plasma levels and zymographic activities of matrix metalloproteinases 2 and 9 in type II diabetics with peripheral arterial disease. *Vascular Medicine.* February 1, 2005 2005;10(1):1-6.

7. Simionescu A, Philips K, Vyavahare N. Elastin-derived peptides and TGF-Î²1 induce osteogenic responses in smooth muscle cells. *Biochemical and Biophysical Research Communications.* 2005;334(2):524-532.

8. Simionescu A, Simionescu DT, Vyavahare NR. Osteogenic responses in fibroblasts activated by elastin degradation products and transforming growth factor-beta1: role of myofibroblasts in vascular calcification. *Am J Pathol.* Jul 2007;171(1):116-123.

9. Nicoloff G, Baydanoff S, Stanimorova N, Petrova C, Cristova P. Relationship between elastin-derived peptides and the development of microvascular complications: A longitudinal study in children with Type 1 (insulin-dependent) diabetes mellitus. *General Pharmacology: The Vascular System.* 2000;35(2):59-64.

10. Winlove CP, Parker KH, Avery NC, Bailey AJ. Interactions of elastin and aorta with sugars in vitro and their effects on biochemical and physical properties. *Diabetologia.* 1996/10/01 1996;39(10):1131-1139.

11. Sakata N, Noma A, Yamamoto Y, et al. Modification of elastin by pentosidine is associated with the calcification of aortic media in patients with end-stage renal disease. *Nephrology Dialysis Transplantation.* August 1, 2003 2003;18(8):1601-1609.

12. Thompson RW. ATVB In Focus: Abdominal Aortic Aneurysms: Pathophysiological Mechanisms and Clinical Implications. *Arteriosclerosis, Thrombosis, and Vascular Biology.* February 1, 2004 2004;24(2):240.

13. Isselbacher EM. Thoracic and Abdominal Aortic Aneurysms. *Circulation.* February 15, 2005 2005;111(6):816-828.

14. Steinmetz EF, Buckley C, Shames ML, et al. Treatment with simvastatin suppresses the development of experimental abdominal aortic aneurysms in normal and hypercholesterolemic mice. *Ann Surg.* Jan 2005;241(1):92-101.

15. Kalyanasundaram A, Elmore JR, Manazer JR, et al. Simvastatin suppresses experimental aortic aneurysm expansion. *J Vasc Surg.* Jan 2006;43(1):117-124.

16. Nagashima H, Aoka Y, Sakomura Y, et al. A 3-hydroxy-3-methylglutaryl coenzyme A reductase inhibitor, cerivastatin, suppresses production of matrix metalloproteinase-9 in human abdominal aortic aneurysm wall. *J Vasc Surg.* Jul 2002;36(1):158-163.

17. Brophy CM, Tilson JE, Tilson MD. Propranolol stimulates the crosslinking of matrix components in skin from the aneurysm-prone blotchy mouse. *J Surg Res.* Apr 1989;46(4):330-332.

18. Ricci MA, Slaiby JM, Gadowski GR, Hendley ED, Nichols P, Pilcher DB. Effects of Hypertension and Propranolol upon Aneurysm Expansion in the Anidjar/Dobrin Aneurysm Modela. *Annals of the New York Academy of Sciences.* 1996;800(1):89-96.

19. Liao S, Miralles M, Kelley BJ, Curci JA, Borhani M, Thompson RW. Suppression of experimental abdominal aortic aneurysms in the rat by treatment with angiotensin-converting enzyme inhibitors. *J Vasc Surg.* May 2001;33(5):1057-1064.

20. Sho E, Chu J, Sho M, et al. Continuous periaortic infusion improves doxycycline efficacy in experimental aortic aneurysms. *J Vasc Surg.* Jun 2004;39(6):1312-1321.

21. Baxter BT, Pearce WH, Waltke EA, et al. Prolonged administration of doxycycline in patients with small asymptomatic abdominal aortic aneurysms: report of a prospective (Phase II) multicenter study. *J Vasc Surg.* Jul 2002;36(1):1-12.

22. Wang M, Thanou M. Targeting nanoparticles to cancer. *Pharmacological Research.* 2010;62(2):90-99.

23. Muro S, Dziubla T, Qiu W, et al. Endothelial Targeting of High-Affinity Multivalent Polymer Nanocarriers Directed to Intercellular Adhesion Molecule 1. *Journal of Pharmacology and Experimental Therapeutics.* June 1, 2006 2006;317(3):1161-1169.

24. Rossin R, Muro S, Welch MJ, Muzykantov VR, Schuster DP. In Vivo Imaging of 64Cu-Labeled Polymer Nanoparticles Targeted to the Lung Endothelium. *Journal of Nuclear Medicine.* January 1, 2008 2008;49(1):103-111.

25. Homem de Bittencourt Jr PI, Lagranha DJ, Maslinkiewicz A, et al. LipoCardium: Endothelium-directed cyclopentenone prostaglandin-based liposome formulation that completely reverses atherosclerotic lesions. *Atherosclerosis.* 2007;193(2):245-258.

26. Paulsson M. Basement membrane proteins: structure, assembly, and cellular interactions. *Crit Rev Biochem Mol Biol.* 1992;27(1-2):93-127.

27. Publishers FSHPeB.

28. Rosenbloom J, Abrams WR, Mecham R. Extracellular matrix 4: the elastic fiber. *The FASEB Journal.* October 1, 1993 1993;7(13):1208-1218.

29. Osborne-Pellegrin MJ, Farjanel J, Hornebeck W. Role of elastase and lysyl oxidase activity in spontaneous rupture of internal elastic lamina in rats. *Arteriosclerosis, Thrombosis, and Vascular Biology.* November 1, 1990 1990;10(6):1136-1146.

30. Isenburg JC, Simionescu DT, Vyavahare NR. Elastin stabilization in cardiovascular implants: improved resistance to enzymatic degradation by treatment with tannic acid. *Biomaterials.* 2004;25(16):3293-3302.

31. Tamburro AM. Elastin: molecular and supramolecular structure. *Progress in clinical and biological research.* 1981;54:45-62.

32. Debelle L, Tamburro AM. Elastin: molecular description and function. *The international journal of biochemistry & cell biology.* Feb 1999;31(2):261-272.

33. Hay ED. Cell biology of extracellular matrix. 1991 Plenum press NYCI.

34. Laban MM. Collagen tissue: implications of its response to stress in vitro. *Arch Phys Med Rehabil.* Sep 1962;43:461-466.

35. http://biochemistry.utoronto.ca/keeley/bch.html.

36. Roach MR, Burton AC. The reason for the shape of the distensibility curves of arteries. *Canadian journal of biochemistry and physiology.* 1957;35(8):681-690.

37. Stromberg DD, Wiederhielm CA. Viscoelastic description of a collagenous tissue in simple elongation. *Journal of Applied Physiology.* June 1, 1969 1969;26(6):857-862.

38. http://helpfromthedoctor.com/blog/2010/07/27/what-is-a-protein/.

39. Rosenbloom J AW, Mecham R. Extracellular matrix 4: the elastic fiber. *FASEB J.* 1993 Oct;7(13):1208-1218.

40. Robert AM RLBaPoetSKCI, III, IV.

41. Ramamurthi A, Vesely I. Evaluation of the matrix-synthesis potential of crosslinked hyaluronan gels for tissue engineering of aortic heart valves. *Biomaterials.* 2005;26(9):999-1010.

42. Kielty CM, Sherratt MJ, Shuttleworth CA. Elastic fibres. *Journal of Cell Science.* July 15, 2002 2002;115(14):2817-2828.

43. Fazio MJ, Mattei MG, Passage E, et al. Human elastin gene: new evidence for localization to the long arm of chromosome 7. *American journal of human genetics.* Apr 1991;48(4):696-703.

44. Saunders NA, Grant ME. Elastin biosynthesis in chick-embryo arteries. Studies on the intracellular site of synthesis of tropoelastin. *Biochem J.* Jul 15 1984;221(2):393-400.

45. Clarke AW, Arnspang EC, Mithieux SM, Korkmaz E, Braet F, Weiss AS. Tropoelastin Massively Associates during Coacervation To Form Quantized Protein Spheres†. *Biochemistry.* 2006/08/01 2006;45(33):9989-9996.

46. Mecham RP. Elastin Synthesis and Fiber Assemblya. *Annals of the New York Academy of Sciences.* 1991;624(1):137-146.

47. Clarke AW, Wise SG, Cain SA, Kielty CM, Weiss AS. Coacervation Is Promoted by Molecular Interactions between the PF2 Segment of Fibrillin-1 and the Domain 4 Region of Tropoelastin†. *Biochemistry.* 2005/08/01 2005;44(30):10271-10281.

48. Hirai M, Ohbayashi T, Horiguchi M, et al. Fibulin-5/DANCE has an elastogenic organizer activity that is abrogated by proteolytic cleavage in vivo. *The Journal of Cell Biology.* March 26, 2007 2007;176(7):1061-1071.

49. Yeo GC, Keeley FW, Weiss AS. Coacervation of tropoelastin. *Advances in colloid and interface science.* Sep 14 2011;167(1-2):94-103.

50. Siegel RC, Pinnell SR, Martin GR. Cross-linking of collagen and elastin. Properties of lysyl oxidase. *Biochemistry.* 1970/11/01 1970;9(23):4486-4492.

51. Kagan HM, Sullivan KA. [35] Lysyl oxidase: Preparation and role in elastin biosynthesis. In: Leon W. Cunningham DWF, ed. *Methods Enzymol.* Vol Volume 82: Academic Press; 1982:637-650.

52. Tu Y, Wise SG, Weiss AS. Stages in tropoelastin coalescence during synthetic elastin hydrogel formation. *Micron.* 2010;41(3):268-272.

53. Tu Y, Weiss AS. Glycosaminoglycan-Mediated Coacervation of Tropoelastin Abolishes the Critical Concentration, Accelerates Coacervate Formation, and Facilitates Spherule Fusion: Implications for Tropoelastin Microassembly. *Biomacromolecules.* 2008/07/01 2008;9(7):1739-1744.

54. Urry D. Entropic elastic processes in protein mechanisms. I. Elastic structure due to an inverse temperature transition and elasticity due to internal chain dynamics. *J Protein Chem.* 1988/02/01 1988;7(1):1-34.

55. Clarke AW, Arnspang EC, Mithieux SM, Korkmaz E, Braet F, Weiss AS. Tropoelastin massively associates during coacervation to form quantized protein spheres. *Biochemistry.* Aug 22 2006;45(33):9989-9996.

56. Bressan GM, Castellani I, Giro MG, Volpin D, Fornieri C, Pasquali Ronchetti I. Banded fibers in Tropoelastin coacervates at physiological temperatures. *Journal of Ultrastructure Research.* 1983;82(3):335-340.

57. Cirulis JT, Bellingham CM, Davis EC, et al. Fibrillins, Fibulins, and Matrix-Associated Glycoprotein Modulate the Kinetics and Morphology of in Vitro Self-Assembly of a Recombinant Elastin-like Polypeptide†. *Biochemistry.* 2008/11/25 2008;47(47):12601-12613.

58. Bressan GM, Pasquali-Ronchetti I, Fornieri C, Mattioli F, Castellani I, Volpin D. Relevance of aggregation properties of tropoelastin to the assembly and structure of elastic fibers. *Journal of Ultrastructure and Molecular Structure Research.* 1986;94(3):209-216.

59. Hu Q, Loeys BL, Coucke PJ, et al. Fibulin-5 mutations: mechanisms of impaired elastic fiber formation in recessive cutis laxa. *Human Molecular Genetics.* December 1, 2006 2006;15(23):3379-3386.

60. Mithieux SM, Wise SG, Raftery MJ, Starcher B, Weiss AS. A model two-component system for studying the architecture of elastin assembly in vitro. *Journal of structural biology.* 2005;149(3):282-289.

61. Keeley FW, Bellingham CM, Woodhouse KA. Elastin as a self–organizing biomaterial: use of recombinantly expressed human elastin polypeptides as a model for investigations of structure and self–assembly of elastin. *Philosophical Transactions of the Royal Society of London. Series B: Biological Sciences.* February 28, 2002 2002;357(1418):185-189.

62. Murie JA. Vascular surgery – 5th edition, R.B. Rutherford (ed.), 285 × 222 mm. Pp. 2266. Illustrated. 1999. Philadelphia, Pennsylvania: W. B. Saunders. £199.00. *British Journal of Surgery.* 2000;87(7):972-973.

63. Tu JV, Pashos CL, Naylor CD, et al. Use of Cardiac Procedures and Outcomes in Elderly Patients with Myocardial Infarction in the United States and Canada. *New England Journal of Medicine.* 1997;336(21):1500-1505.

64. Small-Diameter Vascular Graft Prostheses: Current Status. *Archives Of Physiology And Biochemistry.* 1998;106(2):100-115.

65. www.cardiocheck.co.uk.

66. Rabinovitch M. Molecular pathogenesis of pulmonary arterial hypertension. *The Journal of Clinical Investigation.* 2012;122(12):4306-4313.

67. Meyrick B, Reid L. Ultrastructural findings in lung biopsy material from children with congenital heart defects. *Am J Pathol.* Dec 1980;101(3):527-542.

68. Xu W, Kaneko FT, Zheng S, et al. Increased arginase II and decreased NO synthesis in endothelial cells of patients with pulmonary arterial hypertension. *The FASEB Journal.* September 13, 2004 2004.

69. Christman BW, McPherson CD, Newman JH, et al. An Imbalance between the Excretion of Thromboxane and Prostacyclin Metabolites in Pulmonary Hypertension. *New England Journal of Medicine.* 1992;327(2):70-75.

70. Lehto S, Niskanen L, Suhonen M, Rönnemaa T, Laakso M. Medial Artery Calcification: A Neglected Harbinger of Cardiovascular Complications in Non–Insulin-Dependent Diabetes Mellitus. *Arteriosclerosis, Thrombosis, and Vascular Biology.* August 1, 1996 1996;16(8):978-983.

71. Lau WL, Ix JH. Clinical Detection, Risk Factors, and Cardiovascular Consequences of Medial Arterial Calcification: A Pattern of Vascular Injury Associated With Aberrant Mineral Metabolism. *Seminars in Nephrology.* 2013;33(2):93-105.

72. Gentile S, Bizzarro A, Marmo R, Bellis A, Orlando C. Medial arterial calcification and diabetic neuropathy. *Acta diabet. lat.* 1990/07/01 1990;27(3):243-253.

73. London GM, Guérin AP, Marchais SJ, Métivier F, Pannier B, Adda H. Arterial media calcification in end-stage renal disease: impact on all-cause and cardiovascular mortality. *Nephrology Dialysis Transplantation.* September 1, 2003 2003;18(9):1731-1740.

74. Towler DA, Bidder M, Latifi T, Coleman T, Semenkovich CF. Diet-induced Diabetes Activates an Osteogenic Gene Regulatory Program in the Aortas of Low Density Lipoprotein Receptor-deficient Mice. *Journal of Biological Chemistry.* November 13, 1998 1998;273(46):30427-30434.

75. Cheng S-L, Shao J-S, Charlton-Kachigian N, Loewy AP, Towler DA. Msx2 Promotes Osteogenesis and Suppresses Adipogenic Differentiation of Multipotent Mesenchymal Progenitors. *Journal of Biological Chemistry.* November 14, 2003 2003;278(46):45969-45977.

76. Karsenty G. Minireview: Transcriptional Control of Osteoblast Differentiation. *Endocrinology.* July 1, 2001 2001;142(7):2731-2733.

77. Vattikuti R, Towler DA. Osteogenic regulation of vascular calcification: an early perspective. *American Journal of Physiology - Endocrinology And Metabolism.* May 1, 2004 2004;286(5):E686-E696.

78. Nelson RG, Gohdes DM, Everhart JE, et al. Lower-extremity amputations in NIDDM. 12-yr follow-up study in Pima Indians. *Diabetes care.* Jan 1988;11(1):8-16.

79. http://webhost.ua.ac.be/mct/in_vivo_3/aorta_calcif.htm.

80. http://www.biomedsearch.com/nih/Multi-detector-row-computed tomography/17882427.html.

81. Jovinge S, Ares MPS, Kallin B, Nilsson J. Human Monocytes/Macrophages Release TNF-α in Response to Ox-LDL. *Arteriosclerosis, Thrombosis, and Vascular Biology.* December 1, 1996 1996;16(12):1573-1579.

82. Tintut Y, Patel J, Parhami F, Demer LL. Tumor Necrosis Factor-α Promotes In Vitro Calcification of Vascular Cells via the cAMP Pathway. *Circulation.* November 21, 2000 2000;102(21):2636-2642.

83. Shanahan CM, Cary NRB, Salisbury JR, Proudfoot D, Weissberg PL, Edmonds ME. Medial Localization of Mineralization-Regulating Proteins in Association With Mönckeberg's Sclerosis: Evidence for Smooth Muscle Cell–Mediated Vascular Calcification. *Circulation.* November 23, 1999 1999;100(21):2168-2176.

84. Balica M, Boström K, Shin V, Tillisch K, Demer LL. Calcifying Subpopulation of Bovine Aortic Smooth Muscle Cells Is Responsive to 17β-Estradiol. *Circulation.* April 1, 1997 1997;95(7):1954-1960.

85. Kingsley DM. The TGF-beta superfamily: new members, new receptors, and new genetic tests of function in different organisms. *Genes & Development.* January 1, 1994 1994;8(2):133-146.

86. Watson KE, Bostrom K, Ravindranath R, Lam T, Norton B, Demer LL. TGF-beta 1 and 25-hydroxycholesterol stimulate osteoblast-like vascular cells to calcify. *J Clin Invest.* May 1994;93(5):2106-2113.

87. Grainger DJ, Metcalfe JC, Grace AA, Mosedale DE. Transforming growth factor-beta dynamically regulates vascular smooth muscle differentiation in vivo. *J Cell Sci.* Oct 1998;111 (Pt 19):2977-2988.

88. Lee JS, Basalyga DM, Simionescu A, Isenburg JC, Simionescu DT, Vyavahare NR. Elastin Calcification in the Rat Subdermal Model Is Accompanied by Up-Regulation of Degradative and Osteogenic Cellular Responses. *The American Journal of Pathology*. 2006;168(2):490-498.

89. Sinha S, Heagerty AM, Shuttleworth CA, Kielty CM. Expression of latent TGF-beta binding proteins and association with TGF-beta1 and fibrillin-1 following arterial injury. *Cardiovascular Research.* March 1, 2002 2002;53(4):971-983.

90. Ramirez F, Dietz HC. Marfan syndrome: from molecular pathogenesis to clinical treatment. *Current Opinion in Genetics & Development.* 2007;17(3):252-258.

91. Komori T, Yagi H, Nomura S, et al. Targeted Disruption of Cbfa1 Results in a Complete Lack of Bone Formation owing to Maturational Arrest of Osteoblasts. *Cell.* 1997;89(5):755-764.

92. Bae S-C, Lee YH. Phosphorylation, acetylation and ubiquitination: The molecular basis of RUNX regulation. *Gene.* 2006;366(1):58-66.

93. Jono S, McKee MD, Murry CE, et al. Phosphate Regulation of Vascular Smooth Muscle Cell Calcification. *Circulation Research.* September 29, 2000 2000;87(7):e10-e17.

94. Mornet E. Hypophosphatasia: The mutations in the tissue-nonspecific alkaline phosphatase gene. *Human Mutation.* 2000;15(4):309-315.

95. O'Neill WC. Pyrophosphate, Alkaline Phosphatase, and Vascular Calcification. *Circulation Research.* July 21, 2006 2006;99(2):e2.

96. Boskey AL, Gadaleta S, Gundberg C, Doty SB, Ducy P, Karsenty G. Fourier transform infrared microspectroscopic analysis of bones of osteocalcin-deficient mice provides insight into the function of osteocalcin. *Bone.* 1998;23(3):187-196.

97. Takemoto M, Yokote K, Nishimura M, et al. Enhanced Expression of Osteopontin in Human Diabetic Artery and Analysis of Its Functional Role in Accelerated Atherogenesis. *Arteriosclerosis, Thrombosis, and Vascular Biology.* March 1, 2000 2000;20(3):624-628.

98. Sharon MM, Kalisha DON, Danxia D, et al. Medial artery calcification in ESRD patients is associated with deposition of bone matrix proteins. *Kidney International.* 2002;61(2):638-647.

99. Buján J, Bellón JM, Sabater C, et al. Modifications induced by atherogenic diet in the capacity of the arterial wall in rats to respond to surgical insult. *Atherosclerosis.* 1996;122(2):141-152.

100. Brownlee M. The Pathobiology of Diabetic Complications: A Unifying Mechanism. *Diabetes.* June 1, 2005 2005;54(6):1615-1625.

101. Engerman RL, Kern TS, Larson ME. Nerve conduction and aldose reductase inhibition during 5 years of diabetes or galactosaemia in dogs. *Diabetologia.* 1994/02/01 1994;37(2):141-144.

102. Goldin A, Beckman JA, Schmidt AM, Creager MA. Advanced Glycation End Products: Sparking the Development of Diabetic Vascular Injury. *Circulation.* August 8, 2006 2006;114(6):597-605.

103. Xia P IT, Kern TS, Engerman RL, Oates PJ, King GL. Characterization of the mechanism for the chronic activation of diacylglycerol-protein kinase C pathway in diabetes and hypergalactosemia. *Diabetes.* 1994 Sep;43(9):1122-9.

104. Koya D, King GL. Protein kinase C activation and the development of diabetic complications. *Diabetes.* June 1, 1998 1998;47(6):859-866.

105. Kaufman HW, Kleinberg I. Studies on the incongruent solubility of hydroxyapatite. *Calcif Tissue Int.* Apr 17 1979;27(2):143-151.

106. Ernst E. Chelation Therapy for Peripheral Arterial Occlusive Disease: A Systematic Review. *Circulation.* August 5, 1997 1997;96(3):1031-1033.

107. Godfrey ME. EDTA chelation as a treatment of arteriosclerosis. *The New Zealand medical journal.* Apr 11 1990;103(887):162-163.

108. Chappell LT, Janson M. EDTA chelation therapy in the treatment of vascular disease. *The Journal of cardiovascular nursing.* Apr 1996;10(3):78-86.

109. Clarke NE, Clarke CN, Mosher RE. The in vivo dissolution of metastatic calcium; an approach to atherosclerosis. *The American journal of the medical sciences.* Feb 1955;229(2):142-149.

110. Ernst E. Chelation therapy for coronary heart disease: An overview of all clinical investigations. *American Heart Journal.* 2000;140(1):139-141.

111. Schurgers LJ, Spronk HMH, Soute BAM, Schiffers PM, DeMey JGR, Vermeer C. Regression of warfarin-induced medial elastocalcinosis by high intake of vitamin K in rats. *Blood.* April 1, 2007 2007;109(7):2823-2831.

112. Takemoto M, Liao JK. Pleiotropic Effects of 3-Hydroxy-3-Methylglutaryl Coenzyme A Reductase Inhibitors. *Arterioscler Thromb Vasc Biol.* November 1, 2001 2001;21(11):1712-1719.

113. Crisby M, Nordin-Fredriksson G, Shah PK, Yano J, Zhu J, Nilsson J. Pravastatin Treatment Increases Collagen Content and Decreases Lipid Content, Inflammation, Metalloproteinases, and Cell Death in Human Carotid Plaques : Implications for Plaque Stabilization. *Circulation.* February 20, 2001 2001;103(7):926-933.

114. Wanner C, Krane V, März W, et al. Atorvastatin in Patients with Type 2 Diabetes Mellitus Undergoing Hemodialysis. *New England Journal of Medicine.* 2005;353(3):238-248.

115. Raggi P. Regression of calcified coronary artery plaque assessed by electron beam computed tomography. *Zeitschrift fur Kardiologie.* 2000;89 Suppl 2:135-139.

116. Nakao J, Orimo H, Ooyama T, Shiraki M. Low serum estradiol levels in subjects with arterial calcification. *Atherosclerosis.* Dec 1979;34(4):469-474.

117. McLaughlin VV, Hoff JA, Rich S. Relation between hormone replacement therapy in women and coronary artery disease estimated by electron beam tomography. *American Heart Journal.* 1997;134(6):1115-1119.

118. Hulley S GDBT, et al. RAndomized trial of estrogen plus progestin for secondary prevention of coronary heart disease in postmenopausal women. *JAMA.* 1998;280(7):605-613.

119. Fleckenstein A, Frey M, Zorn J, Fleckenstein-Grün G. The role of calcium in the pathogenesis of experimental arteriosclerosis. *Trends in Pharmacological Sciences.* 1987;8(12):496-501.

120. Strickberger SA, Russek LN, Phair RD. Evidence for increased aortic plasma membrane calcium transport caused by experimental atherosclerosis in rabbits. *Circulation Research.* January 1, 1988 1988;62(1):75-80.

121. Oparil S. Long-term morbidity and mortality trials with amlodipine. *J Cardiovasc Pharmacol.* 1999;33 Suppl 2:S1-6.

122. Neven E, D'Haese PC. Vascular Calcification in Chronic Renal Failure: What Have We Learned From Animal Studies? *Circulation Research.* January 21, 2011 2011;108(2):249-264.

123. Price PA, Faus SA, Williamson MK. Warfarin Causes Rapid Calcification of the Elastic Lamellae in Rat Arteries and Heart Valves. *Arteriosclerosis, Thrombosis, and Vascular Biology.* September 1, 1998 1998;18(9):1400-1407.

124. Howe, Webster. Warfarin exposure and calcification of the arterial system in the rat. *International Journal of Experimental Pathology.* 2000;81(1):51-56.

125. Zebboudj AF, Imura M, Boström K. Matrix GLA Protein, a Regulatory Protein for Bone Morphogenetic Protein-2. *Journal of Biological Chemistry.* February 8, 2002 2002;277(6):4388-4394.

126. Price PA, Faus SA, Williamson MK. Warfarin-Induced Artery Calcification Is Accelerated by Growth and Vitamin D. *Arteriosclerosis, Thrombosis, and Vascular Biology.* February 1, 2000 2000;20(2):317-327.

127. Niederhoffer N, Lartaud-Idjouadiene I, Giummelly P, Duvivier C, Peslin R, Atkinson J. Calcification of Medial Elastic Fibers and Aortic Elasticity. *Hypertension.* April 1, 1997 1997;29(4):999-1006.

128. Jono S, Nishizawa Y, Shioi A, Morii H. Parathyroid Hormone–Related Peptide as a Local Regulator of Vascular Calcification: Its Inhibitory Action on In Vitro Calcification by Bovine Vascular Smooth Muscle Cells. *Arteriosclerosis, Thrombosis, and Vascular Biology.* June 1, 1997 1997;17(6):1135-1142.

129. Jono S, Nishizawa Y, Shioi A, Morii H. 1,25-Dihydroxyvitamin D3 Increases In Vitro Vascular Calcification by Modulating Secretion of Endogenous Parathyroid Hormone–Related Peptide. *Circulation.* September 29, 1998 1998;98(13):1302-1306.

130. Henrion D, Chillon JM, Godeau G, et al. The consequences of aortic calcium overload following vitamin D3 plus nicotine treatment in young rats. *Journal of hypertension.* Oct 1991;9(10):919-926.

131. Luo G, Ducy P, McKee MD, et al. Spontaneous calcification of arteries and cartilage in mice lacking matrix GLA protein. *Nature.* Mar 6 1997;386(6620):78-81.

132. Bucay N, Sarosi I, Dunstan CR, et al. osteoprotegerin-deficient mice develop early onset osteoporosis and arterial□calcification. *Genes & Development.* May 1, 1998 1998;12(9):1260-1268.

133. Galvin KM, Donovan MJ, Lynch CA, et al. A role for smad6 in development and homeostasis of the cardiovascular system. *Nature genetics.* Feb 2000;24(2):171-174.

134. Spicer SS, Lewis SE, Tashian RE, Schulte BA. Mice carrying a CAR-2 null allele lack carbonic anhydrase II immunohistochemically and show vascular calcification. *Am J Pathol.* Apr 1989;134(4):947-954.

135. Pereira L, Lee SY, Gayraud B, et al. Pathogenetic sequence for aneurysm revealed in mice underexpressing fibrillin-1. *Proceedings of the National Academy of Sciences.* March 30, 1999 1999;96(7):3819-3823.

136. Kuro-o M, Matsumura Y, Aizawa H, et al. Mutation of the mouse klotho gene leads to a syndrome resembling ageing. *Nature.* Nov 6 1997;390(6655):45-51.

137. Qiao JH, Xie PZ, Fishbein MC, et al. Pathology of atheromatous lesions in inbred and genetically engineered mice. Genetic determination of arterial calcification. *Arteriosclerosis, Thrombosis, and Vascular Biology.* September 1, 1994 1994;14(9):1480-1497.

138. Roselaar SE, Kakkanathu PX, Daugherty A. Lymphocyte Populations in Atherosclerotic Lesions of ApoE −/− and LDL Receptor −/− Mice: Decreasing Density With Disease Progression. *Arteriosclerosis, Thrombosis, and Vascular Biology.* August 1, 1996 1996;16(8):1013-1018.

139. Paule WJ, Bernick S, Strates B, Nimni ME. Calcification of implanted vascular tissues associated with elastin in an experimental animal model. *Journal of biomedical materials research.* Sep 1992;26(9):1169-1177.

140. Gertz SD, Kurgan A, Eisenberg D. Aneurysm of the rabbit common carotid artery induced by periarterial application of calcium chloride in vivo. *J Clin Invest.* Mar 1988;81(3):649-656.

141. www.ncbi.nlm.nih.gov/pubmedhealth/PMH0001215/figure/A000162.B18072/?report=objectonly.

142. http://www.healthpress.us/wp-content/uploads/2010/12/types-of-aneurysms.gif.

143. Crawford CM, Hurtgen-Grace K, Talarico E, Marley J. Abdominal aortic aneurysm: an illustrated narrative review. *Journal of Manipulative and Physiological Therapeutics.* 2003;26(3):184-195.

144. Newman AB, Arnold AM, Burke GL, O'Leary DH, Manolio TA. Cardiovascular Disease and Mortality in Older Adults with Small Abdominal Aortic Aneurysms Detected by Ultrasonography: The Cardiovascular Health Study. *Annals of Internal Medicine.* February 6, 2001 2001;134(3):182-190.

145. Vardulaki, K A, Walker, et al. *Quantifying the risks of hypertension, age, sex and smoking in patients with abdominal aortic aneurysm.* Vol 87. Chichester, ROYAUME-UNI: Wiley; 2000.

146. Lederle FA, Johnson GR, Wilson SE, et al. Prevalence and associations of abdominal aortic aneurysm detected through screening. Aneurysm Detection and Management (ADAM) Veterans Affairs Cooperative Study Group. *Annals of Internal Medicine.* 1997;126(6):441-449.

147. LaMorte WW, Scott TE, Menzoian JO. Racial differences in the incidence of femoral bypass and abdominal aortic aneurysmectomy in Massachusetts: Relationship to cardiovascular risk factors. *Journal of Vascular Surgery.* 1995;21(3):422-431.

148. Singh K, BÃ¸naa KH, Jacobsen BK, BjÃ¸rk L, Solberg S. Prevalence of and Risk Factors for Abdominal Aortic Aneurysms in a Population-based Study. *American Journal of Epidemiology.* August 1, 2001 2001;154(3):236-244.

149. Alcorn HG, Wolfson SK, Jr., Sutton-Tyrrell K, Kuller LH, O'Leary D. Risk Factors for Abdominal Aortic Aneurysms in Older Adults Enrolled in the Cardiovascular Health Study. *Arterioscler Thromb Vasc Biol.* August 1, 1996 1996;16(8):963-970.

150. Selle JG, Robicsek F, Daugherty HK, Cook JW. Thoracoabdominal aortic aneurysms: a review and current status. *Coll Works Cardiopulm Dis.* Aug 1979;22:79-90.

151. http://www.bmj.com/content/320/7243/1193/F1.large.jpg.

152. Aboulafia DM, Aboulafia ED. Aortic aneurysm-induced disseminated intravascular coagulation. *Ann Vasc Surg.* Jul 1996;10(4):396-405.

153. http://www.bmj.com/content/320/7243/1193.full.

154. Sakalihasan N, Limet R, Defawe OD. Abdominal aortic aneurysm. *The Lancet.* 2005;365(9470):1577-1589.

155. Curci JA, Thompson RW. Adaptive cellular immunity in aortic aneurysms: cause, consequence, or context? *J Clin Invest.* Jul 2004;114(2):168-171.

156. Elefteriades JA. Thoracic Aortic Aneurysm: Reading the Enemy's Playbook. *Current Problems in Cardiology.* 2008;33(5):203-277.

157. Welgus HG, Jeffrey JJ, Stricklin GP, Roswit WT, Eisen AZ. Characteristics of the action of human skin fibroblast collagenase on fibrillar collagen. *J Biol Chem.* Jul 25 1980;255(14):6806-6813.

158. Irizarry E, Newman KM, Gandhi RH, et al. Demonstration of Interstitial Collagenase in Abdominal Aortic Aneurysm Disease. *Journal of Surgical Research.* 1993;54(6):571-574.

159. Senior RM, Griffin GL, Fliszar CJ, Shapiro SD, Goldberg GI, Welgus HG. Human 92- and 72-kilodalton type IV collagenases are elastases. *J Biol Chem.* Apr 25 1991;266(12):7870-7875.

160. Thompson RW, Holmes DR, Mertens RA, et al. Production and localization of 92-kilodalton gelatinase in abdominal aortic aneurysms. An elastolytic metalloproteinase expressed by aneurysm-infiltrating macrophages. *J Clin Invest.* Jul 1995;96(1):318-326.

161. Pyo R, Lee JK, Shipley JM, et al. Targeted gene disruption of matrix metalloproteinase-9 (gelatinase B) suppresses development of experimental abdominal aortic aneurysms. *The Journal of Clinical Investigation.* 2000;105(11):1641-1649.

162. Longo GM, Xiong W, Greiner TC, Zhao Y, Fiotti N, Baxter BT. Matrix metalloproteinases 2 and 9 work in concert to produce aortic aneurysms. *The Journal of Clinical Investigation.* 2002;110(5):625-632.

163. Xiong W, Knispel R, MacTaggart J, Greiner TC, Weiss SJ, Baxter BT. Membrane-type 1 matrix metalloproteinase regulates macrophage-dependent elastolytic activity and aneurysm formation in vivo. *The Journal of biological chemistry.* 2009;284(3):1765-1771.

164. Freestone T, Turner RJ, Coady A, Higman DJ, Greenhalgh RM, Powell JT. Inflammation and Matrix Metalloproteinases in the Enlarging Abdominal Aortic Aneurysm. *Arterioscler Thromb Vasc Biol.* August 1, 1995 1995;15(8):1145-1151.

165. Fontaine V, Jacob M-P, Houard X, et al. Involvement of the Mural Thrombus as a Site of Protease Release and Activation in Human Aortic Aneurysms. *The American Journal of Pathology.* 2002;161(5):1701-1710.

166. Goodall S, Porter KE, Bell PR, Thompson MM. Enhanced invasive properties exhibited by smooth muscle cells are associated with elevated production of MMP-2 in patients with aortic aneurysms. *Eur J Vasc Endovasc Surg.* Jul 2002;24(1):72-80.

167. Shapiro SD, Kobayashi DK, Ley TJ. Cloning and characterization of a unique elastolytic metalloproteinase produced by human alveolar macrophages. *J Biol Chem.* Nov 15 1993;268(32):23824-23829.

168. Curci JA, Liao S, Huffman MD, Shapiro SD, Thompson RW. Expression and localization of macrophage elastase (matrix metalloproteinase-12) in abdominal aortic aneurysms. *The Journal of Clinical Investigation.* 1998;102(11):1900-1910.

169. Lindholt JS VS, Juul S, Henneberg EW, Fasting H. The validity of ultrasonographic scanning as screening method for abdominal aortic aneurysm. *Eur J Vasc Endovasc Surg.* 1999 Jun;17(6):472-5.

170. Sakalihasan N, Limet R, Defawe OD. Abdominal aortic aneurysm. *Lancet.* Apr 30-May 6 2005;365(9470):1577-1589.

171. Schermerhorn M. A 66-year-old man with an abdominal aortic aneurysm: Review of screening and treatment. *JAMA.* 2009;302(18):2015-2022.

172. Arko FR, Lee WA, Hill BB, et al. Aneurysm-related death: primary endpoint analysis for comparison of open and endovascular repair. *J Vasc Surg.* Aug 2002;36(2):297-304.

173. Vega de CÃ©niga M, Estallo L, Barba A, de la Fuente N, Viviens B, GÃ³mez R. Long-Term Cardiovascular Outcome AfterÂ Elective Abdominal Aortic Aneurysm Open Repair. *Annals of vascular surgery.*24(5):655-662.

174. Desai M, Eaton-Evans J, Hillery C, et al. AAA stent-grafts: past problems and future prospects. *Ann Biomed Eng.* Apr;38(4):1259-1275.

175. Coggia M, Javerliat I, Di Centa I, et al. Total laparoscopic infrarenal aortic aneurysm repair: Preliminary results. *Journal of Vascular Surgery.* 2004;40(3):448-454.

176. Parodi JC, Palmaz JC, Barone HD. Transfemoral Intraluminal Graft Implantation for Abdominal Aortic Aneurysms. *Annals of vascular surgery.* 1991;5(6):491-499.

177. Arko FR, Filis KA, Seidel SA, et al. How Many Patients With Infrarenal Aneurysms Are Candidates for Endovascular Repair? The Northern California Experience. *Journal of Endovascular Therapy.* 2004;11(1):33-40.

178. Schurink GWH, Aarts NJM, van Bockel JH. Endoleak after stent-graft treatment of abdominal aortic aneurysm: a meta-analysis of clinical studies. *British Journal of Surgery.* 1999;86(5):581-587.

179. Gilling-Smith G, Brennan J, Harris P, Bakran A, Gould D, McWilliams R. Endotension After Endovascular Aneurysm Repair: Definition, Classification, and Strategies for Surveillance and Intervention. *Journal of Endovascular Surgery.* 1999;6(4):305-307.

180. Skillern CS, Stevens SL, Piercy KT, Donnell RL, Freeman MB, Goldman MH. Endotension in an experimental aneurysm model. *J Vasc Surg.* Oct 2002;36(4):814-817.

181. Drury D, Michaels JA, Jones L, Ayiku L. Systematic review of recent evidence for the safety and efficacy of elective endovascular repair in the management of infrarenal abdominal aortic aneurysm. *British Journal of Surgery.* 2005;92(8):937-946.

182. Zarins CK, Bloch DA, Crabtree T, Matsumoto AH, White RA, Fogarty TJ. Stent graft migration after endovascular aneurysm repair: importance of proximal fixation. *Journal of vascular surgery : official publication, the Society for Vascular Surgery [and] International Society for Cardiovascular Surgery, North American Chapter.* 2003;38(6):1264-1272.

183. Jacobs TS, Won J, Gravereaux EC, et al. Mechanical failure of prosthetic human implants: A 10-year experience with aortic stent graft devices. *Journal of Vascular Surgery.* 2003;37(1):16-26.

184. Steinmetz, Eric F, Buckley, et al. *Treatment with simvastatin suppresses the development of experimental abdominal aortic aneurysms in normal and hypercholesterolemic mice.* Vol 241. Hagerstown, MD, ETATS-UNIS: Lippincott Williams & Wilkins; 2005.

185. Kalyanasundaram A, Elmore JR, Manazer JR, et al. Simvastatin suppresses experimental aortic aneurysm expansion. *Journal of Vascular Surgery.* 2006;43(1):117-117.e139.

186. Nagashima H, Aoka Y, Sakomura Y, et al. A 3-hydroxy-3-methylglutaryl coenzyme A reductase inhibitor, cerivastatin, suppresses production of matrix metalloproteinase-9 in human abdominal aortic aneurysm wall. *Journal of Vascular Surgery.* 2002;36(1):158-163.

187. Sukhija R, Aronow WS, Sandhu R, Kakar P, Babu S. Mortality and Size of Abdominal Aortic Aneurysm at Long-Term Follow-Up of Patients Not Treated Surgically and Treated With and Without Statins. *The American Journal of Cardiology.* 2006;97(2):279-280.

188. Evans J, Powell JT, Schwalbe E, Loftus IM, Thompson MM. Simvastatin Attenuates the Activity of Matrix Metalloprotease-9 in Aneurysmal Aortic Tissue. *European Journal of Vascular and Endovascular Surgery.* 2007;34(3):302-303.

189. Schouten O, van Laanen JHH, Boersma E, et al. Statins are Associated with a Reduced Infrarenal Abdominal Aortic Aneurysm Growth. *European Journal of Vascular and Endovascular Surgery.* 2006;32(1):21-26.

190. Twine CP, Williams IM. Systematic review and meta-analysis of the effects of statin therapy on abdominal aortic aneurysms. *Br J Surg.* Nov 24.

191. Hirsch AT, Haskal ZJ, Hertzer NR, et al. ACC/AHA 2005 Practice Guidelines for the Management of Patients With Peripheral Arterial Disease (Lower Extremity, Renal, Mesenteric, and Abdominal Aortic): A Collaborative Report from the American Association for Vascular Surgery/Society for Vascular Surgery,* Society for Cardiovascular Angiography and Interventions, Society for Vascular Medicine and Biology, Society of Interventional Radiology, and the ACC/AHA Task Force on Practice Guidelines (Writing Committee to Develop Guidelines for the Management of Patients With Peripheral Arterial Disease): Endorsed by the American Association of Cardiovascular and Pulmonary Rehabilitation; National Heart, Lung, and Blood Institute; Society for Vascular Nursing; TransAtlantic Inter-Society Consensus; and Vascular Disease Foundation. *Circulation.* March 21, 2006 2006;113(11):e463-465.

192. Brophy CM, Tilson JE, Tilson MD. Propranolol stimulates the crosslinking of matrix components in skin from the aneurysm-prone Blotchy mouse. *Journal of Surgical Research.* 1989;46(4):330-332.

193. Boucek RJ, Gunja-Smith Z, Noble NL, Simpson CF. Modulation by propranolol of the lysyl cross-links in aortic elastin and collagen of the aneurysm-prone turkey. *Biochemical Pharmacology.* 1983;32(2):275-280.

194. Slaiby JM RM, Gadowski GR, Hendley ED, Pilcher DB. Expansion of aortic aneurysms is reduced by propranolol in a hypertensive rat model. *J Vasc Surg.* 1994 Aug;20(2):178-183.

195. Gadowski GR PD, Ricci MA. Abdominal aortic aneurysm expansion rate: effect of size and beta-adrenergic blockade. *J Vasc Surg.* 1994 Apr;.19(4):727-31.

196. Leach SD, Toole AL, Stern H, DeNatale RW, Tilson MD. Effect of beta-adrenergic blockade on the growth rate of abdominal aortic aneurysms. *Arch Surg.* May 1988;123(5):606-609.

197. The Propranolol Aneurysm Trial I. Propranolol for small abdominal aortic aneurysms: Results of a randomized trial. *Journal of Vascular Surgery.* 2002;35(1):72-79.

198. Lindholt JS, Henneberg EW, Juul S, Fasting H. Impaired results of a randomised double blinded clinical trial of propranolol versus placebo on the expansion rate of small abdominal aortic aneurysms. *Int Angiol.* Mar 1999;18(1):52-57.

199. Daugherty A, Manning MW, Cassis LA. Angiotensin II promotes atherosclerotic lesions and aneurysms in apolipoprotein Eâ€“deficient mice. *The Journal of Clinical Investigation.* 2000;105(11):1605-1612.

200. Cassis LA, Gupte M, Thayer S, et al. ANG II infusion promotes abdominal aortic aneurysms independent of increased blood pressure in hypercholesterolemic mice. *American Journal of Physiology - Heart and Circulatory Physiology.* May 2009 2009;296(5):H1660-H1665.

201. Sasamura H, Itoh H. [Hypertension and arteriosclerosis]. *Nippon Rinsho.*69(1):125-130.

202. Inoue N, Muramatsu M, Jin D, et al. Involvement of Vascular Angiotensin II-Forming Enzymes in the Progression of Aortic Abdominal Aneurysms in Angiotensin II- Infused ApoE-Deficient Mice. *Journal of Atherosclerosis and Thrombosis.* 2009;16(3):164-171.

203. Liao S, Miralles M, Kelley BJ, Curci JA, Borhani M, Thompson RW. Suppression of experimental abdominal aortic aneurysms in the rat by treatment with angiotensin-converting enzyme inhibitors. *Journal of Vascular Surgery.* 2001;33(5):1057-1064.

204. Hackam DG, Thiruchelvam D, Redelmeier DA. Angiotensin-converting enzyme inhibitors and aortic rupture: a population-based case-control study. *The Lancet.* 2006/8/25/ 2006;368(9536):659-665.

205. Sweeting MJ, Thompson SG, Brown LC, Greenhalgh RM, Powell JT. Use of angiotensin converting enzyme inhibitors is associated with increased growth rate of abdominal aortic aneurysms. *Journal of Vascular Surgery.*52(1):1-4.

206. Daugherty A, Manning MW, Cassis LA. Antagonism of AT2 receptors augments Angiotensin II-induced abdominal aortic aneurysms and atherosclerosis. *British Journal of Pharmacology.* 2001;134(4):865-870.

207. Fujiwara Y, Shiraya S, Miyake T, et al. Inhibition of experimental abdominal aortic aneurysm in a rat model by the angiotensin receptor blocker valsartan. *Int J Mol Med.* Dec 2008;22(6):703-708.

208. Manning MW, Cassis LA, Daugherty A. Differential Effects of Doxycycline, a Broad-Spectrum Matrix Metalloproteinase Inhibitor, on Angiotensin II-Induced Atherosclerosis and Abdominal Aortic Aneurysms. *Arterioscler Thromb Vasc Biol.* March 1, 2003 2003;23(3):483-488.

209. Curci JA, Mao D, Bohner DG, et al. Preoperative treatment with doxycycline reduces aortic wall expression and activation of matrix metalloproteinases in patients with abdominal aortic aneurysms. *Journal of Vascular Surgery.* 2000;31(2):325-342.

210. Baxter BT, Pearce WH, Waltke EA, et al. Prolonged administration of doxycycline in patients with small asymptomatic abdominal aortic aneurysms: Report of a prospective (Phase II) multicenter study. *Journal of Vascular Surgery.* 2002;36(1):1-12.

211. Dai J, Louedec L, Philippe M, Michel J-B, Houard X. Effect of blocking platelet activation with AZD6140 on development of abdominal aortic aneurysm in a rat aneurysmal model. *Journal of Vascular Surgery.* 2009;49(3):719-727.

212. Karlsson L, Gnarpe J, Bergqvist D, Lindbäck J, Pärsson H. The effect of azithromycin and Chlamydophilia pneumonia infection on expansion of small abdominal aortic aneurysms - A prospective randomized double-blind trial. *Journal of Vascular Surgery.* 2009;50(1):23-29.

213. Gavrila D, Li WG, McCormick ML, et al. Vitamin E Inhibits Abdominal Aortic Aneurysm Formation in Angiotensin II-Infused Apolipoprotein E-Deficient Mice. *Arterioscler Thromb Vasc Biol.* August 1, 2005 2005;25(8):1671-1677.

214. The effect of vitamin E and beta carotene on the incidence of lung cancer and other cancers in male smokers. The Alpha-Tocopherol, Beta Carotene Cancer Prevention Study Group. *N Engl J Med.* Apr 14 1994;330(15):1029-1035.

215. McCormick ML, Gavrila D, Weintraub NL. Role of Oxidative Stress in the Pathogenesis of Abdominal Aortic Aneurysms. *Arterioscler Thromb Vasc Biol.* March 1, 2007 2007;27(3):461-469.

216. Walton LJ, Franklin IJ, Bayston T, et al. Inhibition of Prostaglandin E2 Synthesis in Abdominal Aortic Aneurysms : Implications for Smooth Muscle Cell Viability, Inflammatory Processes, and the Expansion of Abdominal Aortic Aneurysms. *Circulation.* July 6, 1999 1999;100(1):48-54.

217. King VL, Trivedi DB, Gitlin JM, Loftin CD. Selective Cyclooxygenase-2 Inhibition With Celecoxib Decreases Angiotensin II-Induced Abdominal Aortic Aneurysm Formation in Mice. *Arterioscler Thromb Vasc Biol.* May 1, 2006 2006;26(5):1137-1143.

218. Gitlin JM, Trivedi DB, Langenbach R, Loftin CD. Genetic deficiency of cyclooxygenase-2 attenuates abdominal aortic aneurysm formation in mice. *Cardiovascular Research.* January 1, 2007 2007;73(1):227-236.

219. Dobrin PB, Baumgartner N, Anidjar S, Chejfec G, Mrkvicka R. Inflammatory Aspects of Experimental Aneurysms. *Annals of the New York Academy of Sciences.* 1996;800(1):74-88.

220. Hingorani A, Ascher E, Scheinman M, et al. The effect of tumor necrosis factor binding protein and interleukin-1 receptor antagonist on the development of abdominal aortic aneurysms in a rat model. *J Vasc Surg.* Sep 1998;28(3):522-526.

221. Anidjar S, Salzmann JL, Gentric D, Lagneau P, Camilleri JP, Michel JB. Elastase-induced experimental aneurysms in rats. *Circulation.* September 1, 1990 1990;82(3):973-981.

222. Halpern VJ, Nackman GB, Gandhi RH, et al. The elastase infusion model of experimental aortic aneurysms: synchrony of induction of endogenous proteinases with matrix destruction and inflammatory cell response. *J Vasc Surg.* Jul 1994;20(1):51-60.

223. Nackman GB, Karkowski FJ, Halpern VJ, Gaetz HP, Tilson MD. Elastin degradation products induce adventitial angiogenesis in the Anidjar/Dobrin rat aneurysm model. *Surgery.* 1997;122(1):39-44.

224. Chiou AC, Chiu B, Pearce WH. Murine Aortic Aneurysm Produced by Periarterial Application of Calcium Chloride. *Journal of Surgical Research.* 2001;99(2):371-376.

225. Isenburg JC, Simionescu DT, Starcher BC, Vyavahare NR. Elastin Stabilization for Treatment of Abdominal Aortic Aneurysms. *Circulation.* April 3, 2007 2007;115(13):1729-1737.

226. Daugherty A, Cassis L. Chronic Angiotensin II Infusion Promotes Atherogenesis in Low Density Lipoprotein Receptor −/− Mice. *Annals of the New York Academy of Sciences.* 1999;892(1):108-118.

227. Saraff K, Babamusta F, Cassis LA, Daugherty A. Aortic Dissection Precedes Formation of Aneurysms and Atherosclerosis in Angiotensin II-Infused, Apolipoprotein E-Deficient Mice. *Arterioscler Thromb Vasc Biol.* September 1, 2003 2003;23(9):1621-1626.

228. Manach C, Scalbert A, Morand C, Rémésy C, Jiménez L. Polyphenols: food sources and bioavailability. *The American Journal of Clinical Nutrition.* May 1, 2004 2004;79(5):727-747.

229. Luck G, Liao H, Murray NJ, et al. Polyphenols, astringency and proline-rich proteins. *Phytochemistry.* 1994;37(2):357-371.

230. 1994;89:98. SBHXHEG-piJALCA.

231. Simionescu N, Simionescu M. Galloylglucoses of low molecular weight as mordant in electron microscopy. II. The moiety and functional groups possibly involved in the mordanting effect. *The Journal of Cell Biology.* September 1, 1976 1976;70(3):622-633.

232. Bolwell GP. Plant Polyphenols: Vegetable tannins revisited (1989). By E. Haslam. Chemistry and Pharmacology of Natural Products (J. D. Phillipson, D. C. Ayres and H. Baxter, Eds). Cambridge University Press: Cambridge, Pp. 230, £35/$70. *BioEssays.* 1990;12(9):453-453.

233. Isenburg JC, Simionescu DT, Vyavahare NR. Tannic acid treatment enhances biostability and reduces calcification of glutaraldehyde fixed aortic wall. *Biomaterials.* Apr 2005;26(11):1237-1245.

234. Tedder ME, Liao J, Weed B, et al. Stabilized collagen scaffolds for heart valve tissue engineering. *Tissue engineering. Part A.* Jun 2009;15(6):1257-1268.

235. Chuang TH, Stabler C, Simionescu A, Simionescu DT. Polyphenol-stabilized tubular elastin scaffolds for tissue engineered vascular grafts. *Tissue engineering. Part A.* Oct 2009;15(10):2837-2851.

236. Chow JP, Simionescu DT, Warner H, et al. Mitigation of diabetes-related complications in implanted collagen and elastin scaffolds using matrix-binding polyphenol. *Biomaterials.* 2013;34(3):685-695.

237. Chung K-T, Wei C-I, Johnson MG. Are tannins a double-edged sword in biology and health? *Trends in Food Science & Technology.* 1998;9(4):168-175.

238. Kono S, Ikeda M, Tokudome S, Kuratsune M. A case-control study of gastric cancer and diet in northern Kyushu, Japan. *Japanese journal of cancer research : Gann.* Oct 1988;79(10):1067-1074.

239. Wang ZY, Huang M-T, Ho C-T, et al. Inhibitory Effect of Green Tea on the Growth of Established Skin Papillomas in Mice. *Cancer Research.* December 1, 1992 1992;52(23):6657-6665.

240. Yamane T, Hagiwara N, Tateishi M, et al. Inhibition of azoxymethane-induced colon carcinogenesis in rat by green tea polyphenol fraction. *Japanese journal of cancer research : Gann.* Dec 1991;82(12):1336-1339.

241. Frei B, Higdon JV. Antioxidant Activity of Tea Polyphenols In Vivo: Evidence from Animal Studies. *The Journal of Nutrition.* October 1, 2003 2003;133(10):3275S-3284S.

242. Lee AS, Jung YJ, Kim DH, et al. Epigallocatechin-3-O-gallate decreases tumor necrosis factor-alpha-induced fractalkine expression in endothelial cells by suppressing NF-kappaB. *Cellular physiology and biochemistry : international journal of experimental cellular physiology, biochemistry, and pharmacology.* 2009;24(5-6):503-510.

243. Kim SY, Kim DS, Kwon SB, et al. Protective effects of EGCG on UVB-induced damage in living skin equivalents. *Archives of pharmacal research.* Jul 2005;28(7):784-790.

244. Pan MH, Lin JH, Lin-Shiau SY, Lin JK. Induction of apoptosis by penta-O-galloyl-beta-D-glucose through activation of caspase-3 in human leukemia HL-60 cells. *European journal of pharmacology.* 1999;381(2-3):171-183.

245. Hongbo Hu, Jinhui Zhang, Hyo Jeong Lee, Sung-Hoon Kim, and Junxuan Lü, and Junxuan Lü. Penta-O-galloyl-beta-D-glucose induces S- and G1-cell cycle arrests in prostate cancer cells targeting DNA replication and cyclin D1. *Carcinogenesis.* 2009 May;30(5):818-823.

246. Felipe J, Thomas FM, Kela L, Yanting W, Aleksander H. Ellagic and Tannic Acids Protect Newly Synthesized Elastic Fibers from Premature Enzymatic Degradation in Dermal Fibroblast Cultures. *Journal of Investigative Dermatology.* 2006;126(6):1272-1280.

247. Jorgensen B, Bülow J, Jo/rgensen M, et al. FEMORAL ARTERY RECANALISATION WITH PERCUTANEOUS ANGIOPLASTY AND SEGMENTALLY ENCLOSED PLASMINOGEN ACTIVATOR. *The Lancet.* 1989;333(8647):1106-1108.

248. http://onlinelibrary.wiley.com/doi/10.1002/0471142905.hg1301s31/pdf.

249. Camenzind E, Kint P-P, Di Mario C, et al. Intracoronary Heparin Delivery in Humans : Acute Feasibility and Long-term Results. *Circulation.* November 1, 1995 1995;92(9):2463-2472.

250. http://www.medscape.com/viewarticle/409154_2.

251. Glazier JJ, Hirst JA, Kiernan FJ, et al. Site-specific intracoronary thrombolysis with urokinase-coated hydrogel balloons: Acute and follow-up studies in 95 patients. *Catheterization and Cardiovascular Diagnosis.* 1997;41(3):246-253.

252. http://www.cirse.org/print.php?pid=565&lang=1.

253. Ikeno F, Lyons J, Kaneda H, Baluom M, Benet LZ, Rezaee M. Novel percutaneous adventitial drug delivery system for regional vascular treatment. *Catheterization and Cardiovascular Interventions.* 2004;63(2):222-230.

254. http://www.bacchus-vascular.com/products/trellis/how_it_works.html.

255. Stone GW, Ellis SG, Cannon L, et al. Comparison of a Polymer-Based Paclitaxel-Eluting Stent With a Bare Metal Stent in Patients With Complex Coronary Artery Disease. *JAMA: The Journal of the American Medical Association.* September 14, 2005 2005;294(10):1215-1223.

256. Kajimoto M, Shimono T, Hirano K, et al. Basic fibroblast growth factor slow release stent graft for endovascular aortic aneurysm repair: a canine model experiment. *J Vasc Surg.* Nov 2008;48(5):1306-1314.

257. Villa AE, Guzman LA, Chen W, Golomb G, Levy RJ, Topol EJ. Local delivery of dexamethasone for prevention of neointimal proliferation in a rat model of balloon angioplasty. *J Clin Invest.* Mar 1994;93(3):1243-1249.

258. Okada T, Bark DH, Mayberg MR. Localized Release of Perivascular Heparin Inhibits Intimal Proliferation after Endothelial Injury without Systemic Anticoagulation. *Neurosurgery.* 1989;25(6):892-898.

259. Simons M, Edelman ER, Rosenberg RD. Antisense proliferating cell nuclear antigen oligonucleotides inhibit intimal hyperplasia in a rat carotid artery injury model. *The Journal of Clinical Investigation.* 1994;93(6):2351-2356.

260. Brauner R, Laks H, Drinkwater JDC, et al. Controlled periadventitial administration of verapamil inhibits neointimal smooth muscle cell proliferation and ameliorates vasomotor abnormalities in experimental vein bypass grafts. *The Journal of Thoracic and Cardiovascular Surgery.* 1997;114(1):53-63.

261. Pires NMM, van der Hoeven BL, de Vries MR, et al. Local perivascular delivery of anti-restenotic agents from a drug-eluting poly([epsilon]-caprolactone) stent cuff. *Biomaterials.* 2005;26(26):5386-5394.

262. Yamawaki-Ogata A, Hashizume R, Satake M, et al. A doxycycline loaded, controlled-release, biodegradable fiber for the treatment of aortic aneurysms. *Biomaterials.*31(36):9554-9564.

263. ValÃ©ro F, Hamon M, Fournier C, et al. Intramural Injection of Biodegradable Microspheres as a Local Drug-Delivery System to Inhibit Neointimal Thickening in a Rabbit Model of Balloon Angioplasty. *Journal of Cardiovascular Pharmacology.* 1998;31(4):513-519.

264. Westedt U, Barbu-Tudoran L, Schaper AK, Kalinowski M, Alfke H, Kissel T. Deposition of nanoparticles in the arterial vessel by porous balloon catheters: localization by confocal laser scanning microscopy and transmission electron microscopy. *AAPS PharmSci.* 2002;4(4):E41.

265. Isenburg JC, Karamchandani NV, Simionescu DT, Vyavahare NR. Structural requirements for stabilization of vascular elastin by polyphenolic tannins. *Biomaterials.* 2006;27(19):3645-3651.

266. National Diabetes Fact Sheet, 2011. *Centers for Disease Control and Prevention. National diabetes fact sheet: national estimates and general information on diabetes and prediabetesin the United States, 2011. Atlanta, GA: U.S. Department of Health and Human Services, Centers for Disease Control and Prevention, 2011.*

267. Bobryshev YV, Lord RSA, Warren BA. Calcified deposit formation in intimal thickenings of the human aorta. *Atherosclerosis.* 1995;118(1):9-21.

268. Janzen J, Vuong PN. *Arterial calcifications: morphological aspects and their pathological implications.* Vol 90 Suppl 32001.

269. Johnson RC, Leopold JA, Loscalzo J. Vascular Calcification. *Circulation Research.* November 10, 2006 2006;99(10):1044-1059.

270. Chen NX, Duan D, O'Neill KD, Moe SM. High glucose increases the expression of Cbfa1 and BMP-2 and enhances the calcification of vascular smooth muscle cells. *Nephrology Dialysis Transplantation.* December 1, 2006 2006;21(12):3435-3442.

271. Baydanoff S, Nicoloff G, Alexiev C. Age-related changes in the level of circulating elastin-derived peptides in serum from normal and atherosclerotic subjects. *Atherosclerosis.* 1987;66(1â€“2):163-168.

272. Yu Q, Stamenkovic I. Cell surface-localized matrix metalloproteinase-9 proteolytically activates TGF-Î² and promotes tumor invasion and angiogenesis. *Genes & Development.* January 15, 2000 2000;14(2):163-176.

273. Livak KJ, Schmittgen TD. Analysis of Relative Gene Expression Data Using Real-Time Quantitative PCR and the 2â^'Î"Î"CT Method. *Methods.* 2001;25(4):402-408.

274. Fei T, Zhu S, Xia K, et al. Smad2 mediates Activin/Nodal signaling in mesendoderm differentiation of mouse embryonic stem cells. *Cell Res.* Dec;20(12):1306-1318.

275. Khatiwala CB, Kim PD, Peyton SR, Putnam AJ. ECM Compliance Regulates Osteogenesis by Influencing MAPK Signaling Downstream of RhoA and ROCK. *Journal of Bone and Mineral Research.* 2009;24(5):886-898.

276. Mimori K, Komaki M, Iwasaki K, Ishikawa I. Extracellular Signal-Regulated Kinase 1/2 Is Involved in Ascorbic Acid–Induced Osteoblastic Differentiation in Periodontal Ligament Cells. *Journal of Periodontology.* 2007/02/01 2007;78(2):328-334.

277. Miyazono K. TGF-beta receptors and signal transduction. *Int J Hematol.* Feb 1997;65(2):97-104.

278. Ghuysen-Itard AF, Robert L, Jacob MP. [Effect of elastin peptides on cell proliferation]. *C R Acad Sci III.* 1992;315(12):473-478.

279. Mecham RP, Griffin GL, Madaras JG, Senior RM. Appearance of chemotactic responsiveness to elastin peptides by developing fetal bovine ligament fibroblasts parallels the onset of elastin production. *J Cell Biol.* May 1984;98(5):1813-1816.

280. Robinet A, Fahem A, Cauchard J-H, et al. Elastin-derived peptides enhance angiogenesis by promoting endothelial cell migration and tubulogenesis through upregulation of MT1-MMP. *Journal of Cell Science.* January 15, 2005 2005;118(2):343-356.

281. Jung S, Rutka JT, Hinek A. Tropoelastin and elastin degradation products promote proliferation of human astrocytoma cell lines. *J Neuropathol Exp Neurol.* May 1998;57(5):439-448.

282. Duca L FN, Alix AJ, Haye B, Debelle L. Elastin as a matrikine. *Crit Rev Oncol Hematol.* 2004 Mar;;49(3):235-44.

283. Liu F, Zhong H, Liang JY, et al. Effect of high glucose levels on the calcification of vascular smooth muscle cells by inducing osteoblastic differentiation and intracellular calcium deposition via BMP-2/Cbfalpha-1 pathway. *J Zhejiang Univ Sci B.* Dec;11(12):905-911.

284. BostrÃ¶m KI, Jumabay M, Matveyenko A, Nicholas SB, Yao Y. Activation of Vascular Bone Morphogenetic Protein Signaling in Diabetes Mellitus. *Circulation Research.* December 30, 2010.

285. Shioi A, Nishizawa Y, Jono S, Koyama H, Hosoi M, Morii H. Î²-Glycerophosphate Accelerates Calcification in Cultured Bovine Vascular Smooth Muscle Cells. *Arteriosclerosis, Thrombosis, and Vascular Biology.* November 1, 1995 1995;15(11):2003-2009.

286. Jian B, Narula N, Li QY, Mohler ER, 3rd, Levy RJ. Progression of aortic valve stenosis: TGF-beta1 is present in calcified aortic valve cusps and promotes aortic valve interstitial cell calcification via apoptosis. *Ann Thorac Surg.* Feb 2003;75(2):457-465; discussion 465-456.

287. Tintut Y, Patel J, Parhami F, Demer LL. Tumor Necrosis Factor-Î± Promotes In Vitro Calcification of Vascular Cells via the cAMP Pathway. *Circulation.* November 21, 2000 2000;102(21):2636-2642.

288. Inoki K, Haneda M, Maeda S, Koya D, Kikkawa R. TGF-beta 1 stimulates glucose uptake by enhancing GLUT1 expression in mesangial cells. *Kidney Int.* May 1999;55(5):1704-1712.

289. Inoguchi T, Battan R, Handler E, Sportsman JR, Heath W, King GL. Preferential elevation of protein kinase C isoform beta II and diacylglycerol levels in the aorta and heart of diabetic rats: differential reversibility to glycemic control by islet cell transplantation. *Proc Natl Acad Sci U S A.* Nov 15 1992;89(22):11059-11063.

290. Inoguchi T, Xia P, Kunisaki M, Higashi S, Feener EP, King GL. Insulin's effect on protein kinase C and diacylglycerol induced by diabetes and glucose in vascular tissues. *American Journal of Physiology - Endocrinology And Metabolism.* September 1, 1994 1994;267(3):E369-E379.

291. Ishii H, Jirousek MR, Koya D, et al. Amelioration of Vascular Dysfunctions in Diabetic Rats by an Oral PKC Î² Inhibitor. *Science.* 1996;272(5262):728-731.

292. Koya D, Haneda M, Nakagawa H, et al. Amelioration of accelerated diabetic mesangial expansion by treatment with a PKC Î² inhibitor in diabetic db/db mice, a rodent model for type 2 diabetes. *The FASEB Journal.* March 1, 2000 2000;14(3):439-447.

293. Williams B, Schrier RW. Characterization of glucose-induced in situ protein kinase C activity in cultured vascular smooth muscle cells. *Diabetes.* Nov 1992;41(11):1464-1472.

294. Kunisaki M, Bursell SE, Umeda F, Nawata H, King GL. Normalization of diacylglycerol-protein kinase C activation by vitamin E in aorta of diabetic rats and cultured rat smooth muscle cells exposed to elevated glucose levels. *Diabetes.* Nov 1994;43(11):1372-1377.

295. Lee TS, Saltsman KA, Ohashi H, King GL. Activation of protein kinase C by elevation of glucose concentration: proposal for a mechanism in the development of diabetic vascular complications. *Proc Natl Acad Sci U S A.* Jul 1989;86(13):5141-5145.

296. Koya D, Jirousek MR, Lin YW, Ishii H, Kuboki K, King GL. Characterization of protein kinase C beta isoform activation on the gene expression of transforming growth factor-beta, extracellular matrix components, and prostanoids in the glomeruli of diabetic rats. *J Clin Invest.* Jul 1 1997;100(1):115-126.

297. Fulop T, Jr., Douziech N, Jacob MP, Hauck M, Wallach J, Robert L. Age-related alterations in the signal transduction pathways of the elastin-laminin receptor. *Pathol Biol (Paris).* May 2001;49(4):339-348.

298. Urry DW. Neutral sites for calcium ion binding to elastin and collagen: a charge neutralization theory for calcification and its relationship to atherosclerosis. *Proc Natl Acad Sci U S A.* Apr 1971;68(4):810-814.

299. Coselli JS, Conklin LD, LeMaire SA. Thoracoabdominal aortic aneurysm repair: review and update of current strategies. *Ann Thorac Surg.* November 1, 2002 2002;74(5):S1881-1884.

300. MEMBERS WG, Lloyd-Jones D, Adams RJ, et al. Heart Disease and Stroke Statistics—2010 Update: A Report From the American Heart Association. *Circulation.* February 23, 2010 2010;121(7):e46-e215.

301. Adam van der Vliet J, Boll APM. Abdominal aortic aneurysm. *The Lancet.* 1997;349(9055):863-866.

302. Sho E, Chu J, Sho M, et al. Continuous periaortic infusion improves doxycycline efficacy in experimental aortic aneurysms. *Journal of Vascular Surgery.* 2004;39(6):1312-1321.

303. Manning MW, Cassis LA, Daugherty A. Differential Effects of Doxycycline, a Broad-Spectrum Matrix Metalloproteinase Inhibitor, on Angiotensin II–Induced Atherosclerosis and Abdominal Aortic Aneurysms. *Arteriosclerosis, Thrombosis, and Vascular Biology.* March 1, 2003 2003;23(3):483-488.

304. Galis ZS, Khatri JJ. Matrix Metalloproteinases in Vascular Remodeling and Atherogenesis: The Good, the Bad, and the Ugly. *Circulation Research.* February 22, 2002 2002;90(3):251-262.

305. Isenburg JC, Simionescu DT, Starcher BC, Vyavahare NR. Elastin stabilization for treatment of abdominal aortic aneurysms. *Circulation.* Apr 3 2007;115(13):1729-1737.

306. Partridge SM, Keeley FW. Age Related and Atherosclerotic Changes in Aortic Elastin. In: Wagner W, Clarkson T, eds. *Arterial Mesenchyme and Arteriosclerosis.* Vol 43: Springer US; 1974:173-191.

307. Mecham RP. Methods in elastic tissue biology: Elastin isolation and purification. *Methods.* 2008;45(1):32-41.

308. Gacchina CE, Deb P, Barth JL, Ramamurthi A. Elastogenic inductability of smooth muscle cells from a rat model of late stage abdominal aortic aneurysms. *Tissue engineering. Part A.* Jul 2011;17(13-14):1699-1711.

309. Bailey M, Pillarisetti S, Jones P, Xiao H, Simionescu D, Vyavahare N. Involvement of matrix metalloproteinases and tenascin-C in elastin calcification. *Cardiovascular Pathology.* 2004;13(3):146-155.

310. Isenburg JC, Karamchandani NV, Simionescu DT, Vyavahare NR. Structural requirements for stabilization of vascular elastin by polyphenolic tannins. *Biomaterials.* Jul 2006;27(19):3645-3651.

311. Thompson RW, Holmes DR, Mertens RA, et al. Production and localization of 92-kilodalton gelatinase in abdominal aortic aneurysms. An elastolytic metalloproteinase expressed by aneurysm-infiltrating macrophages. *The Journal of Clinical Investigation.* 1995;96(1):318-326.

312. Freestone T, Turner RJ, Coady A, Higman DJ, Greenhalgh RM, Powell JT. Inflammation and Matrix Metalloproteinases in the Enlarging Abdominal Aortic Aneurysm. *Arteriosclerosis, Thrombosis, and Vascular Biology.* August 1, 1995 1995;15(8):1145-1151.

313. Mecham RP, Broekelmann TJ, Fliszar CJ, Shapiro SD, Welgus HG, Senior RM. Elastin Degradation by Matrix Metalloproteinases: CLEAVAGE SITE SPECIFICITY AND MECHANISMS OF ELASTOLYSIS. *Journal of Biological Chemistry.* July 18, 1997 1997;272(29):18071-18076.

314. Ulrich M, Thomas T, Oliver W. Selective Inactivation of Human Neutrophil Elastase by Synthetic Tannin. *Journal of Investigative Dermatology.* 1991;97(3):529-533.

315. Vayalil PK, Mittal A, Katiyar SK. Proanthocyanidins from grape seeds inhibit expression of matrix metalloproteinases in human prostate carcinoma cells, which is associated with the inhibition of activation of MAPK and NFκB. *Carcinogenesis.* June 1, 2004 2004;25(6):987-995.

316. Demeule M, Brossard M, Pagé M, Gingras D, Béliveau R. Matrix metalloproteinase inhibition by green tea catechins. *Biochimica et Biophysica Acta (BBA) - Protein Structure and Molecular Enzymology.* 2000;1478(1):51-60.

317. Johnson DJ, Robson P, Hew Y, Keeley FW. Decreased Elastin Synthesis in Normal Development and in Long-term Aortic Organ and Cell Cultures Is Related to Rapid and Selective Destabilization of mRNA for Elastin. *Circulation Research.* December 1, 1995 1995;77(6):1107-1113.

318. McMahon M, Faris B, Wolfe BL, et al. Aging effects on the elastin composition in the extracellular matrix of cultured rat aortic smooth muscle cells. *In Vitro Cell Dev Biol.* 1985/12/01 1985;21(12):674-680.

319. Ramanathan R, Tan CH, Das NP. Cytotoxic effect of plant polyphenols and fat-soluble vitamins on malignant human cultured cells. *Cancer letters.* 1992;62(3):217-224.

320. Krettek A, Sukhova GK, Libby P. Elastogenesis in Human Arterial Disease: A Role for Macrophages in Disordered Elastin Synthesis. *Arteriosclerosis, Thrombosis, and Vascular Biology.* April 1, 2003 2003;23(4):582-587.

321. Huffman MD, Curci JA, Moore G, Kerns DB, Starcher BC, Thompson RW. Functional importance of connective tissue repair during the development of experimental abdominal aortic aneurysms. *Surgery.* 2000;128(3):429-438.

322. Maretoshi H, Tetsuya O, Masahito H, et al. Fibulin-5/DANCE has an elastogenic organizer activity that is abrogated by proteolytic cleavage in vivo. *The Journal of Cell Biology.* 2007;176(7).

323. Kagan HM, Sullivan KA. Lysyl oxidase: preparation and role in elastin biosynthesis. *Methods in enzymology.* 1982;82 Pt A:637-650.

324. Ricotta JJ, Green RM, DeWeese JA. Use and limitations of thrombolytic therapy in the treatment of peripheral arterial ischemia: Results of a multi-institutional questionnaire. *Journal of vascular surgery : official publication, the Society for Vascular Surgery.* 1987;6(1):45-50.

325. Schulman S, Beyth RJ, Kearon C, Levine MN. Hemorrhagic complications of anticoagulant and thrombolytic treatment: American College of Chest Physicians Evidence-Based Clinical Practice Guidelines (8th Edition). *Chest.* Jun 2008;133(6 Suppl):257S-298S.

326. Elliott RJ, McGrath LT. Calcification of the human thoracic aorta during aging. *Calcified Tissue International.* 1994;54(4):268-273.

327. Edmonds ME. Medial arterial calcification and diabetes mellitus. *Zeitschrift fÃ¼r Kardiologie.* 2000;89(2):S101-S104.

328. Salusky IB, Goodman WG. Cardiovascular calcification in endâ€stage renal disease. *Nephrology Dialysis Transplantation.* February 1, 2002 2002;17(2):336-339.

329. Aikawa E, Aikawa M, Libby P, et al. Arterial and Aortic Valve Calcification Abolished by Elastolytic Cathepsin S Deficiency in Chronic Renal Disease. *Circulation.* April 7, 2009 2009;119(13):1785-1794.

330. Lederle FA, Johnson GR, Wilson SE, et al. Prevalence and Associations of Abdominal Aortic Aneurysm Detected through Screening. *Annals of Internal Medicine.* 1997;126(6):441-449.

331. Lusis AJ. Atherosclerosis. *Nature.* Sep 14 2000;407(6801):233-241.

332. Sims FH. The Initiation of Intimal Thickening in Human Arteries. *Pathology - Journal of the RCPA.* 2000;32(3):171-175 110.1080/pat.1032.1083.1171.1175.

333. Raines EW, Koyama H, Carragher NO. The Extracellular Matrix Dynamically Regulates Smooth Muscle Cell Responsiveness to PDGFa. *Annals of the New York Academy of Sciences.* 2000;902(1):39-52.

334. Basalyga DM, Simionescu DT, Xiong W, Baxter BT, Starcher BC, Vyavahare NR. Elastin Degradation and Calcification in an Abdominal Aorta Injury Model: Role of Matrix Metalloproteinases. *Circulation.* November 30, 2004 2004;110(22):3480-3487.

335. Melis M, Pace E, Siena L, et al. Biologically Active Intercellular Adhesion Molecule-1 Is Shed as Dimers by a Regulated Mechanism in the Inflamed Pleural Space. *American Journal of Respiratory and Critical Care Medicine.* 2003/04/15 2003;167(8):1131-1138.

336. Bartoli MA, Parodi FE, Chu J, et al. Localized Administration of Doxycycline Suppresses Aortic Dilatation in an Experimental Mouse Model of Abdominal Aortic Aneurysm. *Annals of Vascular Surgery.* 2006;20(2):228-236.

337. Chan JM, Zhang L, Tong R, et al. Spatiotemporal controlled delivery of nanoparticles to injured vasculature. *Proceedings of the National Academy of Sciences.* February 2, 2010;107(5):2213-2218.

338. Sakai LY, Keene DR, Engvall E. Fibrillin, a new 350-kD glycoprotein, is a component of extracellular microfibrils. *The Journal of Cell Biology.* December 1, 1986 1986;103(6):2499-2509.

339. Ashworth JL, Murphy G, Rock MJ, et al. Fibrillin degradation by matrix metalloproteinases: implications for connective tissue remodelling. *Biochem J.* May 15 1999;340 (Pt 1):171-181.

340. Fukuda Y, Ferrans VJ. Pulmonary elastic fiber degradation in paraquat toxicity. An electron microscopic immunohistochemical study. *Journal of submicroscopic cytology and pathology.* Jan 1988;20(1):15-23.

341. Derksen JTP, Morselt HWM, Scherphof GL. Uptake and processing of immunoglobulin-coated liposomes by subpopulations of rat liver macrophages. *Biochimica et Biophysica Acta (BBA) - Molecular Cell Research.* 1988;971(2):127-136.

342. Vonarbourg A, Passirani C, Saulnier P, Benoit J-P. Parameters influencing the stealthiness of colloidal drug delivery systems. *Biomaterials.* 2006;27(24):4356-4373.

343. Knop K, Hoogenboom R, Fischer D, Schubert US. Poly(ethylene glycol) in Drug Delivery: Pros and Cons as Well as Potential Alternatives. *Angewandte Chemie International Edition.* 2010;49(36):6288-6308.

344. Sivaraman B, Ramamurthi A. Multifunctional nanoparticles for doxycycline delivery towards localized elastic matrix stabilization and regenerative repair. *Acta Biomaterialia.* (0).

345. Song C, Labhasetwar V, Cui X, Underwood T, Levy RJ. Arterial uptake of biodegradable nanoparticles for intravascular local drug delivery: Results with an acute dog model. *Journal of Controlled Release.* 1998;54(2):201-211.

346. Cho EC, Au L, Zhang Q, Xia Y. The Effects of Size, Shape, and Surface Functional Group of Gold Nanostructures on Their Adsorption and Internalization by Cells. *Small.*6(4):517-522.

347. Cho EC, Xie J, Wurm PA, Xia Y. Understanding the Role of Surface Charges in Cellular Adsorption versus Internalization by Selectively Removing Gold Nanoparticles on the Cell Surface with a I2/KI Etchant. *Nano Letters.* 2013/04/04 2009;9(3):1080-1084.

348. Luo R, Neu B, Venkatraman SS. Surface Functionalization of Nanoparticles to Control Cell Interactions and Drug Release. *Small.*8(16):2585-2594.

349. Majmudar MD, Yoo J, Keliher EJ, et al. Polymeric Nanoparticle PET/MR Imaging Allows Macrophage Detection in Atherosclerotic Plaques. *Circulation Research.* March 1, 2013 2013;112(5):755-761.

350. Aragnol D, Leserman LD. Immune clearance of liposomes inhibited by an anti-Fc receptor antibody in vivo. *Proceedings of the National Academy of Sciences.* April 1, 1986 1986;83(8):2699-2703.

351. Gabizon AA. Pegylated Liposomal Doxorubicin: Metamorphosis of an Old Drug into a New Form of Chemotherapy. *Cancer Investigation.* 2001;19(4):424-436.

352. Schrama D, Reisfeld RA, Becker JC. Antibody targeted drugs as cancer therapeutics. *Nat Rev Drug Discov.* Feb 2006;5(2):147-159.

353. Kaminski MS, Zasadny KR, Francis IR, et al. Radioimmunotherapy of B-Cell Lymphoma with [131I]Anti-B1 (Anti-CD20) Antibody. *New England Journal of Medicine.* 1993;329(7):459-465.

354. Hudson PJ, Souriau C. Engineered antibodies. *Nat Med.* Jan 2003;9(1):129-134.

355. Yan G, Paul D, Shenshen C, et al. Shape effects of filaments versus spherical particles in flow and drug delivery. *Nature Nanotechnology.* 2007;2(4):249-255.

356. Silvia M, Carmen G, Julie AC, et al. Control of Endothelial Targeting and Intracellular Delivery of Therapeutic Enzymes by Modulating the Size and Shape of ICAM-1-targeted Carriers. *Molecular Therapy.* 2008;16(8):1450-1458.

357. Champion JA, Mitragotri S. Role of target geometry in phagocytosis. *Proceedings of the National Academy of Sciences of the United States of America.* March 28, 2006 2006;103(13):4930-4934.

358. Chiappini C, Tasciotti E, Fakhoury JR, et al. Tailored Porous Silicon Microparticles: Fabrication and Properties. *ChemPhysChem.* 2010;11(5):1029-1035.

359. Gref R, Minamitake Y, Peracchia MT, Trubetskoy V, Torchilin V, Langer R. Biodegradable Long-Circulating Polymeric Nanospheres. *Science.* 1994;263(5153):1600-1603.

360. Pisani E, Ringard C, Nicolas V, et al. Tuning microcapsules surface morphology using blends of homo- and copolymers of PLGA and PLGA-PEG. *Soft Matter.* 2009;5(16):3054-3060.

361. Abdelwahed W, Degobert G, Stainmesse S, Fessi H. Freeze-drying of nanoparticles: Formulation, process and storage considerations. *Advanced Drug Delivery Reviews.* 2006;58(15):1688-1713.

362. Saez A, Guzmán M, Molpeceres J, Aberturas MR. Freeze-drying of polycaprolactone and poly(d,l-lactic-glycolic) nanoparticles induce minor particle size changes affecting the oral pharmacokinetics of loaded drugs. *European Journal of Pharmaceutics and Biopharmaceutics.* 2000;50(3):379-387.

363. Malam Y, Loizidou M, Seifalian AM. Liposomes and nanoparticles: nanosized vehicles for drug delivery in cancer. *Trends in Pharmacological Sciences.* 2009;30(11):592-599.